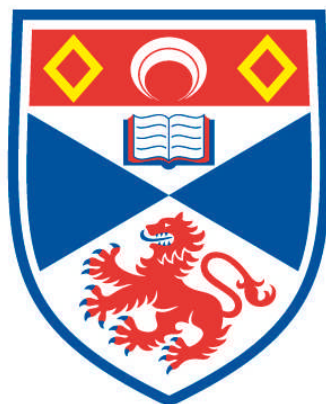


# **SYNTHESIS AND EVALUATION OF B-FLUORO- Γ-AMINOBTYRIC ACID ENANTIOMERS**

**Gildas Deniau**

**A Thesis Submitted for the Degree of PhD  
at the  
University of St Andrews**



**2007**

**Full metadata for this item is available in  
Research@StAndrews:FullText  
at:**

**<http://research-repository.st-andrews.ac.uk/>**

**Please use this identifier to cite or link to this item:**

**<http://hdl.handle.net/10023/362>**

**This item is protected by original copyright**

**This item is licensed under a  
Creative Commons Licence**

# **Synthesis and Evaluation of $\beta$ -Fluoro- -aminobutyric acid enantiomers.**



**A thesis presented for the degree of Doctor of  
Philosophy in the School of Chemistry  
University of St. Andrews**

**Gildas Deniau**

**May 2007**

Марина, Спасибо за твою любовь и веру

*Look at every path closely and deliberately, then ask yourself this crucial question:*

*Does this path have a heart? If it does, then the path is good. If it doesn't, it is of no use.*

Carlos Castaneda

## Declaration

I, Gildas Pascal Deniau, hereby certify that this thesis, which is approximately 52,000 words in length, has been written by me, that it is the record of work carried out by me and that it has not been submitted in any previous application for a higher degree.

Date.....Signature of Candidate.....

I was admitted as a research student in October 2003 and as a candidate for the degree of Doctor of Philosophy in October 2003, the higher study for which this is a record was carried out at the University of St. Andrews between October 2003 and October 2006.

Date.....Signature of Candidate.....

I hereby certify that the candidate has fulfilled the conditions of the Resolution and Regulations appropriate for the Degree of Doctor of Philosophy in the University of St. Andrews and that the candidate is qualified to submit this thesis in application for that degree.

Date.....Signature of Supervisor.....

# Copyright

In submitting this thesis to the University of St. Andrews I wish access to it to be subject to the following conditions: for a period of three years from the date of submission, the thesis shall be withheld from use;

I understand, however, that the title and abstract of the thesis will be published during this period of restricted access; and that after the expiry of this period the thesis will be made available for use in accordance with the regulations of the University Library for the time being in force, subject to any copyright in the work not being affected thereby, and a copy of the work may be made and supplied to any *bona fide* library or research worker, that my thesis will be electronically accessible for personal or research use, and that the library has the right to migrate my thesis into new electronic forms as required to ensure continued access to the thesis. I have obtained any third-party copyright permissions that may be required in order to allow such access and migration.

Date.....Signature of Candidate.....

# Acknowledgements

First, I would like to express my gratitude to my supervisor Professor David O'Hagan. His academic and personal qualities have been much appreciated over the last three years. Also, I am grateful to the University of St. Andrews for an interdisciplinary studentship and to my second supervisor Professor Keith Sillar for his interest in this project.

I wish to thank the technical and support staff at the department for the excellent working conditions throughout my PhD in St. Andrews. Special thanks go to Professor Alexandra M. Z. Slawin for her constant dynamism and expertise, to Melanja Smith and Dr Tomáš Lébl who offer with inexhaustible energy an NMR service of high quality and to Caroline Horsburgh for all mass spectroscopic analyses.

I guess it is now time for me to thank my friends in St Andrews. I have been very happy to meet here such a bunch of interesting people without which the long and dark months of the Scottish winter would have been too gloomy. Fortunately, they were also here to enjoy the long and bright days of summer! At the same time, I would like to thank past and present members of the DOH group for useful and useless discussions about chemistry and hem, not only chemistry. Fumehood neighbours Vincent and Kenny, desk-buddy Luke, sister Natalie, brother Matthieu and Uncles Martin and Cosimo are all warmly and sincerely thanked.

Last but not least, I am extremely thankful to Marina for her understanding and unfailing love which guided me during my time in St. Andrews.

# Table of contents

Abbreviations	ix
Abstract	xi
 <b>Chapter 1: Fluorine in bioactive molecules</b>	
<b>1.1</b> Introduction	1
<b>1.2</b> The significance of fluorine in bioactive molecules	4
1.2.1 Physicochemical properties of fluorine	4
1.2.2 Fluorine in medicinal chemistry	13
<b>1.3</b> The fluorine <i>gauche</i> effect	23
1.3.1 Origin of the <i>gauche</i> effect	23
1.3.2 Uses and applications of the fluorine <i>gauche</i> effect	32
<b>1.4</b> References	42
 <b>Chapter 2: The GABA-mediated inhibition of neuronal signals</b>	
<b>2.1</b> Introduction	46
<b>2.2</b> GABA and GABA receptors as key elements in the CNS	48
2.2.1 The importance of GABA in the CNS	48
2.2.2 GABA <sub>A</sub> and GABA <sub>B</sub> receptors	53
<b>2.3</b> Binding studies of GABA analogues	63

<b>2.4 Steroid modulation of the GABA response</b>	69
2.4.1 The nature of steroid modulation	69
2.4.2 Synthesis of steroid selective inhibitors	75
2.4.3 Biological results	90
2.4.4 Conclusions	92
<b>2.5 References</b>	93

## **Chapter 3: Synthesis and evaluation of 3-fluoro-GABA enantiomers**

<b>3.1 Introduction</b>	98
<b>3.2 Previous syntheses of 3-fluoro-GABA</b>	
3.2.1 The dehydroxyfluorination approach	101
3.2.2 The Gabriel synthesis approach	104
<b>3.3 Amino acids as precursors of 3-fluoro-GABA</b>	
3.3.1 The serine approach	107
3.3.2 The aspartic acid approach	114
<b>3.4 The Phenylalanine route</b>	118
<b>3.5 Conformation and evaluation of 3-fluoro-GABA enantiomers</b>	
3.5.1 Conformational and NMR analyses	133
3.5.2 $pK_a$ studies and conclusions	141
3.5.3 Conclusions	145
<b>3.6 Biological studies</b>	
3.6.1 Studies on GABA receptors	146
3.6.2 Studies of GABA aminotransferase	150
3.6.3 Conclusions	155



<b>3.7</b>	<b>Towards the synthesis of 3-fluoro-GABA analogues</b>	
3.7.1	Synthesis of conformationally constrained GABA analogues	156
3.7.2	Towards the synthesis of a fluorinated analogue of carnitine	162
<b>3.8</b>	<b>References</b>	168

## **Chapter 4: Synthesis of 2-fluorohexane-1,6-diamine and 2-aminomethyl-piperidine from L-lysine**

<b>4.1</b>	<b>Introduction</b>	173
<b>4.2</b>	<b>Synthesis of (2<i>R</i>)-fluorohexane-1,6-diamine</b>	
4.2.1	The lysine approach	175
4.2.2	The <i>N</i> (ε)-Z-L-lysine route	179
<b>4.3</b>	<b>Synthesis of (2<i>R</i>)-aminomethyl-piperidine</b>	185
<b>4.4</b>	<b>References</b>	191

## **Chapter 5: Experimental.**

<b>5.1</b>	<b>General methods</b>	192
<b>5.2</b>	<b>Protocols</b>	194
<b>5.3</b>	<b>References</b>	259
<b>5.4</b>	<b>Crystallographic data</b>	261

# Abbreviations

BnOH:	benzyl alcohol
Boc <sub>2</sub> O:	<i>tert</i> -butoxycarbonyl anhydride
Bn:	benzyl
br s:	broad singlet
BuLi:	butyl lithium
CNS:	central nervous system
CSD:	Cambridge Structural Database
d:	doublet
DAST:	diethylaminosulfur trifluoride
DCM:	dichloromethane
de:	diastereomeric excess
DFT:	density functional theory
4-DMAP:	4-( <i>N,N</i> -dimethylamino)pyridine
DMF:	<i>N,N</i> -dimethylformamide
ee:	enantiomeric excess
eq.:	equivalent
Flp:	(4 <i>R</i> )-fluoroproline
flp:	(4 <i>S</i> )-fluoroproline
3-F-GABA:	3-fluoro- $\gamma$ -aminobutyric acid
GABA:	$\gamma$ -aminobutyric acid
GABA-AT:	$\gamma$ -aminobutyric acid aminotransferase
GAD:	L-glutamic acid decarboxylase
Hz:	Hertz
IR:	Infrared spectroscopy
<i>J</i> :	coupling constant
m:	multiplet
MeCN:	acetonitrile
$\mu$ M:	micromolar ( $10^{-6}$ mol.L <sup>-1</sup> )
Mp:	melting point

Ms <sub>2</sub> O:	methanesulfonic anhydride
( <i>R</i> )-(-)-MTPA-Cl:	( <i>R</i> )-(-)- $\alpha$ -methoxy- $\alpha$ -(trifluoromethyl)phenylacetyl chloride
NMR:	Nuclear magnetic resonance
NOESY:	Nuclear Overhauser effect correlation spectroscopy
17-PA:	(3 $\alpha$ ,5 $\alpha$ )-17-phenylandroster-16-en-3-ol
PLP:	pyridoxal-5'-phosphate
PMP:	pyridoxamine-5'-phosphate
ppm:	parts per million
pTSA:	<i>p</i> -toluenesulfonic acid monohydrate
q:	quartet
QSAR:	quantitative structure-activity relationships
R <sub>f</sub> :	perfluorinated group
RT:	room temperature
s:	singlet
t:	triplet
TBAF:	<i>N</i> -tetrabutylammonium fluoride
Tf <sub>2</sub> O:	trifluoromethanesulfonic anhydride
THF:	tetrahydrofuran
TLC:	thin layer chromatography
TMSCl:	trimethylsilyl chloride
V <sub>w</sub> :	Van der Waals volume

## Abstract

The impact of fluorine in medicinal chemistry is reviewed in the first chapter of this work and the fluorine *gauche* effect, which has not been fully exploited in medicinal chemistry, is also discussed. GABA<sub>A</sub> and GABA<sub>B</sub> receptors are then presented and the synthesis of neurosteroid antagonists acting at GABA<sub>A</sub> receptors is reported. The synthesis of such compounds was motivated to explore the mode of action of neurosteroids at GABA receptors.

The observation that the C-F bond has a strong preference to align *gauche* to the C-N<sup>+</sup> bond in protonated  $\beta$ -fluoroamines stimulated the enantioselective synthesis of 3-fluoro-GABA enantiomers. This was achieved from L- and D- phenylalanine in six steps and in an overall yield of 31%. The preferred conformations of 3-fluoro-GABA in solution are then explored by NMR analysis and *ab initio* calculations. The biological evaluation of 3-fluoro-GABA enantiomers on GABA aminotransferase was then investigated and showed that the (*R*)-enantiomer undergoes HF elimination ten times more rapidly than the (*S*)-enantiomer, suggesting a preferred binding conformation of GABA on GABA aminotransferase. This study demonstrates that the C-F bond can be used as a chemical probe to reveal the binding conformation of a bioactive amine and this offers exciting prospects for future research.

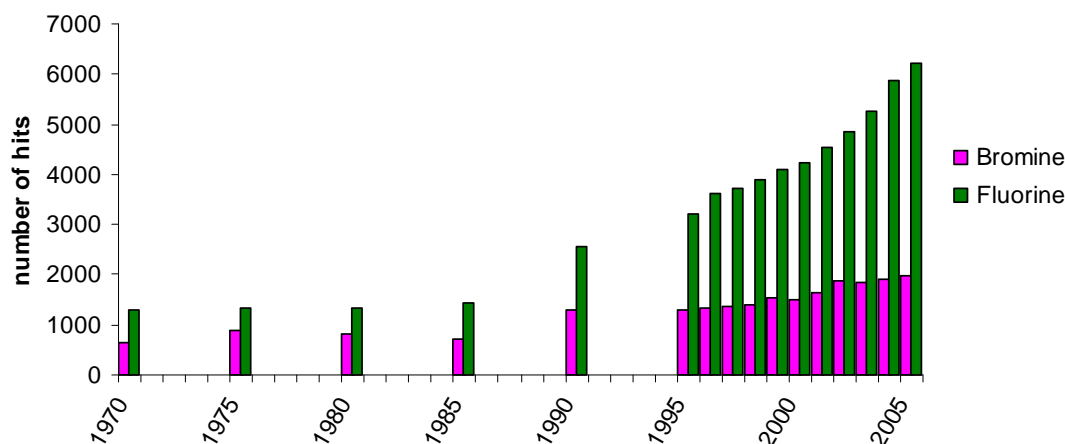
The synthesis of 3-fluoro-GABA from phenylalanine indicated that amino acids are practical starting materials for the preparation of  $\beta$ -fluoroamines. This methodology is applied to L-lysine to generate (2*R*)-fluorohexane-1,6-diamine. The formation of a diamine of potential interest for catalysis is also observed in this synthesis.

## Chapter 1: Fluorine in bioactive molecules

### 1.1 Introduction

"Independent scientific evidence repeatedly showing up over the past 50 years reveals that fluoride allegedly shortens our life span, promotes cancer and various mental disturbances, accelerates osteoporosis and broken hips in old folks, and makes us stupid, docile, and subservient, all in one package."

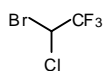
This quote from an article which has spread over the net can be found on many web sites, *e.g.* <http://www.tuberose.com/Fluoride.html>. Although not always based on scientific facts, this article reflects the public concerns about water fluorination in the USA. Certainly, the industrial applications of fluorine chemistry have boomed over the last 60 years and have today a visible impact on everybody's life, not only with fluorinated toothpastes, but also with Teflon<sup>TM</sup> and GoreTex<sup>TM</sup> which are made of perfluorinated polymers. Fluorine chemistry now plays an important role in a wide range of advanced technologies extending from medicinal chemistry to liquid crystals. A quick search on Scifinder shows that hits on "fluorine" have steadily increased over the last 35 years, as illustrated in Graph 1.1.



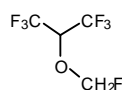
**Graph 1.1:** Evolution of the number of hits on “bromine” and “fluorine” between 1970 and 2005 on SciFinder.

Fluorine was first isolated in 1886 by French chemist Henri Moissan, a discovery for which he received the Nobel Prize just a century ago, in 1906. In the first part of the 20<sup>th</sup> century, fluorine had a significant impact on material science with the discovery of chlorofluorocarbons (CFCs) as refrigerants and the discovery of fluoropolymers.

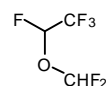
The first application of fluorinated compounds in biology occurred in the early 1950s with the introduction of fluorinated anaesthetics as alternatives for diethyl ether. Halothane (**1**) has long been used as an anaesthetic because of its low blood-gas partition coefficient which shortens the recovery time of patients. In the 1990s, sevoflurane (**2**) and desflurane (**3**) have been found to have lower levels of metabolism and lower blood-gas partition coefficient. They are currently used in anaesthesia.<sup>1</sup>



**1**

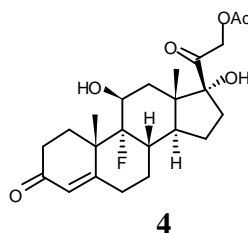


**2**



**3**

It was with the synthesis of 9 $\alpha$ -fluorohydrocortisone acetate (**4**) reported by Fried<sup>2</sup> in 1954 that the potential of fluorine to enhance the pharmacological properties of bioactive molecules was first demonstrated. This work has initiated the development of fluorine first in corticosteroid chemistry but then more widely in the pharmaceutical industry and it is estimated at present that about 20-25% of drugs contain at least one fluorine atom.<sup>3</sup> This is remarkable as fluorine was present in only 5% of pharmaceutical compounds in 1970.



The physicochemical properties of the fluorine atom are presented first in Chapter 1 and the particular reactivity of fluorinated compounds is discussed. The different strategies in which fluorinated compounds are employed in medicinal chemistry are then reviewed. Finally, the ability of fluorine to influence the conformation of molecules and in particular of  $\beta$ -fluoroamines is examined. This conformational influence, often called “fluorine *gauche* effect” is well recognised but its potential in organic or medicinal chemistry has not been fully exploited.

## 1.2 The significance of fluorine in bioactive molecules

### 1.2.1 Physicochemical properties of fluorine

Fluorine is located at the top right hand side of the periodic table and is therefore the most electronegative element (3.98 on the Pauling scale). This high electronegativity is due to the positive charge of the nucleus (+9) which strongly attracts the electrons of the outer shell. The two main consequences of this are that the fluorine atom has a high ionization potential and a low polarisability. As fluorine is much more electronegative than carbon (2.55 on the Pauling scale), the C-F bond presents a significant polar character which contributes to making the C-F bond the strongest bond that carbon can form with any other element. These atomic properties of fluorine account for the thermal and chemical stability of highly fluorinated compounds and their weak intermolecular interactions.

Due to its high electronegativity, fluorine is always a strong electron withdrawing group by the inductive effect. However, it can donate electrons by the mesomeric effect and the three lone pairs on fluorine have to be considered to explain the specific stability of carbocations and carbanions  $\alpha$  or  $\beta$  to a fluorine atom. While  $\alpha$  fluorine stabilises a carbocation by the mesomeric effect,  $\beta$  fluorine destabilises a carbocation by the inductive effect (Figure 1.1).



Figure 1.1: Fluorine stabilises  $\alpha$  carbocations and destabilises  $\beta$  carbocations.



While  $\alpha$  fluorine destabilises a carbanion due to  $n-\pi$  interaction,  $\beta$  fluorine stabilises a carbanion by the inductive effect and also by negative hyperconjugation. (Figure 1.2)



Figure 1.2: Fluorine destabilises  $\alpha$  carbanions, but stabilises  $\beta$  carbanions.

Fluorination induces considerable changes in the electronic distribution of a molecule, again a consequence of fluorine's high electronegativity. Additional to the strength of the C-F bond, fluorine also strengthens C-O, C-C and other C-F bonds when  $\alpha$  to fluorine. This for example accounts for the very good chemical and enzymatic stability of a  $\text{CF}_3$  group.

Changes in electronic distribution imply obvious changes in reactivity. For instance, when fluorine is  $\alpha$ ,  $\beta$  or even  $\gamma$  to the site of a nucleophilic substitution,  $\text{S}_{\text{N}}1$  and  $\text{S}_{\text{N}}2$  reactions are generally disfavoured, because of the inductive effect of fluorine which strengthens the bond to be broken. Thus, fluorine chemists quickly realise that many reaction conditions that work with non fluorinated compounds are not immediately transposable to fluorinated substrates because of the specific reactivity of fluorine, leading often to surprises or disappointments. One example among others is the hydrolysis of a tosylate  $\alpha$  to a  $\text{CF}_3$  group which occurs on the O-S bond and not as expected on the C-O bond<sup>4</sup> (Figure 1.3).

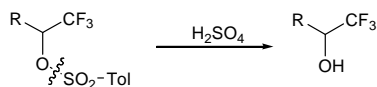


Figure 1.3: Fluorine effect on the hydrolysis of tosylate with CF<sub>3</sub> group in the α position

The presence of a fluorine atom in a molecule also affects the properties of nearby functional groups. Because of its electron withdrawing effect, fluorine causes carboxylic acids, amines and alcohols to be more acidic, an effect which can be dramatic and change the nature, the solubility and the reactivity of a molecule. Table 1.1 and Table 1.2 show the effect of fluorination (mono, di and tri-fluorination) on the pK<sub>a</sub> of acetic acid and on protonated ethylamine. This effect will be discussed in more detail later but it demonstrates here that the pK<sub>a</sub> of bioactive molecules can be modulated by the introduction of fluorine.

Compound	CH <sub>3</sub> CO <sub>2</sub> H	FCH <sub>2</sub> CO <sub>2</sub> H	F <sub>2</sub> CHCO <sub>2</sub> H	F <sub>3</sub> CCO <sub>2</sub> H
pK <sub>a</sub>	4.76	2.59	1.24	0.23

Table 1.1: pK<sub>a</sub> of acetic acid and its α-fluorinated analogues in water at 25 °C.<sup>5</sup>

Compound	CH <sub>3</sub> CH <sub>2</sub> NH <sub>2</sub>	FCH <sub>2</sub> CH <sub>2</sub> NH <sub>2</sub>	F <sub>2</sub> CHCH <sub>2</sub> NH <sub>2</sub>	F <sub>3</sub> CCH <sub>2</sub> NH <sub>2</sub>
pK <sub>a</sub>	10.7	8.97	7.52	5.7

Table 1.2: pK<sub>a</sub> of ethylamine and its β-fluorinated analogues in water.<sup>6</sup>

Fluorine can be used by medicinal chemists as a tool to tune the  $pK_a$  of amines or acids in order to improve for example the solubility, the oral absorption or the bioavailability of a drug. Numerous examples exist in the literature where the introduction of a single fluorine atom has been beneficial on the *in vivo* activity of a bioactive molecule because the  $pK_a$  has changed.<sup>7-9</sup> Modulation of  $pK_a$  can also affect the binding of a drug to its target macromolecule, in a positive or negative way.

A key property of fluorine in medicinal chemistry is its small size. With a van der Waals radius of 1.47 Å, fluorine is the smallest substituent (other than hydrogen's isotopes) that can be used to replace a hydrogen atom (van der Waals radius 1.20 Å). Therefore, the substitution of a hydrogen atom for fluorine doesn't induce much steric or geometrical perturbation and it is well established that enzymes will generally bind the fluorinated analogue of a natural substrate. Thus, fluorine is a good hydrogen mimic and has been widely used in medicinal chemistry in this respect. Counter examples have been published recently where the size of a fluorine atom does induce geometrical changes in sterically hindered systems. Substitution of a hydrogen atom by a fluorine atom prevents for example a  $\beta$ -heptapeptide from folding,<sup>10</sup> but in general such steric effects are small.

Fluorine is actually more isosteric with an oxygen atom, whose van der Waals radius is 1.52 Å.<sup>11</sup> The van der Waals volume ( $V_w$ ) of a hydroxyl group has been calculated to be around 8.04 cm<sup>3</sup>.mol<sup>-1</sup>, but 1.05 cm<sup>3</sup>.mol<sup>-1</sup> is subtracted from this value for each hydrogen bond formed (Table 1.3). The C-F bond for secondary or tertiary fluorine has a  $V_w$  of 6.2 cm<sup>3</sup>.mol<sup>-1</sup> and in the case of aromatic fluorine, this value is 5.8 cm<sup>3</sup>.mol<sup>-1</sup>.<sup>11</sup> Moreover, the lengths of typical C-F and C-O bonds (1.39 vs 1.43 Å) and their comparable electronegativities (oxygen is the next most electronegative element after fluorine) suggest

that fluorine can be regarded also as an isosteric and isopolar replacement for the hydroxyl group.

Atom or group	$V_w$ (cm <sup>3</sup> mol <sup>-1</sup> )
C(primary)-F	5.72
C(secondary)-F	6.20
OH (without hydrogen bond)	8.04
>CF <sub>2</sub>	15.3
>C=O	11.70
CH <sub>3</sub>	13.67
CF <sub>3</sub>	21.3

Table 1.3: van der Waals molar volume  $V_w$  (cm<sup>3</sup> mol<sup>-1</sup>) for various non-fluorinated and fluorinated functional groups.<sup>11, 12</sup>

The major difference between fluorine and the hydroxyl group is the ability of the latter to form strong hydrogen bonds which are indispensable features in biological processes, such as molecular recognition, binding and folding. In contrast, and despite its three lone pairs, fluorine is a weak hydrogen bond acceptor. This is mainly due to its low polarisability: the three lone pairs of electrons are tightly held by the nucleus.

It is clear that fluorine cannot directly replace the role of the acidic hydrogen in a hydrogen bond, but it can indirectly act as a hydrogen bond donor by enhancing the acidity of a geminal proton. This property has been shown for CF<sub>2</sub>H groups where the acidic proton can interact with O=C groups.<sup>13</sup> Curiously, this property has not been discussed much in the literature. It is the ability of fluorine to act as a hydrogen bond acceptor which has been the subject of debate over the last decade.

A hydrogen bond is defined by a C-F...H-X contact shorter than 2.35 Å where X is an electronegative atom such as N or O. Dunitz writes that “organic fluorine hardly ever

accepts hydrogen bonds, that is, it does so only in the absence of a better acceptor”.<sup>14</sup> O’Hagan *et al*<sup>15</sup> have calculated that the strength of a C(sp<sup>3</sup>)-F...H-O bond is 2.38 kcal.mol<sup>-1</sup>, which represents less than half the strength of a C-O...H-O bond (5-10 kcal.mol<sup>-1</sup>). The conclusion is that fluorine is only a weak hydrogen bond acceptor. Furthermore, analysis of the Cambridge Structural Database reveals that short contacts consistent with a true F...H bond are extremely rare.<sup>16</sup> According to Diederich and Müller, they should rather be described as dipolar interactions.<sup>17</sup>

However, it is now recognised that although those interactions are much weaker than C=O...H-X (X= N or O), they do influence molecular packing in crystals.<sup>18</sup> In addition, numerous intermolecular O-H...F-C and N-H...F-C hydrogen bridges have been reported to stabilise the binding of fluorinated compounds to enzyme active sites.<sup>19, 20</sup>

This leads us to a newly recognised interaction described as a C-F orthogonal dipole-dipole interaction<sup>21</sup> between intrinsically polar C-F and C=O bonds. It has been discovered by examination of the Cambridge Structural Database that the C-F bond often points approximately perpendicular to the partially positively charged electrophilic carbon of a C=O or a C≡N bond as shown in Figure 1.4.



Figure 1.4: Schematic representation of C-F interaction with carboxyl and nitrile group.

These interactions have been found in small molecules and in protein-ligand complexes.<sup>17</sup> Initial measurements of these stabilising interactions on a model system gave a relatively low value of about 0.19 to 0.36 kcal.mol<sup>-1</sup> in nonpolar solvents such as chloroform or benzene.<sup>21</sup> By comparison, the average stabilising effect of dipole-dipole

orthogonal  $\text{C}=\text{O}\cdots\text{C}=\text{O}$  interactions have been estimated to be about  $1.9 \text{ kcal.mol}^{-1}$ .<sup>22</sup>  $\text{H}\cdots\text{F}$  bonding in crystal structures have been recently scrutinised in order to discover new motifs which are prone to form stabilising interactions with fluorine and which can render a specific binding site fluorophilic.<sup>17</sup>

There is no doubt that further discussions will arise in the near future on the ability of fluorine to form noncovalent interactions with polar bonds as this is of great interest in medicinal chemistry for understanding the specific binding abilities of fluorinated substrates to macromolecules.

The C-F bond has proved to be a good substitute for C-H or C-OH bonds. In some instances, other fluorinated motifs have been used or suggested to mimic other functional groups of natural substrates. In particular, fluoro olefins are considered good bioisosteres of peptide bonds. When incorporated into a peptide, the geometry, the charge distribution and the dipolar moment of the fluoro olefin are all close enough to those of the peptide bond to be recognised by enzymes. The *trans* double bond maps sterically the length and the angle of the peptide bond and the fluorine introduces the polarity in the olefin unit in a direction similar to the effect of the oxygen in the peptide unit<sup>23</sup> (Figure 1.5). This strategy has been used with success to make peptidase inhibitors.<sup>24</sup> Calculations on dipole moments have shown that trifluoromethylalkene isosteres (**8**) are even better electrostatic mimic of the amide bond.<sup>25</sup>

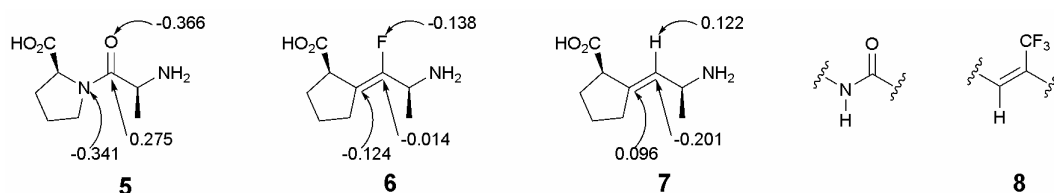
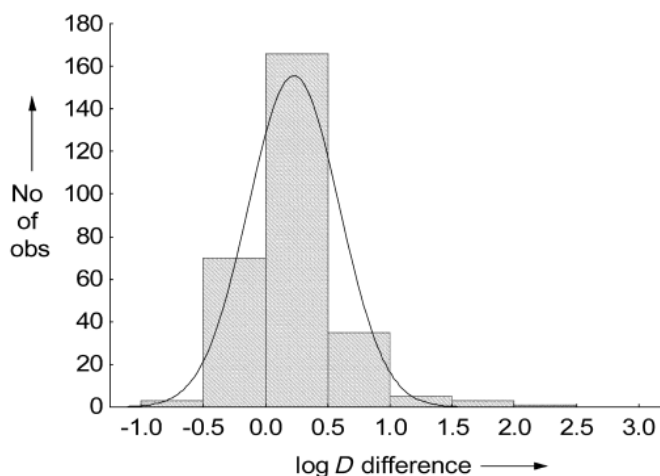


Figure 1.5: Comparison of the charge distribution in dipeptide and dipeptide analogues.<sup>26</sup>

Lipophilicity is another physical property which can be greatly affected by the introduction of one or more fluorine atoms into a molecule. There is no simple relationship between fluorination and lipophilicity, however general rules have been established. Fluorination always increases lipophilicity in the case of aromatic compounds. In the case of aliphatic molecules like alkanes, fluorination usually decreases the lipophilicity but increases the hydrophobicity, such that highly fluorinated or perfluoro compounds are not soluble in organic solvents nor in water but rather form a third phase, a fluorous phase. It is important here to distinguish between lipophilicity and hydrophobicity which reflect the same idea in the case of non fluorinated compounds but which are different with molecules containing several fluorine atoms. This is due to the definition of lipophilicity as the logarithmic coefficient of a compound's distribution between octanol and water at a given pH, usually 7.4. As the solubility of fluorinated compounds usually decreases more in water than in octanol, it seems sometimes that fluorination increases lipophilicity but it just reflects the lack of affinity for both solvents.<sup>26</sup> In any case, it is very difficult to predict the effect of fluorination on the lipophilicity of aliphatic compounds.

This is illustrated by a study conducted by H.J. Böhm on a large number of pairs of molecules, in which one hydrogen atom was substituted by one fluorine atom. Log  $D$  was measured for each compound and the difference in log  $D$  for each pair was calculated. The results presented in Graph **1.2** indicate that fluorination has indeed various effects on lipophilicity. Although this study has been conducted on a structurally limited database of fluorinated compounds, it shows that on average, substitution of one hydrogen atom by a fluorine atom increases lipophilicity slightly, by roughly 0.25 log unit.<sup>8</sup>



Graph 1.2: Histogram of change in log  $D$  observed upon substitution of a hydrogen atom by a fluorine atom.<sup>8</sup>

Lipophilicity is a key parameter in medicinal chemistry. Indeed, a good drug must be lipophilic enough to be able to cross numerous biological membranes, typically lipid bilayer membranes on the way to its target. Then on its target, usually a protein, it partially desolvates to bind on the specific binding site of the macromolecule. Lipophilic interactions are of particular importance for obtaining a good binding affinity and this explains why drugs often possess lipophilic groups such as aromatics or  $\text{CF}_3$ . However, a drug must not be too lipophilic because this reduces its water solubility and its bioavailability. Therefore a balance is required between good lipophilicity and sufficient overall polarity. This can be brought about by fluorine, which can simultaneously increase lipophilicity and dipolar interactions, an interesting intrinsic property of fluorine which is called “the polar hydrophobicity of fluorinated compounds”.<sup>27</sup>



### 1.2.2 Fluorine in medicinal chemistry

We have seen that the introduction of fluorine can change the electron distribution and therefore the biological properties of a molecule. Also, fluorine usually has beneficial effects on lipophilicity and on the  $pK_a$  of drugs, two crucial factors for their transport and their bioavailability. A third important factor for the biological activity of a drug is its metabolism and here too fluorine can play an important role.

Before reaching its target, the drug needs to resist acidic or basic media and numerous adventitious enzymes. For example, rapid oxidative metabolism of lipophilic compounds by liver enzymes, particularly the  $P_{450}$  cytochromes, often reduces the half-life of the drug.  $P_{450}$  cytochromes are oxidative enzymes containing a heme group at the active site and they transform a hydrophobic substrate into a more hydrophilic one by introduction of a hydroxyl group.  $P_{450}$  cytochromes require for reaction one molecule of oxygen, two protons and two electrons. Most aromatic oxidations involve  $P_{450}$  cytochromes with radical-cation intermediates and it seems that the electronic deficiency in the complex  $C\cdots H\cdots O-Fe^{IV}$  is disfavoured by the electron withdrawing effect of a fluorine atom or a fluoroalkyl group. As a result, substituting a C-H by a C-F bond in a molecule can block or reduce its oxidative metabolism by  $P_{450}$  enzymes. This accounts for the plethora of drugs bearing a fluorinated substituent on an aromatic ring, especially in the *para* position. This is the most widely used method to prevent oxidative metabolism of aromatic rings. Figure 1.6 illustrates this idea.<sup>28</sup>

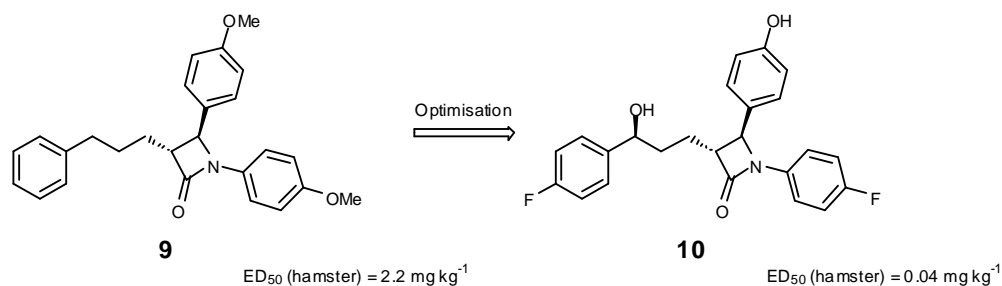


Figure 1.6: Development of Ezetimibe (**10**) as a potent inhibitor of cholesterol absorption.<sup>28</sup>

The ability of fluorine to block oxidative metabolism can also be a problem in some cases when it makes the drug metabolically too stable. Thus, fluorinated compound (**11**) had a half-life of 220 h which was not acceptable for a drug, but substitution of the fluorine by a metabolically labile methyl group shortened the half-life of compound (**12**) to 3.5 h. Celecoxib<sup>29</sup> (**12**) is a cyclooxygenase 2 (COX 2) inhibitor (Figure 1.7).

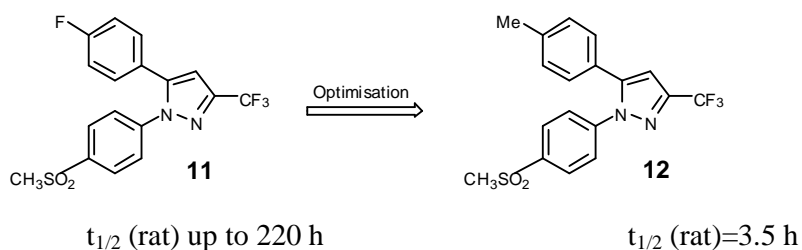
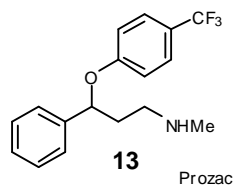


Figure 1.7: Development of Celecoxib (**12**): effect of methyl substitution for fluorine on the half-life of (**11**) and (**12**).<sup>29</sup>

Also, significant levels of non-metabolised fluorinated drugs can be found in wastewater, representing a hazard for the environment and health. ‘The Scotsman’ newspaper reported on 9<sup>th</sup> August 2004 that British drinking water contains fluoxetine (Prozac) (**13**), one of the most prescribed anti-depressant drugs in the world. Fluoxetine is present in wastewater because of the large quantities prescribed but also because it is only partially metabolised in the body before being excreted.



Fluorine is often used to slow down the oxidative metabolism of a drug but in some cases, fluorine can also accelerate such metabolism.<sup>30</sup> Therefore, the introduction of fluorine can not be regarded as a general method to reduce metabolism and it remains a trial and error process in medicinal chemistry development.

Due to the specific electronic effects mentioned previously, fluorine can be used in many ways to design analogues of natural compounds or of natural intermediates, for the purpose of inhibiting enzymes or disclosing enzymatic mechanisms. An example among others is the stabilisation of hemiketals by the inductive effect of fluorine (Figure 1.8), which has been applied to design compounds that mimic the tetrahedral intermediate during the enzymatic cleavage of esters or peptides bonds.

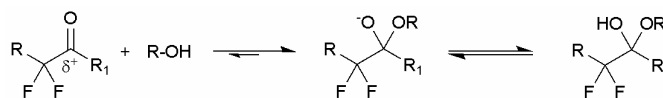
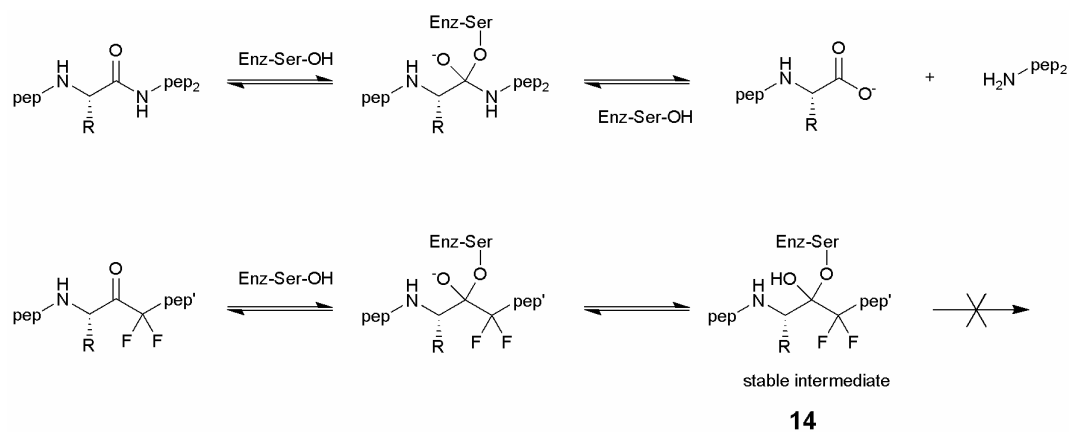


Figure 1.8: Stabilisation of hemiketals by fluorine.

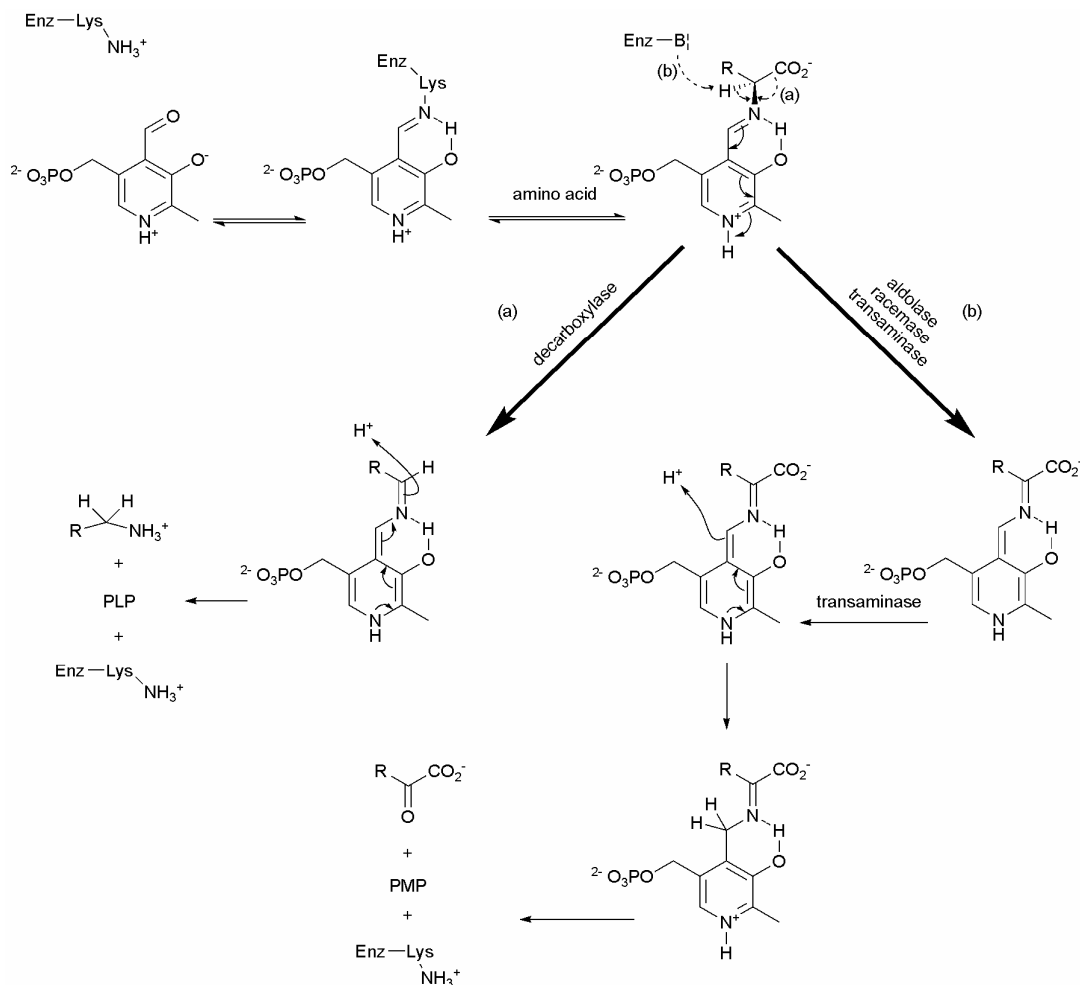
Scheme 1.1 shows the cleavage of a peptide bond by a serine protease and its inhibition by an  $\alpha$ -difluoro-ketomethylene peptide analogue. The application of this strategy is extremely broad. A large number of difluoro- and enantiopure monofluoro-ketomethylene peptides isosteres has been synthesised for this purpose.<sup>31-33</sup> Many of these have been used for the study and the inhibition of different kind of proteases.<sup>26</sup> This inhibition of proteases comes from the propensity of difluoro ketones to form hemiketals.

Consequently, the intermediate (**14**) is stable enough to remain covalently bound in the active site of the enzyme as a more or less irreversible inhibitor which can still be displaced by the natural substrate.



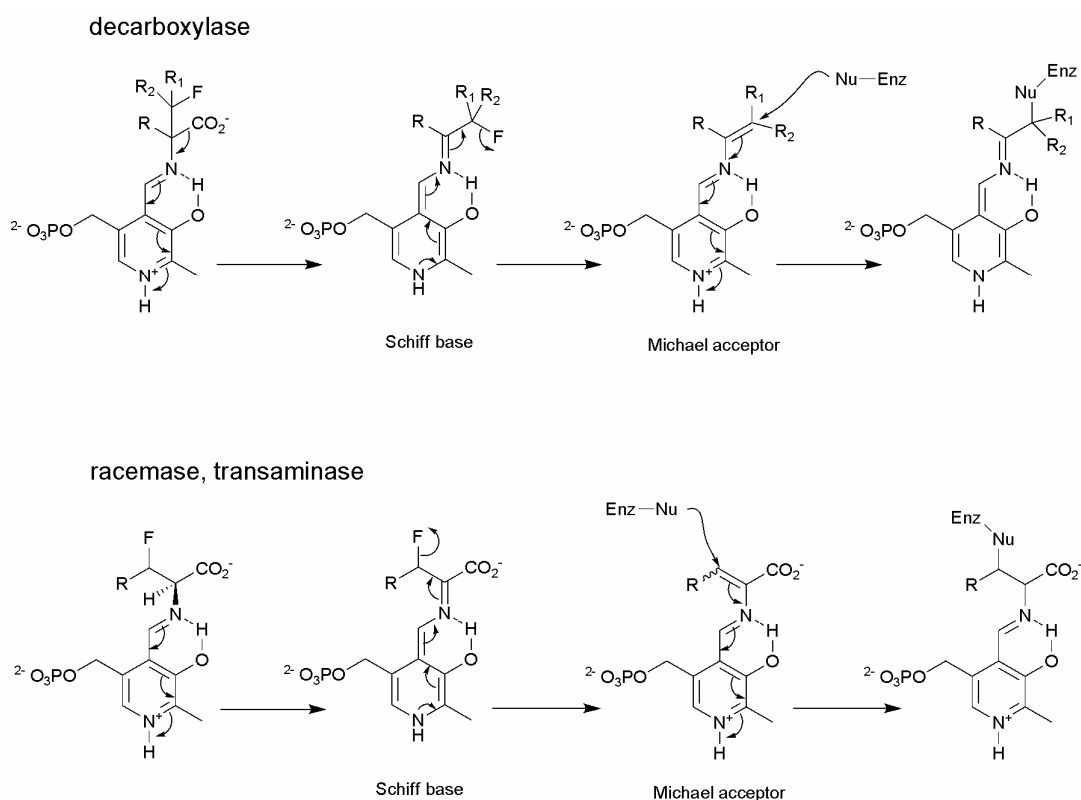
Scheme **1.1**: Inhibition of serine protease by a difluoromethylene peptide isostere.

Fluorine can play many roles in the rational design of fluorinated substrate inhibitors of enzymes. One of particular interest in this context, is the concept of suicide substrates for the inhibition of pyridoxal-5'-phosphate (PLP) dependent enzymes. PLP dependent enzymes form a large family which includes amino acid racemases, decarboxylases and amino transferases. Their biological role is crucial in the control of amino acid and neuroamine metabolism. Scheme 1.2 outlines the general transformation of amino acids into amines or  $\alpha$ -keto acids by PLP dependent enzymes.



Scheme 1.2: Mechanisms of PLP dependent enzymes.

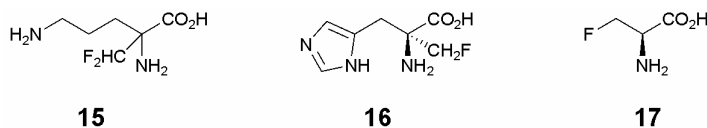
A suicide substrate is usually a compound which by the action of an enzyme can generate a Michael type acceptor species. This species then reacts quickly and irreversibly with a nucleophile located in the active site of the enzyme. In the case of PLP dependent enzymes, suicide substrate inhibitors typically possess at least one fluorine atom  $\beta$  to the amino group linked to the PLP co-factor. This illustrates the biological importance of  $\beta$ -fluoro amines and  $\beta$ -fluoro amino acids. The fluorine can be placed either on the side chain of the amino acid or on a  $\text{CFX}_2$  group in the  $\alpha$ -position, depending on the enzyme (Scheme 1.3). The formation of the Schiff base is facilitated by the electron withdrawing effect of the fluorine which renders the  $\alpha$  proton more acidic. Loss of fluoride generates the active Michael type acceptor which reacts readily with a nucleophilic residue on the enzyme.



Scheme 1.3: Inhibition of PLP dependent enzymes by  $\beta$ -fluoro amino acids.

Scheme 1.3 presents the general mode of action of fluorinated suicide substrates on PLP dependent enzymes. In some cases however, the real mechanism is more complex. The inhibition of PLP dependent enzymes by fluorinated amino acids will be discussed later on the particular case of the GABA transaminase.

Given the physiological importance of those transformations, significant efforts have been made towards the design of fluorinated inhibitors. This has led to some successes in the 1980s. For example,  $\alpha$ -difluoromethylornithine (**15**) was found to be a good irreversible inhibitor of ornithine decarboxylase<sup>34</sup> and it is still used for the treatment of trypanosomiasis also called sleeping sickness. (*S*)-(+)- $\alpha$ -(Fluoromethyl)histidine (**16**) and  $\beta$ -fluoroalanine (**17**) were found to be irreversible inhibitors of histidine decarboxylase<sup>35</sup> and alanine racemase<sup>36, 37</sup> respectively.



The inhibition of PLP enzymes stimulated an early interest in fluorinated amino acids. Recently, they have gained a renewed interest, and this is reflected by an increase in publications in this area. Most of current research on fluorinated amino acids is now focused on their incorporation into enzymes, fluorinated polypeptides and fluorinated  $\beta$ -peptides (peptides made of  $\alpha$ -fluoro- $\beta$ -amino acids). One of the reasons for this interest is that fluorinated amino acids have a significant influence on the conformation, stability and folding of such compounds.

One fluorinated amino acid that has attracted recent interest is 4-fluoroproline. Raines *et al.* have discovered that its substitution for proline or 4-hydroxyproline in the collagen structure produces a thermally more stable helical peptide (Figure 1.9).<sup>38</sup>

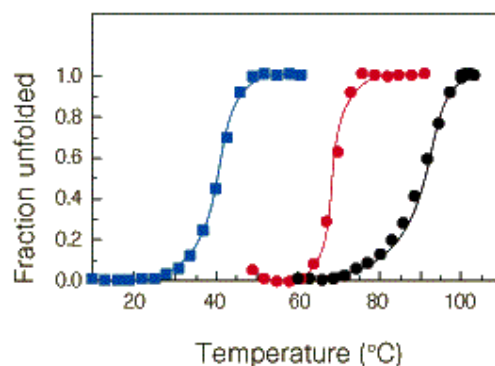


Figure 1.9: Thermal denaturation of collagen-related triple helices.<sup>38</sup>  
 (Proline-Proline-Glycine)<sub>10</sub> (blue):  $T_m(^{\circ}\text{C}) = 41 \pm 1$   
 (Proline-(4*R*)-Hydroxyproline-Glycine)<sub>10</sub> (red):  $T_m(^{\circ}\text{C}) = 69 \pm 1$   
 (Proline-(4*R*)-Fluoroproline-Glycine)<sub>10</sub> (black):  $T_m(^{\circ}\text{C}) = 91 \pm 1$ .  
 $T_m(^{\circ}\text{C})$  is the temperature at the midpoint of the thermal transition curve.

Collagen is the most abundant protein in animals, representing 75% of the weight of human skin for example. In connective tissue, collagen consists of three individual peptide strands folded into a right-handed triple helix. Each strand comprises about 300 tripeptide repeats of the sequence (X-Y-Gly), where proline (Pro) and (4*R*)-hydroxyproline (Hyp) are most prevalent in the X- and Y-positions respectively. The substitution of (4*R*)-hydroxyproline for (4*R*)-fluoroproline confers the greater thermal stability to the decatripeptide, with  $T_m$  rising from 69 °C to 91°C. This striking increase results from stereoelectronic effects.

Molecular modeling of the triple helical (Proline-Proline-Glycine)<sub>10</sub> strands has shown that the pyrrolidine ring of proline adopts preferably a  $C^{\gamma}$ -*endo* ring puckered conformation in the X-position whereas it adopts preferably a  $C^{\gamma}$ -*exo* ring puckered



conformation in the Y-position. Both ring conformations are populated at room temperature in the case of proline, increasing the entropy of the system. But in the case of (4*R*)-fluoroproline, the C $\gamma$ -*exo* ring puckered conformation is greatly favoured. The predisposition of (4*R*)-fluoroproline towards this ring conformation leads in the Y-position to stabilisation of the triple helix.<sup>39</sup> This specific fluorine effect comes from the propensity of the C-F bond to align *gauche* to the C-N bond (Figure 1.10), which will be discussed in section 1.3.

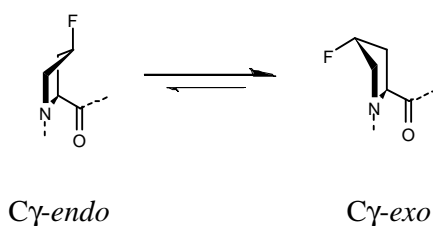


Figure 1.10: Stabilisation of the C $\gamma$ -*exo* ring conformation in the case of (4*R*)-fluoroproline.

The discovery of thermally stable collagen-related peptides is of great interest and opens the way to the production of new biomaterials. To date, the tripeptide unit (Pro-Flp-Gly) offers the greatest thermal stability.<sup>40</sup>

Other recent studies have illustrated the pivotal role that fluorine can have in protein engineering and in influencing peptide conformation. Recently, the St Andrews lab has demonstrated that the incorporation of *threo*- and *erythro* difluorosuccinic acid into small peptides has a strong influence on the peptide conformation.<sup>41, 42</sup> Also,  $\beta$ -peptides have been the subject of many conformational studies since it was shown that they adopt secondary structures similar to their  $\alpha$ -peptidic analogues. As they are metabolically more stable than  $\alpha$ -peptides, this class of compounds has potential as drugs or non-natural polymers. Interesting discoveries have been made in this field, such as the observation that a single stereogenic C-F inversion forces a  $\beta$ -heptapeptide to adopt two totally different

secondary structures.<sup>10</sup> However, despite interesting and often quite dramatic observations, the field of fluorinated  $\beta$ -amino acids and  $\beta$ -polypeptides remains largely unexplored.

Fluorinated amino acids have also been incorporated into proteins with the major advantage that the chemical environment of the fluorinated residue and therefore the folding of the protein can be monitored by  $^{19}\text{F}$  NMR, a technique which is extremely sensitive to the spatial environment.  $^{19}\text{F}$  NMR analysis can then be used to investigate conformational changes in a protein which occur for example when a substrate binds. Moreover, no background fluorine signal is observed from natural proteins. Also, the introduction of fluorine into proteins can induce increased thermal stability<sup>43</sup> or a change in lipophilicity, but the general consequences of the presence of fluorinated amino acids in proteins remain not very well understood. Nevertheless, the early observations obtained from incorporating fluorinated amino acids into peptides and proteins have raised their level of interest and have stimulated the development of new methods of syntheses for fluorinated amino acids.

## 1.3 The fluorine *gauche* effect

### 1.3.1 Origin of the *gauche* effect

Most often, the effects of fluorine on the conformation of large molecules such as peptides cannot be explained by its size, but rather by the stereoelectronic effects induced by the presence of the fluorine atom. Although these effects can be dramatic, they are often omitted in discussions of fluorine in medicinal or organic chemistry, perhaps because such stereoelectronic effects have largely been of academic interest only. People have recently understood how they can be applied advantageously in the design of fluorinated molecules.

The most widely discussed stereoelectronic effect associated with fluorine is undoubtedly the so-called *gauche* effect which recognised that the lowest energy conformation for two vicinal C-F bonds has the two fluorine atoms *gauche* to each other rather than *anti* as one might expect intuitively for steric reasons and dipole repulsion between the electronegative atoms (Figure 1.11).

The simplest and most studied system where the fluorine *gauche* effect is observed is 1,2-difluoroethane (**18**). In 1960, Klaboe<sup>44</sup> showed by analysis of infrared absorption spectra that the *gauche* conformer is more stable than the *anti* conformer. Since this time, many more studies have been carried on the conformational behaviour of this system and NMR data,<sup>45</sup> *ab initio* calculations,<sup>46-48</sup> and X-ray diffraction<sup>49</sup> have all concluded that the *gauche* conformer is more stable than the *anti* conformer by  $\sim 1$  kcal.mol<sup>-1</sup>, an unusual observation which is not seen with 1,2-dichloroethane or 1,2-dibromoethane.

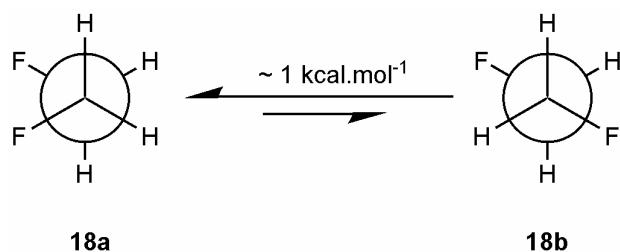


Figure 1.11: Newman projections of the rotamers of 1,2-difluoroethane. The *gauche* conformer (**18a**) is stabilised by  $\sim 1 \text{ kcal.mol}^{-1}$  over the *anti* conformer (**18b**) in the gas phase.<sup>50</sup>

This effect is not limited to 1,2-difluoroethane. Similar observations have been reported on *erythro*- and *threo*-2,3-difluorobutane (**19**) and (**20**): the *gauche* conformers (**19a**) and (**19c**) are more stable in organic solvents as well as in the gas phase. The energy required to bring the two methyl groups into close proximity is overcome by favourable fluorine *gauche* stabilisation.<sup>51</sup> In the case of *threo*-2,3-difluorobutane, the fluorine *gauche* effect and steric interactions reinforce the conformation (**20b**) (Figure 1.12).

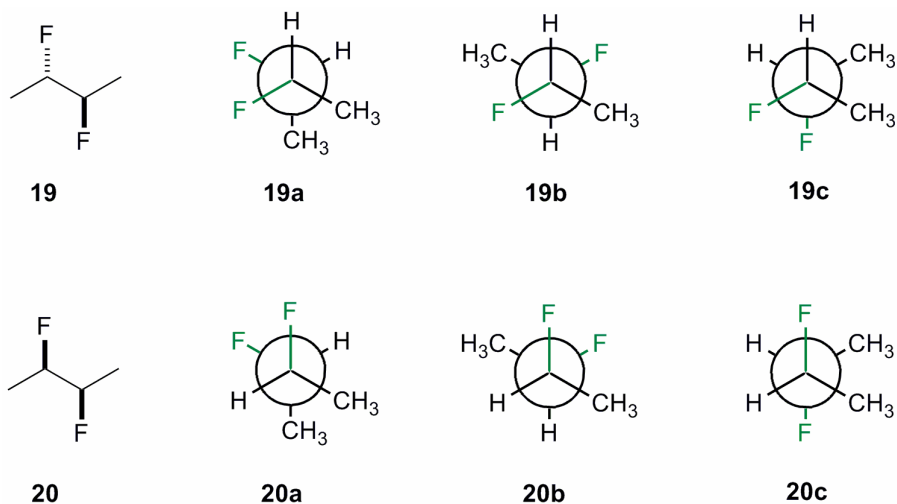


Figure 1.12: Newman projections of the rotamers of *erythro*- and *threo*-2,3-difluorobutane (**19**) and (**20**).

Different explanations have been proposed to rationalise the “*gauche* effect”. The most widely accepted theory comes from the general idea that the preferred conformation places the best  $\sigma$ -donor bond or lone pair, antiperiplanar to the best  $\sigma$ -acceptor bond. This is to conform with the hyperconjugation of the electron-rich bonding  $\sigma$  C-H orbital to the electron-deficient antibonding  $\sigma^*$  C-F orbital, which requires the C-H bond to align antiperiplanar to the C-F bond (Figure 1.13). C-H bonds are generally better  $\sigma$ -donor bonds than C-C bonds.<sup>52</sup>

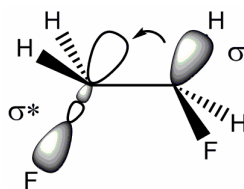


Figure 1.13: Hyperconjugation  $\sigma_{\text{C-H}} \rightarrow \sigma^*_{\text{C-F}}$ .

A so-called “bent-bond” theory has also been advanced by Wiberg<sup>47</sup> to account for the lower energy of the *gauche* conformer. X-ray analyses and *ab initio* calculations have shown that the bond which is defined as the path of maximum charge density between two atoms does not always follow a straight line as it is conventionally represented.<sup>53</sup> In the case of 1,2-difluoroethane, Wiberg explained<sup>54</sup> that the energy difference between the *gauche* and *anti* conformers does not come from stabilisation of the *gauche* but from destabilisation of the *anti* conformer. The strong electronegativity of the fluorine atom induces a distortion of the C-C orbitals to give a C-C bond bent towards the fluorine (Figure 1.14). In the *anti* conformer, the C-C orbitals are bent in opposite direction, leading to decreased overlap and poorer bonding, whereas in the *gauche* conformer, orbitals are bent roughly in the same direction. The concept of bent orbitals has been widely proposed to explain the stability of small rings such as cyclopropanes.

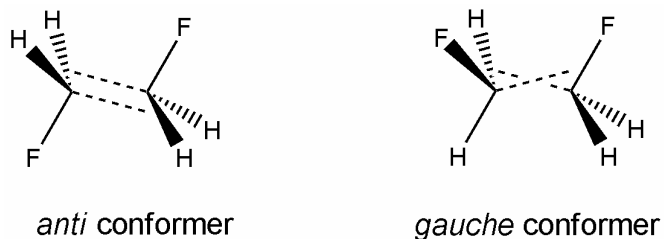


Figure 1.14: Bent bond analysis: The *anti* conformer is destabilised due to a poor  $sp^3$  overlap. The *gauche* conformer overlaps in a better bond.

Likewise, the C=C bond in 1,2-difluoroethene is shown by calculated charge density maps to be distorted in the case of the *trans*-1,2-difluoroethene and bent in the case of the *cis*-1,2-difluoroethene, which accounts for the better stability of the *cis* over the *trans* isomer (Figure 1.15).<sup>54</sup>

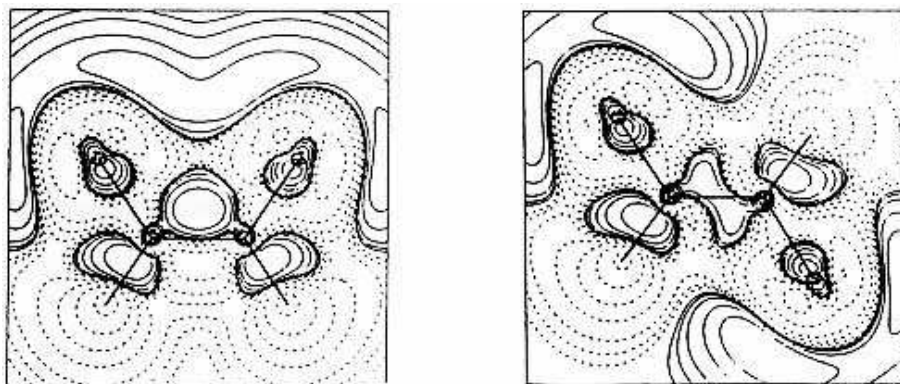


Figure 1.15: Wiberg electron density maps of *cis*-1,2-difluoroethene (left) and *trans*-1,2-difluoroethene (right) calculated using 6-31+G\* basis set.<sup>54</sup>

However a recent study has showed that energy difference “due to bond bending is too small to account for a significant portion of the  $\sim 1 \text{ kcal.mol}^{-1}$  preferential stabilisation of the *gauche* conformer”.<sup>48</sup> It has also been pointed that not only antiperiplanar  $\sigma_{\text{C-H}} \rightarrow \sigma^*_{\text{C-F}}$  should be considered in the hyperconjugation theory (see figure 1.13), but also *cis*  $\sigma_{\text{C-H}} \rightarrow \sigma^*_{\text{C-F}}$  as it appears that hyperconjugation from *cis*  $\sigma_{\text{C-H}}$  accounts for around 25 % of the antiperiplanar  $\sigma_{\text{C-H}}$  hyperconjugation stabilisation (Figure 1.16).<sup>48</sup> This is an important statement and it could explain why the F-C-C-F dihedral angle in X-ray structures<sup>49</sup> of 1,2-difluoroethane is  $68^\circ$  and not  $60^\circ$  as it should be in theory.

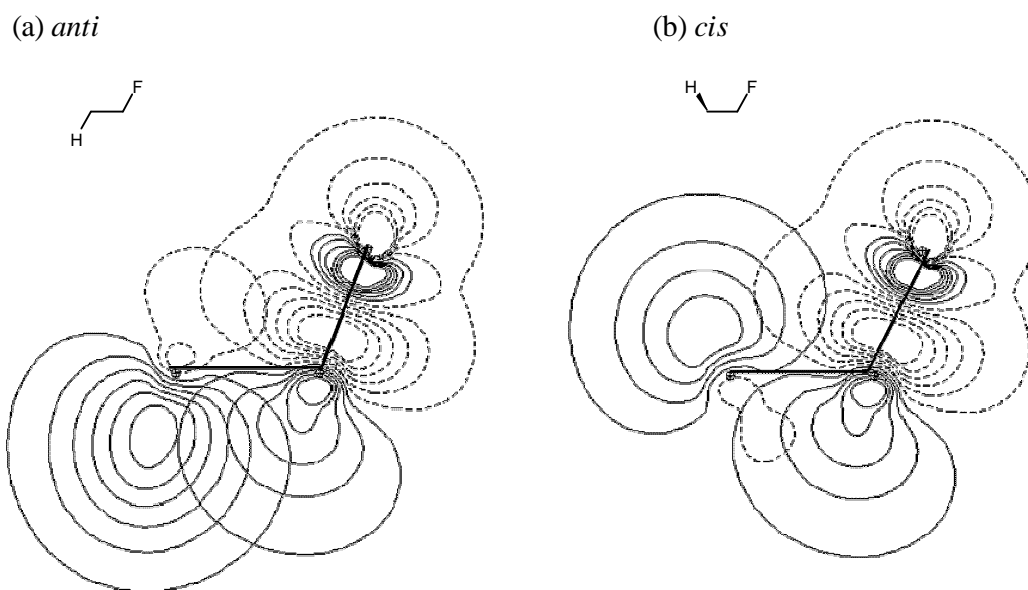


Figure 1.16: *Anti*  $\sigma_{\text{C-H}} \rightarrow \sigma^*_{\text{C-F}}$  and *cis*  $\sigma_{\text{C-H}} \rightarrow \sigma^*_{\text{C-F}}$  orbital overlaps, showing the greater overlap of the main lobe of the *anti* orbital C-H bond with the back lobe of the C-F\* antibond. The orbital contours are shown in the C-C-F plane.<sup>48</sup>

The *gauche* preference is not only observed in vicinal C-F bonds systems. In fact, it is general for any electronegative substituents such as fluorine, oxygen or nitrogen. For example, one C-F bond can be substituted by a C-OH bond, since the electronegativity of the hydroxyl group is only slightly less than that of the fluorine atom. Thus, *gauche* preferences have also been described in  $\beta$ -fluoroalcohols.<sup>55</sup> 2-Fluoroethanol is the simplest  $\beta$ -fluoroalcohol and has been used as a model to study the conformational behaviour of vicinal C-F and C-O bonds. It appears that the molecule adopts clearly a *gauche* conformation (**21a**), stabilised by 2.0 kcal.mol<sup>-1</sup> over the *anti* conformation (**21b**). However, this stabilisation does not originate only from through-bond stereoelectronic effects but rather from an intramolecular O-H...F bond. Indeed, the calculated *gauche* structure (**21c**) which lacks intramolecular O-H...F bond is lower in energy than its *anti* structure (**21d**), but only by 0.1 kcal.mol<sup>-1</sup>. In conclusion, stereoelectronic effects in  $\beta$ -fluoroalcohols contribute only to a very small part in the stabilisation of the *gauche* conformation (Figure 1.17).<sup>55, 56</sup>

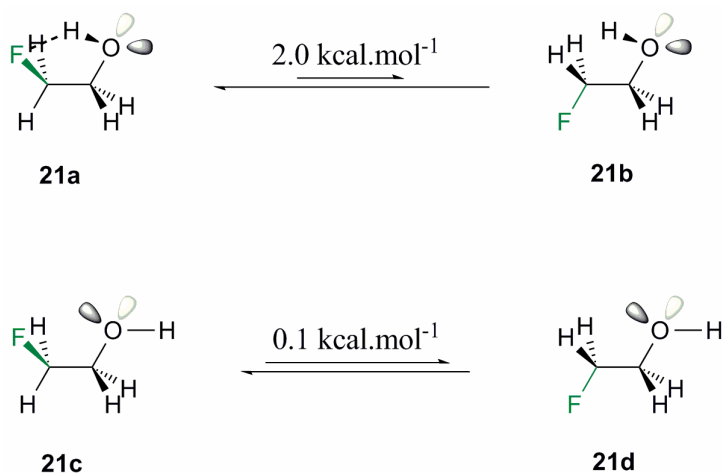


Figure 1.17: Calculated minimum conformations of 2-fluoroethanol: the *gauche* conformer (**21a**) is stabilised by ~2 kcal.mol<sup>-1</sup> due to intramolecular O-H...F bonding.



The *gauche* preference in 2-fluoroethanol arises almost exclusively from intramolecular O-H...F bonding. Therefore it was interesting to investigate the situation when the hydroxyl group becomes protonated. Two factors should reinforce the *gauche* preference: firstly, the positive charge on the oxygen increases the polarisation of the C-O bond which should result in a stronger stereoelectronic effect and a lower  $\sigma^*$  energy. Secondly, the protonated oxygen is a better hydrogen bond donor.

Calculations have shown indeed that the most stable conformation of protonated 2-fluoroethanol (**22a**) is 7.2 kcal.mol<sup>-1</sup> more stable than its *anti* structure (**22b**) and includes an intramolecular O-H...F bond. The calculated *gauche* structure (**22c**) which lacks intramolecular O-H...F bonding is still 4.4 kcal.mol<sup>-1</sup> lower in energy than its corresponding *anti* structure (**22d**) (Figure 1.18). This value represents more than four times the stereoelectronic *gauche* stabilisation in 1,2-difluoroethane and suggests that intramolecular hydrogen bonding accounts for around 2.6 kcal.mol<sup>-1</sup> in the stabilisation, which is close to the value found for the intramolecular O-H...F bonding in the non-protonated species (~2 kcal.mol<sup>-1</sup>).

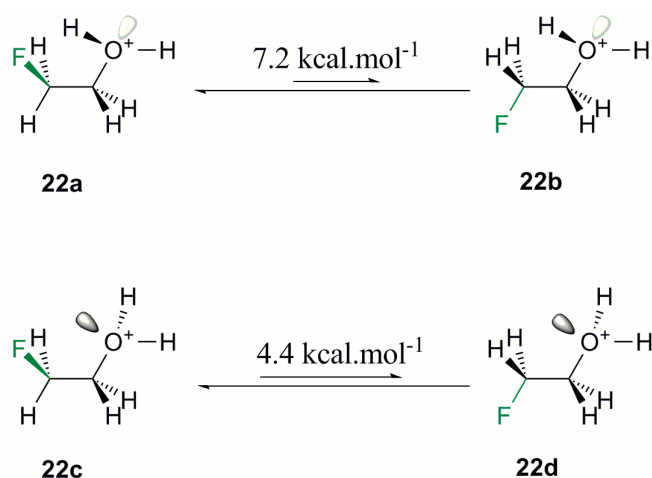


Figure 1.18: Calculated conformations of protonated 2-fluoroethanol: the *gauche* conformer (**22a**) is stabilised by 7.2 kcal.mol<sup>-1</sup> over the *anti* conformer (**22b**) due most probably to stereoelectronic effects and intramolecular O-H...F bonding.

In a similar manner to  $\beta$ -fluoroalcohols,  $\beta$ -fluoroamines exhibit a small *gauche* preference, although this effect is less pronounced as nitrogen is less electronegative. In the case of 2-fluoroethylamine, the *gauche* conformers are stabilised over the *anti* conformer by around 1 kcal.mol<sup>-1</sup>. It seems that this stabilisation, similar to that found in 2-fluoroethanol, arises from intramolecular H...F bonding.<sup>56</sup>

The situation changes dramatically when the nitrogen becomes protonated and a large *gauche* preference is then observed. The *gauche* conformer (**23a**) of 2-fluoroethylammonium is stabilised by 5.8 kcal.mol<sup>-1</sup> over the *anti* conformer (**23b**) as evaluated by density functional theory (DFT) calculations (Figure 1.19).<sup>56</sup> This observation is potentially of some utility as amines are protonated at physiological pH and such an effect will be observed *in vivo* for  $\beta$ -fluoroamines. The large value of 5.8 kcal.mol<sup>-1</sup> indicates that the fluorinated amine is fully populated in the *gauche* conformation in solution.

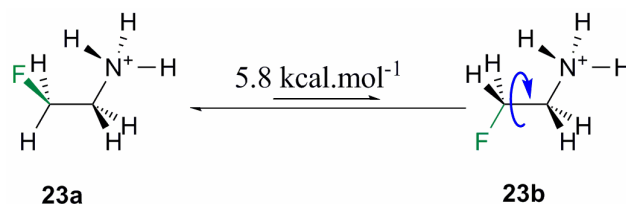


Figure 1.19: The *gauche* conformation of 2-fluoroethylammonium is stabilised by 5.8 kcal.mol<sup>-1</sup> over the *anti* conformation.

Other systems such as 3-fluoropiperidinium (**24**), *N*-methyl-3-fluoropiperidinium (**25**) and *N,N*-dimethyl-3-fluoropiperidinium (**26**) salts have been studied by NMR, *ab initio* calculations and X-ray crystallography. Consistent with the observations described above, a strong preference for *gauche* alignments of the C-F and C-N<sup>+</sup> bonds was observed when the nitrogen is positively charged (Figure 1.20).<sup>57</sup>

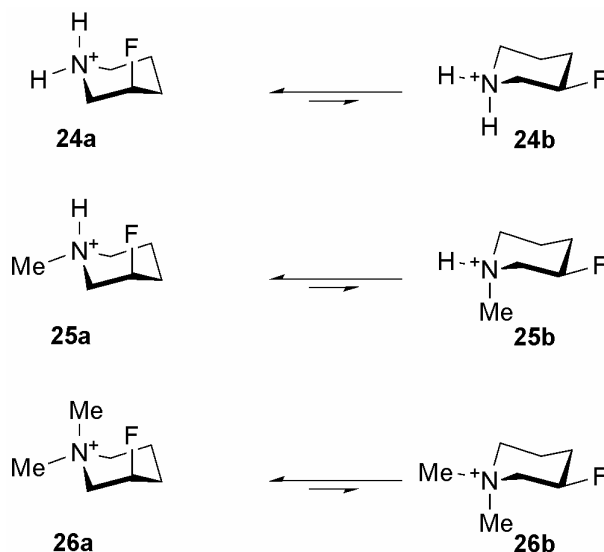


Figure 1.20: Stabilisation of the *gauche* (axial) F-C-C-N<sup>+</sup> conformation over the *anti* (equatorial) conformation in 3-fluoropiperidinium systems.<sup>57</sup>

As the *anti* conformers (**24b**), (**25b**) and (**26b**) were never detected in solution, the *gauche* conformers (**24a**), (**25a**) and (**26a**) were estimated to be at least 2.5 kcal.mol<sup>-1</sup> lower in energy. It is predicted that the stabilising effect lies around 4-5 kcal.mol<sup>-1</sup>. Different parameters could be evoked to explain this effect. Intramolecular C-F...H-N<sup>+</sup> bonding can help stabilise the *gauche* conformation, but it has been shown before that fluorine is only a weak hydrogen bond acceptor. Similarly, through-bond stereoelectronic effects do not contribute to a large stabilisation as no clear *gauche* preference is observed in the neutral system. However, the presence of the positive charge in protonated systems may lower the C-N<sup>+</sup> bond  $\sigma^*$  energy and favour hyperconjugation, but this has not been investigated. It seems that the main explanation for the large F-C-C-N<sup>+</sup> *gauche* preference in these systems is a charge-dipole interaction. This charge-dipole interaction is powerful enough to accommodate the axial orientation of fluorine and the subsequent steric congestion with the two methyl groups in structure (**26a**).

A large number of molecules with the F-C-C-N<sup>+</sup> motif have been synthesised in the St Andrews laboratories and elsewhere. *Gauche* conformations are always observed, indicating that this effect is intrinsic to this motif. Most recently, 2-fluoroethylpyridinium salts have been synthesised and the putative role of hydrogen bonding is suppressed in these systems (27)-(29) (Figure 1.21).<sup>58</sup> The charge-dipole interaction in the F-C-C-N<sup>+</sup> *gauche* preference is a reasonable working hypothesis, especially as the C-F bond has a strong dipole. However, further studies are required to fully understand the origin of the *gauche* preference in such charged  $\beta$ -fluoroamines.

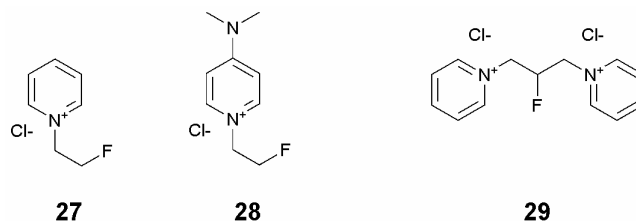


Figure 1.21: Examples of molecules bearing the F-C-C-N<sup>+</sup> motif that are enable to form an intramolecular N-H...F bond.

### 1.3.2 Uses and applications of the C-F...N<sup>+</sup>-C interaction

The persistence of the axial orientation for fluorine in 3-fluoropiperidinium systems (24)-(26) suggests that the incorporation of a C-F bond  $\beta$  to a protonated nitrogen can influence the conformation of rings in the solid state and in solution. With this idea in mind, 3-fluoro-1,5-diazacyclooctane HBr salt (30) has been prepared.<sup>59</sup> The fluorine atom should engage in two C-F...N<sup>+</sup> interactions and therefore influence the conformation of this large flexible ring system. DFT calculations have predicted the conformation with fluorine in the axial position (30a) to be 9.2 kcal.mol<sup>-1</sup> lower in energy than the

conformation with fluorine in the equatorial position (**30b**). The X-ray structure of (**30**) has confirmed that fluorine occupies the axial position with no evidence of molecules bearing fluorine in an equatorial position.<sup>59</sup>

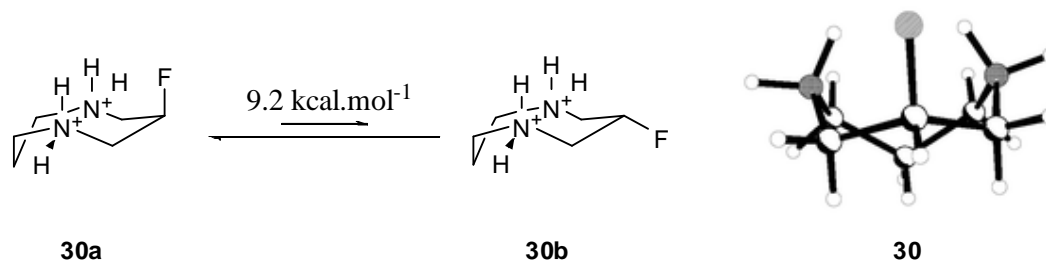
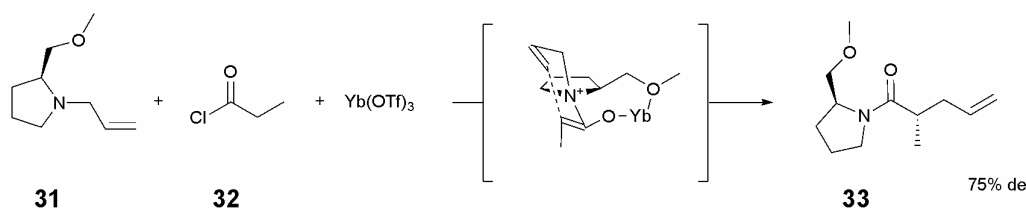


Figure 1.22: The conformation with fluorine axial (**30a**) is greatly favoured over equatorial (**30b**).

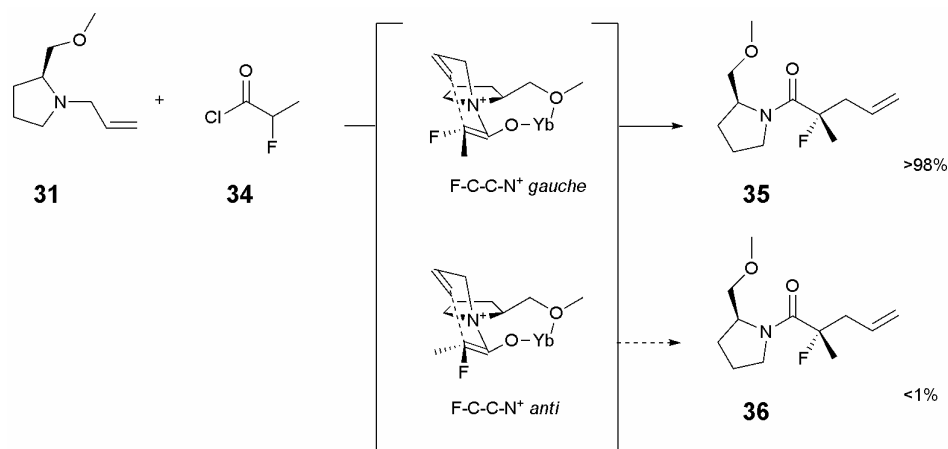
It follows that the C-F bond could be used as a tool to influence the solution conformation of biologically active amines, exactly as it does in the ring system shown above. There are several reasons for exploring this: Firstly, the substitution of hydrogen by fluorine does not induce a significant steric change in the molecule which will maintain its steric profile for binding to the target protein. Also, biologically active amines are usually protonated at physiological pH, so the large conformational preference ( $4\text{--}5 \text{ kcal.mol}^{-1}$ ) for the *gauche* orientation of the F-C-C-N<sup>+</sup> motif should influence, if not limit the solution conformation of the molecule. This means that a  $\beta$ -fluorinated amine is not able to access all conformations available to the non-fluorinated analogue, allowing the significant biologically active conformations of the given amine to be explored. Finally, the introduction of fluorine alters the pK<sub>a</sub> of the bio-active amines. This can have positive or negative consequences for their activity but it is anticipated that the fluorinated amines will remain sufficiently basic to be protonated at physiological pH.

Testing the validity of this concept was exciting and the synthesis of 3-fluoro- $\gamma$ -aminobutyric acid was undertaken in this perceptive. The main focus of this research is to explore the conformational consequences of C-F bond on a bio-active  $\beta$ -fluoroamine.

It has been argued that the C-F bond has the potential to be a powerful tool in influencing the conformation of organic molecules, and particularly  $\beta$ -fluoroamines. The ability could also be used advantageously in asymmetric synthesis to stabilise or destabilise charged reaction intermediates or transition states. However, after browsing the literature, it appears that very few articles report on the role of fluorine in influencing the stereochemical outcome of an organic reaction. One example comes from the St Andrews laboratories. Scheme 1.4 describes the zwitterionic aza-Claisen rearrangement of (*S*)-*N*-allyl-2(methoxymethyl)-pyrrolidine (**31**) with propionyl chloride (**32**) and a Lewis acid. The reaction proceeded with a 75% de.



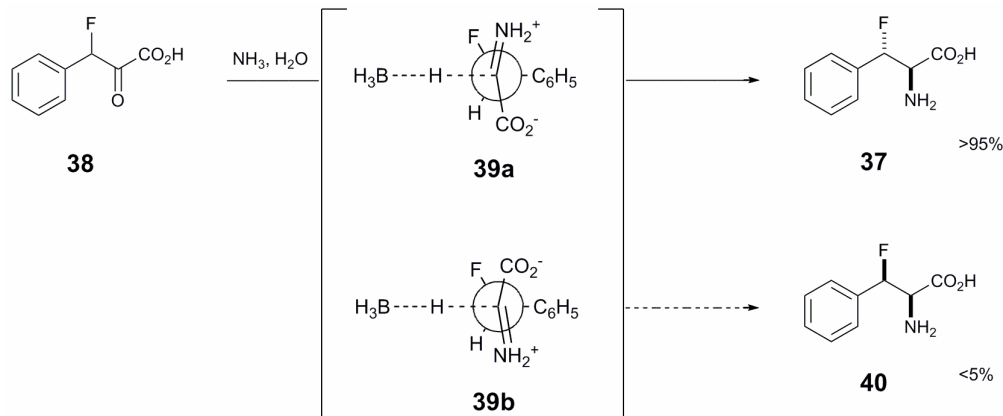
Scheme 1.4: Aza-Claisen rearrangement with propionyl chloride.



Scheme 1.5: The orientation of the C-F bond in the transition state can affect the stereochemical outcome of the zwitterionic aza-Claisen rearrangement.

When 2-fluoropropionyl chloride (**34**) was used instead, the reaction proceeded with a 99% de. It is thought that the C-F bond influences the diastereoselectivity of the reaction by stabilising the transition state where the C-F bond aligns *gauche* to the C-N<sup>+</sup> bond and conversely destabilises the alternative diastereoisomeric transition state, where the C-F bond is *anti* to the C-N<sup>+</sup> bond (Scheme 1.5).<sup>60</sup>

Another example where the orientation of a C-F bond vicinal to a C-N<sup>+</sup> bond is likely to control the stereoselectivity of a reaction has been reported for the synthesis of *erythro*-3-fluorophenylalanine (**37**). Reductive amination of 3-fluorophenylpyruvate (**38**) with NaBH<sub>4</sub> proved to be stereoselective, affording the *erythro* isomer in >90% de (Scheme 1.6).



Scheme 1.6: Transition state models for reduction of  $\alpha$ -iminium-3-benzene-3-fluoropropanoic acid (**39**).<sup>61</sup>

According to the Felkin model, the reduction occurs through either transition state (**39a**) or (**39b**). The former leads to the formation of the *erythro* compound (**37**) and the latter to the *threo* compound (**40**). The transition state (**39a**) is probably stabilised by the

*gauche* relationship between the C-F and the C-N<sup>+</sup> bonds. This accounts for the >95% stereoselectivity of the reduction.<sup>61</sup>

Although applications of such interactions with fluorine in asymmetric organic synthesis are rare, they do exist and raise the significance of the C-F...C-N<sup>+</sup> interactions in influencing the relative stability of transition states and therefore in inducing stereoselectivity in asymmetric reactions.

It has already been noted that (4*R*)-fluoroproline in the Yaa position of collagen peptides increases thermal stability. This example demonstrates that fluorine stereoelectronic effects can be advantageously applied to peptide chemistry. (4*R*)-Fluoroproline adopts the Cγ-*exo* ring conformation to allow the C-F bond to align *gauche* to the C-N bond in a typical *gauche* effect (see also Figure 1.10). Similarly, (4*S*)-fluoroproline adopts the Cγ-*endo* ring conformation, which provides some stability in the Xaa position. The Cγ-*endo* conformer requires the pyrrolidine ring to pucker towards the proline carbonyl (Figure 1.23).

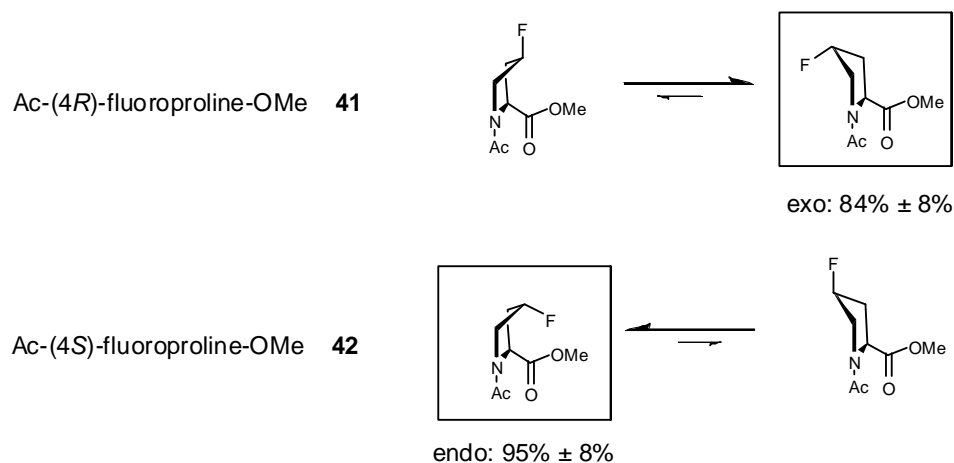
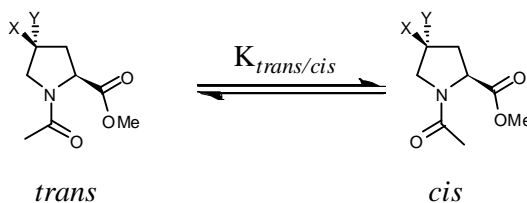


Figure 1.23: Preferred conformations of (4*R*)- and (4*S*)-fluoroproline derivatives (**41**) and (**42**) and the relative populations of the *endo* and *exo* conformations in dioxane at 25 °C.<sup>62</sup>



All peptide bonds in the collagen triple helix are in the *trans* conformation,<sup>63</sup> therefore the predisposition of proline derivatives to adopt a *trans* conformation should decrease the entropic penalty for triple helix formation. (4*R*)-Fluoroproline has the highest  $K_{trans/cis}$  (Table 1.4) and accordingly stabilises the triple helix formation when located at the Yaa position, more than (4*S*)-fluoroproline in the Xaa position (Table 1.5).



Xaa	X	Y	$K_{trans/cis}$
proline	H	H	4.6
(4 <i>R</i> )-hydroxy-proline	H	OH	6.1
(4 <i>S</i> )-hydroxy-proline	OH	H	2.4
(4 <i>R</i> )-fluoro-proline	H	F	6.7
(4 <i>S</i> )-fluoro-proline	F	H	2.5

Table 1.4: Values of  $K_{trans/cis}$  for 4-substituted proline residues measured in D<sub>2</sub>O at 25 °C.<sup>64</sup>

	$T_m$ (°C)
(Pro-Pro-Gly) <sub>7</sub>	-6
(Pro-(4 <i>R</i> )Flpro-Gly) <sub>7</sub>	45
((4 <i>S</i> )Flpro-Pro-Gly) <sub>7</sub>	33
((4 <i>S</i> )Flpro-(4 <i>R</i> )Flpro-Gly) <sub>7</sub>	8

Table 1.5: Effect of 4-fluoroproline on the conformational stability of a collagen triple helix with (XaaYaaGly)<sub>7</sub> strands.<sup>40</sup>

There is a correlation between high  $K_{trans/cis}$  and the stability of the collagen helix, but other factors, such as steric considerations are also important.<sup>39, 40</sup> By constructing constrained proline analogues, Raines *et al.* showed that changes in *trans/cis* ratio arise from changes in ring pucker.<sup>64</sup> However, the correlation between  $K_{trans/cis}$  and *exo/endo* conformations is not well established. As described, (4*R*)-fluoroproline adopts the  $C\gamma$ -*exo* conformation and has a high  $K_{trans/cis}$  whereas (4*S*)-fluoroproline adopts the  $C\gamma$ -*endo* conformation but has a much lower  $K_{trans/cis}$  suggesting that the *trans* conformation is much less stable in this case.

How does this difference between the two arise? It has been advanced that in the case of (4*R*)-fluoroproline, the oxygen of the amide points towards the carbon of the methyl ester in a  $n \rightarrow \pi^*$  stabilising interaction (**41b**). In the case of (4*S*)-fluoroproline, this  $n \rightarrow \pi^*$  interaction is less stabilising because the oxygen of the amide and the carboxylic group are further apart due to the  $C\gamma$ -*endo* conformation. Moreover, the fluorine interacts unfavourably with the oxygen of the methyl ester in the *trans* conformation (**42b**), which disfavors the  $n \rightarrow \pi^*$  interaction. (Figure 1.24).<sup>62, 64</sup>

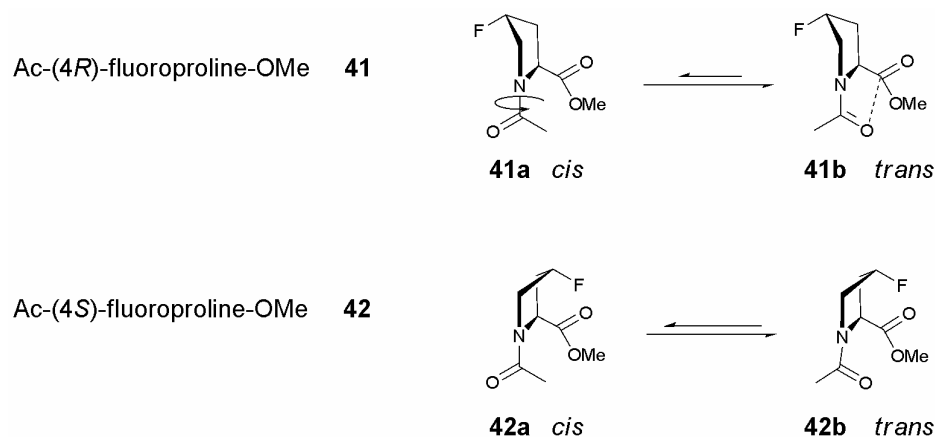


Figure 1.24: Stabilisation of the *trans* conformer (**41b**) by  $n \rightarrow \pi^*$  interaction and destabilisation of the *trans* conformer (**42b**) due to unfavourable steric interactions between the nonbonded electrons on the fluoro and ester groups, which disfavors the  $n \rightarrow \pi^*$  interaction.<sup>64</sup>

Although it has not been discussed in the literature, the relative destabilisation of the *trans* conformer of Ac-(4*S*)-fluoroproline-OMe (**42b**) could also be explained in terms of an unfavourable dipole-dipole interaction between the C-F bond and the amide bond. This explanation could also account for the higher *trans/cis* ratio of Ac-(4*R*)-fluoroproline-OMe as a dipole-dipole interaction between the C-F and the amide bond would also destabilise the *cis* conformer (**41a**) (Figure 1.25).

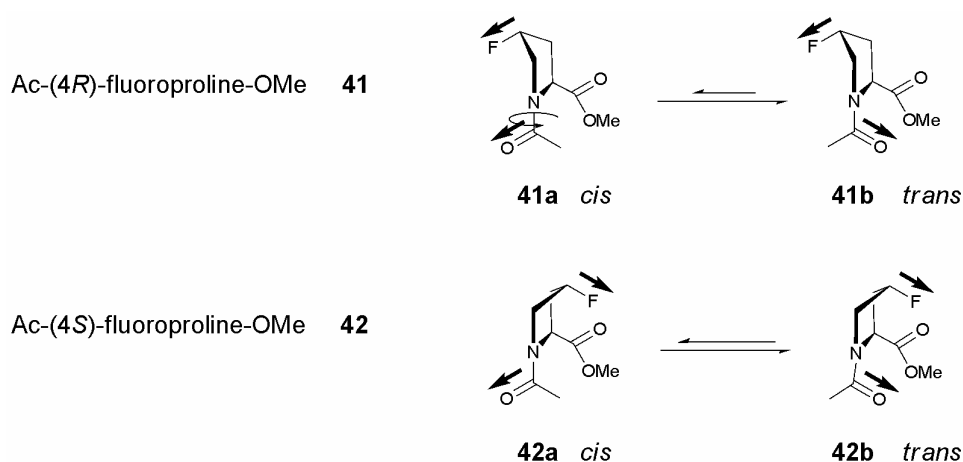


Figure 1.25: Destabilisation of the *cis* conformer (**41a**) and *trans* conformer (**42b**) due to dipole-dipole interaction.

This analysis shows that the propensity of proline residues to adopt either the *trans* or *cis* conformation has a decisive effect on the conformation stability of proline-rich peptides. It also demonstrates that the fluorine *gauche* effect and its potential use in influencing the conformation of polypeptides are fully acknowledged and have already been utilised.

It is important to note that proline has a crucial role also in the folding of proteins by causing turns in  $\beta$ -sheets or by promoting  $\alpha$ -helix stability. Lummis and Beene<sup>65</sup> have shown that striking structural and functional consequences are observed when unnatural

proline analogues with different  $K_{trans/cis}$  values are substituted for a proline residue at a specific position in the sequence of the 5-hydroxytryptamine type 3 receptor (5-HT<sub>3</sub> receptor). 5-HT<sub>3</sub> receptors are, like GABA<sub>A</sub> receptors, neurotransmitter-gated ion channels, members of the Cys-loop receptor superfamily.

Their study showed that proline analogues that strongly favour the *trans* conformer produced non-functional channels, *i.e.* channels unable to open. Conversely, proline analogues with a high preference for the *cis* conformation produced channels which stay open longer, suggesting that the *cis/trans* isomerisation of this proline residue provides the switch that interconverts the open and closed state of the channel (Figure 1.26). In this case however, (4*R*)-fluoroproline and (4*S*)-fluoroproline showed little difference from the natural proline residue.

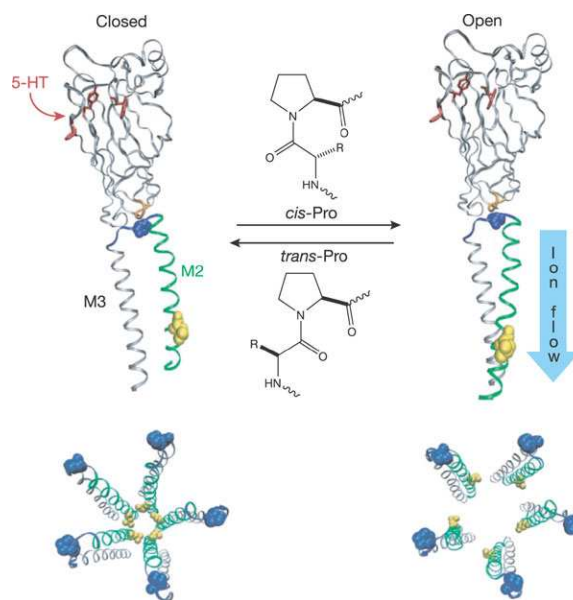


Figure 1.26: A proposed gating mechanism. A single 5-HT<sub>3</sub> receptor subunit is depicted, illustrating how *trans/cis* isomerisation could function as a switch between the open and closed state of the channel.<sup>65</sup>

This provided an important insight into understanding the gating mechanism of ligand-gated ion channels receptors. But it is still unclear how the binding of a small molecule, such as acetylcholine, serotonin (5-hydroxytryptamine) or GABA, can operate the conformational changes in the receptor which open the channel pore, located about 60 Å away from the binding site of the neurotransmitter. The biological role of GABA and its binding on GABA<sub>A</sub> and GABA<sub>B</sub> receptors are the subjects of Chapter 2.

## 1.4 References

- <sup>1</sup> D. Halpern, *J. Fluorine Chem.*, 2002, **118**, 47-53.
- <sup>2</sup> J. Fried and E. F. Sabo, *J. Am. Chem. Soc.*, 1954, **76**, 1455-1456.
- <sup>3</sup> C. Isanbor and D. O'Hagan, *J. Fluorine Chem.*, 2006, **127**, 303-319.
- <sup>4</sup> V. M. Kanagasabapathy, J. F. Sawyer, and T. T. Tidwell, *J. Org. Chem.*, 1985, **50**, 503-509.
- <sup>5</sup> C. Swain and N. M. J. Rupniak, *Annu. Rep. Med. Chem.*, 1999, **34**, 51-60.
- <sup>6</sup> *MedChem Database, Biobyte Corporation and Pomona College*, 2002.
- <sup>7</sup> M. B. van Niel, I. Collins, M. S. Beer, H. B. Broughton, S. K. F. Cheng, S. C. Goodacre, A. Heald, K. L. Locker, A. M. MacLeod, D. Morrison, C. R. Moyes, D. O'Connor, A. Pike, M. Rowley, M. G. N. Russell, B. Sohal, J. A. Stanton, S. Thomas, H. Verrier, A. P. Watt, and J. L. Castro, *J. Med. Chem.*, 1999, **42**, 2087-2104.
- <sup>8</sup> H.-J. Boehm, D. Banner, S. Bendels, M. Kansy, B. Kuhn, K. Mueller, U. Obst-Sander, and M. Stahl, *ChemBioChem*, 2004, **5**, 637-643.
- <sup>9</sup> S. Kim, S. Y. Hwang, Y. K. Kim, M. Yun, and Y. S. Oh, *Bioorg. Med. Chem. Lett.*, 1997, **7**, 769-774.
- <sup>10</sup> R. I. Mathad, F. Gessier, D. Seebach, and B. Jaun, *Helv. Chim. Acta*, 2005, **88**, 266-280.
- <sup>11</sup> A. Bondi, *J. Phys. Chem.*, 1964, **68**, 441-451.
- <sup>12</sup> V. A. Sonoshonok, *Enantiocontrolled Synthesis of Fluoro-organic Compounds*, John Wiley & Sons Ltd, 1999.
- <sup>13</sup> J. A. Erickson and J. I. McLoughlin, *J. Org. Chem.*, 1995, **60**, 1626-1631.
- <sup>14</sup> J. D. Dunitz, *ChemBioChem*, 2004, **5**, 614-621.
- <sup>15</sup> J. A. K. Howard, V. J. Hoy, D. O'Hagan, and G. T. Smith, *Tetrahedron*, 1996, **52**, 12613-12622.
- <sup>16</sup> J. D. Dunitz and R. Taylor, *Chem.--Eur. J.*, 1997, **3**, 89-98.
- <sup>17</sup> J. A. Olsen, D. W. Banner, P. Seiler, B. Wagner, T. Tschopp, U. Obst-Sander, M. Kansy, K. Mueller, and F. Diederich, *ChemBioChem*, 2004, **5**, 666-675.
- <sup>18</sup> R. Froehlich, T. C. Rosen, O. G. J. Meyer, K. Rissanen, and G. Haufe, *J. Mol. Struct.*, 2006, **787**, 50-62.

- <sup>19</sup> D. O'Hagan and H. S. Rzepa, *Chem. Commun.*, 1997, 645-652.
- <sup>20</sup> G. M. Dubowchik, V. M. Vrudhula, B. Dasgupta, J. Ditta, T. Chen, S. Sheriff, K. Sipman, M. Witmer, J. Tredup, D. M. Vyas, T. A. Verdoorn, S. Bollini, and A. Vinitsky, *Org. Lett.*, 2001, **3**, 3987-3990.
- <sup>21</sup> R. Paulini, K. Mueller, and F. Diederich, *Angew. Chem., Int. Ed.*, 2005, **44**, 1788-1805.
- <sup>22</sup> A. Gavezzotti, *J. Phys. Chem.*, 1990, **94**, 4319-4325.
- <sup>23</sup> R. J. Abraham, S. L. R. Ellison, P. Schonholzer, and W. A. Thomas, *Tetrahedron*, 1986, **42**, 2101-2110.
- <sup>24</sup> P. A. Bartlett and A. Otake, *J. Org. Chem.*, 1995, **60**, 3107-3111.
- <sup>25</sup> P. Wipf, T. C. Henninger, and S. J. Geib, *J. Org. Chem.*, 1998, **63**, 6088-6089.
- <sup>26</sup> J. P. Begue and D. Bonnet-Delpon, *Chimie bioorganique et medicinale du fluor*, CNRS editions, 2005.
- <sup>27</sup> J. C. Biffinger, H. W. Kim, and S. G. DiMagno, *ChemBioChem*, 2004, **5**, 622-627.
- <sup>28</sup> J. W. Clader, *J. Med. Chem.*, 2004, **47**, 1-9.
- <sup>29</sup> T. D. Penning, J. J. Talley, S. R. Bertenshaw, J. S. Carter, P. W. Collins, S. Docter, M. J. Graneto, L. F. Lee, J. W. Malecha, J. M. Miyashiro, R. S. Rogers, D. J. Rogier, S. S. Yu, G. D. Anderson, E. G. Burton, J. N. Cogburn, S. A. Gregory, C. M. Koboldt, W. E. Perkins, K. Seibert, A. W. Veenhuizen, Y. Y. Zhang, and P. C. Isakson, *J. Med. Chem.*, 1997, **40**, 1347-1365.
- <sup>30</sup> J. G. Dingwall, *Pestic. Sci.*, 1994, **41**, 259-267.
- <sup>31</sup> M. H. Gelb, J. P. Svaren, and R. H. Abeles, *Biochemistry*, 1985, **24**, 1813-1817.
- <sup>32</sup> R. V. Hoffman and J. Tao, *J. Org. Chem.*, 1999, **64**, 126-132.
- <sup>33</sup> A. G. Myers, J. K. Barbay, and B. Zhong, *J. Am. Chem. Soc.*, 2001, **123**, 7207-7219.
- <sup>34</sup> B. W. Metcalf, P. Bey, C. Danzin, M. J. Jung, P. Casara, and J. P. Vever, *J. Am. Chem. Soc.*, 1978, **100**, 2551-2553.
- <sup>35</sup> G. Granerus, J. H. Olafsson, and G. Roupe, *Agents Actions*, 1985, **16**, 244-248.
- <sup>36</sup> J. Kollonitsch and L. Barash, *J. Am. Chem. Soc.*, 1976, **98**, 5591-5593.
- <sup>37</sup> E. A. Wang and C. Walsh, *Biochemistry*, 1981, **20**, 7539-7546.
- <sup>38</sup> S. K. Holmgren, K. M. Taylor, L. E. Bretscher, and R. T. Raines, *Nature*, 1998, **392**, 666-667.
- <sup>39</sup> J. A. Hodges and R. T. Raines, *J. Am. Chem. Soc.*, 2005, **127**, 15923-15932.
- <sup>40</sup> M. D. Shoulders, J. A. Hodges, and R. T. Raines, *J. Am. Chem. Soc.*, 2006, **128**, 8112-8113.

- <sup>41</sup> M. Schueler, D. O'Hagan, and A. M. Z. Slawin, *Chem. Commun.*, 2005, 4324-4326.
- <sup>42</sup> D. O'Hagan, H. S. Rzepa, M. Schuler, and A. M. Z. Slawin, *Beilstein J. Org. Chem.*, 2006, **2**, No pp given.
- <sup>43</sup> Y. Tang, G. Ghirlanda, W. A. Petka, T. Nakajima, W. F. DeGrado, and D. A. Tirrell, *Angew. Chem., Int. Ed.*, 2001, **40**, 1494-1496.
- <sup>44</sup> P. Klaboe and J. R. Nielsen, *J. Chem. Phys.*, 1960, **33**, 1764-1774.
- <sup>45</sup> T. Hirano, S. Nonoyama, T. Miyajima, Y. Kurita, T. Kawamura, and H. Sato, *J. Chem. Soc., Chem. Commun.*, 1986, 606-607.
- <sup>46</sup> D. A. Dixon and B. E. Smart, *J. Phys. Chem.*, 1988, **92**, 2729-2733.
- <sup>47</sup> K. B. Wiberg, *Acc. Chem. Res.*, 1996, **29**, 229-234.
- <sup>48</sup> L. Goodman, H. Gu, and V. Pophristic, *J. Phys. Chem. A*, 2005, **109**, 1223-1229.
- <sup>49</sup> F. Akkerman, J. Buschmann, D. Lentz, P. Luger, and E. Roedel, *J. Chem. Crystallogr.*, 2003, **33**, 969-975.
- <sup>50</sup> J. R. Durig, J. Liu, T. S. Little, and V. F. Kalasinsky, *J. Phys. Chem.*, 1992, **96**, 8224-8233.
- <sup>51</sup> G. Angelini, E. Gavuzzo, A. L. Segre, and M. Speranza, *J. Phys. Chem.*, 1990, **94**, 8762-8766.
- <sup>52</sup> P. R. Rablen, R. W. Hoffmann, D. A. Hrovat, and W. T. Borden, *J. Chem. Soc., Perkin Trans. 2*, 1999, 1719-1726.
- <sup>53</sup> G. R. Runtz, R. F. W. Bader, and R. R. Messer, *Can. J. Chem.*, 1977, **55**, 3040-3045.
- <sup>54</sup> K. B. Wiberg, M. A. Murcko, K. E. Laidig, and P. J. MacDougall, *J. Phys. Chem.*, 1990, **94**, 6956-6959.
- <sup>55</sup> D. A. Dixon and B. E. Smart, *J. Phys. Chem.*, 1991, **95**, 1609-1612.
- <sup>56</sup> C. R. S. Briggs, M. J. Allen, D. O'Hagan, D. J. Tozer, A. M. Z. Slawin, A. E. Goeta, and J. A. K. Howard, *Org. Biomol. Chem.*, 2004, **2**, 732-740.
- <sup>57</sup> A. Sun, D. C. Lankin, K. Hardcastle, and J. P. Snyder, *Chem.--Eur. J.*, 2005, **11**, 1579-1591.
- <sup>58</sup> N. E. J. Gooseman, 'The  $\beta$ -fluorine $\cdots$ ammonium interaction in ring systems, PhD Thesis', St andrews University, 2007.
- <sup>59</sup> N. E. J. Gooseman, D. O'Hagan, A. M. Z. Slawin, A. M. Teale, D. J. Tozer, and R. J. Young, *Chem. Commun.*, 2006, 3190-3192.
- <sup>60</sup> K. Tenza, S. Northen Julian, D. O'Hagan, and M. Z. Slawin Alexandra, *Beilstein J. Org. Chem.*, 2005, **1**, 13.



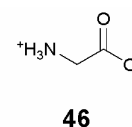
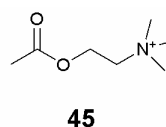
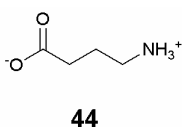
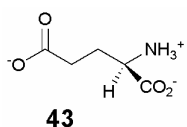
- <sup>61</sup> T. Tsushima, K. Kawada, J. Nishikawa, T. Sato, K. Tori, T. Tsuji, and S. Misaki, *J. Org. Chem.*, 1984, **49**, 1163-1169.
- <sup>62</sup> M. L. DeRider, S. J. Wilkens, M. J. Waddell, L. E. Bretscher, F. Weinhold, R. T. Raines, and J. L. Markley, *J. Am. Chem. Soc.*, 2002, **124**, 2497-2505.
- <sup>63</sup> J. Bella, M. Eaton, B. Brodsky, and H. M. Berman, *Science*, 1994, **266**, 75-81.
- <sup>64</sup> C. L. Jenkins, G. Lin, J. Duo, D. Rapolu, I. A. Guzei, R. T. Raines, and G. R. Krow, *J. Org. Chem.*, 2004, **69**, 8565-8573.
- <sup>65</sup> S. C. R. Lummis, D. L. Beene, L. W. Lee, H. A. Lester, R. W. Broadhurst, and D. A. Dougherty, *Nature*, 2005, **438**, 248-252.

## Chapter 2: The GABA-mediated inhibition of neuronal signals.

### 2.1 Introduction

The brain and the central nervous system (CNS) of human beings are probably the most sophisticated machineries in nature and certainly the most intriguing parts of ourselves. For example, little is known about the mechanisms involved in memory or information storage in the brain. The propagation of neuronal signals from the brain to the muscles is also a very complex system controlled or affected by a huge number of parameters which are not all identified. It is however crucial for the development of modern science to understand how neurons communicate between each other.

Synapses are regions between neurons where the electric neuronal signal is converted into a chemical signal and transmitted to another neuron. When the electric signal depolarises the pre-synaptic nerve terminal, a neurotransmitter released from storage vesicles diffuses the short distance to the post-synaptic membrane where it binds to its receptors and opens a channel through which ions can flow into the post-synaptic neuron. The main neurotransmitters in the CNS are glutamate (**43**),  $\gamma$ -aminobutyric acid (GABA) (**44**), acetylcholine (**45**) and glycine (**46**).

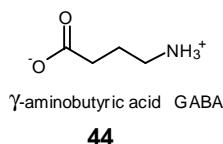


GABA is the main inhibitory neurotransmitter with, depending on the brain region, 20-50% of neuronal synapses estimated to be GABAergic (*i.e.* to synthesise and to utilise GABA as their primary neurotransmitter).<sup>1, 2</sup> Its binding on the post-synaptic membrane causes the cell to hyperpolarise and thus to be less likely to fire, by allowing either a flow of chloride anions into the cell or a flow of cations out of the cell. GABA is involved in a wide range of physiological functions such as respiration,<sup>3, 4</sup> locomotion,<sup>5</sup> pain,<sup>6</sup> memory<sup>7, 8</sup> and sleep<sup>9</sup> and its receptors are the target of many important drugs.

Chapter 2 outlines the central role of GABA in the CNS and the pharmaceutical importance of its receptors. The structures of GABA<sub>A</sub> and GABA<sub>B</sub> receptors are then discussed, as well as the models of GABA binding sites which have been proposed. The aim of the second part of this chapter is to discern the active conformations of GABA on its different binding sites. For that purpose, GABA analogues and their biological activities are reviewed and compared. The last part of this chapter presents the synthesis of neurosteroids which interact with GABA. Their synthesis was motivated to explore the mode of action of neurosteroids on the GABA receptors, a relationship that is not well understood.

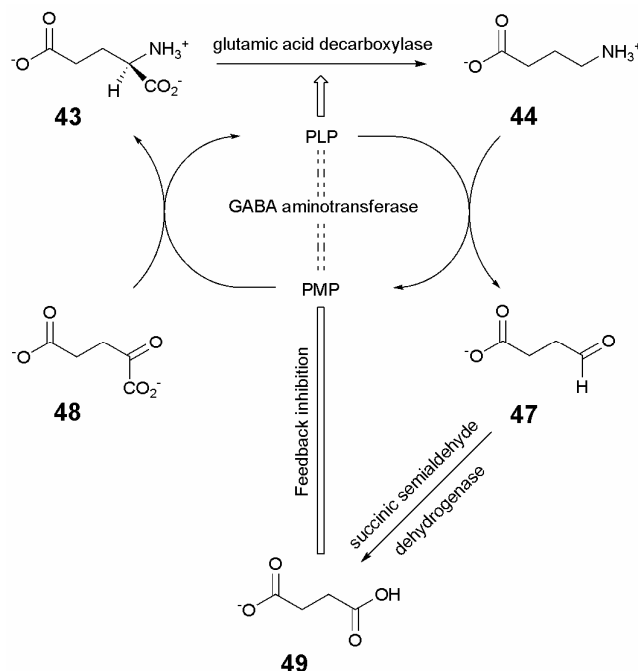
## 2.2 GABA and GABA receptors as key elements of the CNS.

### 2.2.1 The importance of GABA in the CNS



GABA ( $\gamma$ -aminobutyric acid) (**44**) is the most prevalent inhibitory neurotransmitter in the CNS. It is synthesised from L-glutamate (**43**) by the action of L-glutamic acid decarboxylase (GAD) which is a PLP-dependent enzyme. The mechanism of this transformation is outlined in Scheme **1.2**. The action of this enzyme is of huge importance as it converts the main excitatory neurotransmitter (glutamate) into the main inhibitory neurotransmitter (GABA).

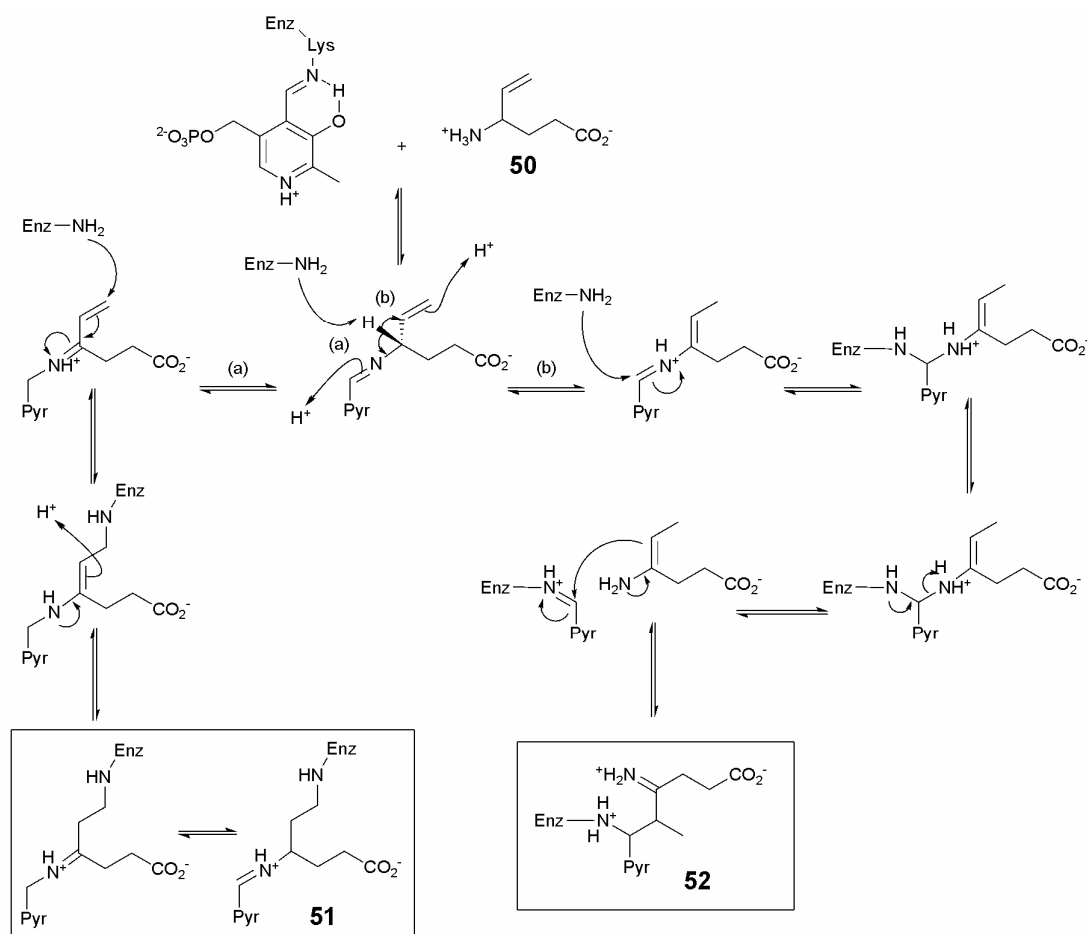
GABA is then metabolised to succinic semialdehyde (**47**) by the enzyme GABA aminotransferase (GABA-AT) which is also a PLP-dependent enzyme. It converts PLP to PMP, then PMP is restored to PLP by transamination with  $\alpha$ -ketoglutarate (**48**), regenerating L-glutamate. Succinic semialdehyde is converted by succinic semialdehyde dehydrogenase (SSADH) to succinate (**49**), which has a negative-feedback inhibition on the enzyme GAD. This auto-regulated system keeps the concentration of GABA in the CNS constant as the production of GABA is inhibited by an increased concentration of the end-product succinic acid (Scheme **2.1**).



Scheme 2.1: Biosynthetic pathway and metabolism of GABA.

Dysfunctions in the regulation of GABA lead to abnormal concentrations of the neurotransmitter and have serious effects on the propagation of neuronal signals. Particularly critical are depleted concentrations of GABA which are related to major neurological disorders such as Parkinson's disease,<sup>10</sup> Alzheimer's disease,<sup>11</sup> epilepsy,<sup>12</sup> anxiety or depression.<sup>13</sup> These syndromes affect a large proportion of the population especially in industrialised countries and over the years, the pharmaceutical industry has introduced a number of drugs to the market to treat these disorders.

There are different ways of enhancing the action of GABA. The first method is to inhibit GABA metabolism, that is, to block the action of GABA aminotransferase. This is the mode of action of Vigabatrin (**50**), sold in the United Kingdom under the trade name Sabril® and used successfully to treat epilepsy.<sup>14, 15</sup> Vigabatrin is a mechanism-based irreversible inhibitor of GABA-AT (Scheme 2.2), with only the (*S*)-enantiomer displaying pharmaceutical activity.<sup>16, 17</sup> Sabril® however is sold as a racemate.



Scheme 2.2: Mechanisms of inactivation of GABA-AT by vigabatrin.<sup>18</sup>

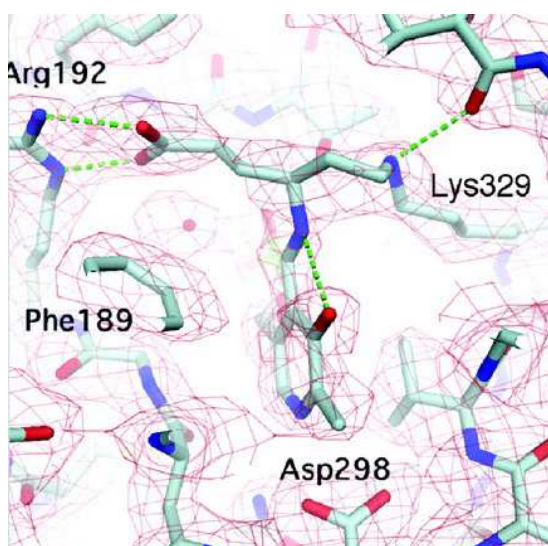
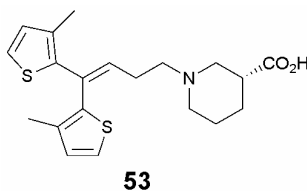


Figure 2.1: Active site of GABA-AT after modification with vigabatrin. The ternary adduct has been modelled according to structure (51).<sup>19</sup>

The crystal structure of GABA-AT was reported in 1999.<sup>20</sup> More recently, GABA-AT and vigabatrin have been co-crystallised and the ternary adduct (**51**) of Lys329, PLP-co-factor and vigabatrin was found in the active site (Figure 2.1). This finding supports the Michael addition mechanism (pathway *a*) however the enamine mechanism (pathway *b*) can not be ruled out.<sup>19</sup>

A second method to enhance the action of GABA is to reduce its reuptake by neuronal GABA transporters. Reuptake into presynaptic terminals or surrounding glial cells constitutes the primary mechanism for terminating inhibitory GABAergic neurotransmission. Therefore, selective GABA uptake inhibitors, like Tiagabine<sup>21, 22</sup> (**53**) exhibit interesting anticonvulsant activities. Tiagabine is used clinically for the treatment of epileptic disorders.<sup>23</sup> By binding GABA transporters, this drug permits more GABA to be available for receptor binding on the surface of the postsynaptic membrane. GABA transporters have been cloned and shown to be members of the large family of Na<sup>+</sup>-dependent neurotransmitter transporters<sup>24</sup> but no crystal structure nor homology model is available yet.



A third way of enhancing GABA availability is to stimulate its biosynthesis but no drug using this strategy has been clinically approved so far. Instead, most of the drugs potentiating the effects of GABA act by binding to GABA receptors, but on a different binding site to GABA itself. Such compounds have little or no intrinsic activity in the absence of GABA. They are called positive allosteric modulators of GABA and represent a large family of compounds which includes the clinically important barbiturates, benzodiazepines and neurosteroids as well as ethanol, halothane (**1**) and etomidate (**54**).

Barbiturates have been used since the early 1900s as sedative-hypnotics, anticonvulsants and anaesthetics. The most representative compound of this class is pentobarbitone (**55**) which is the oldest anticonvulsant still in use, although barbiturates as a class have been largely supplanted by benzodiazepines which have fewer undesired side effects.<sup>25</sup>

Diazepam (**56**), marketed under the name Valium® is certainly the best known benzodiazepine. It was the top selling drug in the 1970s and is still in use today. More recently, neurosteroids have also been found to modulate the activity of GABA. The term “neurosteroid” refers to steroids which, independent of their origin, are capable of modifying neural activities.<sup>26</sup> One of the most potent endogenous neurosteroids is allopregnanolone (**57**) which has been recognised to have potential therapeutic applications as an anaesthetic.<sup>27</sup>

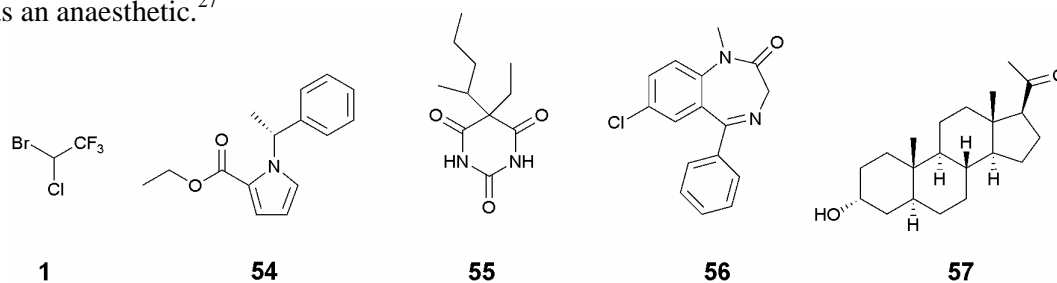


Figure 2.2: Representative compounds known to act as positive allosteric modulators of the GABA-mediated inhibition of neuronal signals.

The five compounds shown above are clinically used or have potential use as anaesthetics. They are believed to act at GABA receptors, although their modes of action remain elusive. Their structural variety is remarkable and suggests that GABA receptors possess numerous binding sites for allosteric modulation. It could also be that multiple types of GABA receptors with diverse pharmacological profiles are expressed heterogeneously in the CNS. Disclosing the structural and pharmaceutical specificities of GABA receptors is a current challenge for both academic research and the pharmaceutical industry.



### 2.2.2 GABA<sub>A</sub> and GABA<sub>B</sub> receptors

The action of GABA is mediated mostly by two structurally and pharmacologically distinct receptors, termed GABA<sub>A</sub> and GABA<sub>B</sub> receptors. The GABA<sub>A</sub> receptors are ligand-gated chloride ion channels conveying the fast synaptic transmission. They are antagonised by bicuculline (**58**) and are insensitive to baclofen (**59**). GABA<sub>B</sub> receptors operate *via* second messenger systems and are coupled to Ca<sup>2+</sup> and K<sup>+</sup> ions channels through G-proteins. They produce slow, longer-lasting inhibition,<sup>28</sup> are activated by baclofen and are insensitive to bicuculline. Both receptors have been cloned, GABA<sub>A</sub> first in 1987<sup>29</sup> and GABA<sub>B</sub> in 1997<sup>30</sup> but progress to establish their precise structure, as well as ligand binding and gating mechanisms have been hindered due to their membrane-bound protein nature, which is not conducive to structural determination by usual methods such as X-ray crystallography.

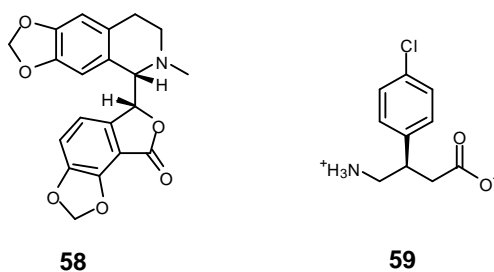


Figure 2.3: Bicuculline (**58**) is a selective GABA<sub>A</sub> antagonist and (*R*)-baclofen (**59**) is a selective GABA<sub>B</sub> agonist.

Bicuculline and (*R*)-baclofen constitute molecular tools for biologists to selectively “close” or “open” GABA receptors in order to understand their specific pharmacology.

GABA<sub>A</sub> receptors have generated a lot of interest due to their physiological significance and their complexity. They have been described as “the most complicated of the superfamily of ligand-gated ion channels in term of the large number of receptor subtypes and also the variety of ligands that interact with specific sites on the receptors”.<sup>25</sup>

Indeed, GABA<sub>A</sub> receptors are composed of five subunits drawn from a library of sixteen subunits ( $\alpha$ 1- $\alpha$ 6,  $\beta$ 1- $\beta$ 3,  $\gamma$ 1- $\gamma$ 3,  $\delta$ ,  $\epsilon$ ,  $\pi$  and  $\theta$ ). This structural diversity allows the expression of approximately thirty different functional isoforms of GABA<sub>A</sub> receptors which are heterogeneously expressed in the CNS and exhibit distinct physiological and pharmacological properties.<sup>31</sup> Individual neurons can also produce different receptor subtypes. In most cases, functional receptors require the presence of  $\alpha$  and  $\beta$  subunits and the most quantitatively prevalent receptor isoform is believed to have the structure  $2\alpha 2\beta 1\gamma$ . This composition is used as a model for GABA<sub>A</sub> receptors.

The GABA binding sites are located at the interfaces of the  $\alpha$  and the  $\beta$  subunits.<sup>32</sup> There are therefore two GABA binding sites on the GABA<sub>A</sub> receptor and two molecules of the neurotransmitter are required to initiate the sequence of conformational changes which ultimately results in the opening of the chloride ion channel.

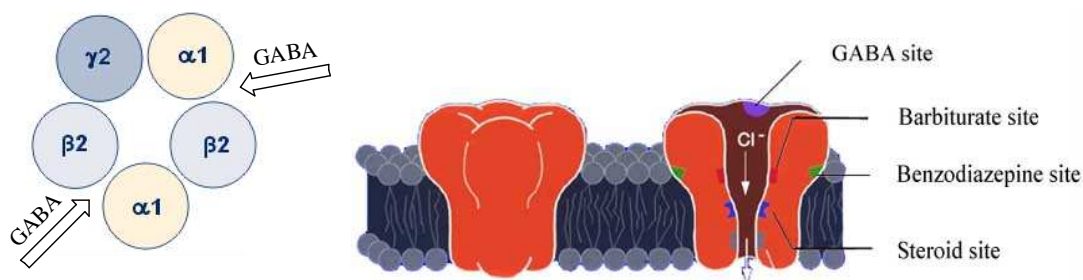


Figure 2.4: Schematic representations of the GABA<sub>A</sub> receptor.

No crystal structure of the GABA<sub>A</sub> receptor has been published to date and this seriously impedes efforts to characterise precisely the structure of the GABA binding site. To circumvent this problem, three-dimensional models have been constructed by comparison with crystal structures of related proteins. The first protein which served as a template for the development of homology models of the GABA<sub>A</sub> receptor was the acetylcholine binding protein, a soluble analogue of the nicotinic acetylcholine receptor amino-terminal domain. Its crystal structure was reported in 2001.<sup>33</sup> More recently in 2005, a crystallographic model based on cryo-electron microscopic analyses of the acetylcholine (ACh) receptor in *Torpedo* electric ray post-synaptic membranes revealed with more accuracy the structure of Cys-loop receptor-coupled ion channels.<sup>34</sup> ACh and GABA<sub>A</sub> receptors have similar structure as they belong to the same family of transmembrane pentameric Cys-loop receptor ion channels.

Comparative modelling, also called homology modelling is based on the observation that in protein families, structure is more conserved than sequence.<sup>35</sup> Therefore, knowing the sequence and the structure of an ACh receptor, and the sequence of the GABA<sub>A</sub> receptor, it is possible to align by comparison the target sequence with the template structure. By this method, one obtains a model whose validity depends on the sequence analogy between the template and the target.

GABA<sub>A</sub> receptors have been modelled using this concept and the results depend on the alignment technique and on the template(s) used.<sup>36-42</sup>

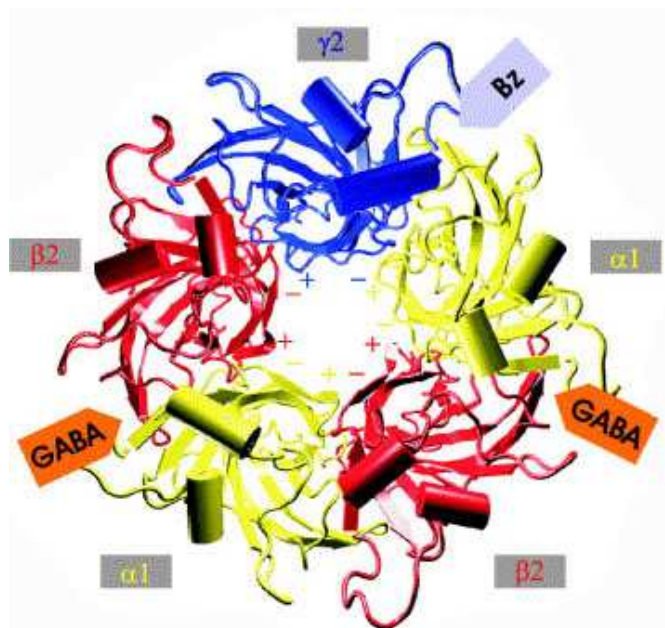


Figure 2.5: Model structure of the extracellular domain of GABA<sub>A</sub> receptors published in 2003.<sup>41</sup>

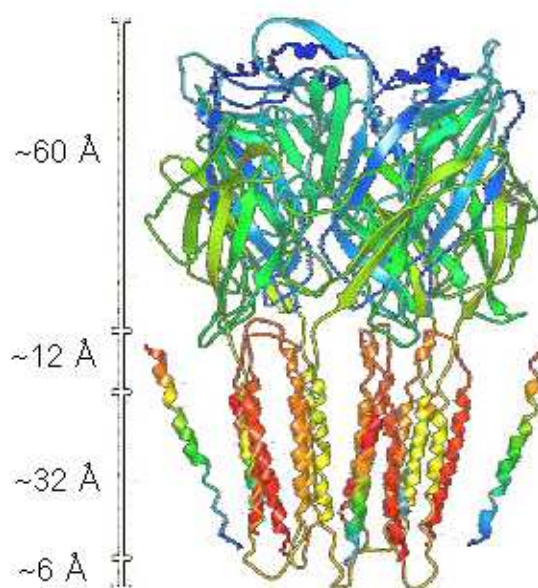


Figure 2.6: Model structure of the GABA<sub>A</sub> receptor showing the extracellular domain (β-strand rich) and the transmembrane domain (α-helix) published in 2007.<sup>42</sup>

Together with photolabelling techniques and substituted cysteine accessibility method (SCAM), homology modelling provides a better picture of the GABA<sub>A</sub> receptor and the GABA binding site structures. To date, multiple residues have been shown to contribute to the formation of the GABA binding site. These are Phe64, Arg66, Arg119, Ile120, Arg176, Val178, Val180 and Asp183 of the  $\alpha_1$  subunit, and Tyr97, Leu99, Tyr157, Thr160, Thr202, Ser204, Tyr205, Arg207, and Ser209 of the  $\beta_2$  subunit.<sup>43-45</sup>

From these elements, a model of the GABA binding site on the GABA<sub>A</sub> receptor has been constructed (Figure 2.7).<sup>38</sup> Note that GABA is drawn in a fully extended conformation. It is however very difficult to assess the validity and the accuracy of this model.

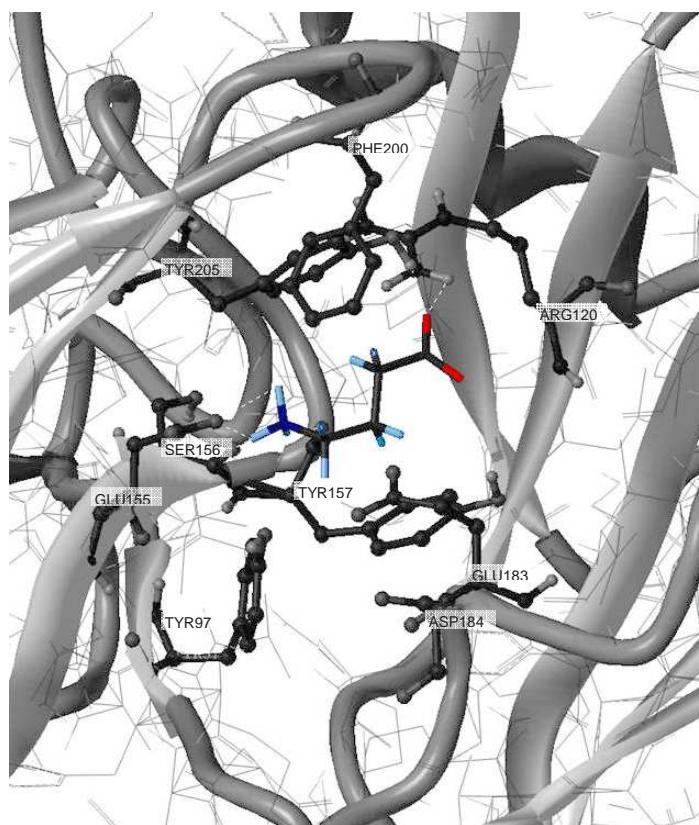


Figure 2.7: Model binding of GABA to the GABA<sub>A</sub> binding site published in 2006.<sup>38</sup>

Another GABA<sub>A</sub> binding site model has been proposed recently after the observation that the amino group of GABA is in close contact with the aromatic ring of Tyr97 in a cation- $\pi$  interaction. The GABA binding pocket is described as an aromatic pocket (Figure 2.8).<sup>46</sup>

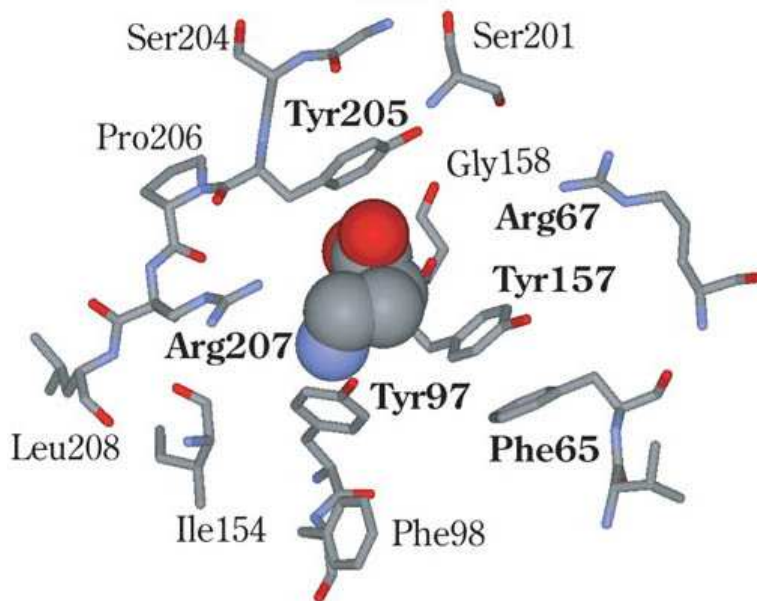


Figure 2.8: GABA molecule docked into the proposed aromatic pocket published in 2007.<sup>46</sup>

The last two years have witnessed great progress in the modelling and the understanding of the GABA<sub>A</sub> structure in order to disclose the structures of ligand recognition sites and gating mechanisms. This is currently a very active area of research and the convergence of different techniques will undoubtedly lead to the discovery of the full GABA<sub>A</sub> receptor structure at an atomic level in the next few years.

It should also be mentioned that interesting studies have been published on the structure of GABA<sub>C</sub> receptors which are a subtype of lower complexity of GABA<sub>A</sub> receptors.<sup>47, 48</sup>

GABA<sub>B</sub> receptors were pharmacologically characterised in 1980<sup>49</sup> but their structure was fully elucidated only in 1998 with the discovery that they are heterodimeric G-protein coupled receptors, formed from the GABA<sub>B1</sub> and GABA<sub>B2</sub> subunits, both of which are required to generate functional receptors.<sup>50</sup> The GABA binding site is located on GABA<sub>B1</sub> whereas GABA<sub>B2</sub> is responsible for G-protein coupling (Figure 2.9). No isoform of the GABA<sub>B2</sub> subunit has been reported yet but the GABA<sub>B1</sub> subunit exists mainly in two isoforms, GABA<sub>B(1a)</sub> and GABA<sub>B(1b)</sub>. The former is predominant in the developing brain whereas the latter is the main isoform in the adult brain.<sup>51</sup>

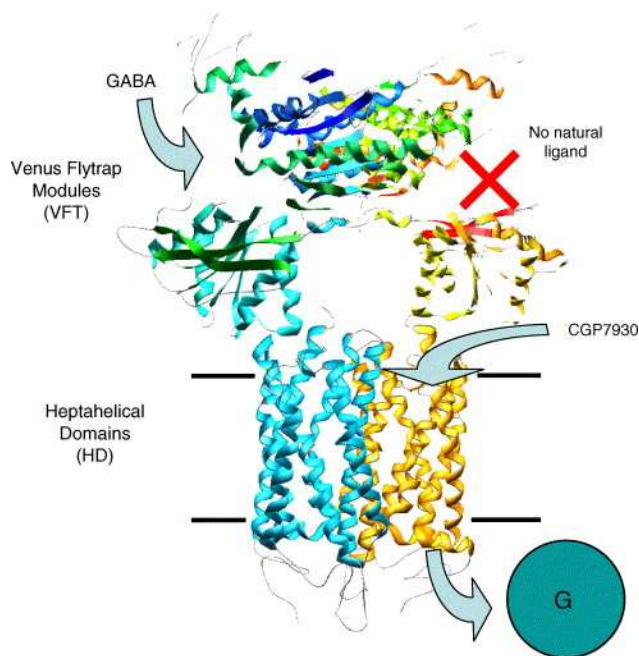


Figure 2.9: Proposed structural organisation of the heteromeric GABA<sub>B</sub> receptor. Classical GABA<sub>B</sub> ligands bind in the cleft of the GABA<sub>B1</sub> VFT shown on the left.<sup>52</sup>

Mutational studies of the GABA<sub>B</sub> binding site, guided by homology models have shown that the Ser246, Ser269, Glu465 residues in lobe I in addition to Tyr366 and Tyr385 in lobe II are important for agonist and antagonist binding.<sup>53</sup> These homology models of the GABA<sub>B</sub> binding site have been built using the structure of leucine/isoleucine/valine-



binding proteins (Figures 2.10 and 2.11).<sup>54, 55</sup> It is worth noting that the phenyl ring of baclofen (**59**) can fit well between Tyr366 and Tyr395 and form a possible  $\pi$ - $\pi$  stacking interaction with those groups.

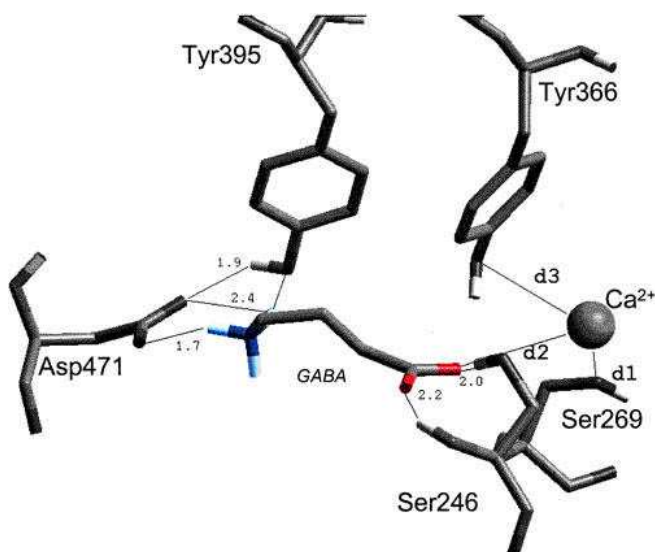


Figure 2.10: Model of GABA and Ca<sup>2+</sup> docked into the ligand-binding site of GABA<sub>B1</sub> published in 2001.<sup>54</sup>

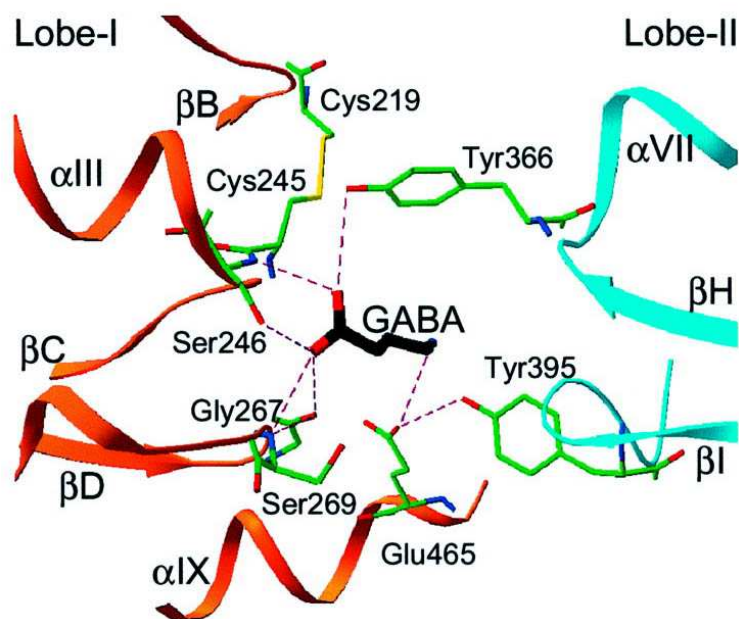
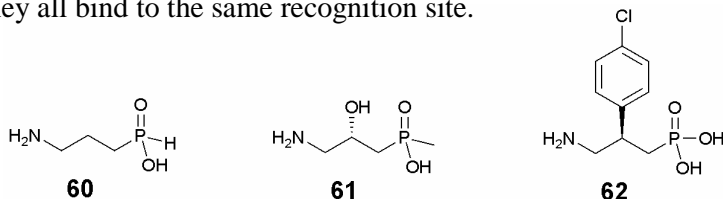


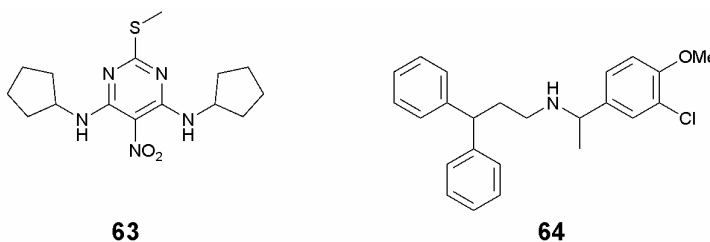
Figure 2.11: Model of GABA docked into the ligand-binding site of GABA<sub>B1</sub> published in 2002.<sup>55</sup>



Unlike GABA<sub>A</sub> receptors, the pharmacological diversity of GABA<sub>B</sub> receptors seems limited. In fact, the agonist baclofen (**59**) introduced to the market in 1972 to treat neuronal seizures is still the prototype of selective GABA<sub>B</sub> receptor agonists. The similar structures of selective agonists (**60**)<sup>56</sup> and (**61**)<sup>57</sup> and the antagonist (*R*)-phaclofen (**62**)<sup>58</sup> suggests that they all bind to the same recognition site.



However, intensive high-throughput screening in the last few years has revealed some structurally different allosteric compounds, such as GS39783 (**63**) or 3-chloro-4-methoxyfendiline (**64**) which have potential clinical applications.<sup>59</sup> They are thought to bind to the GABA<sub>B2</sub> subunit. The discovery of this allosteric modulation has suddenly turned GABA<sub>B</sub> receptors into more attractive targets for anaesthetic drugs.



A combination of mutational and computational studies has allowed convincing GABA binding site models for GABA<sub>A</sub> and GABA<sub>B</sub> receptors to be constructed. This will help to reveal how the GABA molecule is orientated in its binding sites in order for example, to design more potent analogues. It should also give a better understanding of the conformational changes induced by GABA binding in order to disclose at the atomic level the gating mechanism of GABA receptors.

Homology modelling is certainly a useful tool to approach the three dimensional structure of proteins for which no crystal structure is available. However, the dynamics and the complex structural changes which occur during receptor activation render the current models inadequate for designing new potent modulators of the GABA<sub>A</sub> or GABA<sub>B</sub> receptors. In fact, QSAR analyses have proven so far to be the method of choice over the last 40 years and an impressive number of GABA analogues have been designed and found to selectively bind only one receptor of the GABA system.

Selective GABA agonists or antagonists are valuable pharmaceutical tools that can be used as molecular keys to selectively open or close GABA receptor subtypes in order to elucidate their specific functions. In addition, selective GABA agonists can also have therapeutic applications.

## 2.3 Binding studies of GABA analogues

GABA is a conformationally flexible molecule. It is achiral but it binds to chiral proteins, namely GABA<sub>A</sub> and GABA<sub>B</sub> receptors, GABA transporters and GABA aminotransferase. The fact that some GABA analogues of restricted conformation exhibit selectivity to the above proteins indicates that GABA binds in diverse conformations to its binding sites.

Despite the intensive efforts made to define the “active conformations” of GABA and despite the relatively large number of analogues which exhibit selectivity to one protein, little is known of the preferred binding conformations of GABA. The difficulty in solving this question lies in the fact that the potency of GABA analogues depends not only on their conformation in the binding site, but also in their ability to approach this site and to initiate the conformational changes which result in the activation of GABA receptors. The conformations of GABA can be characterised by the distance between the nitrogen and the carbon of the carboxylate,  $\delta_{(N-C)}$  and by two torsion angles  $\tau_N$  and  $\tau_C$  as shown in Figure 2.12.

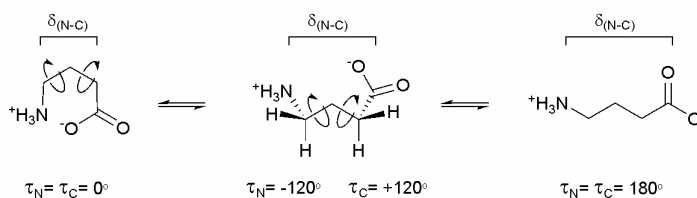


Figure 2.12: Characteristic parameters of GABA conformations.

Some interesting reviews have been published in the last twenty years, in order to draw a general picture of the preferred binding conformations of GABA and eventually to construct 3-D pharmacophore models for GABA binding.<sup>60-63</sup> Tables **2.1** and **2.2** present the structures of some conformationally restricted GABA analogues as well as their biological activities on GABA<sub>A</sub>, GABA<sub>B</sub> binding and GABA uptake. The values are given relative to the activity of GABA which has been assigned the value 100. Also given in Table **2.1** and **2.2** are  $\delta_{(N-C)}$ ,  $\tau_N$  and  $\tau_C$  values.

Curiously, the  $\delta_{(N-C)}$  distance is not a determining factor in GABA<sub>A</sub> binding ability, as potent GABA<sub>A</sub> agonists have  $\delta_{(N-C)}$  values ranging from 4.29 to 4.97 Å. This still indicates that GABA binds to GABA<sub>A</sub> receptors in a partially extended conformation. It is assumed that the carboxylate binds first to an arginine residue (either  $\alpha_1$ Arg66,  $\alpha_1$ Arg119 or  $\beta_2$ Arg207)<sup>46, 63, 64</sup> and that the side chain of this arginine possesses some flexibility within the binding pocket. The ligand then accommodates itself in the binding site to present the ammonium group to either some counter ion or a  $\pi$ -system.<sup>46</sup>

It appears after examination of Table **2.1** that negative values for both  $\tau_N$  and  $\tau_C$  are associated with high activity towards GABA<sub>A</sub> receptors. This is particularly clear by comparing the activities of the enantiomers **(70)**-**(71)**, **(72)**-**(73)** and **(74)**-**(75)**.

However, defining further the preferred torsion angles  $\tau_N$  and  $\tau_C$  for GABA<sub>A</sub> binding is very speculative. It seems that compounds with  $\tau_C$  between -140° and -180° have good GABA<sub>A</sub> activities. Similarly,  $\tau_N$  between -130° and -170° give good GABA<sub>A</sub> activity as indicated by **(73)**, **(75)** and **(77)**. This however doesn't account for the high efficacies of isoguvacine **(66)** and THIP **(67)** which have  $\tau_N$  values between -11° and +50°, depending on which GABA backbone, as well as which six-membered ring conformation is considered.

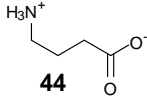
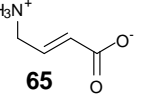
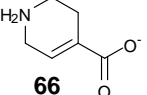
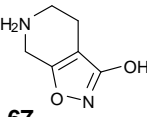
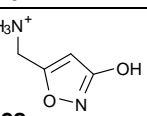
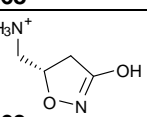
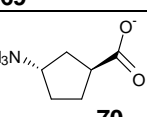
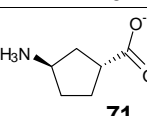
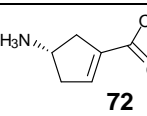
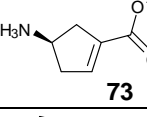
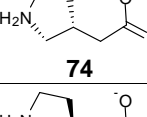
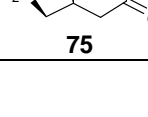
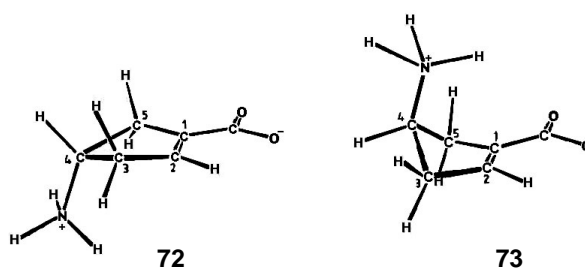
compound	Structure	GABA <sub>A</sub>	GABA <sub>B</sub>	GABA uptake	$\delta_{(N-C)}$	T <sub>N</sub>	T <sub>C</sub>
GABA	 <b>44</b>	100	100	100	2.72-4.96	free	free
<i>Trans</i> -aminocrotonic acid	 <b>65</b>	41	1.3	31.5	4.29-4.94	free	180°
Isoguvacine	 <b>66</b>	~100	<1	<1	4.29	±11° ±50°	±178° ±160°
THIP	 <b>67</b>	33	<1	<1	4.22	±10° ±49°	±179° ±158°
Muscimol	 <b>68</b>	550	1.3	1.3	4.29-4.68	free	180°
(S)-(+)-dihydro-muscimol	 <b>69</b>	825	0.2	<1	3.77-4.73	free	-144°
(1 <i>S</i> ,3 <i>S</i> )- <i>trans</i> -ACP	 <b>70</b>	~500	Not tested	<1	4.97	-132°	-140°
(1 <i>R</i> ,3 <i>R</i> )- <i>trans</i> -ACP	 <b>71</b>	2.5	Not tested	~200	4.97	+132°	+140°
(4 <i>S</i> )-ACP-1-ene	 <b>72</b>	~160	Not tested	<1	4.96	-139°	-168°
(4 <i>R</i> )-ACP-1-ene	 <b>73</b>	<1	Not tested	50	4.96	+139°	+168°
( <i>R</i> )-homo-β-proline	 <b>74</b>	47	<1	188	4.24-4.88	-167°	free
( <i>S</i> )-homo-β-proline	 <b>75</b>	3.7	0.4	111	4.24-4.88	+167°	free

Table 2.1: Biological activities of GABA analogues.<sup>60, 62, 65</sup> (cont. overleaf)

compound	Structure	GABA <sub>A</sub>	GABA <sub>B</sub>	GABA uptake	$\delta_{(N-C)}$	T <sub>N</sub>	T <sub>C</sub>
(S)-(+)-3-OH-GABA <b>76</b>		8.3	1.3	10.3	2.72-4.96	free	free
(R)-(-)-3-OH-GABA <b>77</b>		3.3	8.6	4.5	2.72-4.96	free	free
(RS)-3-OMe-GABA <b>78</b>		<1	<1	<1	2.72-4.96	free	free
(R)-(-)-baclofen <b>59</b>		<1	38.5	1	3.12-4.89	free	free

Table 2.2: Biological activities of GABA analogues.<sup>60, 62</sup>

A comparison of the activities of enantiomers (**72**) and (**73**), (4*S*)- and (4*R*)-(+)-4-aminocyclopent-1-ene carboxylic acid, reveals stereochemical details on the active conformations of GABA in the GABA<sub>A</sub> receptor and the GABA uptake sites. Indeed, (**72**) and (**73**) differ only by the orientation of the amino group, but (4*S*)-(**72**) is GABA<sub>A</sub> selective whereas (4*R*)-(**73**) is GABA uptake selective. The other set of enantiomers (**70**)-(**71**) also indicates that the conformation (*S*) is required for GABA<sub>A</sub> binding activity. The preferred  $\tau_N$ , shown below for (**72**), is around  $-115^\circ$ .<sup>61</sup> It was assigned  $-139^\circ$  in Table 2.1.<sup>62</sup>

Figure 2.13: Best fit structures of (**72**) and (**73**) for the GABA<sub>A</sub> receptor and the uptake site respectively.<sup>61</sup>

Less information is available for selective GABA<sub>B</sub> ligands. To date, only two GABA analogues are reported to possess relatively good selectivity towards GABA<sub>B</sub> receptors: these are (*R*)-baclofen (**59**) and (*R*)-3-hydroxy-GABA (**77**). Interestingly, (**77**) shows a small preference for the GABA<sub>B</sub> receptor whereas its enantiomer (**76**) demonstrates the opposite selectivity and is more active as a GABA<sub>A</sub> agonist. It is however difficult to draw any conclusion for GABA<sub>B</sub> ligands because no conformationally restricted compound with potent GABA<sub>B</sub> activity has yet been found.

It should be noted that the polar hydroxyl group of (*R*)-3-hydroxy-GABA (**77**) has the opposite stereochemical orientation to the lipophilic aromatic group of (*R*)-baclofen. Substitution of the hydroxyl by a methoxyl group suppresses the activity in (**78**), strongly suggesting that the hydroxyl interacts with polar residues on one side of the GABA<sub>B</sub> binding site. Conversely, the aromatic group of baclofen is directed into a lipophilic cavity on the other side. Since both ionised groups NH<sub>3</sub><sup>+</sup> and CO<sub>2</sub><sup>-</sup> tend to orient away from the lipophilic cavity, it was suggested that the GABA<sub>B</sub> binding site prefers to bind GABA conformations having opposite signs for  $\tau_N$  and  $\tau_C$  (butterfly conformations).<sup>62</sup>

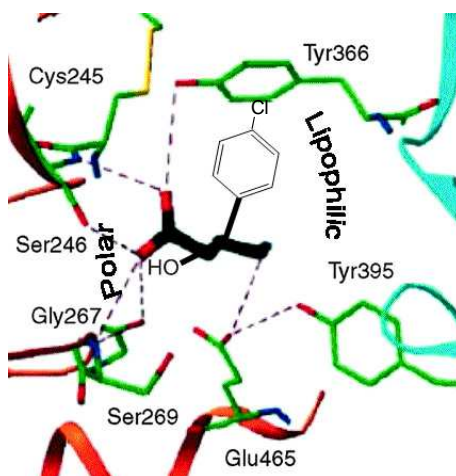
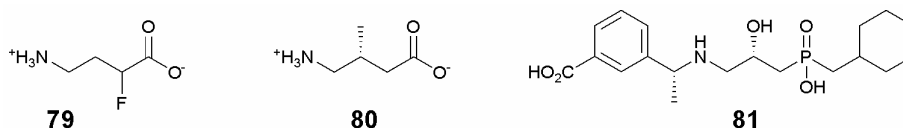


Figure 2.14: Model of the GABA<sub>B</sub> binding site showing the lipophilic cavity on the right hand side of the GABA molecule and the polar cavity on the left hand side (adapted from J. Kniazeff *et al.*, *J. Neurosci.*, 2002).<sup>55</sup>

Other GABA analogues have been tested on the GABA system. 2-Fluoro-GABA (**79**) for example was found to have good GABA uptake binding potency, being 2.3 times less potent than GABA (43% of the GABA activity).<sup>66, 67</sup>

Interestingly, (*R*)-3-methyl-GABA (**80**) was found to be an activator of L-glutamic acid decarboxylase (GAD). Activation of GAD results in an increase in the GABA concentration in the CNS, which confers (*R*)-3-methyl-GABA (**80**) with anticonvulsant properties. Compound (**80**) was found to have the best *in vitro* activity on purified pig brain GAD of all GABA analogues tested in Silverman's studies. However, its *in vivo* anticonvulsant activity was found to be modest. Compound (**80**) appears to allosterically activate GAD, increasing  $V_{\max}$  without affecting the  $K_m$  of L-glutamate. Its enantiomer, (*S*)-3-methyl-GABA, has very little potency.<sup>68, 69</sup>



Binding studies with GABA analogues have furnished valuable information for the design of new ligands. For example, specific GABA<sub>B</sub> antagonists *e.g.* compound (**81**) with a hydroxyl group at the 3-position and with the (*R*) stereochemistry, have been designed from the observation that (**77**) is GABA<sub>B</sub> selective.<sup>70, 71</sup>

3D-pharmacophore models based on the analyses of known ligands have been constructed, but often in the context of identifying low-potency GABA agonists or antagonists. Indeed, neither full GABA agonists nor antagonists may be useful therapeutic agents; therefore efforts have not focused on discovering highly potent GABA analogues, which are of academic interest only. This is one of the numerous reasons why the active

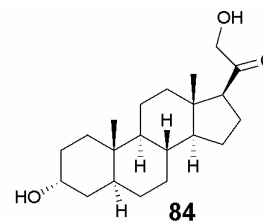
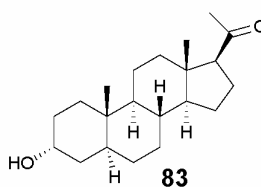
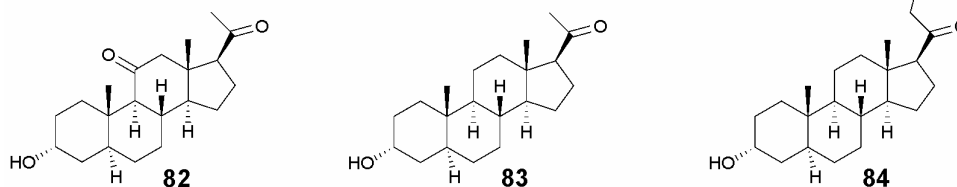


conformations of GABA on GABA<sub>A</sub> and GABA<sub>B</sub> receptors are still elusive. However, the data in Tables 2.1 and 2.2 will surely prove to be useful once precise models of the GABA binding sites can be constructed or once the crystal structures of GABA receptors can be solved.

## 2.4 Steroid modulation of the GABA response

### 2.4.1 The nature of steroid modulation

The anaesthetic action of endogenous steroids was first observed in 1941<sup>72</sup> but it was only in 1984 that their ability to enhance neuronal inhibition *via* the GABA<sub>A</sub> receptor was demonstrated.<sup>73</sup> The synthetic steroid alphaxalone, 5 $\alpha$ -pregnan-11,20-dione (**82**) as well as endogenous steroids allopregnanolone, 5 $\alpha$ -pregnan-3 $\alpha$ -ol-20-one (**83**) and tetrahydrodeoxycorticosterone (THDOC), 5 $\alpha$ -pregnan-3 $\alpha$ ,21-diol-20-one (**84**) are all active at low nanomolar concentrations and are believed to enhance the interactions of GABA with the GABA<sub>A</sub> receptor, thereby stabilising the open state of the receptor channel complex.<sup>74</sup> However, at higher concentrations, steroids directly activate the GABA<sub>A</sub> receptor in the absence of GABA. This dual effect indicates that the steroid-mediated potentiation of GABA occurs in two distinct ways which has long complicated the elucidation of their mode of action.

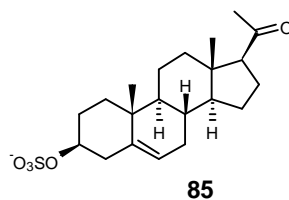


Strong indications such as the selective and enantioselective nature of the steroid potentiation suggest the existence of a specific steroid recognition site on the GABA<sub>A</sub> receptor. It is selective because steroids have no effect on the GABA<sub>B</sub> receptor and enantioselective because *ent*-allopregnanolone, the non-natural enantiomer of allopregnanolone (**83**) is much less active than its natural counterpart.<sup>75</sup>

Over the past ten years, numerous studies have been carried out on neurosteroids acting at GABA<sub>A</sub> receptors. Interest has been stimulated by the therapeutic potential of such neurosteroids as anticonvulsants, sedatives and hypnotics<sup>76</sup> and also by the lack of knowledge concerning their mode of action.

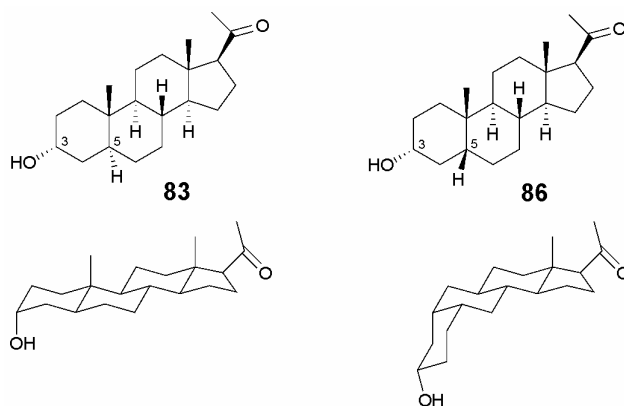
Analogues of the most potent neurosteroids have been synthesised and their biological activity on GABA<sub>A</sub> receptors was tested. This has allowed different classes of steroids to be determined.

Thus, 3 $\beta$ -steroids were found to be non-competitive antagonists: they inhibit the potentiation induced by 3 $\alpha$ -steroids through activation-dependent blocking of GABA<sub>A</sub> receptors but they also reduce barbiturate and GABA potentiation.<sup>77</sup> 3 $\beta$ -Sulfate steroids such as pregnenolone sulphate (**85**) have similar effects.



The 5 $\beta$ -steroids were found to have similar activity to 5 $\alpha$ -steroids on GABA potentiation.<sup>78</sup> This was a rather surprising result as 5 $\alpha$ - and 5 $\beta$ -steroids belong to two distinct structural classes with a different backbone and might be expected to bind quite

differently to the recognition site. Allopregnanolone (**83**) and pregnanolone (5 $\beta$ -pregnan-3 $\alpha$ -ol-20-one) (**86**) are typical representatives of both classes.



Significant progress in understanding the neurosteroid-mediated action on GABA<sub>A</sub> receptors was made in 2006 in a landmark article published in *Nature* by A. M. Hosie and T. G. Smart.<sup>79</sup> They discovered that neurosteroids regulate GABA<sub>A</sub> receptors through two discrete transmembrane sites: one site mediates the potentiating effect and the other the direct activation effect. They succeeded in localising the potentiation site by constructing chimera GABA<sub>A</sub> receptors having low potentiation sensitivity and lacking direct activation by neurosteroids. After identification of the subunit domain critical for potentiation, they mutated several polar residues and determined that Thr236 on the  $\alpha$ 1 subunit was critical for steroid activation and Gln241 also on the  $\alpha$ 1 subunit essential for steroid potentiation. By constructing homology models, they could then locate Thr236 and Gln241 and identify the other amino acid residues involved in the binding sites. Figures **2.15** and **2.16** show the neurosteroid activation site and potentiation site respectively.

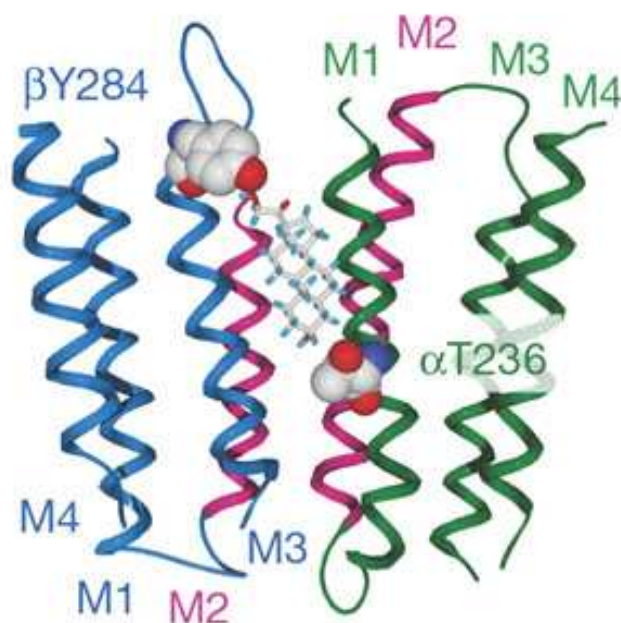


Figure **2.15**: Neurosteroid activation binding site spanning the  $\beta/\alpha$ -subunit interface. View through the lipid bilayer of model GABA<sub>A</sub> receptor transmembrane region with a bound THDOC molecule.  $\alpha$ Thr236 and  $\beta$ Tyr284 are predicted to face the surrounding lipid.<sup>79</sup>

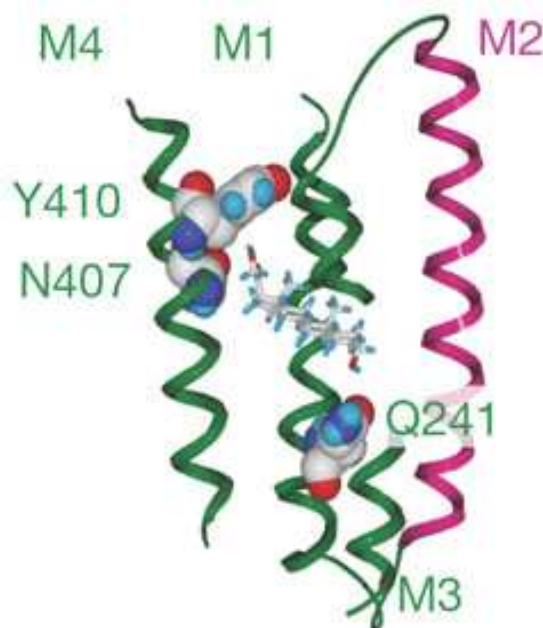


Figure **2.16**: Neurosteroid potentiation binding site. Ribbon structure of  $\alpha$ -subunit M1–M4, showing  $\alpha$ Gln241,  $\alpha$ Asn407 and  $\alpha$ Tyr410 docking with a THDOC molecule, viewed from the lipid bilayer. The channel lining the M2 domain is shown in purple, and a section of M3 is omitted for clarity.<sup>79</sup>

Both binding sites are located in the transmembrane domain and are only accessible to hydrophobic molecules, although the potentiation site seems to lie at the base of a water-filled cavity between the  $\alpha$  subunit's M1-M4 domains. It was found that the potentiation site cannot distinguish between  $5\alpha$ - and  $5\beta$ -reduced steroids whereas the activation site may differentiate the two classes and have a different pharmacophore. As outlined in Figure 2.17, significant receptor activation by neurosteroids relies on occupancy of both the activation and potentiation sites, which is in accordance with the fact that direct activation is appreciable only at high concentration.

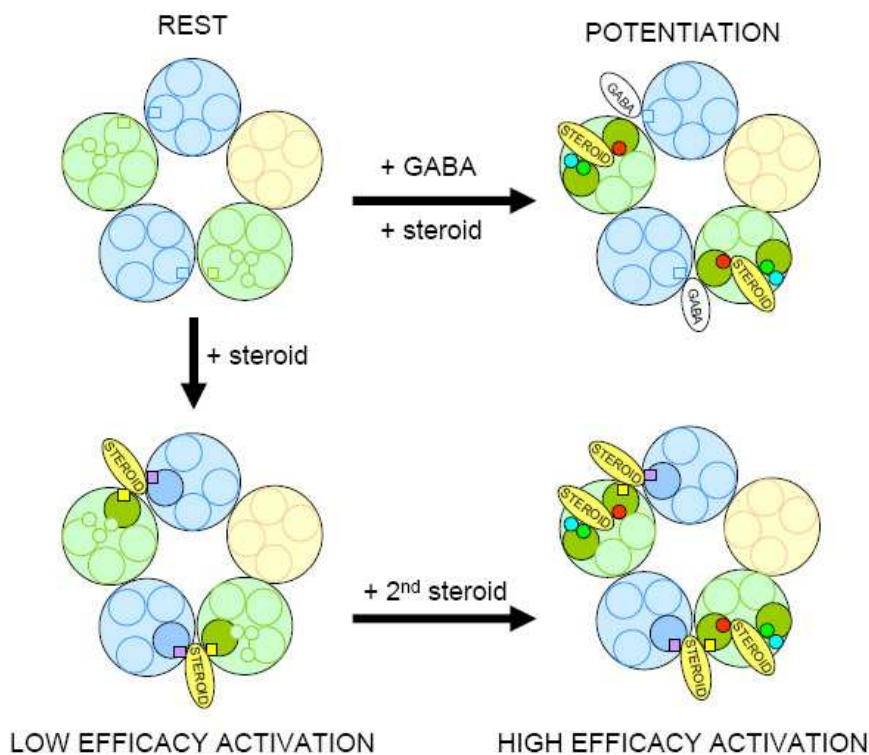
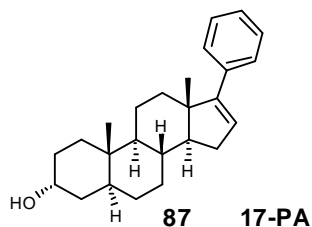


Figure 2.17: Diagram of the GABA<sub>A</sub> receptor indicating how the occupation of the neurosteroid binding sites affects receptor activation and the potentiation of GABA responses. Neurosteroid activation of GABA<sub>A</sub> receptors is proposed to be a two-step process. Binding to the activation site is followed by occupation of the potentiation site.<sup>79</sup>

The identification of the steroid binding sites allows a better understanding of their mode of action and now allows the building of more precise 3-D binding site models and the design of new neurosteroids displaying improved potentiation or activation responses.

The design of selective antagonists is pharmacologically pertinent as such compounds could be used in anaesthesia to selectively reverse the anaesthetic effects of sedative steroids, to help patients recover after surgery for example. Selective antagonists may also help shed light on the physiological function of GABA-potentiating neurosteroids in health and disease.

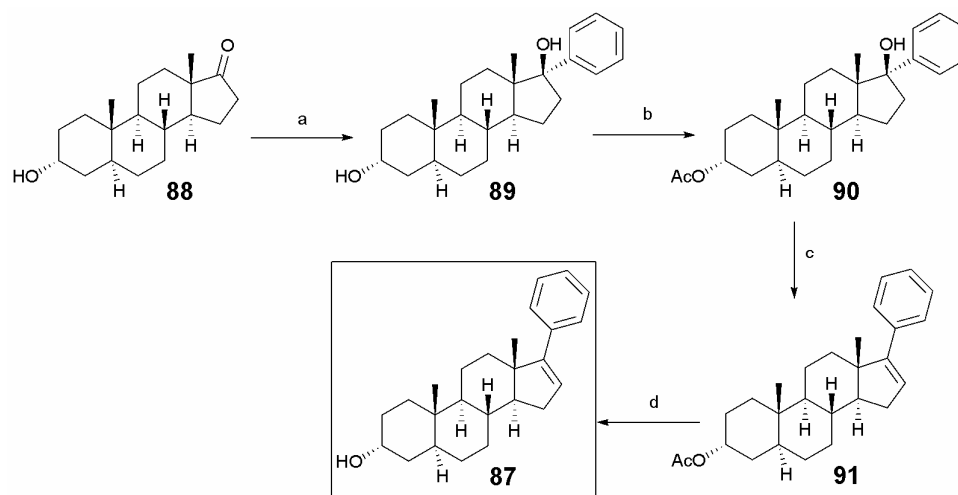
However, only one compound has been reported to date to act as a selective steroid antagonist. Its structure was published in 2004<sup>80</sup> and immediately raised the interest of neurobiologists. (3 $\alpha$ ,5 $\alpha$ )-17-Phenylandroster-16-en-3-ol, (17-PA) (**87**) was found to selectively antagonise 5 $\alpha$ -reduced neurosteroid effects at GABA<sub>A</sub> receptors whereas 5 $\beta$ -reduced steroids were only weakly affected. 17-PA (**87**) was also reported to have little or no effect on baseline GABA responses and barbiturate potentiation.<sup>80</sup> Thus 17-PA represented in 2004 an attractive pharmaceutical tool of a new class to explore neurosteroids effects.



Our collaborators from the School of Neurobiology in Dundee had developed an interest in this compound. It was decided to undertake the synthesis of 17-PA and to develop a series of analogues bearing different substituents on the aromatic ring in order to explore structure-activity relationships.

## 2.4.2 Synthesis of steroid selective inhibitors

The synthesis of 17-PA (**87**) which was reported by Covey *et al.*,<sup>80</sup> starts from commercially available androsterone (**88**). Addition of phenyllithium generated diol (3 $\alpha$ ,5 $\alpha$ ,17 $\beta$ )-17-phenylandrosterane,3,17-diol (**89**) which was then acetylated at the 3-position. Dehydration of tertiary alcohol (**90**) was achieved by adding methanesulfonyl chloride and triethylamine in DCM. Subsequent hydrolysis of the acetate furnished 17-PA as a white solid in 4 steps and 39% overall yield (Scheme 2.3).

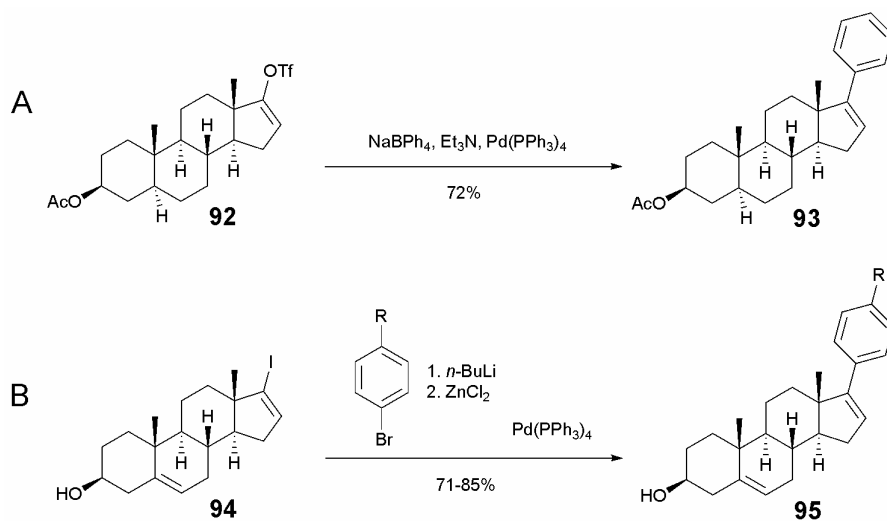


Scheme 2.3: Synthesis of 17-PA (**87**) from androsterone (**88**) as reported by Covey *et al.*<sup>80</sup>  
 Reagents and conditions: a) PhLi, THF, 0 °C to 25 °C, 5 h, 44%; b) Ac<sub>2</sub>O, pyridine, DMAP, 25 °C, 5 min, 95%; c) MsCl, Et<sub>3</sub>N, DCM, 0 °C, 40 min, 99%; d) NaOH, H<sub>2</sub>O, MeOH, 65 °C, 1 h, 95%.

Different approaches can be considered for the synthesis of 17-PA, but although steroid chemistry is well documented, only a few examples of C<sup>17</sup>-phenyl-substituted steroids have been reported.

The use of palladium chemistry represents a possible alternative to the above synthesis of 17-PA. It was reported for example that the palladium-catalyzed cross-

coupling of sodium tetraphenylborate ( $\text{NaBPh}_4$ ) with vinyl triflates<sup>81</sup> proceeds smoothly and in good yields (Scheme 2.4 A). However, very few derivatives of tetraphenylborates are commercially available which renders this method unattractive to the generating of a series of 17-PA analogues with different substituents on the aromatic ring. Likewise, Negishi coupling of arylzinc chlorides with vinyl iodides<sup>82</sup> can be envisaged as an alternative strategy to 17-PA (**87**) (Scheme 2.4 B). This method is appealing as it directly furnishes the unsaturated steroid and avoids the tedious protection-deprotection sequence shown in Scheme 2.3. Although these alternative methods were potential candidates, it was decided to follow the published synthesis in the first instance.<sup>80</sup>



Scheme 2.4: Syntheses of 17-PA analogues (**93**) and (**95**) illustrating possible alternative syntheses to 17-PA.<sup>81, 82</sup>

Phenyllithium was generated *in situ* by lithium-bromine exchange using  $n\text{-BuLi}$  and bromobenzene in dry  $\text{Et}_2\text{O}$  at 0 °C. This mixture was added to a solution of androsterone (**88**) in THF and after work-up and purification, diol (**89**) was obtained. The procedures followed that described in the original report<sup>80</sup> and gave (**89**) as a colorless solid in a modest 43% yield. The low conversion is mainly due to the propensity of ketone (**88**) to enolise in the presence of aryllithium. Also, 20% of unreacted starting material was

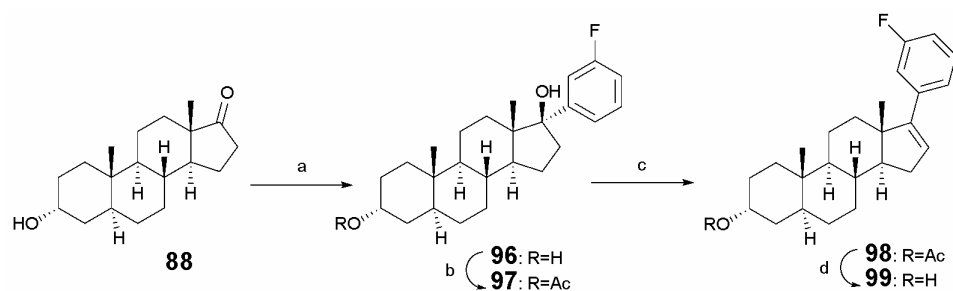


recovered from this reaction. For the rest of the synthesis, the published reaction conditions were strictly followed and compounds (**89**), (**90**), (**91**) and 17-PA (**87**) were obtained in yields similar to those reported. All characterisation data were in accordance with the published data.

With this reference compound in hand and a working knowledge of the route, we then addressed the synthesis of fluorinated analogues of 17-PA. As described in chapter 1, it was anticipated that the introduction of fluorine should induce only minor steric changes without altering the pharmacological profile of 17-PA.

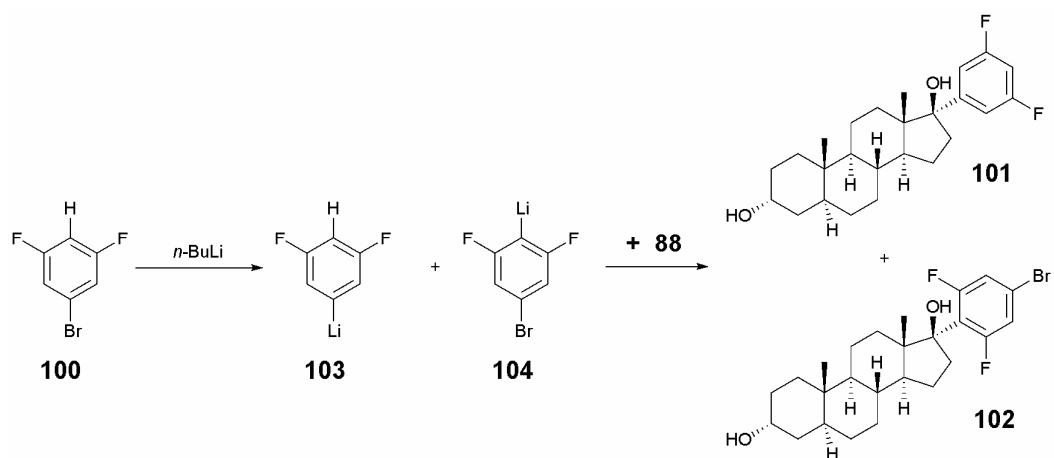
The synthesis of the *meta*-fluorinated 17-PA analogue was first investigated. Presumably, a fluorine atom in the *meta*-position on the aromatic ring induces some steric and electronic dissymmetry that can be accommodated in the recognition site by the free rotation of the ring. This might be beneficial for the biological activity of the compound.

3-Fluorophenyllithium was prepared by reacting *n*-BuLi with 3-fluorobromobenzene in dry Et<sub>2</sub>O at -78 °C. Low temperature was required to prevent decomposition of the fluorinated aryllithium. The mixture was then added at -78 °C to a solution of androsterone in THF. It should be noted that androsterone was not soluble in Et<sub>2</sub>O which might be preferable for this kind of reaction. After work-up and purification, the product (3 $\alpha$ ,5 $\alpha$ ,17 $\beta$ )-17-(*m*-fluorophenyl)androstane-3,17-diol (**96**) was obtained as a colourless solid in a low 31% yield. Acetylation of (**96**) under the reaction conditions used for the synthesis of 17-PA gave (**97**) in 80% yield. Subsequent dehydration of the tertiary alcohol and hydrolysis of the acetate as described previously, furnished the target compound (3 $\alpha$ ,5 $\alpha$ )-17-(*m*-fluorophenyl)androst-16-en-3-ol (**99**) as a colourless solid in 15% overall yield from androsterone (Scheme 2.5).



Scheme **2.5**: Synthesis of the *m*-fluorophenyl analogue of 17-PA (**99**) using published reaction conditions.<sup>80</sup> Reagents and conditions: a) 3-Fluorobromobenzene, *n*-BuLi, Et<sub>2</sub>O, -78 °C to 25 °C, 15 h, 31%; b) Ac<sub>2</sub>O, pyridine, DMAP, 25 °C, 15 min, 80%; c) MsCl, Et<sub>3</sub>N, CH<sub>2</sub>Cl<sub>2</sub>, 0 °C, 45 min, 67%; d) NaOH, H<sub>2</sub>O, MeOH, 65 °C, 1 h, 90%.

The synthesis of the *meta*-difluorophenyl analogue was then addressed. *n*-BuLi was added at -78 °C to a solution of 3,5-difluorobromobenzene (**100**) in Et<sub>2</sub>O. The mixture was stirred for 3 h and added at -78 °C to a solution of androsterone in THF. TLC analysis showed a complex mixture of products and purification of the crude material by column chromatography proved to be difficult. However, NMR and mass spectroscopy analyses of selected fractions were found to be consistent with the formation of two main products, (**101**) and (**102**) although these compounds could not be fully purified.



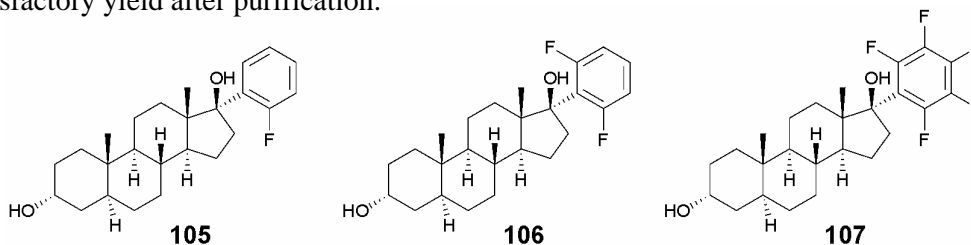
Scheme **2.6**: Attempted synthesis of (**101**). The combined electron withdrawing effect of the two fluorine atoms render the *ortho* hydrogen susceptible to exchange, leading to a mixture of (**103**) and (**104**).

As shown on Scheme 2.6, the increased acidity of the hydrogen atom *ortho* to the fluorine atoms promotes lithium-hydrogen exchange to the detriment of lithium-bromine exchange, leading to a mixture of 1,3-difluorophenyl-5-lithium (**103**) and 1,3-difluorophenyl-2-lithium (**104**). This generates the product mixture of (**101**) and (**102**) after reaction with androsterone.

This example shows the importance of controlling and understanding the formation of the phenyllithium derivative for the synthesis of 17-PA analogues. The lithium-bromine exchange reaction using *n*-BuLi and an aryl bromide was first described in 1938 by Wittig and co-workers<sup>83</sup> and has been widely used since then. Yet, its mechanism remains unclear because competing reactions such as  $\beta$ -eliminations and Wurtz-type couplings as well as the fact that organolithium compounds do not exist as monomers in solution, complicate its examination. Halophilic attack of *n*-BuLi to the halogen or a radical-mediated process are the two main explanations for this mechanism.<sup>84</sup>

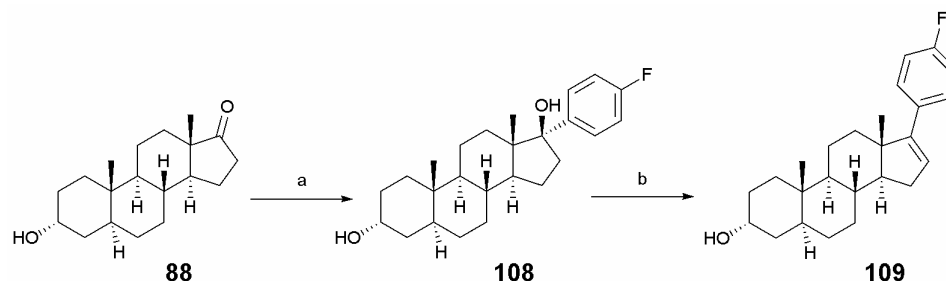
The particular reactivity of fluorinated bromobenzenes with *n*-BuLi has also been studied. Generally, fluorinated phenyllithiums are stable only at very low temperature. In the case of *ortho*-fluorophenyllithiums, elimination of LiF occurs above -50 °C and generates benzyne.<sup>84-87</sup>

Preparation of the fluorinated analogues of 17-PA, (**105**), (**106**) and (**107**) were also attempted but were unsuccessful, either because the lithium-bromine or lithium-hydrogen exchange reaction failed or because the fluorinated steroid could not be obtained in a satisfactory yield after purification.



The synthesis of the *para*-fluorinated analogue (**109**) of 17-PA was however successful. Preparation of 4-fluorophenyllithium was achieved by reacting *n*-BuLi with 4-fluorobromobenzene in Et<sub>2</sub>O. The mixture was then added at -78 °C to a solution of androsterone in THF. After work-up and purification, (3 $\alpha$ ,5 $\alpha$ ,17 $\beta$ )-17-(*p*-fluorophenyl)androstane-3,17-diol (**108**) was obtained in 40% yield. The development of a strongly UV-active compound after leaving (**108**) in CHCl<sub>3</sub> for a few days was an indication that the tertiary alcohol was not stable under acidic conditions. It is known that tertiary alcohols are prone to dehydrate by an E1 mechanism. Therefore, the acid-catalysed dehydration of (**108**) was attempted in order to shorten the synthesis of these 17-PA analogues to two steps. A catalytic amount of *p*-toluenesulfonic acid monohydrate (pTSA) was added to a solution of (**108**) in DCM and the mixture was heated under reflux for 4 h.

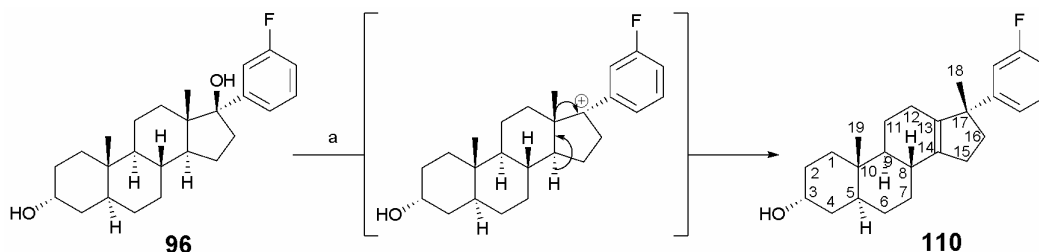
NMR analysis of the crude material revealed the formation of the desired product (3 $\alpha$ ,5 $\alpha$ )-17-(*p*-fluorophenyl)androst-16-en-3-ol (**109**) along with a slightly less polar compound (~15% according to crude NMR analysis). The separation by column chromatography of these two products was achievable but difficult. Nevertheless, (**109**) was obtained as a colourless solid in 60% yield from (**108**) and was fully characterised (Scheme 2.7).



Scheme 2.7: Synthesis of the *p*-fluorophenyl analogue of 17-PA (**109**).  
 Reagents and conditions: a) 4-Fluorobromobenzene, *n*-BuLi, Et<sub>2</sub>O, -78 °C to 25 °C, 12 h, 40%;  
 b) pTSA, DCM, reflux, 4 h, 60%.

As shown in Scheme 2.7, the *para*-fluorophenyl analogue (**109**) of 17-PA could be prepared in two steps from androsterone by direct dehydration of the tertiary alcohol under acidic conditions. It was interesting to examine whether the *meta*-fluorophenyl analogue (**99**) could also be prepared by this shorter route.

Accordingly, a solution of (**96**) in DCM was treated with pTSA and heated under reflux. Forcing conditions (*i.e.* two equivalents of pTSA and heating under reflux for 5 h) had to be applied to achieve complete dehydration of (**96**). A mixture of two products was obtained but this time, the major one was not the expected strongly UV-active compound (**99**). Despite the difficulty of separating the two products by column chromatography, it was possible to isolate the unknown compound in 52% yield. NMR analysis revealed the absence of the ethylenic proton on C<sup>16</sup> and a different pattern in <sup>1</sup>H NMR and <sup>13</sup>C NMR on the D ring of the steroid. The structure of compound (**110**) was elucidated by NMR analyses, in collaboration with Dr Tomáš Lébl at the University of St Andrews. The <sup>13</sup>C NMR spectrum of (**110**) was also fully assigned (Scheme 2.8).



Scheme 2.8: Formation of 17 $\alpha$ -(*m*-fluorophenyl)-17 $\beta$ -methyl-5 $\alpha$ -androsten-13-3 $\alpha$ -ol (**110**) by Wagner-Meerwein rearrangement under acidic conditions.

The structure of (**110**) shows that the methyl group C<sup>18</sup>H<sub>3</sub> has migrated from C<sup>13</sup> to C<sup>17</sup>. This type of rearrangement on similar substrates has been observed on many occasions.<sup>88-93</sup> After elimination of H<sub>2</sub>O and the development of a carbocation on C<sup>17</sup>, the adjacent methyl group, which stands almost perpendicular to the skeleton of the steroid,

migrates to C<sup>17</sup>, generating a carbocation on C<sup>13</sup>. Subsequent elimination of H<sup>14</sup> gives the product (**110**). Full assignment of the structure was necessary because the <sup>13</sup>C NMR spectrum presented only twenty-four distinct peaks for twenty-five expected carbons. It was found that C<sup>2</sup> and C<sup>6</sup> have exactly the same chemical shift. High resolution mass spectroscopy confirmed the chemical composition of (**110**) to be C<sub>25</sub>H<sub>33</sub>OF.

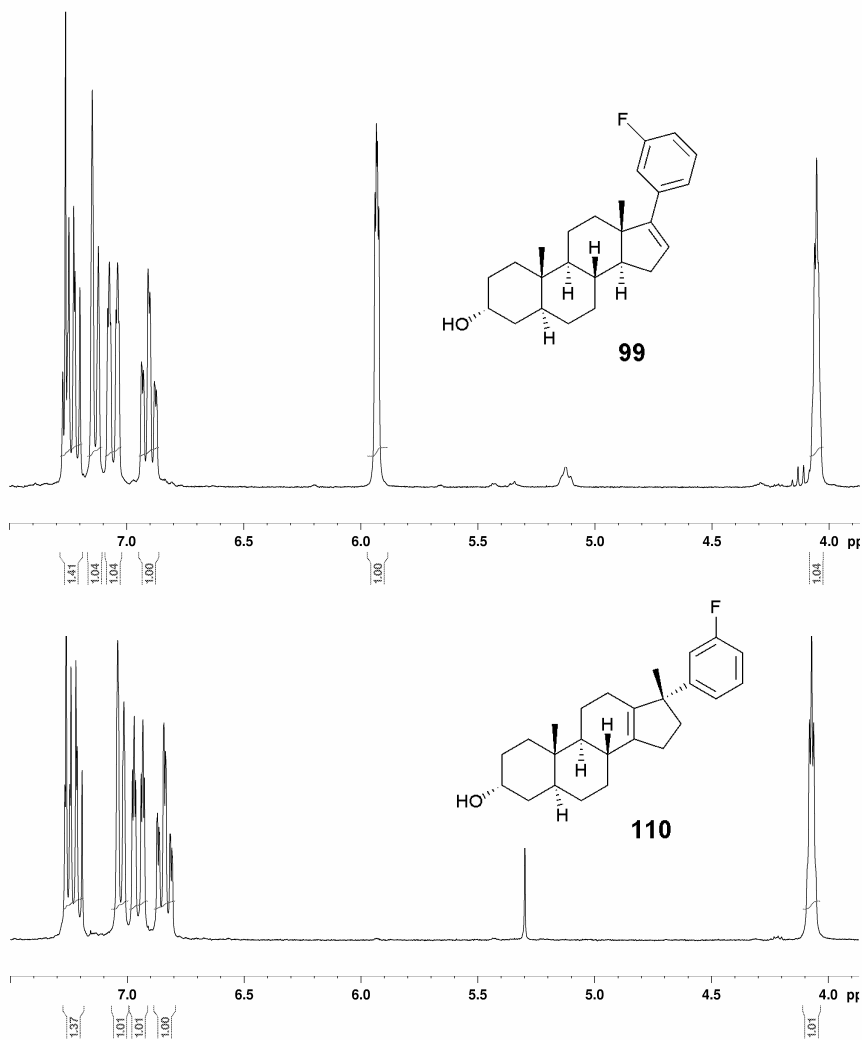
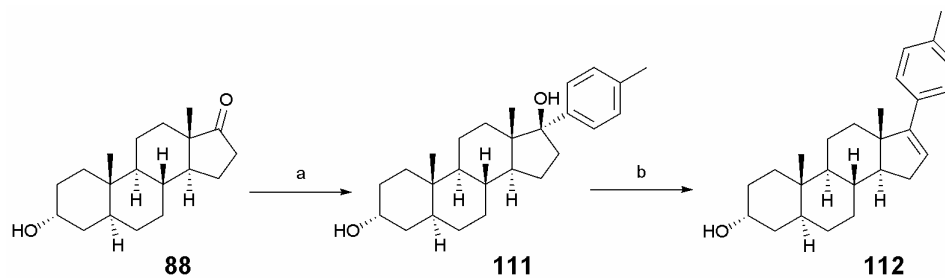


Figure 2.18: <sup>1</sup>H NMR spectra of (**99**) (above) showing the presence of the ethylenic proton H<sup>16</sup> at 5.93 ppm. This signal has disappeared on the <sup>1</sup>H NMR spectrum of (**110**).

The reactivity of the *meta*-fluorophenyl steroid (**96**) is noticeably different from that of the *para*-fluorophenyl steroid (**108**) and illustrates the significance of the fluorine position on reactivity. It seems according to these two examples that fluorine in the *meta*-position destabilises the carbocation on C<sup>17</sup> due to the inductive effect and promotes the rearrangement whereas in the *para*-position, fluorine stabilises the positive charge by the mesomeric effect and promotes the formation of the desired product.

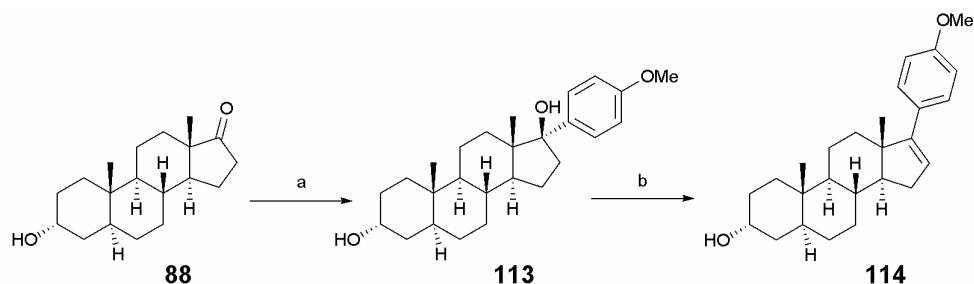
This early indication that electron-donating groups on the aromatic ring may favour the dehydration of the tertiary alcohol under acidic conditions prompted us to synthesise the *para*-methyl (**112**) and the *para*-methoxyl (**114**) derivatives. The *para*-methyl derivative of 17-PA was synthesised in a two-step sequence by addition at RT of a solution of *p*-toluenelithium in Et<sub>2</sub>O to a solution of androsterone in THF followed by dehydration of the tertiary alcohol (**111**) with pTSA in DCM (Scheme 2.10).



Scheme 2.10: Synthesis of the *p*-toluene analogue of 17-PA (**112**).  
Reagents and conditions: a) 4-bromotoluene, *n*-BuLi, Et<sub>2</sub>O, RT, 12 h, 43%;  
b) pTSA, DCM, RT, 2 days, 71%.

The rearranged product was formed in less than 5 % conversion in this case and (3 $\alpha$ ,5 $\alpha$ )-(17-*p*-toluene)androst-16-en-3-ol (**112**) was obtained as a colourless solid in a 71% yield.

The *para*-methoxyl analogue was prepared using the same sequence. It is interesting to note that the tertiary alcohol (**113**) could not be kept in solution and dehydrated rapidly. This is consistent with the donor ability of the methoxyl group. The dehydration step was therefore straightforward as a catalytic amount of pTSA with stirring at RT for 8 h was sufficient to isolate, after purification, the desired product (3 $\alpha$ ,5 $\alpha$ )-17-(*p*-methoxyphenyl)androst-16-en-3-ol (**114**) as a colourless solid in 90% yield. No side product was detected in this reaction (Scheme 2.11).



Scheme 2.11: Synthesis of the *p*-methoxyl analogue of 17-PA (**114**).  
Reagents and conditions: a) 4-bromoanisole, *n*-BuLi, Et<sub>2</sub>O, RT, 12 h, 30%;  
b) pTSA, DCM, RT, 8 h, 90%.

This two-step procedure is very convenient for the preparation of the *p*-methyl- and the *p*-methoxyl analogues of 17-PA (**112**) and (**114**) and is appreciably shorter than the published four-step route to 17-PA.

However, in the situations where a significant amount of undesired product is formed during the acid-mediated dehydration step, the four-step procedure is recommended. This is because the desired product and the rearranged compound are not easily separable. Moreover, the desired product is generally isolated in low yields when the aromatic ring does not bear electron-donating substituents.

The outcome of the dehydration of the tertiary alcohol under acidic conditions strongly depends on the nature and the position of the substituent on the aromatic ring. It is



tempting to correlate the amount of rearranged product to the Hammett parameter of the substituent (Table 2.3).

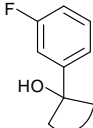
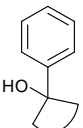
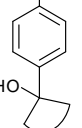
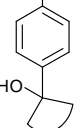
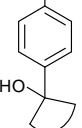
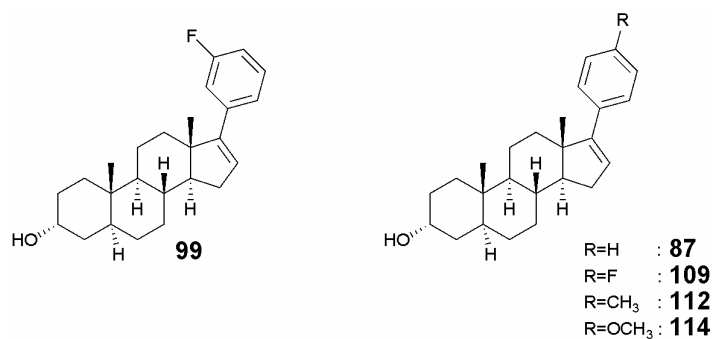
Structure	 <b>96</b>	 <b>89</b>	 <b>108</b>	 <b>111</b>	 <b>113</b>
% of rearranged product	~75	30	15	~5	0
$\sigma$	+0.34	0	+0.06 (or +0.15) <sup>94</sup>	-0.17	-0.29

Table 2.3: Influence of the aromatic substituent on dehydration under acidic conditions.

It seems clear from Table 2.3 that the more electron-donating the substituent, the less favoured is the rearranged product. It is also clear that such substituents promote elimination of H<sub>2</sub>O by stabilising the subsequent carbocation on C<sup>17</sup>. Elimination of H<sup>16</sup> results then in the formation of the conjugated olefin product (**102**). If the carbocation at C<sup>17</sup> is destabilised by an electron-withdrawing substituent, it quickly rearranges by migration of the methyl group to a more stable carbocation on C<sup>13</sup>. This is then followed by elimination of H<sup>14</sup> to form the rearranged product.

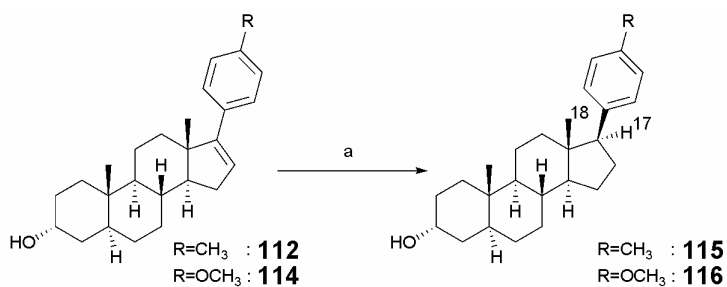
Although the Hammett parameter of fluorine in the *para*-position is positive, it appears from Table 2.3 that it can stabilise the carbocation at C<sup>17</sup> better than hydrogen. It is recognised by both theoretical and experimental observations that fluorine, despite being considered as an electron-withdrawing substituent has an ability to stabilise a positive charge at the *para*-position, because its  $\pi$ -donor ability overcomes its  $\sigma$ -electron-withdrawing effect.<sup>95-97</sup> Conversely at the *meta*-position, only the  $\sigma$ -electron-withdrawing effect is observed.

At the end of this aspect of the study, a set of five compounds, bearing different substituents on the aromatic ring, was prepared.



In order to add some structural diversity in this series of 17-PA analogues, it was decided to hydrogenate the C<sup>16</sup>-C<sup>17</sup> double bond. The hydrogenation is face selective and the resulting saturated compound has the lipophilic aromatic group above the D ring of the steroid in a similar orientation to the acetate moiety in allopregnanolone (**83**).

In this event, the *para*-methyl (**112**) and *para*-methoxyl (**114**) analogues of 17-PA were hydrogenated with palladium on carbon as a catalyst. This furnished the saturated compounds (**115**) and (**116**) in good yields and as single stereoisomers (Scheme 2.12).

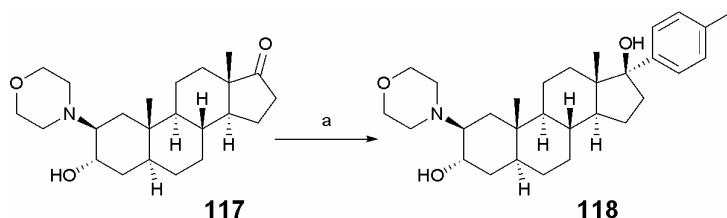


Scheme 2.12: Preparation of saturated 17-PA analogues.  
 Reagents and conditions: a) Pd/C, H<sub>2</sub> (1 atm), EtOAc, 91-93%.

The hydrogenation of each double bond is diastereoselective and the stereochemistry at C<sup>17</sup> was confirmed by NOESY experiments on (**115**), showing that the protons of the C<sup>18</sup> methyl group are close to the aromatic protons and not on the same side as H<sup>17</sup>.

The observation by Prof. Lambert that the steroid analogues of 17-PA were very poorly water-soluble, even at the  $\mu\text{M}$  concentrations required for biological assays spurred us on to synthesise more polar analogues. Organon Ltd is a company which has a lot of experience in the synthesis of steroids. They have developed water-soluble analogues of androsterone and allopregnanolone<sup>98, 99</sup> and generously supplied us with 2 $\beta$ -(4-morpholinyl)-3 $\alpha$ -hydroxy-5 $\alpha$ -androstan-17-one (**117**) as a starting material. The adjunction of a morpholino group at the 2-position generally improves the water solubility without altering the pharmacological profile of steroids, certainly in most cases.

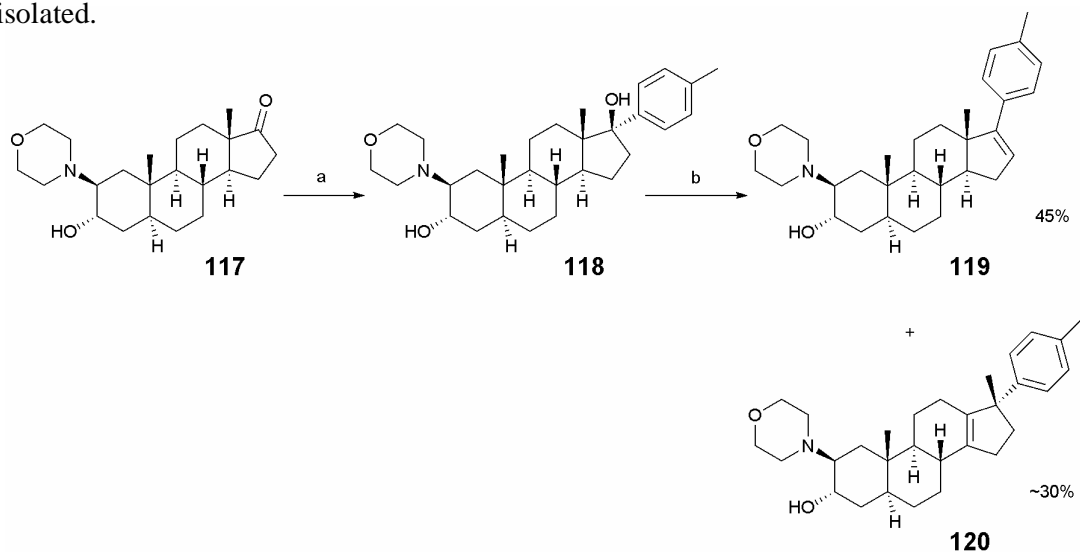
A solution of (**117**) in THF was treated at RT with a solution of *p*-toluenelithium in Et<sub>2</sub>O prepared by addition of *p*-bromotoluene and *n*-BuLi at RT. After work-up and purification, (**118**) was obtained as a white solid in 50% yield (Scheme 2.13).



Scheme 2.13: Preparation of (**118**).  
Reagents and conditions: a) 4-Bromotoluene, *n*-BuLi, Et<sub>2</sub>O, RT, 12 h, 50%.

The dehydration of diol (**118**) to generate the target unsaturated compound (**119**) was expected to proceed similarly to the non-morpholino series. It proved however to be much more difficult. Addition of pTSA to (**118**) did not produce any elimination even after

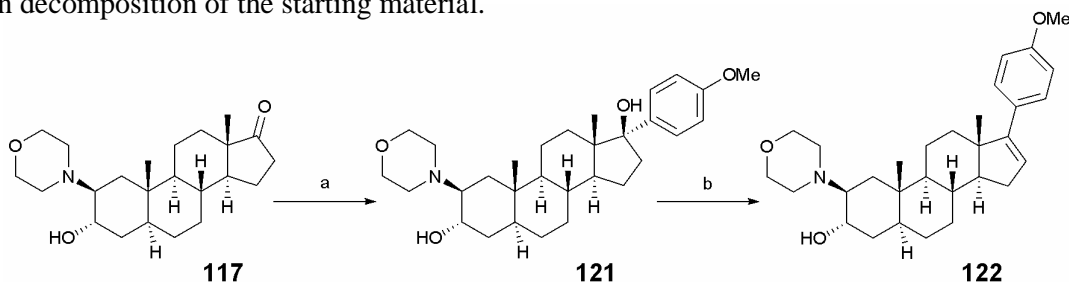
adding more than one equivalent and heating under reflux in DCM for 24 h. After screening various dehydration conditions, including the use of HCl in ether, trifluoroacetic acid, and bases such as DBU, it was found that the addition of trimethylsilyl chloride gave the best results. Thus, treating (**118**) in MeCN with five equivalents of TMSCl for an extended period gave 2 $\beta$ -(4-morpholinyl)-(3 $\alpha$ ,5 $\alpha$ )-(17-*p*-toluene)androst-16-en-3-ol (**119**) as a white solid in 45% yield. The TMS-protected alcohol which probably forms at C<sup>3</sup> is hydrolysed *in situ* by quenching the reaction with potassium carbonate allowing the free alcohol at C<sup>3</sup> to be recovered. It is not clear why TMSCl is the best reagent in this case (Scheme 2.14). The modest yield of the reaction is due to the difficulty in purifying the desired product and to the probable formation of the rearranged compound (**120**) in ~30% conversion, according to NMR analysis of the crude reaction mixture. (**120**) was not isolated.



Scheme 2.14: Synthesis of (**119**). Reagents and conditions: a) 4-Bromotoluene, *n*-BuLi, Et<sub>2</sub>O, RT, 12 h, 50%; b) TMSCl, MeCN, 50 °C, 3 days, K<sub>2</sub>CO<sub>3</sub>, 45%.

The *para*-methoxyl analogue (**122**) was prepared in a similar manner (Scheme 2.15). The dehydration of tertiary alcohol (**121**) was more straightforward here than in the previous case although (**121**) was markedly more stable under acidic conditions

than the non-morpholino compound (**113**). It is probably the nitrogen of the morpholino group that protonates first, but this does not fully explain why the tertiary alcohol on the right-hand side of the molecule does not dehydrate so readily under acidic conditions. It was found that addition of pTSA failed to form (**122**) and forcing conditions resulted only in decomposition of the starting material.

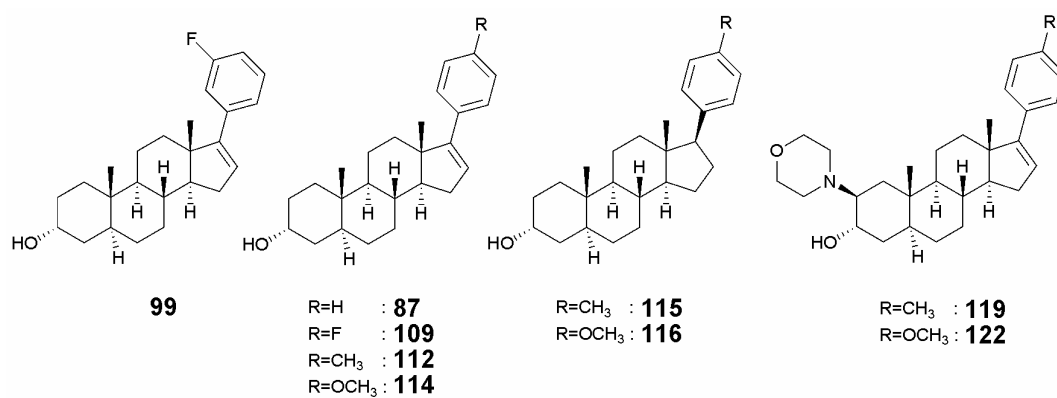


Scheme **2.15**: Synthesis of (**122**). Reagents and conditions: a) 4-Bromoanisole, *n*-BuLi, Et<sub>2</sub>O, RT, 18 h, 37%; b) TMSCl, DCM, RT, 24 h, K<sub>2</sub>CO<sub>3</sub>, 62%.

The target product 2 $\beta$ -(4-morpholinyl)-(3 $\alpha$ ,5 $\alpha$ )-17-(*p*-methoxyphenyl)androst-16-en-3-ol (**122**) was finally obtained in 62% yield by addition of TMSCl and stirring at RT for 24 h. The compound resulting from the Wagner-Meerwein rearrangement, as well as other by-products were detected in the crude mixture but not purified.

### 2.4.3 Biological results

A total of nine steroids were prepared in this project. They were all given to our collaborators at the School of Neurobiology at Ninewells Hospital in Dundee to be tested on recombinant GABA<sub>A</sub> receptors expressed in *Xenopus laevis* oocytes.



The inhibitory action of 17-PA (**87**) against 5 $\alpha$ - and 5 $\beta$ -steroids was assessed and found to be in accordance with the results published by Mennerick *et al.*<sup>80</sup> Preliminary results suggested that *para* substitution (F, CH<sub>3</sub> and OMe) had a significant impact on the biological activity, but a definitive assessment was not forthcoming due mainly to poor solubility.

The discovery of 17-PA was considered at the time of its publication as an important development in the understanding of the steroid modulation of the GABA-response. 17-PA remains today a unique pharmaceutical tool to block the action of anaesthetic neurosteroids on GABA<sub>A</sub> receptors but the more recent publication by M. Hosie and T. G. Smart<sup>79</sup> has somewhat reduced the interest for 17-PA since the existence and the localisation of two discrete binding sites have now been established.

The future of 17-PA and 17-PA analogues lies in the fact that they remain the only selective steroid antagonists identified. However, 17-PA is not an ideal compound to work with: high concentration (10  $\mu$ M) is required to obtain a maximum of around 40% inhibition of the potentiating effect induced by allopregnanolone at 300 nM. This shows that 17-PA is not a potent antagonist and its structure should be taken only as a lead for the development of more efficient antagonists. Improving the water-solubility of 17-PA may reduce the concentration needed and modifying its structure at C<sup>17</sup> may result in better inhibition.

The low water-solubility of 17-PA undeniably constitutes its major drawback. It is hoped that the morphilino-analogues (**119**) and (**122**) will exhibit better activities. Despite the morphilino group, we found that (**122**) was insoluble at 10  $\mu$ M in ethanol and addition of DMSO was necessary to solubilise the steroid. Neurobiologists also observed that 17-PA in DMSO partially precipitates during the biological assays once added into water. Increasing the ionic strength of the solution with a suitable buffer or using surfactants or complexing agents such as cyclodextrins<sup>100, 101</sup> may hold the compound in solution. However optimisation of the solubility to improve the assay by such methods was not explored.

More studies are required to define the role of 17-PA in blocking respectively the activation (*i.e.* direct gating) and the potentiation effects of neurosteroids. The localisation of the two steroid binding sites should inspire neurobiologists to design new experiments with 17-PA analogues. It was found in 2004 that 17-PA was more effective at blocking the activation effects of allopregnanolone than the potentiation effects, but this led to the wrong suggestion that allopregnanolone may act at a single binding site.<sup>80</sup>

### 2.4.4 Conclusions

The preparation of nine 17-PA analogues bearing different substituents on the aromatic ring was achieved in this project. Some compounds were prepared following the four-step synthesis published by Covey *et al.*<sup>80</sup> Some others were prepared using a two-step sequence which proved convenient with electron donating substituents on the aromatic ring. However, the formation of a rearranged product was also observed. This work is a first step towards the design of more potent neurosteroid antagonists. Evaluating their biological activities and possibly docking them into the modelled steroid binding sites developed by M. Hosie and T. G. Smart<sup>79</sup> should give useful information for the design of a second generation of 17-PA analogues.

17-PA (**87**) and 2 $\beta$ -(4-morpholinyl)-(3 $\alpha$ ,5 $\alpha$ )-17-(*p*-methoxyphenyl)androst-16-en-3-ol (**122**) were re-crystallised from DCM and *n*-hexane and the colourless needles obtained were suitable for X-ray crystallography. Their crystal structures, which were solved by Prof. Alexandra Slawin (St Andrews), could be used later for the design of other 17-PA analogues (Figure 2.19).

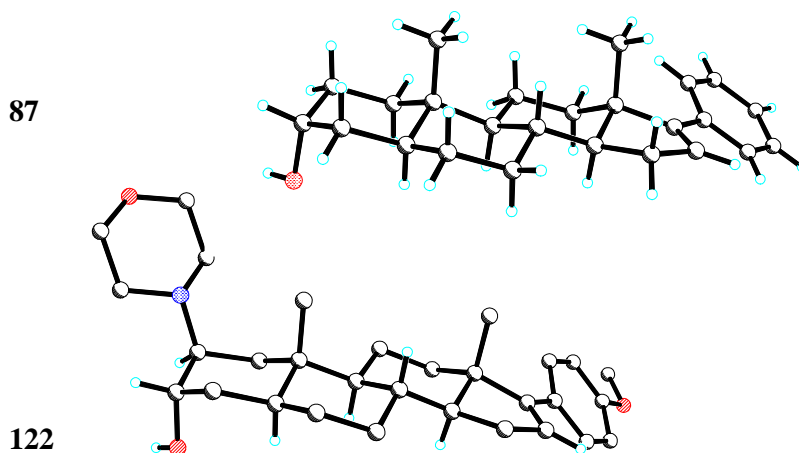


Figure 2.19: X-ray structures of 17-PA (**87**) and the more water-soluble 17-PA analogue (**122**) bearing a morpholino group at the 2-position and a methoxy group at the *para*-position on the aromatic ring.



## 2.5 References

- <sup>1</sup> F. E. Bloom and L. L. Iversen, *Nature*, 1971, **229**, 628-630.
- <sup>2</sup> A. B. Young and D. Chu, *Drug Dev. Res.*, 1990, **21**, 161-167.
- <sup>3</sup> A. L. Bianchi, M. Denavit-Saubie, and J. Champagnat, *Physiol. Rev.*, 1995, **75**, 1-45.
- <sup>4</sup> O. Pierrefiche, A. S. Foutz, and M. Denavit-Saubie, *Brain Res.*, 1993, **605**, 77-84.
- <sup>5</sup> L. S. Wong, G. Eshel, J. Dreher, J. Ong, and D. M. Jackson, *Pharmacol., Biochem. Behav.*, 1991, **38**, 829-835.
- <sup>6</sup> M. J. Millan, *Prog. Neurobiol.*, 1999, **57**, 1-164.
- <sup>7</sup> N. Pitsikas, A. E. Rigamonti, S. G. Cella, and E. E. Muller, *Neuroscience*, 2003, **118**, 1121-1127.
- <sup>8</sup> I. Izquierdo and J. H. Medina, *Trends Pharmacol. Sci.*, 1991, **12**, 260-265.
- <sup>9</sup> C. Gottesmann, *Neuroscience*, 2002, **111**, 231-239.
- <sup>10</sup> O. Hornykiewicz, K. G. Lloyd, and L. Davidson, in *GABA in Nervous System Functions*, ed. E. Roberts, T. N. Chase, and D. B. Tower, Raven Press, New York, 1976.
- <sup>11</sup> T. Aoyagi, T. Wada, M. Nagai, F. Kojima, S. Harada, T. Takeuchi, H. Takahashi, K. Hirokawa, and T. Tsumita, *Chem. Pharm. Bull.*, 1990, **38**, 1748-1749.
- <sup>12</sup> K. Gale, *Epilepsia*, 1989, **30**, 1-11.
- <sup>13</sup> D. A. Slaterry and J. F. Cryan, *Drug Dev. Res.*, 2006, **67**, 477-494.
- <sup>14</sup> B. Lippert, B. W. Metcalf, M. J. Jung, and P. Casara, *Eur. J. Biochem.*, 1977, **74**, 441-445.
- <sup>15</sup> J. A. Davies, *Seizure*, 1995, **4**, 267-271.
- <sup>16</sup> L. Gram, O. M. Larsson, A. Johnsen, and A. Schousboe, *Br. J. Clin. Pharmacol.*, 1989, **27**, 13-17.
- <sup>17</sup> L. Nagarajan, T. Schramm, D. B. Appleton, C. J. Burke, and M. J. Eadie, *Clin. Exp. Neurol.*, 1993, **30**, 127-136.
- <sup>18</sup> S. Choi, P. Storici, T. Schirmer, and R. B. Silverman, *J. Am. Chem. Soc.*, 2002, **124**, 1620-1624.

- <sup>19</sup> P. Storici, D. De Biase, F. Bossa, S. Bruno, A. Mozzarelli, C. Peneff, R. B. Silverman, and T. Schirmer, *J. Biol. Chem.*, 2004, **279**, 363-373.
- <sup>20</sup> P. Storici, G. Capitani, D. De Biase, M. Moser, R. A. John, J. N. Jansonius, and T. Schirmer, *Biochemistry*, 1999, **38**, 8628-8634.
- <sup>21</sup> S. Hog, R. Greenwood Jeremy, B. Madsen Karsten, M. Larsson Orla, B. Frolund, A. Schousboe, P. Krosggaard-Larsen, and P. Clausen Rasmus, *Curr. Top. Med. Chem.*, 2006, **6**, 1861-1882.
- <sup>22</sup> P. Krosggaard-Larsen, B. Frolund, and K. Frydenvang, *Curr. Pharm. Des.*, 2000, **6**, 1193-1209.
- <sup>23</sup> P. D. Suzdak and J. A. Jansen, *Epilepsia*, 1995, **36**, 612-626.
- <sup>24</sup> J. Guastella, N. Nelson, H. Nelson, L. Czyzyk, S. Keynan, M. C. Miedel, N. Davidson, H. A. Lester, and B. I. Kanner, *Science*, 1990, **249**, 1303-1306.
- <sup>25</sup> G. A. R. Johnston, *Pharmacol. Ther.*, 1996, **69**, 173-198.
- <sup>26</sup> B. O. Dubrovsky, *Prog. Neuro-Psychopharmacol. Biol. Psychiatry*, 2005, **29**, 169-192.
- <sup>27</sup> D. Bitran, R. J. Hilvers, and C. K. Kellogg, *Brain Res.*, 1991, **561**, 157-161.
- <sup>28</sup> D. I. B. Kerr and J. Ong, *Pharmacol. Ther.*, 1995, **67**, 187-246.
- <sup>29</sup> P. R. Schofield, M. G. Darlison, N. Fujita, D. R. Burt, F. A. Stephenson, H. Rodriguez, L. M. Rhee, J. Ramachandran, V. Reale, and et al., *Nature*, 1987, **328**, 221-227.
- <sup>30</sup> K. Kaupmann, K. Huggel, J. Heid, P. J. Flor, S. Bischoff, S. J. Mickel, G. McMaster, C. Angst, H. Bittiger, W. Froestl, and B. Bettler, *Nature*, 1997, **386**, 239-246.
- <sup>31</sup> W. Sieghart and G. Sperk, *Curr. Top. Med. Chem.*, 2002, **2**, 795-816.
- <sup>32</sup> R. Baur and E. Sigel, *J. Neurochem.*, 2003, **87**, 325-332.
- <sup>33</sup> K. Brejc, W. J. van Dijk, R. V. Klaassen, M. Schuurmans, J. van der Oost, A. B. Smit, and L. K. Sixma, *Nature*, 2001, **411**, 269-276.
- <sup>34</sup> N. Unwin, *J. Mol. Biol.*, 2005, **346**, 967-989.
- <sup>35</sup> R. B. Russell, M. A. S. Saqi, R. A. Sayle, P. A. Bates, and M. J. E. Sternberg, *J. Mol. Biol.*, 1997, **269**, 423-439.
- <sup>36</sup> Y. Muroi, C. Czajkowski, and M. B. Jackson, *Biochemistry*, 2006, **45**, 7013-7022.
- <sup>37</sup> J. Mercado and C. Czajkowski, *J. Neurosci.*, 2006, **26**, 2031-2040.
- <sup>38</sup> V. I. Chupakhin, V. A. Palyulin, and N. S. Zefirov, *Dokl. Biochem. Biophys.*, 2006, **408**, 169-174.
- <sup>39</sup> M. Ernst, S. Bruckner, S. Boresch, and W. Sieghart, *Mol. Pharmacol.*, 2005, **68**, 1291-1300.

- <sup>40</sup> J. R. Trudell and E. Bertaccini, *J. Mol. Graphics Modell.*, 2004, **23**, 39-49.
- <sup>41</sup> M. Ernst, D. Brauchart, S. Boresch, and W. Sieghart, *Neuroscience*, 2003, **119**, 933-943.
- <sup>42</sup> V. Campagna-Slater and D. F. Weaver, *J. Mol. Graphics Modell.*, 2007, **25**, 721-730.
- <sup>43</sup> J. G. Newell, R. A. McDevitt, and C. Czajkowski, *J. Neurosci.*, 2004, **24**, 11226-11235.
- <sup>44</sup> J. G. Newell and C. Czajkowski, *J. Biol. Chem.*, 2003, **278**, 13166-13172.
- <sup>45</sup> A. J. Boileau, A. R. Evers, A. F. Davis, and C. Czajkowski, *J. Neurosci.*, 1999, **19**, 4847-4854.
- <sup>46</sup> C. L. Padgett, A. P. Hanek, H. A. Lester, D. A. Dougherty, and S. C. R. Lummis, *J. Neurosci.*, 2007, **27**, 886-892.
- <sup>47</sup> N. J. Harrison and S. C. R. Lummis, *J. Mol. Model.*, 2006, **12**, 317-324.
- <sup>48</sup> N. J. Harrison and S. C. R. Lummis, *J. Biol. Chem.*, 2006, **281**, 24455-24461.
- <sup>49</sup> N. G. Bowery, D. R. Hill, A. L. Hudson, A. Doble, D. N. Middlemiss, J. Shaw, and M. Turnbull, *Nature*, 1980, **283**, 92-94.
- <sup>50</sup> K. Kaupmann, B. Malitschek, V. Schuler, J. Heid, W. Froestl, P. Beck, J. Mosbacher, S. Bischoff, A. Kulik, R. Shigemoto, A. Karschin, and B. Bettler, *Nature*, 1998, **396**, 683-687.
- <sup>51</sup> J. F. Cryan and K. Kaupmann, *Trends Pharmacol. Sci.*, 2005, **26**, 36-43.
- <sup>52</sup> J.-P. Pin, J. Kniazeff, V. Binet, J. Liu, D. Maurel, T. Galvez, B. Duthey, M. Havlickova, J. Blahos, L. Prezeau, and P. Rondard, *Biochem. Pharmacol.*, 2004, **68**, 1565-1572.
- <sup>53</sup> B. Bettler, K. Kaupmann, J. Mosbacher, and M. Gassmann, *Physiol. Rev.*, 2004, **84**, 835-867.
- <sup>54</sup> G. Costantino, A. Macchiarulo, A. E. Guadix, and R. Pellicciari, *J. Med. Chem.*, 2001, **44**, 1827-1832.
- <sup>55</sup> J. Kniazeff, T. Galvez, G. Labesse, and J.-P. Pin, *J. Neurosci.*, 2002, **22**, 7352-7361.
- <sup>56</sup> N. G. Bowery, B. Bettler, W. Froestl, J. P. Gallagher, F. Marshall, M. Raiteri, T. I. Bonner, and S. J. Enna, *Pharmacological Reviews*, 2002, **54**, 247-264.
- <sup>57</sup> J. Ong, S. Bexis, V. Marino, D. A. S. Parker, D. I. B. Kerr, and W. Froestl, *Eur. J. Pharmacol.*, 2001, **412**, 27-37.
- <sup>58</sup> W. Froestl, S. J. Mickel, R. G. Hall, G. von Sprecher, D. Strub, P. A. Baumann, F. Brugger, C. Gentsch, J. Jaekel, and et al., *J. Med. Chem.*, 1995, **38**, 3297-3312.
- <sup>59</sup> J. Ong and D. I. B. Kerr, *CNS Drug Reviews*, 2005, **11**, 317-334.

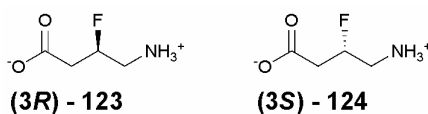
- <sup>60</sup> E. Falch, A. Hedegaard, L. Nielsen, B. R. Jensen, H. Hjeds, and P. Krogsgaard-Larsen, *J. Neurochem.*, 1986, **47**, 898-903.
- <sup>61</sup> R. D. Allan, H. W. Dickenson, and J. Fong, *Eur. J. Pharmacol.*, 1986, **122**, 339-348.
- <sup>62</sup> M. Simonyi, *Enantiomer*, 1996, **1**, 403-414.
- <sup>63</sup> P. Krogsgaard-Larsen, B. Frolund, and T. Liljefors, *Chem. Rec.*, 2002, **2**, 419-430.
- <sup>64</sup> P. Krogsgaard-Larsen, B. Frolund, T. Liljefors, and B. Ebert, *Biochem. Pharmacol.*, 2004, **68**, 1573-1580.
- <sup>65</sup> L. Nielsen, L. Brehm, and P. Krogsgaard-Larsen, *J. Med. Chem.*, 1990, **33**, 71-77.
- <sup>66</sup> V. N'Goka, G. Schlewer, J. M. Linget, J. P. Chambon, and C. G. Wermuth, *J. Med. Chem.*, 1991, **34**, 2547-2557.
- <sup>67</sup> L. L. Iversen and G. A. R. Johnston, *J. Neurochem.*, 1971, **18**, 1939-1950.
- <sup>68</sup> R. B. Silverman, R. Andruszkiewicz, S. M. Nanavati, C. P. Taylor, and M. G. Vartanian, *J. Med. Chem.*, 1991, **34**, 2295-2298.
- <sup>69</sup> R. Andruszkiewicz and R. B. Silverman, *J. Biol. Chem.*, 1990, **265**, 22288-22291.
- <sup>70</sup> S. J. Enna, S. A. Reisman, and J. A. Stanford, *Neurosci. Lett.*, 2006, **406**, 102-106.
- <sup>71</sup> S. Badran, M. Schmutz, and H.-R. Olpe, *Eur. J. Pharmacol.*, 1997, **333**, 135-142.
- <sup>72</sup> H. Selye, *Proc. Soc. Exp. Biol. Med.*, 1941, **46**, 116-121.
- <sup>73</sup> N. L. Harrison and M. A. Simmonds, *Brain Res.*, 1984, **323**, 287-292.
- <sup>74</sup> H. Callachan, G. A. Cottrell, N. Y. Hather, J. J. Lambert, J. M. Nooney, and J. A. Peters, *Proc. R. Soc. London, B*, 1987, **231**, 359-369.
- <sup>75</sup> Y. Hu, L. L. Wittmer, M. Kalkbrenner, A. S. Evers, C. F. Zorumski, and D. F. Covey, *J. Chem. Soc., Perkin Trans. 1*, 1997, **24**, 3665-3671.
- <sup>76</sup> J. W. Sear, *Eur. J. Anaesthesiol.*, 1998, **15**, 129-132.
- <sup>77</sup> M. Wang, Y. He, L. N. Eisenman, C. Fields, C.-M. Zeng, J. Mathews, A. Benz, T. Fu, E. Zorumski, J. H. Steinbach, D. F. Covey, C. F. Zorumski, and S. Mennerick, *J. Neurosci.*, 2002, **22**, 3366-3375.
- <sup>78</sup> D. F. Covey, A. S. Evers, S. Mennerick, C. F. Zorumski, and R. H. Purdy, *Brain. Res. Rev.*, 2001, **37**, 91-97.
- <sup>79</sup> A. M. Hosie, M. E. Wilkins, H. M. A. da Silva, and T. G. Smart, *Nature*, 2006, **444**, 486-489.
- <sup>80</sup> S. Mennerick, Y. He, X. Jiang, B. D. Manion, M. Wang, A. Shute, A. Benz, A. S. Evers, D. F. Covey, and C. F. Zorumski, *Mol. Pharmacol.*, 2004, **65**, 1191-1197.
- <sup>81</sup> P. G. Ciattini, E. Morera, and G. Ortar, *Tetrahedron Lett.*, 1992, **33**, 4815-4818.

- <sup>82</sup> A. Przewdziecka, A. Kurek-Tyrlik, and J. Wicha, *Collect. Czech. Chem. Commun.*, 2002, **67**, 1658-1668.
- <sup>83</sup> G. Wittig, U. Pockels, and H. Droge, *Chem. Ber.*, 1938, **71B**, 1903-1912.
- <sup>84</sup> W. F. Bailey and J. J. Patricia, *J. Organomet. Chem.*, 1988, **352**, 1-46.
- <sup>85</sup> M. Schlosser, *Angew. Chem., Int. Ed.*, 2005, **44**, 376-393.
- <sup>86</sup> M. Schlosser and C. Heiss, *Eur. J. Org. Chem.*, 2003, 4618-4624.
- <sup>87</sup> H. Gilman and R. D. Gorsich, *J. Am. Chem. Soc.*, 1956, **78**, 2217-2222.
- <sup>88</sup> P. Tapolcsanyi, J. Welfling, E. Mernyak, and G. Schneider, *Monatsh. Chem.*, 2004, **135**, 1129-1136.
- <sup>89</sup> P. Tapolcsanyi, J. Welfling, and G. Schneider, *Steroids*, 2001, **66**, 623-635.
- <sup>90</sup> P. Bydal, K.-M. Sam, and D. Poirier, *Steroids*, 1996, **61**, 349-353.
- <sup>91</sup> V. Kumar, C. Rodger, and M. R. Bell, *J. Org. Chem.*, 1995, **60**, 4591-4594.
- <sup>92</sup> D. G. Loughhead, *J. Org. Chem.*, 1985, **50**, 3931-3934.
- <sup>93</sup> G. Ortar and I. Torrini, *Tetrahedron*, 1977, **33**, 859-863.
- <sup>94</sup> M. Sjöstrom and S. Wold, *Chem. Scr.*, 1976, **9**, 200-210.
- <sup>95</sup> R. Yamdagni and P. Kebarle, *J. Am. Chem. Soc.*, 1976, **98**, 1320-1324.
- <sup>96</sup> T. X. Carroll, T. D. Thomas, H. Bergersen, K. J. Borge, and L. J. Strehle, *J. Org. Chem.*, 2006, **71**, 1961-1968.
- <sup>97</sup> Z. B. Maksic, B. Kovacevic, and D. Kovacek, *J. Phys. Chem. A*, 1997, **101**, 7446-7453.
- <sup>98</sup> C. L. Hewett, D. S. Savage, J. J. Lewis, and M. F. Sugrue, *J. Pharm. Pharmacol.*, 1964, **16**, 765-767.
- <sup>99</sup> A. Anderson, A. C. Boyd, A. Byford, A. C. Campbell, D. K. Gemmell, N. M. Hamilton, D. R. Hill, C. Hill-Venning, J. J. Lambert, M. S. Maidment, V. May, R. J. Marshall, J. A. Peters, D. C. Rees, D. Stevenson, and H. Sundaram, *J. Med. Chem.*, 1997, **40**, 1668-1681.
- <sup>100</sup> M. E. Brewster, K. S. Estes, and N. Bodor, *J. Parenter. Sci. Technol.*, 1989, **43**, 262-265.
- <sup>101</sup> K. S. Cameron, J. K. Clark, A. Cooper, L. Fielding, R. Palin, S. J. Rutherford, and M. Q. Zhang, *Org. Lett.*, 2002, **4**, 3403-3406.

## Chapter 3: Synthesis and evaluation of 3-fluoro-GABA enantiomers.

### 3.1 Introduction

This chapter describes the enantioselective synthesis and analysis of the enantiomers of 3-fluoro- $\gamma$ -aminobutyric acid (**123**) and (**124**).



The presence of fluorine at the 3-position in (**123**) and (**124**) is expected to influence the conformational populations of the molecules, particularly with respect to C-F and C-N<sup>+</sup> bonds orientations. A strong *gauche* effect is observed in protonated  $\beta$ -fluoroamines, where the ammonium group prefers to align *gauche* to the C-F bond. This situation exists in 3-F-GABA and *gauche* conformations are estimated to be 4-5 kcal.mol<sup>-1</sup> lower in energy than the conformations where the C-N<sup>+</sup> bond is *anti* to the C-F bond. With such an energy difference, the *anti* conformations will hardly be populated in solution and we can assume that either (**123**) or (**124**) will be a poor mimic of GABA if the binding conformations to a GABA receptor or enzyme required the C-F and C-N<sup>+</sup> bonds to adopt an *anti* relationship. Thus, the introduction of the C-F bond can be viewed as a tool to influence the conformation of GABA and explore the conformational requirements for

GABA binding to a target protein. The torsion angle  $\tau_N$  of 3-F-GABA is limited in this case to only two values for each enantiomer, corresponding to the two most stable conformations:  $-60^\circ$  and  $+180^\circ$  for (3*R*)-F-GABA and  $+60^\circ$  and  $+180^\circ$  for (3*S*)-F-GABA. It follows that the two enantiomers (**123**) and (**124**) are likely to display different biological activities on GABA receptors as they can adopt distinctive conformations (Figure 3.1).

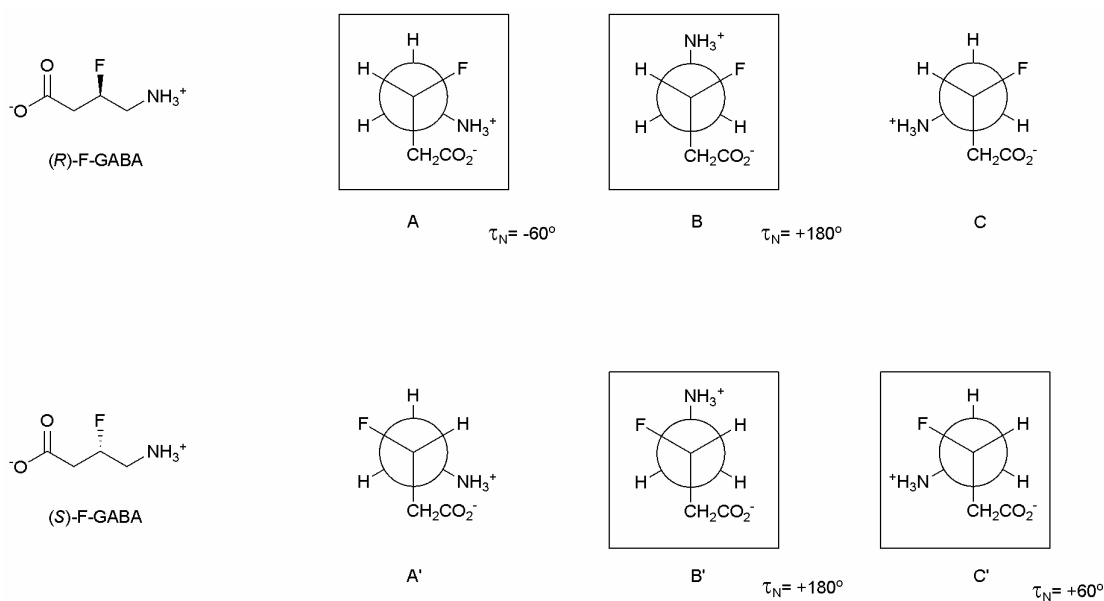


Figure 3.1: Newman projections along the F-C-C-N<sup>+</sup> bond showing the three staggered conformations for both enantiomers (3*R*)-F-GABA and (3*S*)-F-GABA. The conformations highlighted in boxes are predicted to be the most populated in solution as they have C-F/C-N<sup>+</sup> *gauche* relationships.

Figure 3.1 shows the different staggered conformations A/A', B/B' and C/C' with rotation around the C-C-C-N<sup>+</sup> bond and for which  $\tau_N$  has the values  $-60^\circ$ ,  $+180^\circ$  and  $+60^\circ$  respectively. Both enantiomers (3*R*)- and (3*S*)-F-GABA can access the B/B' conformation in which the fluorine atom and the ammonium group are *gauche*. As the conformations with the fluorine *anti* to the amino group are expected not to be significantly populated in solution, conformation C is not accessible to (3*R*)-F-GABA and conformation A' is not accessible to (3*S*)-F-GABA.

It follows that a comparison of the relative biological activities of (3*R*)- and (3*S*)-F-GABA on GABA binding sites should reveal the active conformations of GABA. For example, if the biological activity of (3*R*)- and (3*S*)-F-GABA on a GABA receptor were found to be similar, this would suggest that the active conformations have  $\tau_N$  values close to  $+180^\circ$  (conformer B/B'). Conversely, if (3*R*)-F-GABA was significantly more active than its enantiomer, we could conclude that the most active conformation at this GABA receptor is close to  $\tau_N = -60^\circ$  (conformer A/A'). If (3*S*)-F-GABA was more active than its enantiomer, then conformer C/C' would be more relevant. Experiments can be conducted on GABA<sub>A</sub> or GABA<sub>B</sub> receptors, GABA transporters and the metabolising enzyme GABA aminotransferase. The working hypothesis implies that GABA recognition sites do not distinguish between conformations B and B' which differ only by the orientation of the fluorine atom. This appears a reasonable assumption at the outset as fluorine is a good hydrogen mimic introducing only a minor steric perturbation.

The 3-F-GABA enantiomers have never previously been synthesised or evaluated in any biological system. It was considered that such an evaluation should furnish useful additional information on active GABA conformations. Such information can be compared with the accumulated data from previous experiments using constrained GABA analogues (see Tables **2.1** and **2.2**).

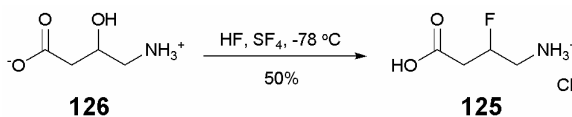
Additionally, the synthesis of 3-F-GABA enantiomers was motivated to validate the concept of using the C-F bond as a new tool to influence the conformational mobility of biologically active amines.



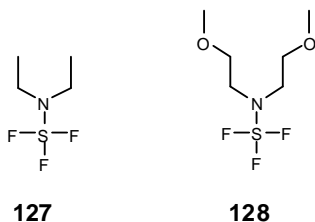
## 3.2 Previous syntheses of 3-Fluoro-GABA

### 3.2.1 The dehydrofluorination approach

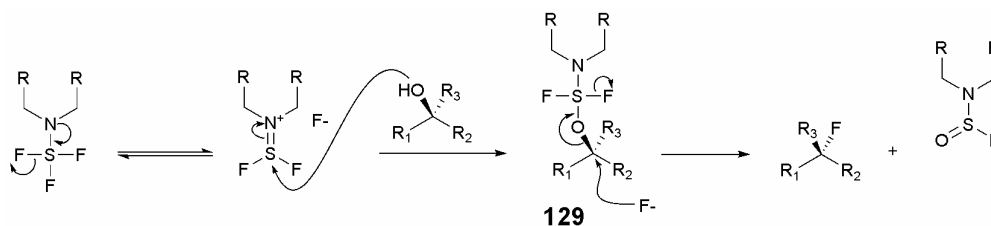
Prior to this study, only racemic 3-fluoro- $\gamma$ -aminobutyric acid (**125**) has been reported. The synthesis, published in 1979 by J. Kollonitsch *et al.*<sup>1</sup> involved fluorination of DL-3-hydroxy- $\gamma$ -aminobutyric acid (**126**) in anhydrous liquid HF with SF<sub>4</sub> at -78 °C. After ion-exchange purification and re-crystallisation from EtOH, racemic 3-F-GABA (**125**) was obtained in 50% yield (Scheme 3.1). The method is rather expeditious as the target molecule is prepared in a single step and interestingly, no protection of the amine or the carboxylic acid is required. Unfortunately, it makes use of quite hazardous chemicals which cannot be readily manipulated in a standard research laboratory. Moreover, this method is not applicable to the preparation of enantiopure 3-F-GABA from the enantiopure precursor alcohol, as such fluorodehydroxylation reactions using SF<sub>4</sub> are known to proceed *via* both S<sub>N</sub>1 and S<sub>N</sub>2 mechanisms. Therefore, the reaction of enantiopure 3-hydroxy-GABA with SF<sub>4</sub> would probably not result in a complete inversion of stereochemistry.



Scheme 3.1: Preparation of 3-F-GABA using the SF<sub>4</sub> methodology.<sup>1</sup>



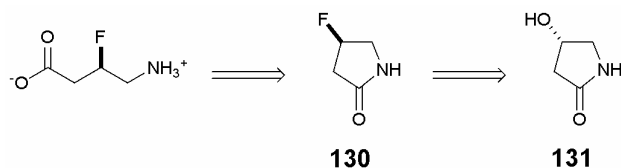
In order to overcome the limitations of the  $\text{SF}_4$  methodology, milder fluorinating agents such as diethylaminesulfur trifluoride (DAST) (**127**) and the thermally more stable bis(2-methoxyethyl)aminosulfur trifluoride (Deoxofluor<sup>TM</sup>) (**128**) have been developed. The mechanism for the fluorination of alcohols using such fluorinating agents proceeds *via* the formation of an alkoxydialkylaminosulfur difluoride intermediate (**129**), followed by the nucleophilic attack of the fluoride ion in a predominant  $\text{S}_{\text{N}}2$  mechanism (Scheme 3.2).



Scheme 3.2: Schematic mechanism of the deoxofluorination of an alcohol with a dialkylaminesulfur trifluoride fluorinating agent.

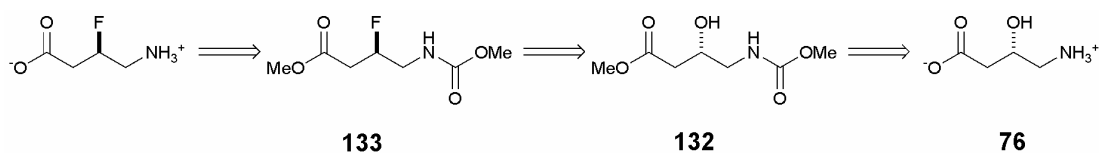
Deoxofluorination is a practical and widely used method for the introduction of a fluorine atom into an organic molecule. In retrosynthetic analyses, the nucleophilic replacement of oxygen with fluorine is an obvious option, but it is not always the most successful as illustrated in the following pages. Indeed, due to the very poor nucleophilicity and the high basicity of fluoride ion, deoxofluorination is often accompanied by loss of stereochemistry, elimination or rearrangements resulting from neighbouring group participation.

Previously in the St Andrews labs (R. Gilmour, 2002),<sup>2</sup> a first retrosynthetic approach towards the synthesis of enantiopure 3-F-GABA was explored. The retrosynthetic analysis in Scheme 3.3 shows that 3-F-GABA is accessible by hydrolysis of 4-fluoropyrrolidin-2-one (**130**) which can itself be obtained from commercially available 4-hydroxypyrrolidin-2-one (**131**) by deoxofluorination. This constituted a very direct strategy for the preparation of 3-F-GABA. Unfortunately, fluorination of (**131**) with DAST under a variety of conditions failed to produce (**130**).<sup>2</sup> Mesylation of (**131**) followed by treatment with tetrabutylammonium fluoride (TBAF) was also unsuccessful.



Scheme 3.3: First retrosynthetic analysis to 3-F-GABA.<sup>2</sup>

An alternative retrosynthesis was developed, starting from (3*S*)-hydroxy- $\gamma$ -aminobutyric acid (**76**) and using a classical protection-deprotection sequence as shown in Scheme 3.4. The most problematic step in this synthesis was the fluorination of (**132**) which afforded an inseparable 1:1 mixture of (**133**) and of an elimination product.



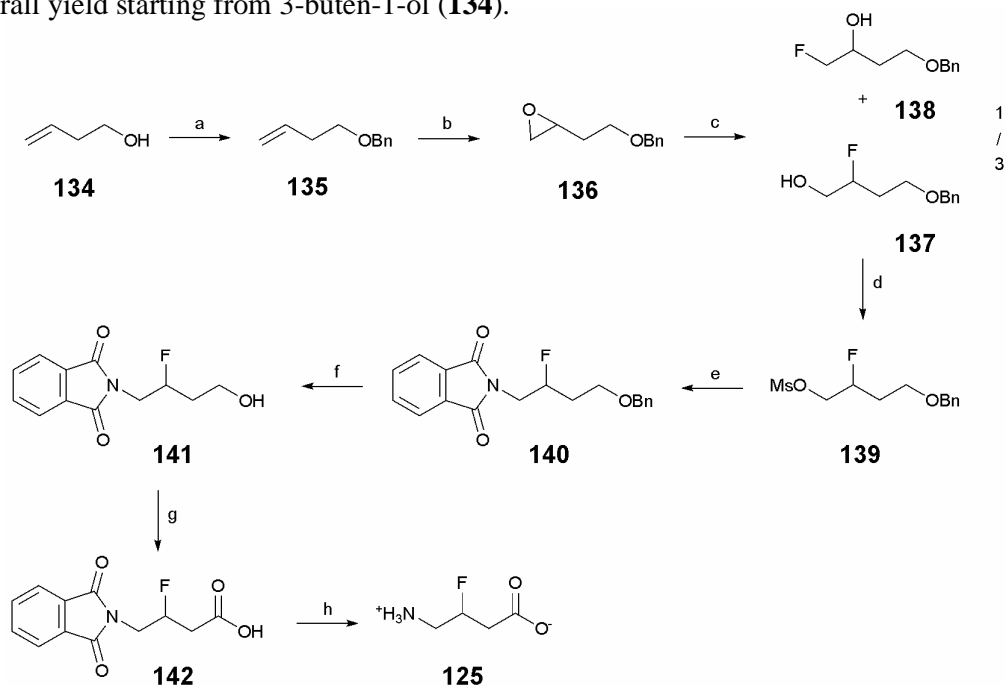
Scheme 3.4: Alternative retrosynthesis starting from 3-hydroxy-GABA.<sup>2</sup>

Attempts to transform the elimination product into a more polar constituent by Sharpless dihydroxylation met with some success but demonstrated the impracticality of this synthesis as a reasonable preparative method.<sup>2</sup> Other protecting groups were also

explored but without significant success. Again, mesylation of (**132**) followed by reaction with TBAF failed to produce the desired product. In retrospect, conversion of the amine into a dimethoxycarbamate or use of Deoxofluor may have reduced the production of the elimination product but this was not explored.

### 3.2.2 The Gabriel synthesis approach

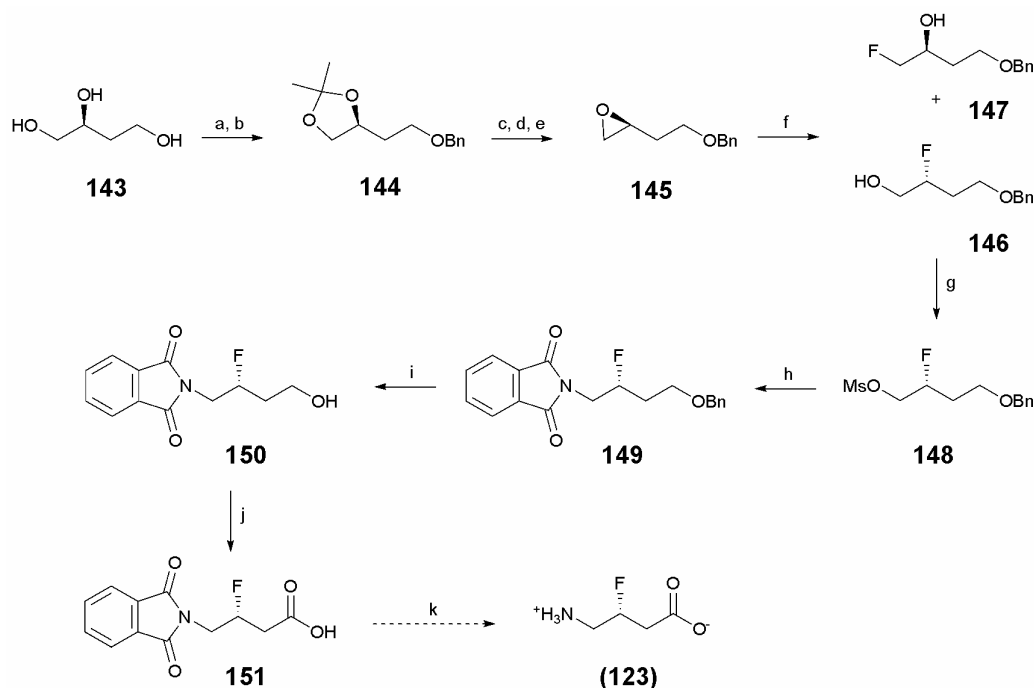
Due to the lack of success of the direct deoxofluorination methods described above, an approach was taken to introduce the fluorine atom at an early stage of the synthesis and to construct 3-F-GABA from a simple building block. Scheme 3.5 shows the eight-step route of racemic 3-F-GABA developed by Dr. F. Chorki in St Andrews.<sup>3</sup> This route was successful but was inefficient and gave only 37 mgs of racemic 3-F-GABA (**126**) in 3% overall yield starting from 3-buten-1-ol (**134**).



Scheme 3.5: Synthesis of racemic 3-F-GABA using the Gabriel synthesis approach.<sup>3</sup> Reagents and conditions: a) NaH, BnBr, THF, 96%; b) *m*CPBA, DCM, 95%; c) HF-Pyridine, DCM, 59%; d) MsCl, Et<sub>3</sub>N, DMAP, THF, 64%; e) Potassium phthalimide, DMF, reflux, 75%; f) H<sub>2</sub>, P=40 bars, Pd(OH)<sub>2</sub>/C, 40%; g) NaIO<sub>4</sub>, RuCl<sub>3</sub>·xH<sub>2</sub>O, CCl<sub>4</sub>/MeCN/H<sub>2</sub>O, 65%; h) H<sub>2</sub>NNH<sub>2</sub>·H<sub>2</sub>O, EtOH, 44%.

The key step in the above synthesis is the hydrogen fluoride mediated ring opening of epoxide (**136**) which gave a 3:1 mixture of regioisomers (**137**) and (**138**). Fortunately, they could be separated by column chromatography.

With some of the elements of this route in place, a strategy evolved to address an enantioselective synthesis of (3*R*)-F-GABA (Scheme 3.6). Starting from commercially available (*S*)-1,2,4-butanetriol, the chiral epoxide (**145**) was obtained in five steps and in 50% overall yield. The subsequent steps were similar to those already developed for the racemic synthesis. A small amount of (**123**) was prepared but it was not pure and its enantiopurity was not evaluated.



Scheme 3.6: Enantioselective preparation of (3*R*)-F-GABA using the Gabriel synthesis approach. Reagents and conditions: a) Acetone, *p*TsOH (cat), RT, 24 h, 95%; b) NaH, BnBr, THF, RT, 24 h, 92%; c) AcOH/H<sub>2</sub>O, 50° C, 1 h, 88%; d) TsCl, Pyridine, RT, 7 h, 76%; e) Triton B, Et<sub>2</sub>O, RT, 85%; f) HF-Pyridine, DCM, 47%; g) MsCl, Pyridine, DMAP, THF, 70%; h) Potassium phthalimide, DMF, reflux, 65%; i) H<sub>2</sub>, P=40 bars, Pd(OH)<sub>2</sub>/C, 50%; j) NaIO<sub>4</sub>, RuCl<sub>3</sub>·xH<sub>2</sub>O, CCl<sub>4</sub>/MeCN/H<sub>2</sub>O, 60%; k) H<sub>2</sub>NNH<sub>2</sub>·H<sub>2</sub>O, EtOH.

In addition to the large number of steps and the poor overall yield, this synthesis presented two additional problems. The first one is the opening of the enantiomerically pure epoxide (**145**) with HF which can result in some cases in a significant loss of stereochemistry.<sup>4</sup> The second problem is the cleavage of the phthalimide group with hydrazine in the final step. A long reaction time was required to achieve an acceptable conversion but this also promoted the formation of a by-product by  $\beta$ -elimination. More problematic was the presence of another zwitterionic amino acid by-product which could not be separated from 3-F-GABA. This by-product was identical spectroscopically to GABA and could have formed by reduction of the  $\beta$ -elimination product with hydrazine. Reduction of unsaturated compounds with hydrazine in the presence of oxygen has been reported.<sup>5</sup> The nucleophilic substitution of fluorine by hydrazine has also been demonstrated in 1997 by M. Bols.<sup>6</sup>

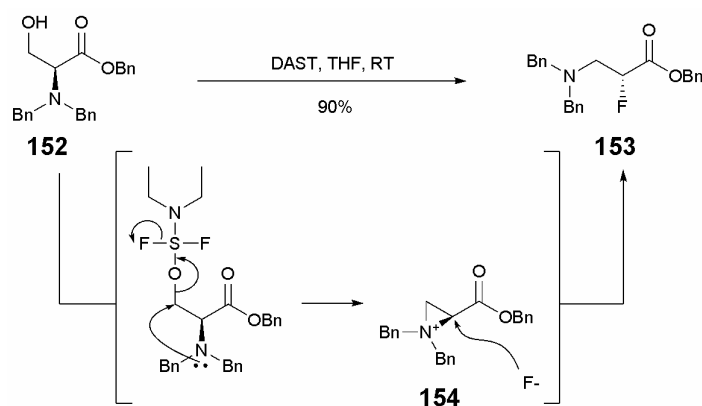
Therefore, it appears from this work that, due to the complications occurring during its hydrolysis with hydrazine, phthalimide is not a suitable protecting group for the synthesis of such  $\beta$ -fluoroamines.

The apparent simplicity of 3-F-GABA as a target molecule and the unsuccessful efforts experienced in its synthesis, emphasize the difficulties and the frustrations which often come with the synthesis of fluorinated organic molecules. The recognition that a reaction first published in 1982 could be used for the synthesis of 3-F-GABA in an enantioselective manner gave a new impulse to this project.

### 3.3 Amino acids as precursors of 3-Fluoro-GABA

#### 3.3.1 The serine approach

A. Shanzer and L. Somekh observed in 1982 that treatment of *N,N*-dibenzyl-L-serine benzyl ester (**152**) with DAST provided *N,N*-dibenzyl- $\alpha$ -fluoro- $\beta$ -alanine benzyl ester (**153**) in 90% yield and in an enantiomerically pure form.<sup>7</sup> The proposed mechanism for this transformation *via* an aziridinium intermediate (**154**) is presented in Scheme 3.7.

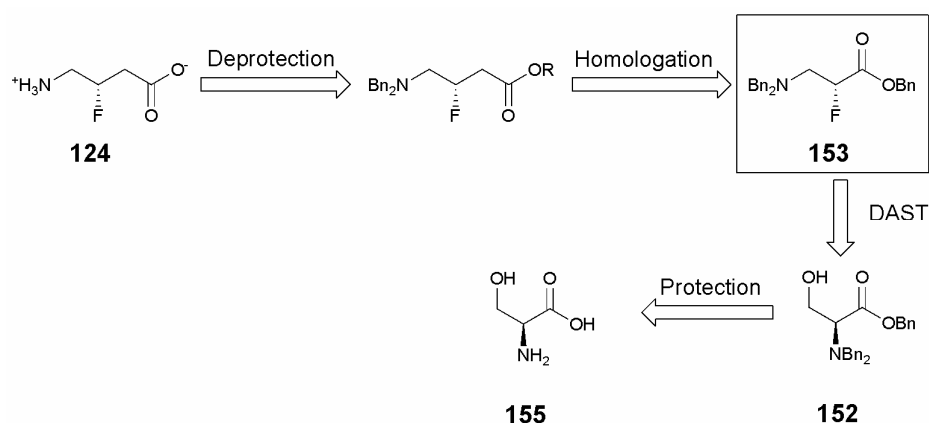


Scheme 3.7: Synthesis of (2*R*)-3-(dibenzylamino)-2-fluoropropanoic benzyl ester (**153**) from (2*S*)-dibenzylamino-3-hydroxypropanoic acid benzyl ester (**152**) *via* formation of the aziridinium (**154**).<sup>7</sup>

This reaction has been reproduced several times<sup>8-11</sup> in the last twenty years and the product has been used for the building of chemical probes<sup>10, 11</sup> or for studies of  $\beta$ -peptide conformations.<sup>8, 9</sup> The formation of aziridinium (**154**) as an intermediate in the above reaction has been confirmed and can be explained by the fact that intramolecular reactions are faster than intermolecular reactions. It also shows that the dibenzyl-protected amine is

more nucleophilic than fluoride anion. The opening of aziridinium (**154**) by fluoride is both regio- and enantio-selective. The stereointegrity of this reaction<sup>7, 11</sup> makes the DAST-mediated rearrangement of  $\beta$ -hydroxylamines a useful method for the synthesis of enantiopure  $\beta$ -fluoroamines.

The applicability of this reaction for the enantioselective synthesis of 3-F-GABA is evident. *N,N*-Dibenzyl- $\alpha$ -fluoro- $\beta$ -alanine benzyl ester (**153**) emerges as a precursor to (3*S*)-F-GABA as indicated in the retrosynthetic analysis shown below (Scheme 3.8).



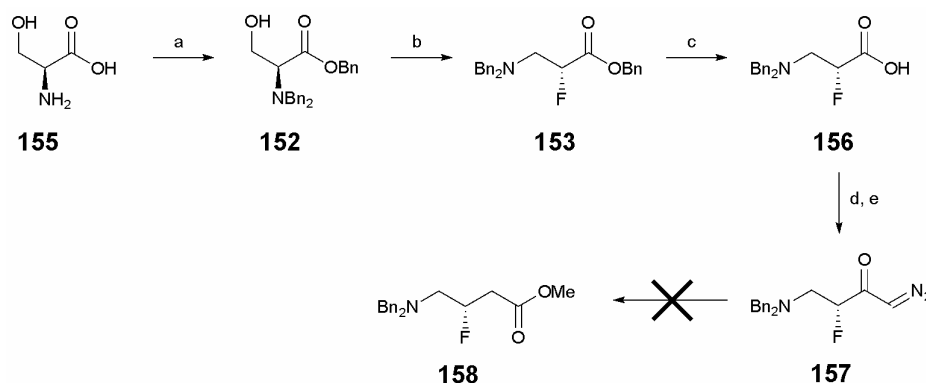
Scheme 3.8: Retrosynthetic analysis starting from L-serine.

(3*S*)- And (3*R*)-F-GABA are according to the proposed retrosynthesis, accessible from L- and D-serine respectively. The key step for this approach is the homologation of the  $\alpha$ -fluoro-ester (**153**). Typically, carboxylic acids can be homologated smoothly using the Arndt-Eistert procedure, a convenient and widely used method which converts simple  $\alpha$ -amino acids into  $\beta$ -amino acids in only two steps.<sup>12, 13</sup>

Accordingly, L-serine (**155**) was tribenzylated using standard procedures<sup>8, 14</sup> to give (2*S*)-(dibenzylamino)-3-hydroxypropionic acid benzyl ester (**152**) in 51% yield. This

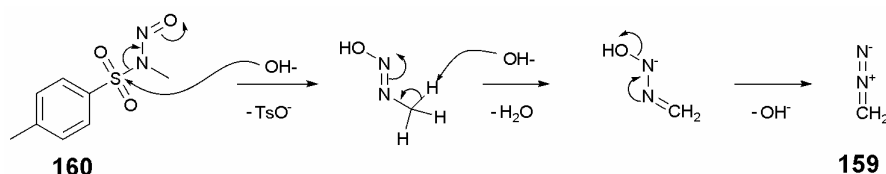


compound was then dissolved in THF and reacted with DAST, affording (**153**) in 85% yield. The reaction proceeded very cleanly and the product had spectroscopic data identical to those reported in the literature.<sup>14</sup> Mild alkaline hydrolysis of the benzyl ester with LiOH gave the carboxylic acid (**156**) in 74% yield. It is noteworthy that mild alkaline hydrolyses of  $\alpha$ -fluoro-esters have been reported to proceed without loss of enantiopurity at the stereogenic centre.<sup>10, 15</sup> The free acid was then converted to the acyl chloride with  $\text{SOCl}_2$  and was directly added into an ethereal solution of diazomethane to generate diazoketone (**157**) (Scheme 3.9).



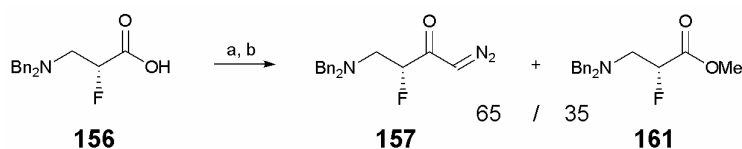
Scheme 3.9: Attempted synthesis of 4-dibenzylamino-(3S)-fluorobutyric acid methyl ester (**158**) via Arndt-Eistert homologation of acid (**156**). Reagents and conditions: a)  $\text{BnBr}$ ,  $\text{K}_2\text{CO}_3$ ,  $\text{NaOH}$ ,  $\text{H}_2\text{O}$ ,  $100^\circ\text{C}$ , 1 h, 51%; b) DAST, THF,  $0^\circ\text{C}$ , 85%; c)  $\text{LiOH}$  0.5 N, THF, RT, 18 h, 74%; d)  $\text{SOCl}_2$ , DCM, reflux, 2 h; e)  $\text{CH}_2\text{N}_2$ , THF, RT, 14 h.

Diazomethane was prepared from Diazald® (Scheme 3.10) using published procedures.<sup>16, 17</sup>



Scheme 3.10: Schematic mechanism of the preparation of diazomethane (**159**) from Diazald® (**160**).

Only a few  $\alpha$ -fluorodiazoketones have been reported in the literature<sup>18-20</sup> and most of these have been described as reasonably stable. In our case, (3*R*)-1-diazo-4-(dibenzylamino)-3-fluorobutan-2-one (**157**) was not purified but was characterised by full NMR analysis and by IR analysis which showed the typical absorption of the N=N bond at 2112 cm<sup>-1</sup>. However, diazoketone (**157**) was contaminated with a significant amount of methyl ester (**161**), arising from direct esterification of the carboxylic acid (**156**) with diazomethane. This is probably due to incomplete conversion to the acyl chloride or competing hydrolysis. The ratio of the mixture (**157**)/(**161**) was determined by NMR to be around 65/35.



Scheme 3.11: Preparation of diazoketone (**157**) and methyl ester (**161**) from carboxylic acid (**156**). Reagents and conditions: a) SOCl<sub>2</sub>, DCM, reflux, 2 h; b) CH<sub>2</sub>N<sub>2</sub>, THF, RT, 14 h.

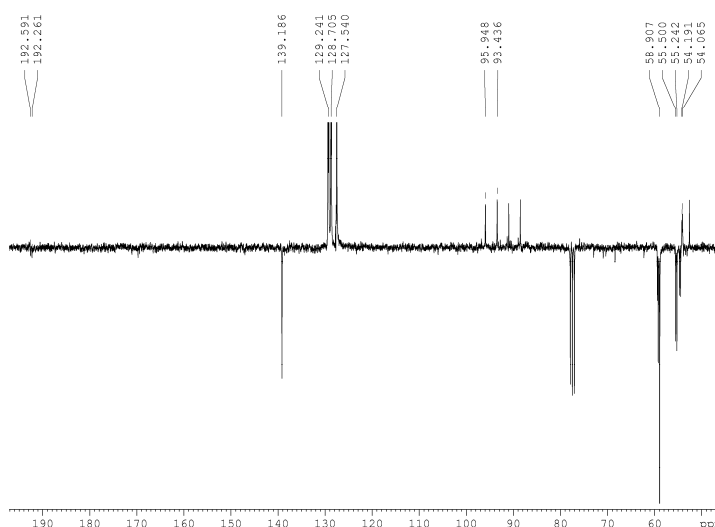


Figure 3.2: DEPT NMR spectrum (CDCl<sub>3</sub>, 75 MHz) of fluorinated diazoketone (**157**) contaminated with methyl ester (**161**).

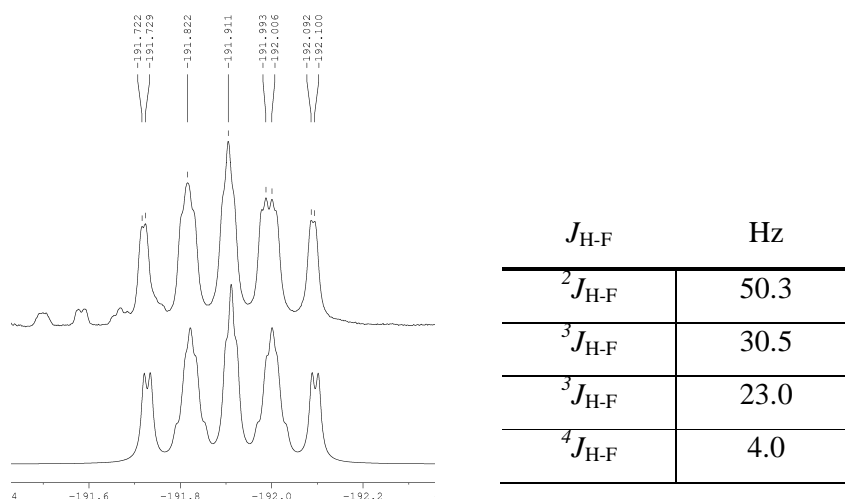
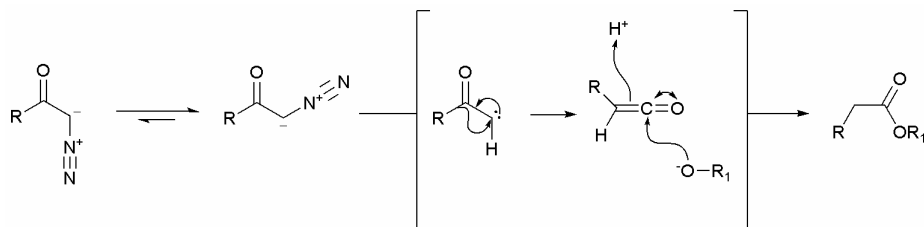


Figure 3.3:  $^{19}\text{F}$  NMR spectrum of the diazoketone (above) and its simulated spectrum (below) from which  $J_{\text{H-F}}$  couplings are extracted.

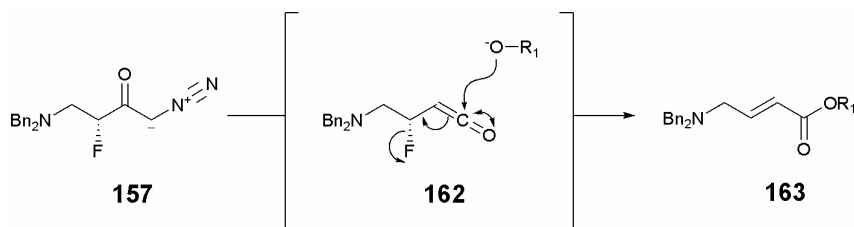
The key step for the Arndt-Eistert homologation procedure is the Wolff rearrangement<sup>21</sup> from the diazoketone which forms a ketene intermediate, which is subsequently hydrolysed to the homologated ester. More than one hundred years after its discovery, questions remain about the mechanism of this rearrangement, for example whether the loss of  $\text{N}_2$  is concerted or not, with the migration of the alkyl group. It seems that both pathways co-exist although it has been suggested that diazoketones adopt the Z conformation in the Wolff rearrangement. In this conformation, the migrating and leaving groups are antiperiplanar, which indicates -at least- a partially concerted mechanism (Scheme 3.12). The migratory aptitude of the R group has also been studied and it appears that phenyl groups migrate faster than methyl groups.



Scheme 3.12: Schematic mechanism of the Wolff rearrangement.

Perfluorinated alkyl groups display a poor ability to migrate in the Wolff rearrangement<sup>22, 23</sup> and E. R. Larsen *et al.* have shown that perfluorinated acids failed to undergo the Arndt-Eistert reaction in a normal manner. They concluded after a series of experiments that at least two methylene groups are required between the carbonyl and the perfluorinated chain for the Wolff rearrangement to proceed conveniently.<sup>24</sup> Interestingly, trifluoroacetic acid is conveniently homologated using standard conditions,<sup>24-26</sup> and it is not clear why this should be so.

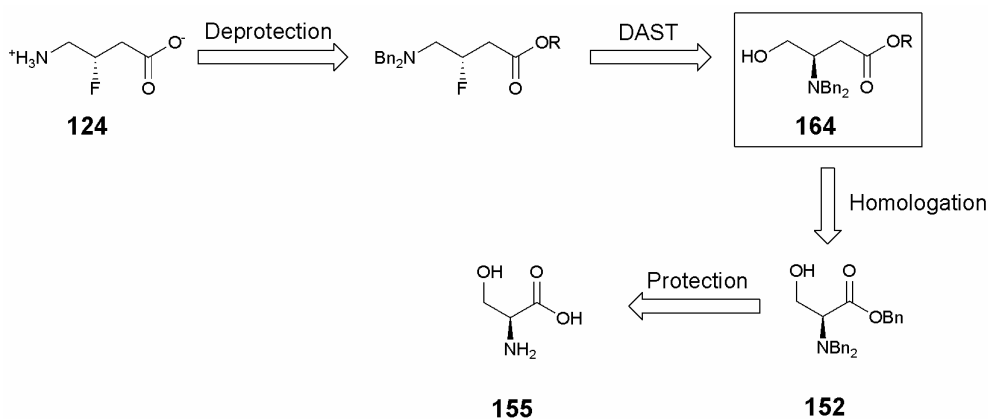
It was exciting to test the feasibility of the Wolff rearrangement on  $\alpha$ -fluorodiazoketone (**157**). Successful homologation of (**156**) to  $\beta$ -fluoroacid (**158**) using the Arndt-Eistert procedure, would open up a new route to this class of compounds for which very few methods have been developed. In the event, (**157**) failed to undergo the Wolff rearrangement in our hands. Crude diazoketone (**157**) was dissolved in various solvents (BnOH, THF/water, DCM/MeOH), the solution was protected from the light and the catalyst silver benzoate  $C_7H_5O_2Ag$  was added to the mixture at 10-20 mole %. Sonication, heating or addition of Lewis acids also failed to induce the desired rearrangement. It is not clear why the homologation of this  $\alpha$ -fluorodiazoketone did not proceed in the expected way but two explanations can be advanced: firstly, the presence of fluorine could reduce the migrating ability of the alkyl group. Secondly, if ketene (**162**) does form, its hydrolysis could result in loss of fluoride (Scheme **3.13**). The later explanation appears more probable as unsaturated compounds were detected in the crude mixture after the Wolff rearrangement but it was not possible to isolate any homologated product from the reactions.



Scheme **3.13**: Putative mechanism of the Wolff rearrangement on  $\alpha$ -fluorodiazoketone (**157**).

At this stage, it is not possible to give a definitive answer about the aptitude of  $\alpha$ -fluorodiazoketones to undergo the Wolff rearrangement and further experiments perhaps merit investigations. However, the lack of success during this work and the lack of precedent in the literature suggest that  $\alpha$ -fluorodiazoketones are unsuitable substrates for the Arndt-Eistert reaction. This led us to reconsider our approach to the synthesis of 3-F-GABA.

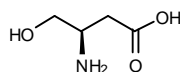
As homologation appeared not to be compatible with an  $\alpha$ -fluorinated substrate, the order of the fluorination and homologation steps presented in Scheme **3.9** was inverted. Accordingly, the  $\beta$ -homoserine derivative (**164**) now emerges as the key compound in the new retrosynthesis (Scheme **3.14**).



Scheme **3.14**: Revised retrosynthetic analysis.

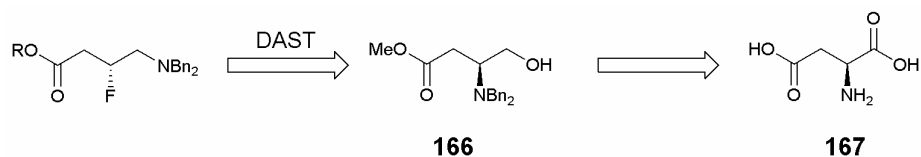
### 3.3.2 The aspartic acid approach

Fluorination *via* the aziridinium intermediate (**154**) as shown in scheme 3.7 is obviously not limited to serine derivatives and can be applied to any *N,N*-dibenzyl-protected  $\beta$ -amino-alcohol. In fact, similar rearrangements have been observed with various *N,N*-dimethyl- $\beta$ -amino-alcohols<sup>27</sup> and *N*-piperidine- $\beta$ -alcohols,<sup>28</sup> which extends the scope of this reaction. Thus, fluorination of  $\beta$ -homoserine derivative (**164**) with DAST or Deoxofluor is expected to behave similarly to that experienced previously with benzylated serine (**152**), although the regioselectivity of the opening of the aziridinium might be less specific in this case.



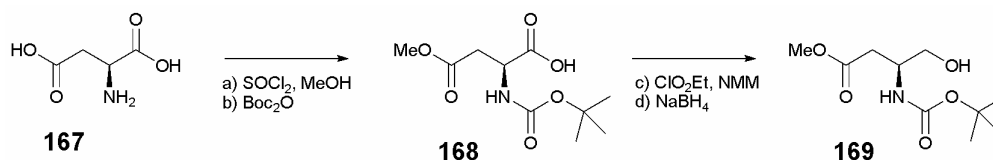
**165**

$\beta$ -Homoserine (**165**) is a well known compound for which different syntheses have been reported. However, homologation procedures such as Arndt-Eistert or Kowalski<sup>29</sup> procedures are not attractive in this case because scale up of these procedures is impractical and expensive. An efficient method giving access to (**164**) or its enantiomer (**166**), avoiding tedious protection-deprotection manipulations was needed. It rapidly emerged that aspartic acid, which contains four carbons like GABA, was an ideal starting material for the synthesis of 3-F-GABA. Scheme 3.15 shows the key intermediates of the retrosynthetic analysis starting from aspartic acid (**167**).



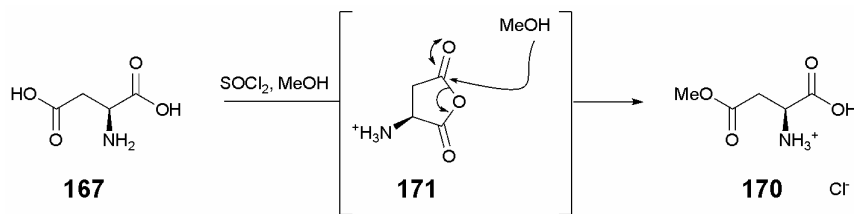
Scheme 3.15: Retrosynthetic analysis starting from L-aspartic acid.

The synthesis of  $\beta$ -aminoalcohol (**166**) from L-aspartic acid (**167**) requires selective reduction of the  $\alpha$ -carbonyl in the presence of the  $\beta$ -carbonyl group of the side chain. This has already been reported many times.<sup>30-32</sup> Typically, aspartic acid is selectively esterified, Boc-protected and then reduced with sodium borohydride  $\text{NaBH}_4$  or borane  $\text{BH}_3$  (Scheme 3.16).

Scheme 3.16: Example of a preparation of (**169**).<sup>30, 33, 34</sup>

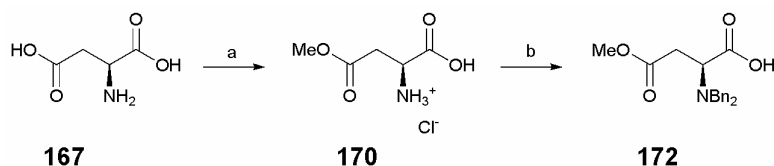
The fluorination step with DAST requires a *N,N*-dibenzyl-protected nitrogen and can not be performed on a Boc-protected amino acid such as (**169**). It was therefore decided, in order to reduce the number of synthetic steps and protecting group manipulations to attempt the reduction reaction on a dibenzyl-protected amino acid. Accordingly, a new route was designed and it started with the esterification of aspartic acid.

The selective  $\beta$ -esterification of aspartic acid was straightforward, using the procedure published in the 1950s by D. Coleman.<sup>33</sup> Addition of thionyl chloride to a methanolic solution of aspartic acid furnished, after re-crystallisation from  $\text{EtOH}/\text{Et}_2\text{O}$ ,  $\beta$ -methyl aspartate hydrochloride (**170**) in 70% yield. The selectivity of the reaction originates from the formation of the anhydride (**171**) which is opened by methanol in a  $\beta/\alpha$  ratio higher than eight (Scheme 3.17).<sup>35</sup>



Scheme 3.17: Preparation of β-methyl aspartate hydrochloride (**170**).

The dibenzyl protection of the amino group was achieved by reductive amination, a method which does not affect the free α-carbonyl. The reaction proceeded smoothly, by addition of benzaldehyde and sodium cyanoborohydride to a solution of amino acid (**170**) in methanol. NaCNBH<sub>3</sub> reduces imines but is not reactive enough to reduce esters or carboxylic acids. In the event, (*S*)-*N,N*-dibenzylaspartic acid β-methyl ester (**172**) was isolated in 64% yield (Scheme 3.18).



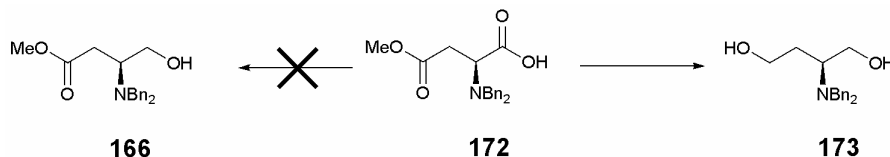
Scheme 3.18: Synthesis of (**172**) from L-aspartic acid *via* reductive amination. Reagents and conditions: a) SOCl<sub>2</sub>, MeOH, RT, 62%; b) benzaldehyde, NaCNBH<sub>3</sub>, MeOH, 64%.

Compound (**172**) now bears differentiated carboxylate groups which were anticipated to react differently in the presence of a reducing agent such as borane BH<sub>3</sub> which is known to efficiently reduce carboxylic acids but not esters.<sup>36</sup>

However, such experiments with BH<sub>3</sub> failed. No reaction was observed after addition of one or two equivalents of BH<sub>3</sub>, at room temperature or even after reflux in THF. The addition of three or more equivalents of BH<sub>3</sub>, and heating under reflux, resulted in a complex mixture of non-reacted, partially reduced and doubly-reduced products, showing that the reduction of (**172**) with borane is not selective. More forcing conditions



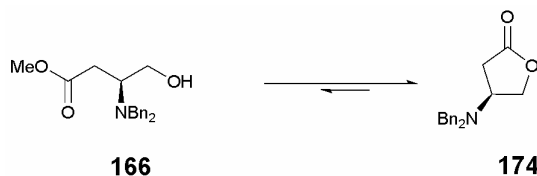
produced the doubly-reduced chiral diol (**173**) which was isolated in 75% yield (Scheme 3.19).



Scheme 3.19: Reduction of (**172**) with borane is not selective.

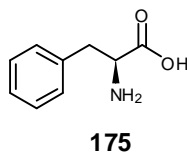
This unsuccessful result illustrated that dibenzyl-protection of the amine renders the reduction of the  $\alpha$ -carboxylic acid more difficult. The conclusion is that  $\beta$ -homoserine is more conveniently synthesised by the method showed on Scheme 3.16 which involves protection of the nitrogen as a carbamate and then reduction with  $\text{NaBH}_4$ .

Examination of the literature revealed that compound (**166**) is unstable in solution and prone to lactonisation<sup>37, 38</sup> (Scheme 3.20). In fact, it has been reported to lactonise quantitatively after a few days in the refrigerator.<sup>37</sup> Although the ring open form can be recovered by acidic treatment, this behaviour mitigates against (**166**) as a good substrate for the fluorination reaction.



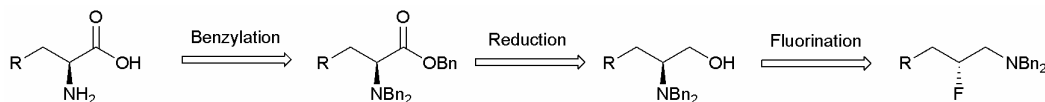
Scheme 3.20: Lactonisation of (**166**).

Therefore, investigations of the route using aspartic acid as a starting material were discontinued at this point. Once again, a new approach was required and again, it was decided to begin the synthesis of 3-F-GABA from another natural amino acid. This time, phenylalanine (**175**) was chosen.



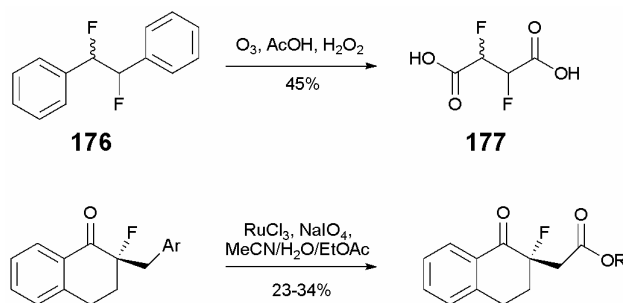
### 3.4 The phenylalanine route

Amino acids are potentially practical starting materials for the synthesis of enantiopure  $\beta$ -fluoroamines as illustrated by the sequence in Scheme 3.21. They are conveniently reduced to  $\beta$ -hydroxylamines and have the potential to be transformed into  $\beta$ -fluoroamines by fluorination with DAST or Deoxofluor.



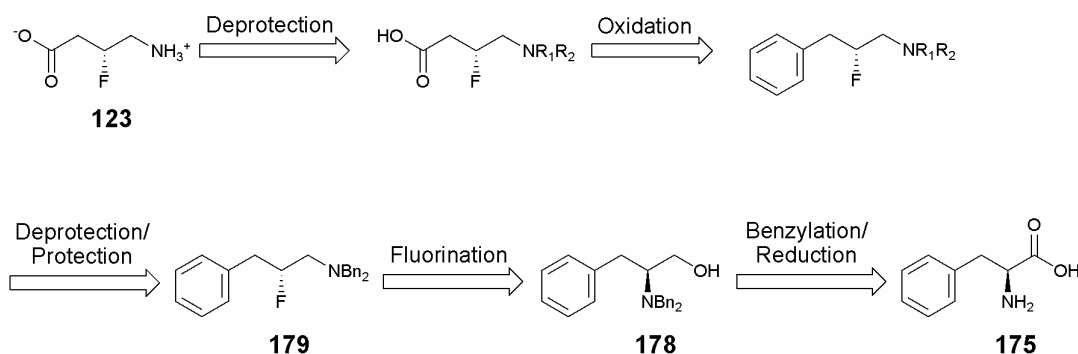
Scheme 3.21: Schematic synthesis of enantiopure  $\beta$ -fluoroamines from  $\alpha$ -amino acids.

In the context of 3-F-GABA synthesis, substituent R could clearly be a carboxylic acid but competing lactonisation occurs in this case as discussed above. Interestingly, aromatic rings can be used as masked carboxylic acid functionalities where the carboxylic acid is released by ozonolysis, potassium permanganate<sup>39</sup> or ruthenium-catalysed oxidations. M. Schüler in the St Andrews lab, recently demonstrated the applicability of this approach on fluorinated substrates by converting 1,2-difluoro-diphenylethane (**176**) into 2,3-difluorosuccinic acid (**177**) by ozonolysis.<sup>40, 41</sup> Ruthenium-catalysed oxidations of aromatic rings can also be conducted with fluorinated substrates (Scheme 3.22).<sup>42-46</sup>



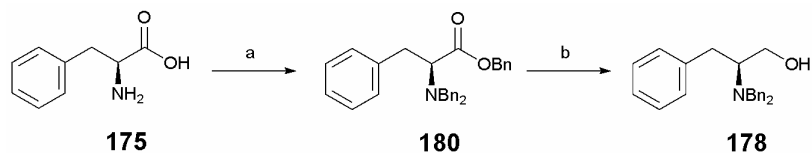
Scheme 3.22: Examples of ozonolysis (above) and ruthenium-catalysed oxidations (below) on fluorinated substrates.<sup>41, 44</sup>

The envisaged retrosynthetic analysis starting from L-phenylalanine (**175**) is outlined in Scheme 3.23. This synthesis contains two important steps which involve fluorination of (**178**) and then oxidation of the phenyl ring. Prior to the oxidation step, it is required to convert the dibenzyl protecting group of (**179**) into a group compatible with oxidation conditions.



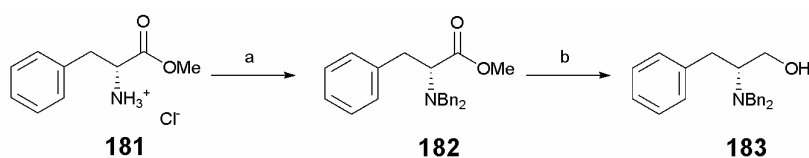
Scheme 3.23: Retrosynthetic analysis starting from L-phenylalanine.

Preparation of amino alcohol (**178**) was straightforward and was achieved using published procedures.<sup>47-49</sup> Accordingly, L-phenylalanine was perbenzylated using benzyl bromide and  $K_2CO_3$  in EtOH. This reaction was performed on a large scale and the crude product obtained after work-up appeared clean enough to be taken through directly for the further step. However, an analytical sample of (2*S*)-(dibenzylamino)-3-phenylpropanoic acid benzyl ester (**180**) was obtained after purification. Reduction of (**180**) was achieved with  $LiAlH_4$  in THF at 0 °C. The excess of  $LiAlH_4$  was quenched by the careful addition of water. After work-up and purification, (2*S*)-(dibenzylamino)-3-phenylpropan-1-ol (**178**) was obtained in 85% yield over two steps as a colourless solid (Scheme 3.24).



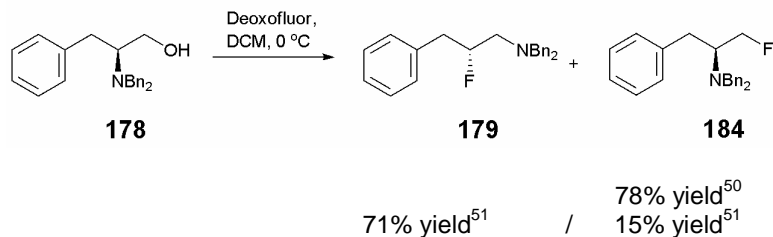
Scheme 3.24: Preparation of (2*S*)-(dibenzylamino)-3-phenylpropan-1-ol (**178**) from L-phenylalanine.<sup>47-49</sup> Reagents and conditions: a) BnBr, K<sub>2</sub>CO<sub>3</sub>, EtOH, 70 °C, 3 days; b) LiAlH<sub>4</sub>, THF, 0 °C, 2 h, 85%.

The (*R*)-enantiomer (**183**) was prepared in a similar manner to the (*S*)-enantiomer from D-phenylalanine methyl ester hydrochloride (**181**) (Scheme 3.25).



Scheme 3.25: Preparation of (2*R*)-(dibenzylamino)-3-phenylpropan-1-ol (**183**) from D-phenylalanine methyl ester hydrochloride. Reagents and conditions: a) BnBr, K<sub>2</sub>CO<sub>3</sub>, MeCN, 80 °C, 16 h, 79%; b) LiAlH<sub>4</sub>, THF, 0 °C, 2 h, 93%.

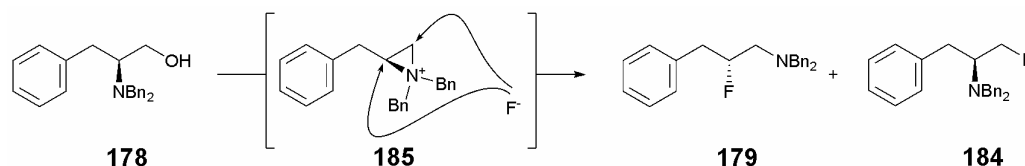
Fluorination of (**178**) with Deoxofluor was reported in 2002 to give the non-rearranged product (2*S*)-*N,N*-dibenzyl-1-fluoro-3-phenylpropan-2-amine (**184**) in 78% isolated yield.<sup>50</sup> However, in 2004, the reaction was reported to give a mixture of (**179**) and (**184**) in a 4:1 ratio (Scheme 3.26) favouring the rearranged product.<sup>51</sup> The later publication was an encouraging observation for our synthesis of 3-F-GABA.



Scheme 3.26: Fluorination of (**178**) as reported by J. M. Shreeve *et al.*<sup>50, 51</sup>

The fluorination of *N,N*-dibenzyl- $\beta$ -amino alcohols is reported to be concentration-dependent, with a higher concentration of Deoxofluor benefiting the formation of the non-rearranged product, possibly by direct substitution.<sup>51</sup> It was therefore decided to perform the fluorination of (**178**) under more dilute conditions.

Accordingly, 0.6 mM solution of Deoxofluor in DCM was added dropwise at -10 °C to a 0.1 mM solution of (**178**) in DCM. The reaction mixture was allowed to warm slowly to room temperature and was stirred for 15 h. After work-up and purification by flash chromatography, the desired product (**179**) was obtained as a colourless oil in 75% yield and the isomer (**184**) isolated in ~12% yield. The dilute reaction conditions appear to favour the intramolecular reaction and the formation of the aziridinium ring (**185**). Consequently, the formation of (**184**) results most probably from non-regioselective opening of aziridinium (**185**) by fluoride (Scheme 3.27).



Scheme 3.27: Proposed mechanism for the formation of (**179**) and (**184**).  
Reagents and conditions: Deoxofluor, DCM, -10 °C, 75% (**179**).

The influence of solvent and temperature on the regioselectivity of aziridinium ring-opening was found to be very limited. DCM was the most convenient solvent for this reaction, providing a high ratio (**179**)/(**184**) (Table 3.3). Carrying out the reaction at room temperature, -10 °C or -78 °C had no significant impact on the ratio (**179**)/(**184**). Also, DAST and Deoxofluor gave very similar results. This series of experiments indicated that the regioselectivity of the reaction could not be easily improved but this was not essential as (2*R*)-*N,N*-dibenzyl-2-fluoro-3-phenylpropan-1-amine (**179**) could be isolated readily and

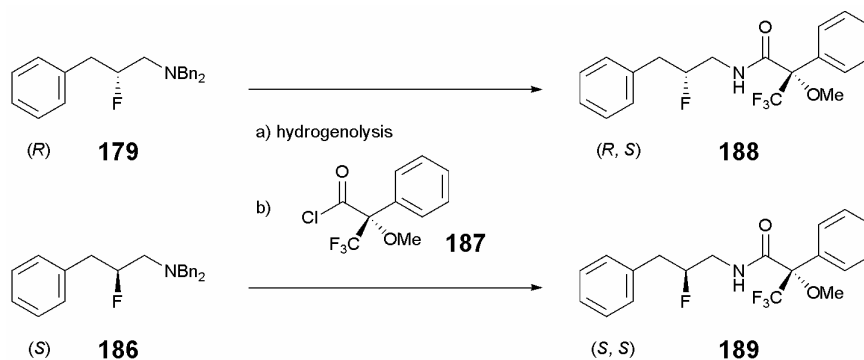
in good isolated yield (75% yield). The enantiomer (2*S*)-*N,N*-dibenzyl-2-fluoro-3-phenylpropan-1-amine (**186**) was obtained similarly in 76% yield from (**183**).

Solvent	Ratio <b>179/184</b> (at 0 °C)
THF	73/27
MeCN	74/26
DCM	80/20
CCl <sub>4</sub> /DCM (3/1)	82/18

Table 3.1: Ratio **179/184** of the fluorination reaction in various solvents. Ratio was measured directly by <sup>19</sup>F NMR analysis.

The enantioselectivity of the fluorination reaction with substrate (**178**) was not previously reported in the literature and although this type of rearrangement was found to be enantioselective on the serine derivative (**152**), possible involvement of a phenonium anion<sup>41</sup> or a S<sub>N</sub>1 pathway had the potential to reduce the enantiopurity. Also, the α<sub>D</sub> values of enantiomers (**179**) and (**186**) were found to be very low ([α]<sub>D</sub><sup>20</sup> +1.1 and -1.0 respectively) so that enantiopurity could not be determined by measurement of the optical activity. It was therefore essential to verify the enantioselectivity of the reaction and this was accomplished with Mosher's amides, which are the most widely used chiral derivatising agents for assessing enantiopurity of chiral amines.<sup>52</sup>

Using parallel procedures, both the (*R*)- and (*S*)- enantiomers (**179**) and (**186**) were debenzylated by hydrogenolysis in MeOH using Pd(OH)<sub>2</sub>/C as a catalyst. After filtration of the solids and evaporation of the solvent, the crude amines were directly coupled to (*R*)-(-)-MTPA-Cl (**187**) with DMAP and Et<sub>3</sub>N in DCM. The reactions were quenched by the addition of water and the solvents were removed. The residues were finally taken up in CDCl<sub>3</sub> and analysed by <sup>19</sup>F NMR (Scheme 3.28).



Scheme 3.28: Preparation of the Mosher's amides (**188**) and (**189**).

The  $^{19}\text{F}$  NMR signal for the fluorine at the stereogenic centre for compounds (**188**), (**189**) and the mixture of the two diastereoisomers is shown in Figure 3.4. Single peaks are observed for pure Mosher's amides derived from enantiomers (**179**) and (**186**) suggesting that the two enantiomers are enantiopure. To confirm that peaks at -184.87 ppm for (*R, S*) (**188**) and -184.73 ppm for (*S, S*) (**189**) are not artefacts, the two Mosher's amides were then mixed in one tube and the NMR spectrum of the mix showed unambiguously two distinct peaks, proving the very high enantioselectivity of the fluorination reaction.

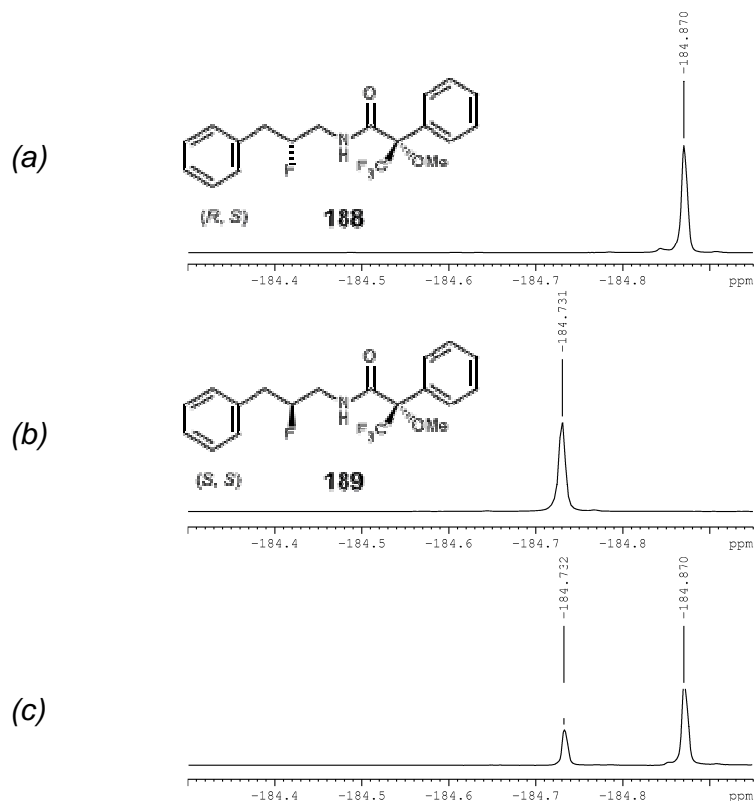
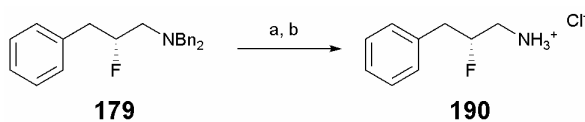


Figure 3.4:  $^{19}\text{F}$  NMR analysis of Mosher's amides (**188**) (spectrum *a*) and (**189**) (spectrum *b*) and mix of (**188**) and (**189**) (spectrum *c*) showing the high enantiopurity of amines (**179**) and (**186**).

In appropriate cases, absolute configuration can be determined by X-ray crystal structure analysis. For that reason, the hydrochloric salt of the dibenzyl-protected amine (**179**) was prepared. Thus, (**179**) was first subjected to hydrogenolysis, and after filtration of the palladium catalyst, 1 M HCl in diethyl ether was added to the methanolic solution of the amine to generate the hydrochloride (Scheme 3.29).



Scheme 3.29: Preparation of (2*R*)-fluoro-3-phenylpropan-1-amine hydrochloride (**190**)  
Reagents and conditions: a)  $\text{Pd}(\text{OH})_2/\text{C}$ ,  $\text{H}_2$ , MeOH; b) HCl, EtOH/Et<sub>2</sub>O, 76%.



Crystals of the hydrochloric salt (**190**) were obtained by re-crystallisation from EtOH/Et<sub>2</sub>O and one of these was amenable to crystal structure analysis. X-ray analysis confirmed the absolute configuration of the amine to be (*R*). The C-F bond lies *gauche* to the C-N<sup>+</sup> bond, with a torsion angle F-C-C-N<sup>+</sup> of 62.9° (Figure 3.5). This is consistent with recent observations indicating this as a preferred conformation in β-fluoroamines.

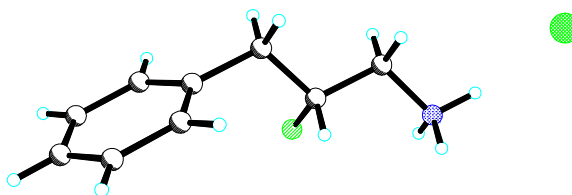
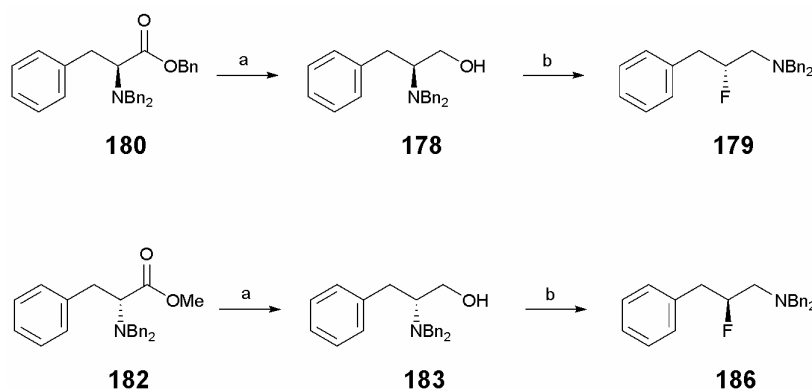


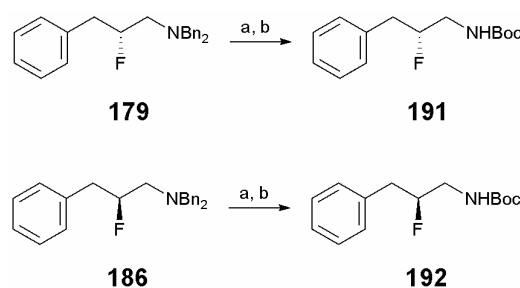
Figure 3.5: The absolute configuration of (**190**) was determined by X-ray structure analysis to be (*R*).



Scheme 3.30: Enantioselective syntheses of chiral β-fluoroamines (**179**) and (**186**) from L- and D-phenylalanine derivatives (**180**) and (**182**) respectively. Reagents and conditions: LiAlH<sub>4</sub>, THF, 0 °C, 2 h, 85-93%; b) Deoxofluor, DCM, -10 °C, 15 h, 75-76%.

As the enantiopurity and the absolute configuration of β-fluoroamines (**179**) and (**186**) was unambiguously established, the synthesis could be progressed toward the oxidation of the phenyl ring.

A suitable protecting group, stable under strongly oxidative conditions and preferably easily introduced and removed was required to replace the dibenzyl protecting group. Examination of the literature revealed many examples of Sharpless oxidations carried out with a Boc-protected amine.<sup>53-55</sup> Therefore, (**179**) and (**186**) were converted using standard procedures into (*R*)- and (*S*)-*tert*-butyl-2-fluoro-3-phenylpropylcarbamate (**191**) and (**192**) respectively as indicated in Scheme 3.31. The two enantiomers were obtained as colourless crystals amenable to X-ray structure analyses (Figure 3.6).



Scheme 3.31: Preparation of *N*-Boc-protected amines (**191**) and (**192**).  
Reagents and conditions: a)  $\text{Pd}(\text{OH})_2/\text{C}$ ,  $\text{H}_2$ , MeOH, 3 h; b)  $\text{Boc}_2\text{O}$ , 14 h, RT, 90%.

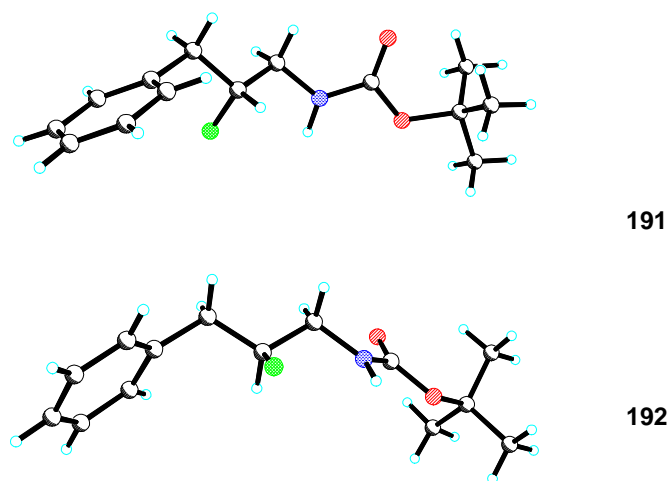


Figure 3.6: X-ray crystal structures of enantiomers (*R*)-(**191**) and (*S*)-(**192**).  
Torsion angles F-C-C-N are  $-66.8^\circ$  in (**191**) and  $66.4^\circ$  in (**192**).

Aromatic compounds (**191**) and (**192**) were then subjected to ruthenium-catalysed oxidation following Sharpless conditions.<sup>56</sup> Enantiomer (**191**) was mixed in a biphasic solution ( $\text{CCl}_4/\text{MeCN}/\text{H}_2\text{O}$ ; 1/1/1.5) with sodium periodate  $\text{NaIO}_4$  (20 equivalents). Ruthenium trichloride hydrate  $\text{RuCl}_3 \cdot x\text{H}_2\text{O}$  was then added (6-10% mol eq.) and the mixture was vigorously stirred at room temperature for two to four days. Filtration over Celite followed by evaporation of  $\text{CCl}_4$  and then extraction of the aqueous phase into EtOAc emerged as the most practical work-up. Disappointingly,  $^{19}\text{F}$  NMR analysis of the crude material showed the formation of several fluorinated products which could not be easily isolated by flash column chromatography (Figure 3.7). The oxidised product may have been formed in a low yield but the purification proved too problematical. Encouragingly, no aromatic products were detected in the reaction.

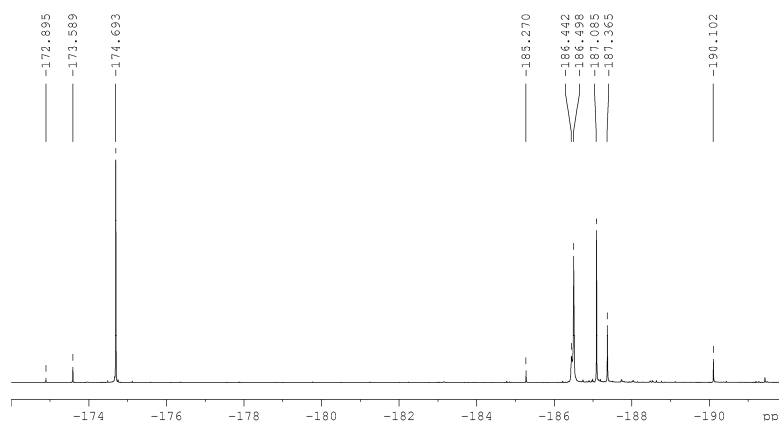
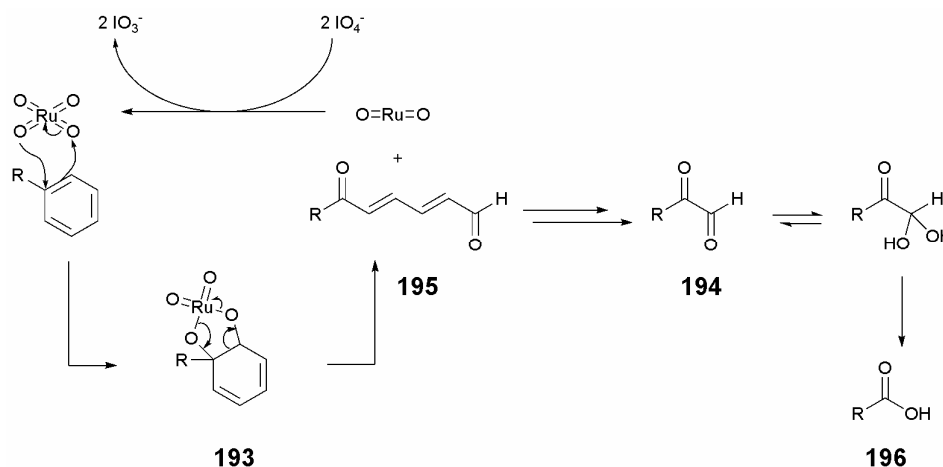


Figure 3.7:  $^{19}\text{F}$  NMR spectrum ( $\text{CDCl}_3$  at 280 MHz) of the crude material from the ruthenium-catalysed oxidation of (**191**).

The oxidative cleavage of aromatic rings by ruthenium is believed to proceed according to the simplified mechanism showed in Scheme 3.32.  $\text{RuCl}_3$  is first oxidised by water to give  $\text{RuO}_2$  which is further oxidised to the active ruthenium tetroxide species by concomitant reduction of  $\text{IO}_4^-$  to  $\text{IO}_3^-$ .  $\text{RuO}_4$  adds at the IPSCO carbon of the aromatic ring to form intermediate (**193**). Note that addition at another position on the ring leads to the formation of the same intermediate (**194**).<sup>57</sup> The C-C bond cleavage of (**193**) results in the formation of aldehyde (**195**) which is further oxidised in a similar manner to compound (**194**). Under Sharpless conditions, (**194**) becomes hydrated and then oxidised by periodate or ruthenium oxide to generate carboxylic acid (**196**).

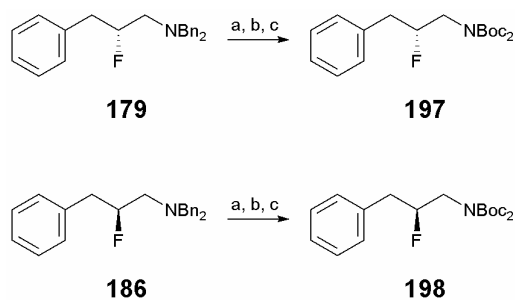


Scheme 3.32: Schematic mechanism of the ruthenium-catalysed oxidative cleavage of aromatic ring.

Although the oxidation of *N*-Boc-2-fluoro-3-phenylpropylamine (**191**) turned out to be disappointing, the fact that the aromatic oxidation had occurred was encouraging and prompted further investigation to optimise the reaction. As stated in the literature,<sup>58</sup> the reaction time of the oxidation was found to be significantly shortened by the addition of  $\text{HIO}_4$  instead of  $\text{NaIO}_4$  as co-oxidant, but this again, gave rise to a complex mixture of

compounds. Conversely, addition of  $\text{NaHCO}_3$  was prejudicial to the reaction and a substantial amount of starting material was recovered, even after longer reaction times. It is also clear from the literature that the oxidation is very temperature-sensitive and must be carried out between 25 °C and 40 °C.<sup>58</sup> It can stop if the temperature falls below 20°C or if stirring is insufficient. Hence, the reaction mixture was immersed in a temperature-controlled water bath at 25 °C and the development of a black-coloured spot, which indicates the presence of oxidised ruthenium, was also carefully examined. After modifications to the reaction conditions failed to produce any improved results, it was decided to undertake the oxidation step with a different substrate and to prepare the di-Boc-protected amines (**197**) and (**198**).

The second *tert*-butylcarbonyl group was introduced onto (**179**) and (**186**) using standard methodology, in aprotic solvent with a catalytic amount of DMAP. The removal of the dibenzyl group, and its replacement with a diBoc group was performed in one step, by evaporating MeOH after installation of the first Boc group, dissolving the residue in MeCN and heating the mixture under reflux after addition of  $\text{Boc}_2\text{O}$  and DMAP. Accordingly, the di-Boc-protected amine was obtained as a colourless oil in 80% yield from the dibenzyl protected amine (Scheme 3.33).



Scheme 3.33: Preparation of *N,N*-diBoc-protected amines (**197**) and (**198**).  
 Reagents and conditions: a)  $\text{Pd}(\text{OH})_2/\text{C}$ ,  $\text{H}_2$ , MeOH, 3 h; b)  $\text{Boc}_2\text{O}$ , RT, 14 h;  
 c)  $\text{Boc}_2\text{O}$ , DMAP, MeCN, 80 °C, 14 h, 78-80%.

Subjecting compounds (**197**) and (**198**) to the standard Sharpless conditions furnished the targeted products (*R*)- and (*S*)- *N,N*-diBoc-3-fluoro-GABA (**199**) and (**200**). The reaction was surprisingly clean as shown by the  $^{19}\text{F}$  and  $^1\text{H}$  NMR spectra of the crude product mixture. The only problem encountered in this reaction was the cleavage of one Boc group which presumably occurred during the acidic extraction of the aqueous phase. This could be avoided by extracting the water phase without acid but with a large volume of EtOAc. Purification by flash column chromatography afforded (**199**) and (**200**) in 75% and 76% yield respectively, showing the reliability and efficiency of this transformation.

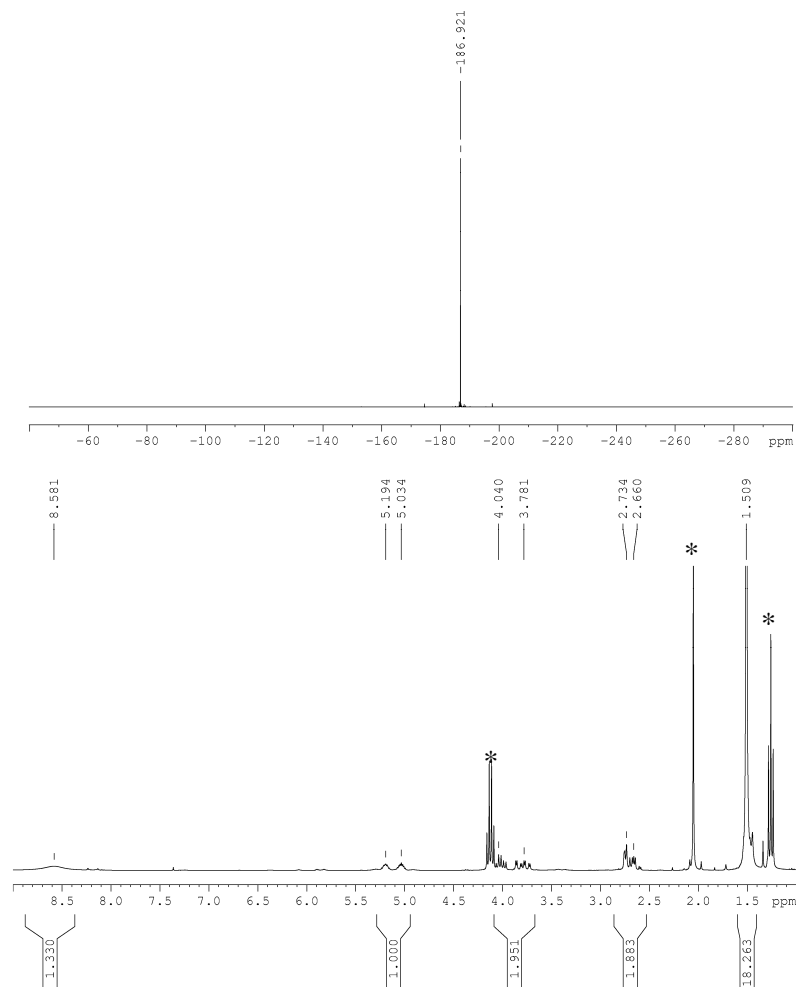
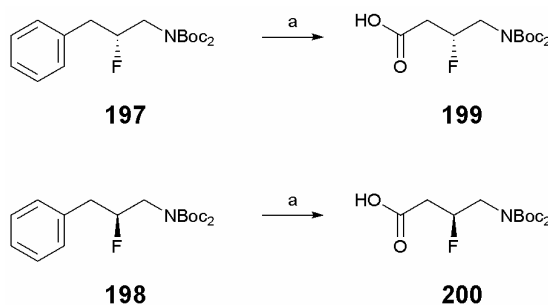


Figure 3.8:  $^{19}\text{F}$  (in  $\text{CDCl}_3$  at 280 MHz) and  $^1\text{H}$  NMR spectra (in  $\text{CDCl}_3$  at 300 MHz) of crude (**199**) product showing a clean conversion. The  $^1\text{H}$  NMR spectrum is contaminated only by residual EtOAc.



Scheme 3.34: Syntheses of (**199**) and (**200**) by ruthenium-catalysed oxidative cleavage of aromatic ring. Reagents and conditions:  $\text{NaIO}_4$  (18 eq),  $\text{RuCl}_3 \cdot x\text{H}_2\text{O}$  (6% mol),  $\text{CCl}_4/\text{MeCN}/\text{H}_2\text{O}$ , 25 °C, 3 days, 75-76%.

The final step of the synthesis required acidic cleavage of the *tert*-butylcarbonyl groups, for which trifluoroacetic acid (TFA) is a common reagent. However, TFA can be difficult to separate from amines and we have found during our synthesis of racemic 3-fluoro-GABA that purification on ion-exchange column can also be problematic. Consequently, it was judged that removal of the diBoc group would be more conveniently achieved with HCl gas. Re-crystallisation would then yield 3-fluoro-GABA as its hydrochloride salt.

Deprotection of the Boc protecting groups, followed by purification were indeed straightforward: HCl gas, generated by addition of concentrated sulfuric acid on sodium chloride was bubbled through a solution of (**199**) or (**200**) in dry DCM at 0 °C. Precipitation of the 3-fluoro-GABA hydrochloric salt occurred within 10 minutes, and single re-crystallisation from EtOH and  $\text{Et}_2\text{O}$  afforded (3*R*)- and (3*S*)-fluoro-4-aminobutyric acid hydrochloride (**123**) and (**124**) as colourless crystalline solids, in around 80% yield (Scheme 3.35).



Scheme 3.35: Synthesis of (3*R*)- and (3*S*)-fluoro-GABA hydrochloride by HCl gas treatment of diBoc-protected amines (**199**) and (**200**).

Reagents and conditions: a) HCl gas, DCM, 0 °C, 10 min, 80%

In order to confirm the integrity and absolute stereochemistry of the products, X-ray crystallography was explored. Obtaining crystals suitable for X-ray structure analysis was however more challenging than expected as the compounds re-crystallised as light flakes. Finally and despite the small size of the crystals, sufficient diffraction enabled structure elucidation of (3*R*)- and (3*S*)-fluoro-GABA hydrochloride, (**123**) and (**124**) (Figure 3.9).

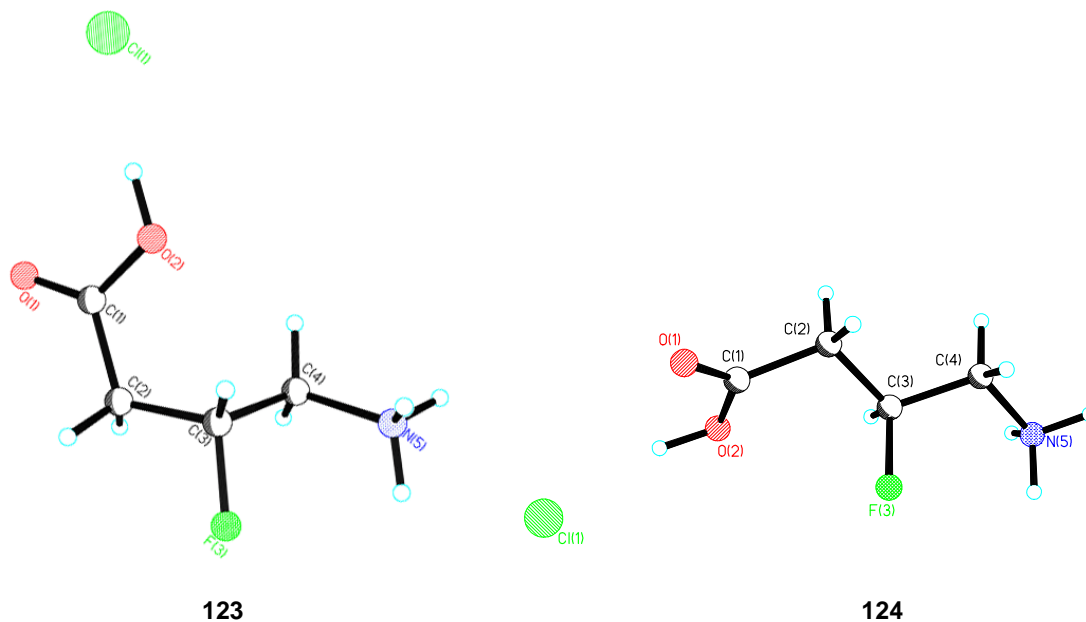


Figure 3.9: X-ray crystal structures of (3*R*)-fluoro-GABA.HCl (**123**) and (3*S*)-fluoro-GABA.HCl (**124**).



## 3.5 Conformation and evaluation of 3-Fluoro-GABA enantiomers

### 3.5.1 Conformational and NMR analyses

As expected, the ammonium aligns *gauche* to the fluorine in both enantiomers (3*R*)- and (3*S*)-fluoro-GABA hydrochloride (Figure 3.9). The F-C-C-N<sup>+</sup> torsion angle is -56.0° for the (*R*)-enantiomer and 64.8° for the (*S*)-enantiomer and although these two values are different, they remain close to the perfect *gauche* angle ( $\pm 60^\circ$ ). It is perhaps not surprising that both enantiomers re-crystallised in different conformations as 3-F-GABA, like GABA, is a flexible molecule. The (*S*)-enantiomer crystallised in a fully extended conformation, having the ammonium group and the four carbons in a same plane. The (*R*)-enantiomer adopted a slightly twisted conformation, with the carbon of the carbonyl pointing out of the plane formed by the ammonium and the three other carbons. The different conformations observed between the two enantiomers probably result from slightly different crystallisation conditions.

Crystal structures of GABA hydrochloride are available from the Cambridge Structural Database, under the codes GAMBAC01 and GAMBAC10. Both structures show GABA.HCl in an extended conformation (Figure 3.10 A). Also, at least three different conformations were found for GABA re-crystallised as a zwitterion (GAMBUT01, GAMBUT04 and GAMBUT10), indicating the flexibility of the molecule (Figure 3.10 B, C and D).

X-ray structure analysis confirms that 3-F-GABA and GABA can access various conformations in the solid state, but it gives only limited information on the most stable

conformation in solution. The conformational behaviour of 3-F-GABA in aqueous solution is important in understanding its binding properties on GABA recognition sites.

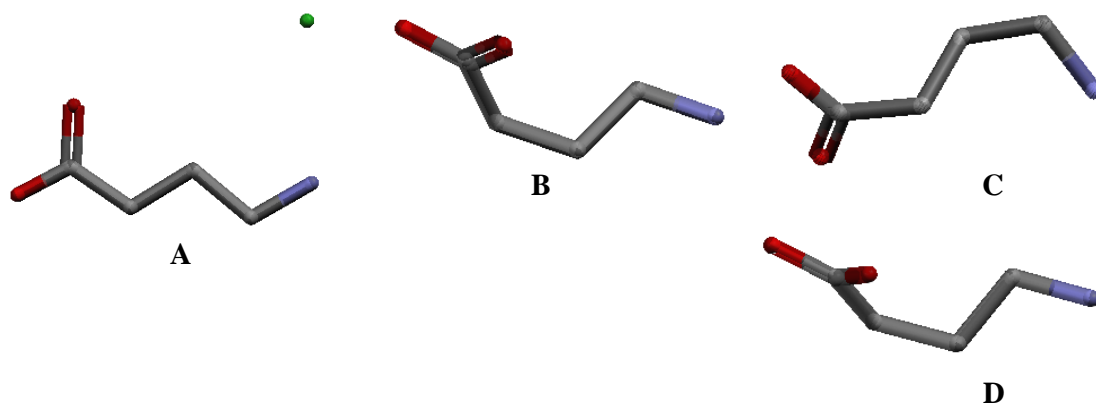


Figure 3.10: Crystal structures and conformations of GABA.HCl (A) and GABA (B, C and D) obtained from the CSD.

Similarly, the identification of low energy rotamer structures of GABA in the aqueous phase can furnish useful information on possible relevant biologically active conformations.  $^1\text{H}$  NMR analysis is not useful for a conformational analysis of GABA due to the achirality and rotational mobility of the molecule (Figure 3.11). *Ab initio* calculations however have proven to be more informative in the case of small molecules such as glycine,<sup>59</sup> adrenaline<sup>60</sup> or glutamic acid.<sup>61</sup> The neurotransmitter GABA has also been studied in this way,<sup>61-63</sup> and recently, M. J. Jordan *et al.* have investigated GABA and GABA analogues structures in aqueous solution using computational methods.<sup>64, 65</sup>

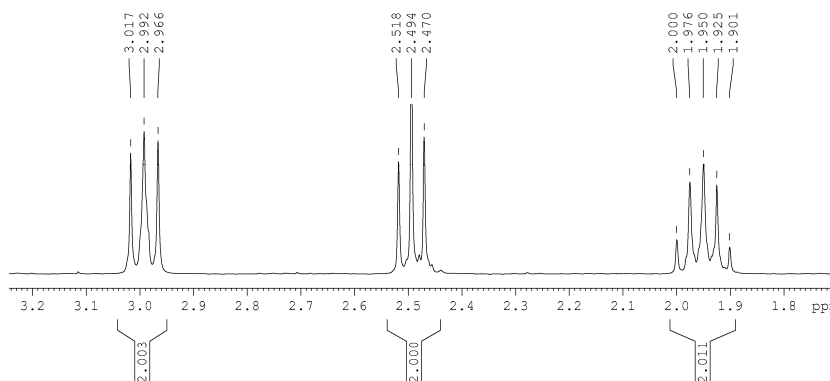


Figure 3.11:  $^1\text{H}$  NMR spectrum of GABA in MeOD (300 MHz).

The major problem facing computational chemists is to adequately model the hydration of GABA in order to obtain geometries related to experimental results. It is known that GABA exists in solution as a zwitterion and binds GABA<sub>A</sub> receptors in extended conformations. Failure to account for GABA's hydration gives misleading conclusions that neutral or folded structures are the most stable in solution. Hydration of GABA can be modelled by the explicit inclusion of water molecules or by estimating long-range water interactions with GABA using a polarised continuum model with the dielectric constant associated with water. In this model, GABA is enclosed into a water cavity with a surface built according to GABA's van der Waals surface.<sup>66</sup> To date, computation is still limited in such predictions and it was stated in 2004 that by using an *ab initio* approach, "it remains unclear ... which conformation, or conformations of GABA are biologically active."<sup>65</sup>

Thanks to the presence of fluorine, the solution conformations of 3-fluoro-GABA can be disclosed more readily by the careful interpretation of the <sup>19</sup>F and <sup>1</sup>H NMR spectra which contain much more information than the <sup>1</sup>H NMR spectrum of GABA. The stereogenic centre present in 3-F-GABA renders the protons of both methylene groups diastereotopic, with different coupling constants with the fluorine atom. This can be observed in the <sup>19</sup>F NMR spectrum which is a multiplicity of 25 signals (Figure 3.12). A total of 32 lines is expected in theory from the coupling of five protons but some peaks clearly overlap. Because of the high resolution of the <sup>19</sup>F NMR multiplicity, an attempt was made to extract the coupling constants from the spectrum. With the coupling constants in hand, it is then possible to reconstruct the geometry of the molecule and suggest the stable conformation(s) of 3-F-GABA in solution.

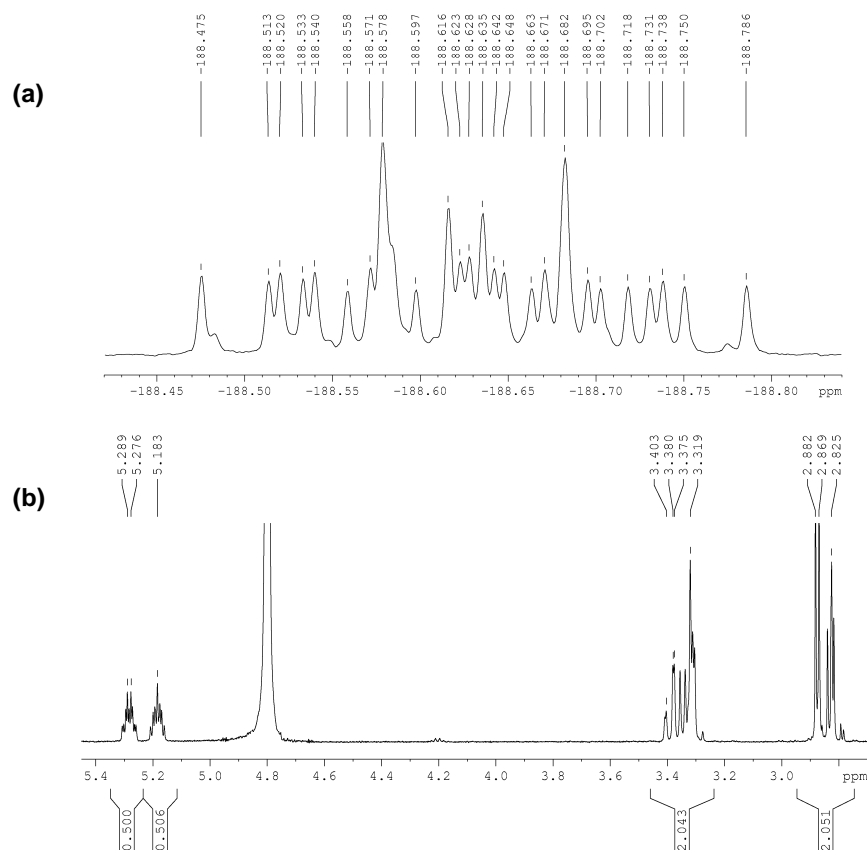


Figure 3.12: <sup>19</sup>F NMR (a) and <sup>1</sup>H NMR (b) spectra of 3-F-GABA in D<sub>2</sub>O at 500 MHz.

The similar chemical shifts of the diastereotopic protons and their large  $J_{\text{HF}}$  coupling constants generate a second-order spectrum where coupling constants cannot be read directly. To access these values, it proved necessary to simulate the spectrum and retrieve the coupling constants in that way. The NMR simulation software DAISY which is part of the NMR processing package TOPSPIN was used for this study.

In a separate evaluation, theoretical values for all coupling constants of the 3-F-GABA six-spin system were calculated *ab initio* (Dr Tanja van Mourik, St Andrews University). Firstly, the ten most stable conformers were identified and optimised using Density Functional Theory (DFT) with the B3LYP<sup>67</sup> functional and the 6-31+G\* basis set (Figure 3.13). The coupling constants of ten conformers were then calculated and are presented in Table 3.2.

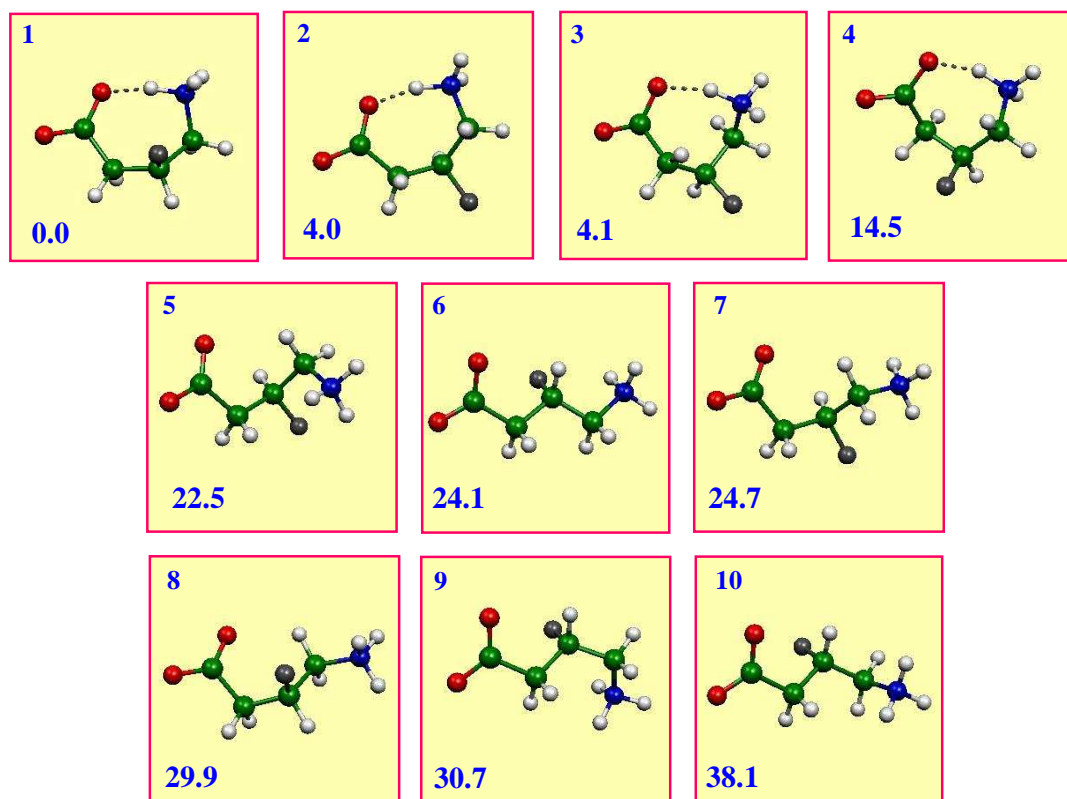
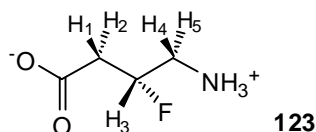


Figure 3.13: Ten most stable conformers of 3-F-GABA calculated using DFT.

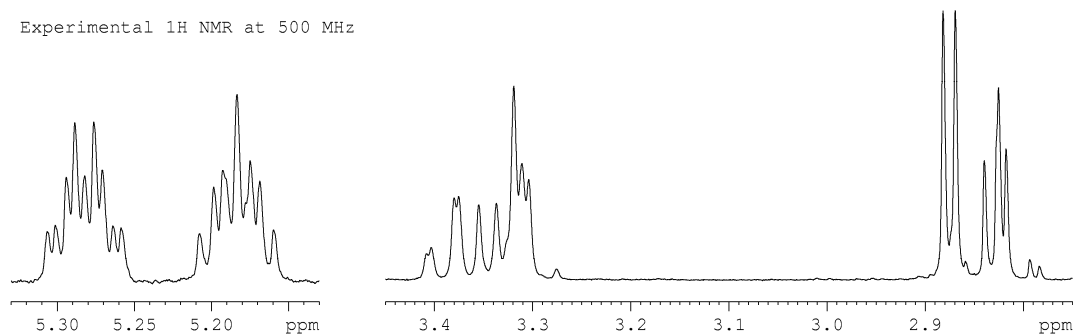


N°	$\Delta E_0$ (kJ/mol)	$^3J_{H5-F}$	$^3J_{H4-F}$	$^3J_{H3-H4}$	$^3J_{H3-H5}$	$^3J_{H2-F}$	$^3J_{H1-F}$	$^3J_{H1-H3}$	$^3J_{H2-H3}$	$^2J_{H4-H5}$	$^2J_{H1-H2}$	$^2J_{H3-F}$
1	0.00	2.59	28.80	0.47	6.20	4.60	49.22	1.73	6.61	-14.18	-17.70	47.95
2	3.95	-1.40	13.97	2.04	10.46	4.43	15.53	2.73	11.22	-12.46	-16.43	47.64
3	4.09	17.27	33.99	1.02	4.45	1.23	22.58	7.91	10.48	-15.04	-11.88	51.54
4	14.53	-1.40	17.76	8.05	8.84	17.75	49.93	3.00	4.78	-12.44	-15.75	52.74
5	22.50	7.09	30.59	0.99	4.65	4.35	11.13	4.69	12.34	-14.20	-17.27	48.65
6	24.10	8.75	27.52	1.97	11.06	14.37	51.73	1.37	10.78	-13.94	-16.10	55.54
7	24.69	9.80	30.51	1.75	10.12	3.49	14.19	4.21	11.29	-13.75	-16.52	56.42
8	29.90	10.70	29.62	1.65	10.50	5.53	52.26	1.57	6.37	-14.58	-16.18	56.84
9	30.67	6.75	29.05	1.20	4.18	15.03	49.78	1.25	11.82	-14.32	-15.69	47.85
10	38.07	0.20	8.36	3.31	11.04	14.37	51.73	1.37	10.78	-13.94	-16.10	55.54

Table 3.2: Relative energy and coupling constants of the ten most stable conformers calculated with DFT-B3LYP for 3-F-GABA.

The four lowest energy structures in Figure **3.13** have intramolecular hydrogen bonding between the ammonium and the carboxylate groups, and although they emerged as the lowest energy conformers, they are not expected to be relevant in an aqueous medium. The next six structures are more interesting, especially structures **6** and **7** which closely mimic the conformations found in the solid state structures of (3*S*)-F-GABA.HCl and (3*R*)-F-GABA.HCl (Figure **3.9**). The coupling constants associated with conformation **6** were then entered into the NMR simulation software DAISY and used as approximate values which were then refined by the software several times by iteration to match the simulated spectrum with the experimental one. It was finally possible to find a good match between the experimental spectrum and the simulated one (Figure **3.14** and **3.15**). The coupling constants determined by the software were found to match equally well for the  $^1\text{H}$  NMR and  $^{19}\text{F}$  NMR recorded at 400 MHz and 500 MHz (Table **3.3**).

Experimental  $^1\text{H}$  NMR at 500 MHz



Simulated  $^1\text{H}$  NMR at 500 MHz

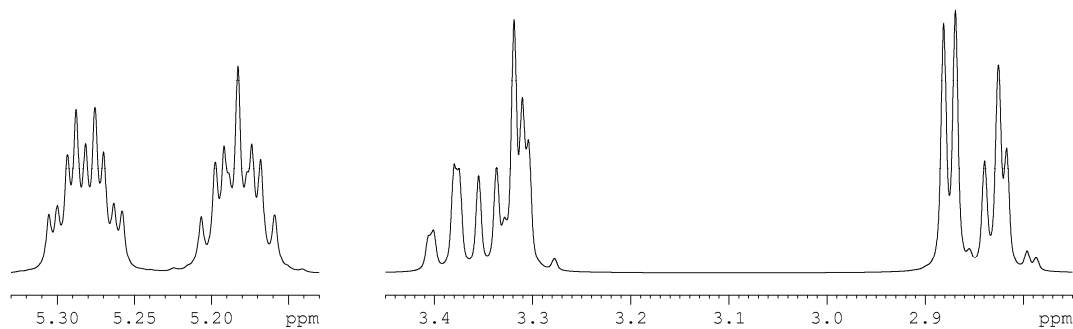
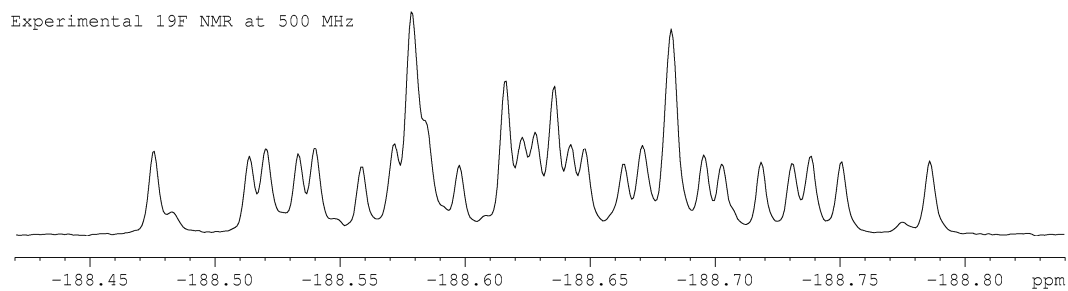
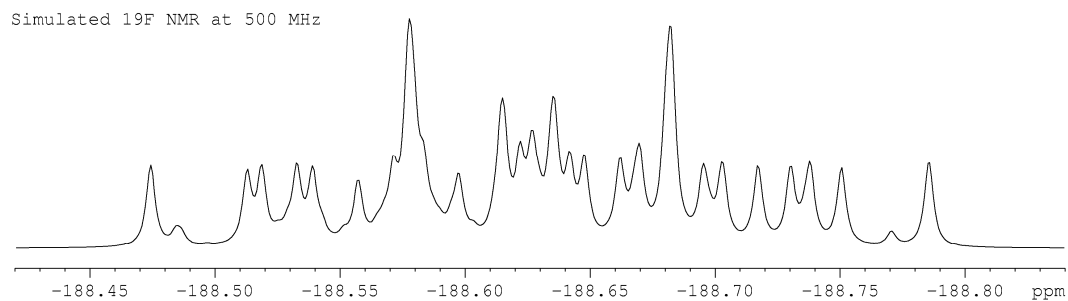


**Figure 3.14:** Experimental (above) and simulated (below)  $^1\text{H}$  NMR spectra of 3-F-GABA at 500 MHz in  $\text{D}_2\text{O}$  at 25 °C.

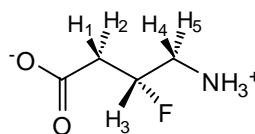
Experimental  $^{19}\text{F}$  NMR at 500 MHz



Simulated  $^{19}\text{F}$  NMR at 500 MHz



**Figure 3.15:** Experimental (above) and simulated (below)  $^{19}\text{F}$  NMR spectra of 3-F-GABA at 500 MHz in  $\text{D}_2\text{O}$  at 25 °C.

**123**

	H <sup>1</sup>	H <sup>2</sup>	H <sup>3</sup>	H <sup>4</sup>	H <sup>5</sup>
F	31.33	17.02	49.43	34.04	14.55
H <sup>1</sup>		-15.03	3.97	0	0
H <sup>2</sup>			8.05	0	0
H <sup>3</sup>				2.34	9.47
H <sup>4</sup>					-13.11

Table **3.3**: Experimental coupling constants extracted from simulated NMR spectra.

The experimental coupling constants in Table **3.3** can then be used to reconstruct the most appropriate geometries of 3-F-GABA conformers. As 3-F-GABA has a degree of conformational flexibility, it is expected that it can adopt several low-energy conformations in solution, particularly with rotation around the C<sub>2</sub>-C<sub>3</sub> bond. The coupling constants in Table **3.3** are consistent with an extended structure of 3-F-GABA in solution (such as structure **6**) computational studies are expected to confirm this.



### 3.5.2 pKa studies

The introduction of a fluorine atom does not induce a significant steric perturbation but it can of course change the electronic distribution in the molecule. This aspect of fluorine substitution has to be taken into account during the design of fluorinated medicinal chemistry compounds and in particular, in the case of  $\beta$ -fluorinated amines, as it is known that the fluorine causes adjacent functional groups to become more acidic. The effect of fluorine substitution on the pKa of primary amines is not well documented but a few reports indicate that it lowers the pKa by one to two pKa units (Figure 3.16).

In the case of 3-fluoro-GABA, fluorine can potentially influence the zwitterionic nature of the molecule by lowering the pKa of the amine and this could affect its protonation *in vivo*. It was therefore of interest to measure the pKa of 3-fluoro-GABA.

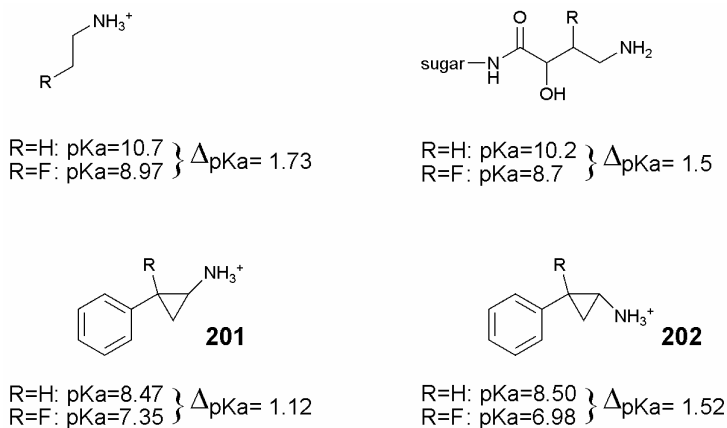


Figure 3.16: Examples of the fluorine substitution on the pKa of some primary amines.<sup>68, 69</sup>

It is noteworthy that the pKa of cyclopropylamine (**201**) which has a fluorine atom and an ammonium group locked in a *cis* relationship, is almost 0.4 of a pKa unit higher than isomer (**202**) in which the fluorine and ammonium substituents are *anti*.<sup>69</sup> Cyclopropylamine (**201**) is therefore less acidic than (**202**) and less prone to deprotonate. The lower acidity of (**201**) can be accounted for by an optimal charge...dipole interaction which stabilises the molecule and makes it more difficult to abstract a proton from the ammonium group (Figure 3.17). It follows that conformations which have the C-F and the C-N<sup>+</sup> bonds *gauche* are more difficult to deprotonate than those in which the C-F and C-N<sup>+</sup> bonds are *anti*.

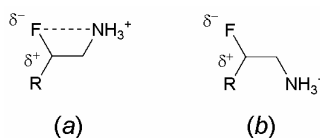
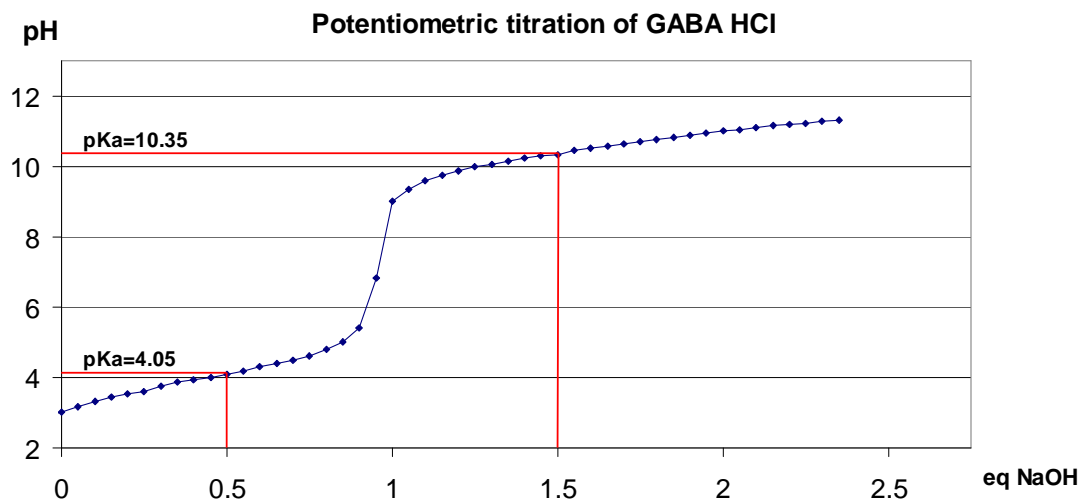


Figure 3.17: Stabilising charge...dipole interaction in (a).

The pKa values of GABA measured in water at 25 °C are 4.03 and 10.55.<sup>70, 71</sup> Before measuring 3-F-GABA hydrochloride, the potentiometric titration of GABA hydrochloride was carried out in order to validate the titration method.

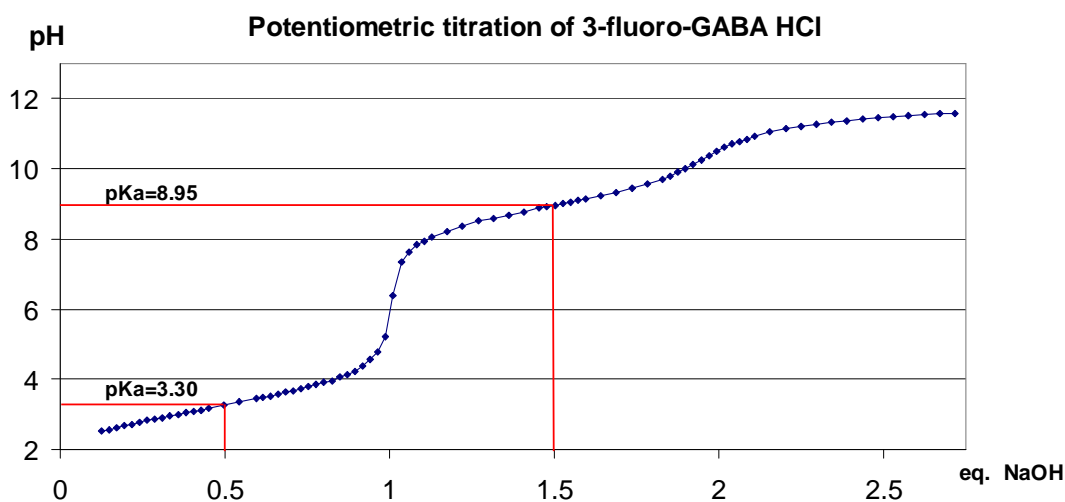
Accordingly, GABA HCl (6 mg) was diluted in pure deionised water (2 mL) and the solution was immersed in a temperature-controlled water bath at 25 °C and magnetically stirred. A pH electrode designed for the titration of small volumes was soaked into the GABA solution and the pH values were read on a pH meter which had previously been calibrated with standard solutions at pH 4 and pH 7. The NaOH titration solution ( $2.073 \times 10^{-2}$  mol.L<sup>-1</sup>) was calibrated with a known tartaric acid solution by acid-base titration using phenolphthalein as an indicator. Under these conditions, the added volume of NaOH solution at the equivalent point was around 2 mL, which induced a significant dilution factor. However, after minor correction, the experimental pKa values

for GABA. HCl turned out to be very close to the theoretical ones, confirming that this titration method was reliable (Graph 3.1). The pKa values can be read graphically on the curve in Graph 3.1 or more accurately from the volume of NaOH ( $2.073 \times 10^{-2} \text{ mol.L}^{-1}$ ) added.



Graph 3.1: Potentiometric titration of GABA HCl.

Similarly, 3-fluoro-GABA HCl (7.1 mg) was titrated against NaOH solution and the titration curve is presented in Graph 3.2. The experimental pKa values can be read graphically on the curve and according to the volume of NaOH ( $2.073 \times 10^{-2} \text{ mol.L}^{-1}$ ) added.



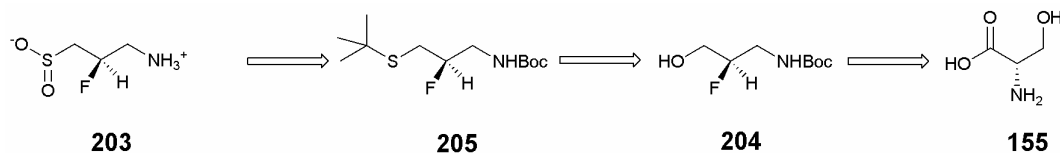
Graph 3.2: Potentiometric titration of 3-F-GABA HCl.

As illustrated on the titration curve in Graph 3.2, the fluorine substituent in 3-F-GABA lowers the pKa of the carboxylic acid by 0.75 pKa unit and the amine by 1.6 pKa unit (Table 3.4). The pKa value of 3-F-GABA (pKa=8.95) is in the same range as other fluorinated primary amines, such as fluoroethylamine (pKa=8.97) and fluorinated GABA analogue (2*R*)-(3-amino-2-fluoropropyl)sulfinic acid (**203**) (pKa= 8.5), a structure that was recently published in 2007.<sup>72</sup>

	pKa <sub>1</sub>	pKa <sub>2</sub>
GABA.HCl	4.03	10.55
3-F-GABA.HCl	3.30	8.95

Table 3.4: pKa of GABA.HCl and 3-F-GABA.HCl

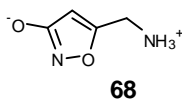
Interestingly, (**203**) was prepared from *tert*-(2*R*)-fluoro-3-hydroxypropylcarbamate (**204**) by mesylation and reaction with *tert*-butyl thiol. Sulfide (**205**) was then oxidised with *m*CPBA and reacted with trifluoromethanesulfonic acid to give (**203**). Compound (**204**) was presumably prepared from L-serine (**155**) as described previously but details of the synthesis were not given as a patent was deposited by AstraZeneca for this class of compounds.<sup>73, 74</sup>



Scheme 3.36: Schematic synthesis of novel fluorinated GABA analogue (**203**).<sup>72-74</sup>

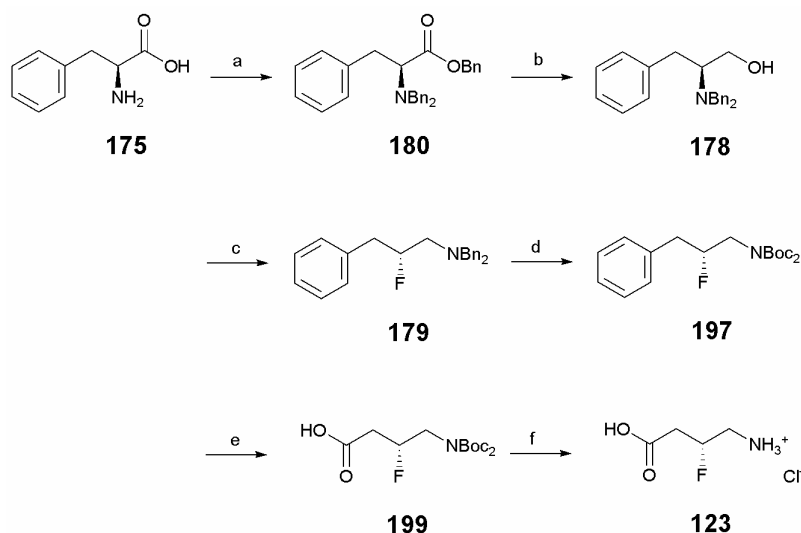
A pKa of 8.95 signifies that 3-F-GABA will exist as a zwitterion *in vivo* and therefore will likely behave as a GABA analogue in that respect. pKa values are most probably not determining factors for the binding affinity of GABA analogues. As an example, muscimol (**68**) also shown in Table 2.1 is one of the most potent GABA analogue

at GABA<sub>A</sub> receptors but has pK<sub>a</sub> values of 4.8 and 8.4. Muscimol is isolated from the white-spotted red mushroom *Amanita Muscaria*.



### 3.5.3 Conclusions

The first successful enantioselective synthesis of both (3*R*)- and (3*S*)-fluoro-GABA hydrochloride was executed as summarised in Scheme 3.37. Over 100 mgs of both enantiomers were obtained in six steps and in an overall yield of 31% from L-phenylalanine and D-phenylalanine methyl ester hydrochloride respectively. In this synthesis, it was shown that the fluorination of the dibenzylamino alcohol (**178**) is enantioselective and that the oxidation of the aromatic ring proceeds cleanly to furnish the carboxylic acid (**199**). More generally, this synthesis shows that enantiopure β-fluoroamines are accessible from α-amino acids.



Scheme 3.37: Enantioselective synthesis of (3*R*)-fluoro-GABA hydrochloride (**123**) from L-phenylalanine (**175**). Reagents and conditions: a) BnBr, K<sub>2</sub>CO<sub>3</sub>, EtOH, 90%; b) LiAlH<sub>4</sub>, THF, 95%; c) Deoxo-Fluor<sup>TM</sup>, DCM, 75%; d) 1. Pd(OH)<sub>2</sub>/C, H<sub>2</sub>, Boc<sub>2</sub>O, MeOH, 2. Boc<sub>2</sub>O, DMAP, MeCN, 80%; e) NaIO<sub>4</sub>, RuCl<sub>3</sub>, CCl<sub>4</sub>/MeCN/H<sub>2</sub>O, 76%; f) HCl gas, DCM, 80%.

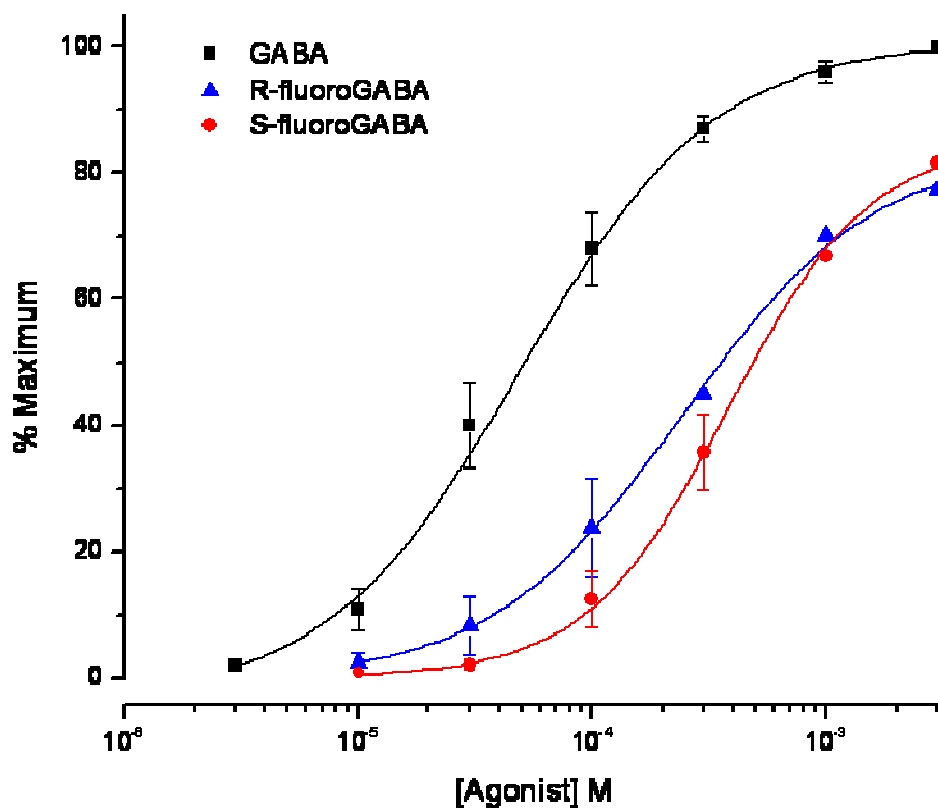
## 3.6 Biological studies

### 3.6.1 Studies on GABA receptors

The activities of 3-F-GABA enantiomers were evaluated at the School of Neurobiology at Ninewells Hospital in Dundee on recombinant GABA<sub>A</sub> receptors expressed in *Xenopus laevis* oocytes. To generate cloned GABA<sub>A</sub> receptors, DNAs encoding the human GABA<sub>A</sub>  $\alpha_1\beta_2\gamma_2$  subunits were used to produce cRNA transcripts, which were injected intranuclearly into *Xenopus laevis* oocytes. Recordings were then made from oocytes two to twelve days after cRNA injection. Such a procedure allows the expression of human GABA<sub>A</sub> receptors at the surface of oocyte membranes and this has proven to be an effective experimental model for exploring GABA induced chloride flux across membranes. The activities of GABA agonists were measured by recording induced currents at a holding potential of  $-60\text{mV}$ . In the data presented below,  $E_{\text{max}}$  refers to the maximal current produced by a saturating concentration of the agonist and  $\text{EC}_{50}$  refers to the concentration of agonist that produces a response 50% of the maximum  $E_{\text{max}}$ .

Unfortunately, a comprehensive study on the effects of 3-F-GABA enantiomers at GABA<sub>A</sub> receptors can not be presented here as, to date, only preliminary results were obtained from biological testing. Nevertheless, a general picture of the action of 3-F-GABA enantiomers on human GABA<sub>A</sub> receptors can be drawn and it appears that (3*R*)- and (3*S*)-fluoro-GABA have similar activity on GABA<sub>A</sub> receptors (Table 3.5 and Graph 3.3).

	$E_{\max}$	$EC_{50}$
GABA	100%	$4.9 \cdot 10^{-5}$ M
(3 <i>R</i> )-F-GABA	77%	$2.4 \cdot 10^{-4}$ M
(3 <i>S</i> )-F-GABA	82%	$3.8 \cdot 10^{-4}$ M

Table 3.5: Activities of GABA and 3-F-GABA enantiomers on GABA<sub>A</sub> receptors.Graph 3.3: Activities of GABA (■), (3*R*)-F-GABA (▲) and (3*S*)-F-GABA (●) on GABA<sub>A</sub> receptors.

The curves in Graph 3.3 indicate that (3*R*)-fluoro-GABA (**123**) requires to be seven times more concentrated than GABA to reach the  $EC_{50}$  response of GABA, and in that respect, the (*R*)-enantiomer is 14% as active as GABA on GABA<sub>A</sub> receptors. The (*S*)-enantiomer is only 10% as active. By comparison, (3*R*)-hydroxy-GABA is 3.3% as active as GABA and (3*S*)-hydroxy-GABA is 8.3% as active (see Table 2.2 p 66). Drawing any

conclusion at this point would be too speculative, but it appears from these data that; firstly, GABA<sub>A</sub> receptors do not distinguish significantly between (*R*)- and (*S*)-enantiomers, suggesting that  $\tau_N$  in GABA binding conformations is close to 180° and that, 3-F-GABA, despite its close steric resemblance with GABA, exhibits poor binding activity. It is hoped that further experiments will allow the respective biological effects of both enantiomers to be refined.

3-F-GABA enantiomers were also tested on a whole tadpole system where the effects of GABA and 3-F-GABA were observed for motorneuronal activity associated with the fictive swimming response of the tadpole (Figure 3.18). The experiments were conducted at the School of Biology in St Andrews in Prof. K. Silar's research labs.

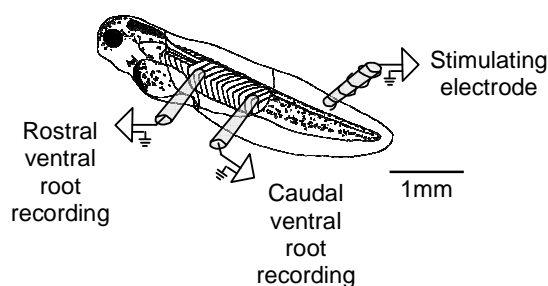
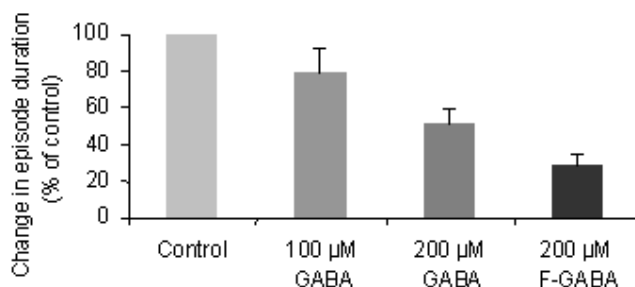


Figure 3.18: Schematic representation of the biological tests conducted on tadpoles.

Experiments performed on racemic 3-F-GABA (prepared by F. Chorki) showed that the compound largely retained the properties of GABA and bind to both GABA<sub>A</sub> and GABA<sub>B</sub> receptors. The GABA<sub>B</sub> response was indicated by the reversal of its effects by selective GABA<sub>A</sub> and GABA<sub>B</sub> antagonists.<sup>75</sup> It was also noticed that 3-F-GABA, when compared to GABA, reduced significantly the swim episode duration of the tadpole (Graph 3.4). The swim episode duration is the time between the first and the last burst in the swimming episode provoked by the stimulation of the nervous system. The fact that the

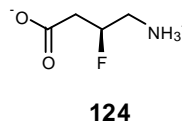
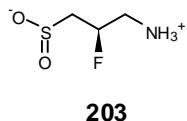


tadpole stopped swimming quicker with 3-F-GABA suggested that it remained available longer than GABA, which could be the result of a lower affinity of 3-F-GABA for GABA transporters or that it is metabolised more slowly by GABA aminotransferase.



Graph 3.4: Analysis of the effect of GABA and racemic 3-F-GABA on swim episode duration.<sup>75</sup>

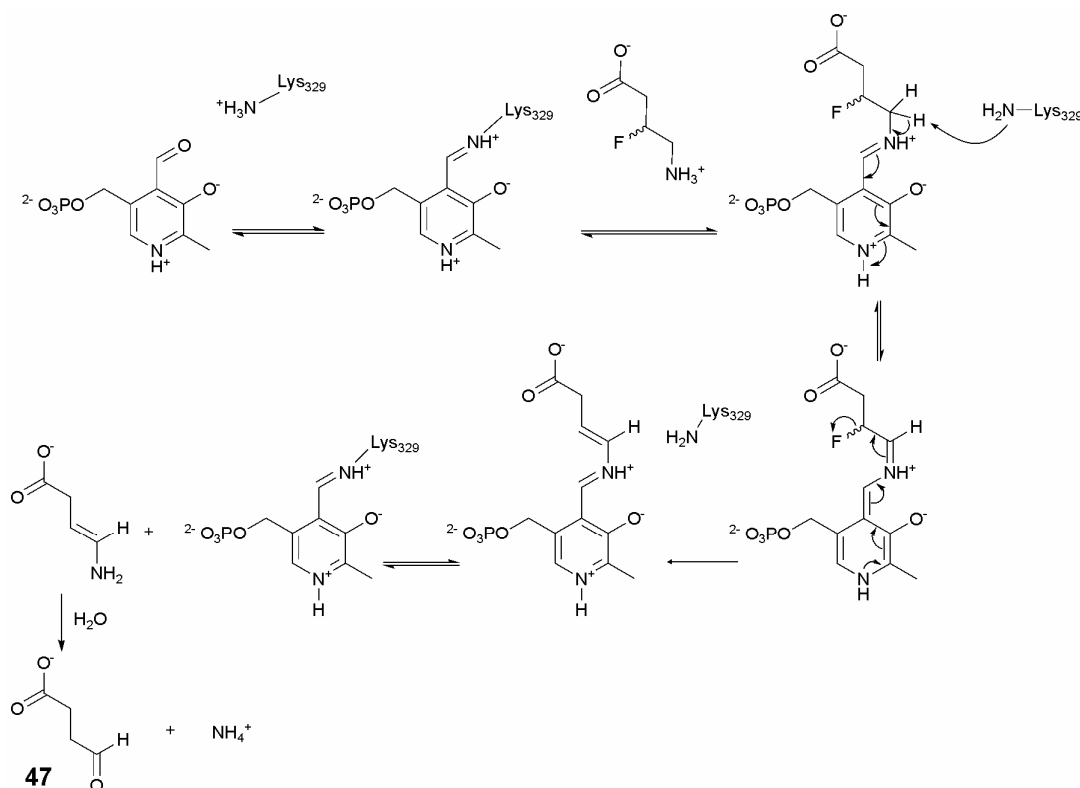
Experiments performed on enantiopure 3-F-GABA showed a clear difference in the swimming response between the (*R*)- and (*S*)-enantiomers, with (*S*) being more potent than (*R*). When GABA<sub>A</sub> receptors were blocked with bicuculline (**58**), a marked difference was still observed between the two enantiomers. It was advanced that 3-F-GABA and particularly the (*S*)-enantiomer was GABA<sub>B</sub> selective. Interestingly, very few compounds are known to exhibit selective GABA<sub>B</sub> activity, baclofen (**59**) being the only GABA<sub>B</sub> agonist approved for clinical use. But recently, (2*R*)-(3-amino-2-fluoropropyl)sulfinic acid (**203**) was reported to have a high GABA<sub>B</sub>/GABA<sub>A</sub> selectivity.<sup>72, 73</sup>



The close structural and stereochemical analogy between (**203**) and (3*S*)-F-GABA (**124**) clearly support the idea that the latter is GABA<sub>B</sub> selective, but *in vivo* experiments on tadpoles are unsuitable to validate this hypothesis. However, it could be confirmed by experiments on cloned GABA<sub>B</sub> receptors. Obviously, such experiments merit investigation.

### 3.6.2 Studies on GABA aminotransferase

Early observations that racemic 3-F-GABA might remain metabolically available for longer than GABA prompted us to test 3-F-GABA enantiomers as substrates or inhibitors of GABA aminotransferase (GABA AT). As stated in chapter 2, GABA AT is a PLP-dependent enzyme which metabolises GABA to succinic semialdehyde (**47**) (Scheme 1.3 and 2.1). In 1981, R. Silverman *et al.*<sup>76</sup> investigated the activity of racemic 3-F-GABA and found that it was a substrate for GABA AT but without conversion of PLP to PMP. 3-F-GABA was able to bind to the enzyme but was not oxidised to succinic semialdehyde in the normal manner with concomitant PLP reduction to PMP (see scheme 1.3). Instead, it emerged that the enzyme catalysed the elimination of HF from the substrate, converting it ultimately to succinic semialdehyde by a process summarised in Scheme 3.38.



Scheme 3.38: Elimination of HF from 3-F-GABA catalysed by GABA AT.

Samples of the 3-F-GABA enantiomers were sent to Prof. R. Silverman at the Northwestern University of Evanston (Illinois, USA) to be evaluated with GABA AT. Consistent with the previous results with racemic 3-F-GABA, neither enantiomer was found to be a substrate for transamination but both underwent HF elimination. Interestingly, elimination of HF from the (*R*)-enantiomer proceeded at a rate of  $6.63 \times 10^{-2}$   $\mu\text{moles} \cdot \text{min}^{-1} \cdot \text{mg}^{-1}$  whereas HF elimination from (*S*)-enantiomer was ten times slower at  $6.26 \times 10^{-3}$   $\mu\text{moles} \cdot \text{min}^{-1} \cdot \text{mg}^{-1}$ . These values were obtained using a fluoride ion selective electrode, but HF elimination was also measured by the evaluation of succinic semialdehyde production.<sup>77</sup> However, the rate of succinic semialdehyde production from (*S*)-enantiomer was too slow to calculate kinetic constants using this method.

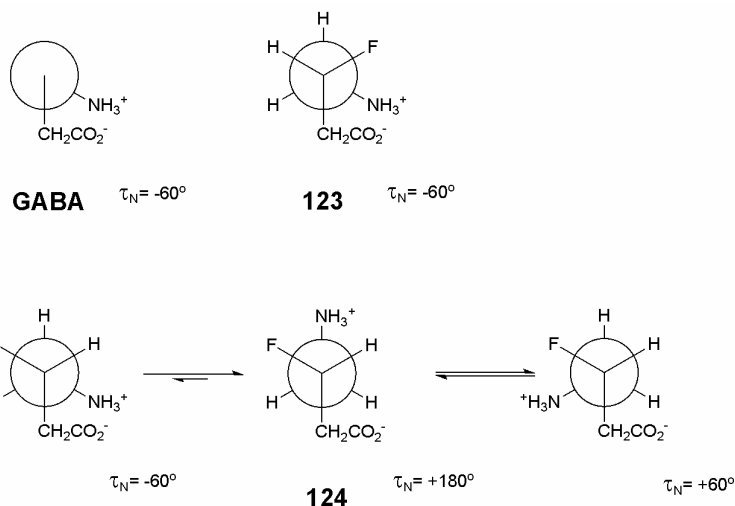
The ability of both enantiomers of 3-F-GABA to bind to the active site of GABA AT was then examined. In order to achieve this, (3*R*)- and (3*S*)-F-GABA were assayed as competitive inhibitors of GABA transamination according to the following principle: the oxidation of one molecule of GABA to succinic semialdehyde generates one molecule of PMP, which in the presence of radiolabeled [<sup>14</sup>C]  $\alpha$ -ketoglutarate (**48**) produces one molecule of radiolabeled [<sup>14</sup>C] L-glutamate (**43**) (see Scheme **2.1**). 3-F-GABA does not generate PMP, therefore the amount of  $\alpha$ -ketoglutarate converted to (**43**) is representative of GABA transamination. The conversion of (**48**) to (**43**) was then measured with different concentrations of (3*R*)- and (3*S*)-F-GABA (Table **3.6**). In the event, it was found that the (*R*)-enantiomer (**123**) showed substantial competitive inhibition of GABA transamination whereas the (*S*)-enantiomer (**124**) showed no significant inhibition.

Concentration of 3-F-GABA enantiomer (nM)	% $\alpha$ -KG ( <b>48</b> ) converted to Glu ( <b>43</b> )/unit time	
	(3 <i>R</i> )-F-GABA ( <b>123</b> )	(3 <i>S</i> )-F-GABA ( <b>124</b> )
0.000	6.79	6.79
0.050	6.97	7.28
0.250	3.89	7.00
0.500	1.87	7.23
1.000	0.97	6.74

Table **3.6**: Inhibition of GABA transamination as measured by a reduction in the rate of conversion of [ $^{14}\text{C}$ ]  $\alpha$ -ketoglutarate to [ $^{14}\text{C}$ ] L-glutamate over 15 min.<sup>77</sup>

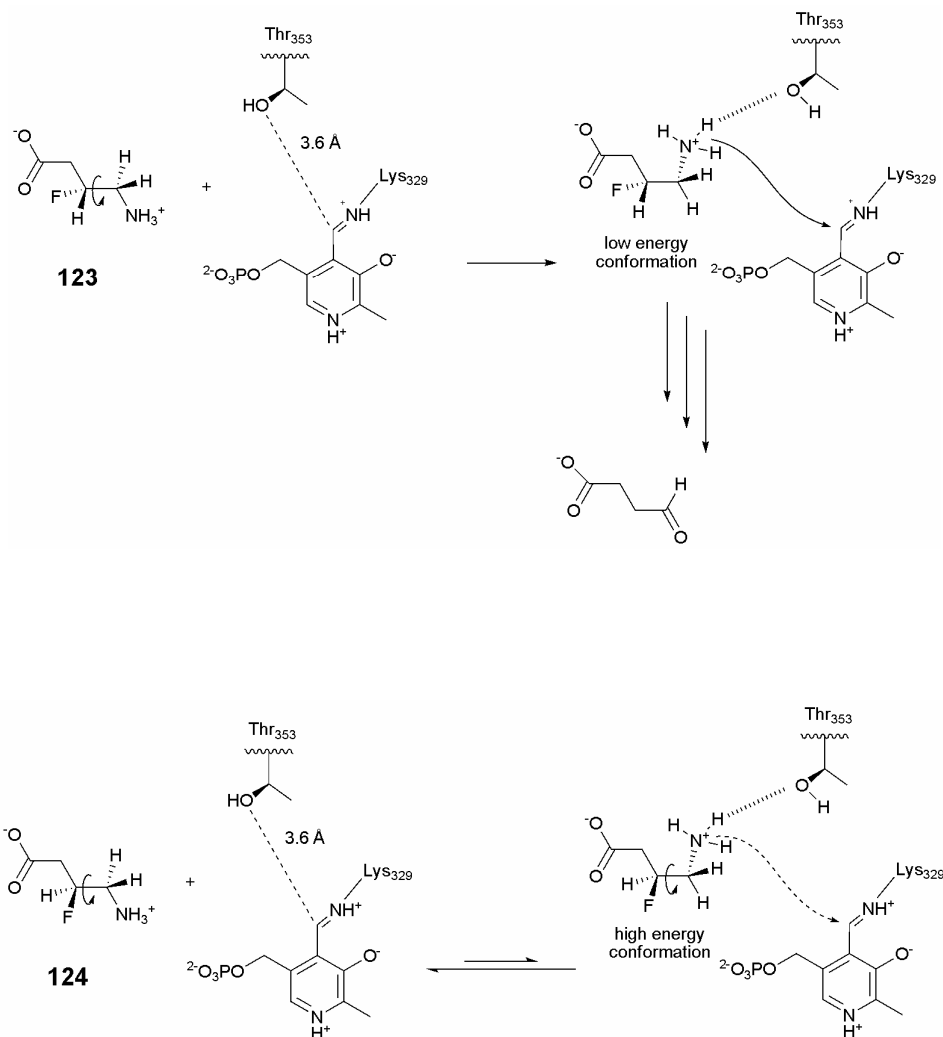
The data in Table **3.6** clearly indicate that the (*S*)-enantiomer does not bind well to the active site of GABA AT, as such binding would inhibit the transamination of GABA, resulting in a reduction in the rate of glutamate production. Conversely, the (*R*)-enantiomer causes inhibition of transamination, suggesting that this enantiomer binds much more efficiently to the enzyme. In another experiment, it was shown that the (*R*)-enantiomer inhibited GABA AT at least ten times better than the (*S*)-enantiomer, indicating an improved binding affinity of (*R*) over (*S*).

These findings suggests that the preferred conformation in solution of (3*R*)-F-GABA (**123**) is more optimal for binding to the enzyme than the preferred conformation in solution of (3*S*)-F-GABA (**124**). A possible interpretation of these results, based on the conformational analysis shown in Figure **3.1** (p 99) is that the preferred torsion angle  $\tau_{\text{N}}$  for binding to the GABA AT is close to  $-60^\circ$ . Only the (*R*)-enantiomer can access this binding conformation whereas in the case of the (*S*)-enantiomer, such a conformation is much higher in energy. The preferred binding modes of GABA, (3*R*)- and (3*S*)-F-GABA are described in Scheme **3.39**.



Scheme **3.39**: Topological description of the preferred binding conformations of GABA and 3-F-GABA enantiomers for GABA AT. In (3*S*)-F-GABA (**124**), the conformation with  $\tau_N = -60^\circ$  is high in energy due to the *anti* relationship of the C-F and C-N<sup>+</sup> bonds.

The difference in binding affinity of both enantiomers (3*R*)- and (3*S*)-F-GABA is interpreted as an indication that GABA binds to GABA AT with a torsion angle  $\tau_N$  close to  $-60^\circ$ . This statement is supported by mechanistic considerations of 3-F-GABA binding to the active site of GABA AT. After entering the substrate binding site of GABA AT, the substrate follows a cascade reaction involving, first the deprotonation of one ammonium proton, then the attack to the imine carbon of the Lys329-PLP adduct and then the formation of the 3-F-GABA-PLP adduct. The approach of the nucleophilic amino group of 3-F-GABA to the electrophilic imine carbon occurs with a Bürgi-Dunitz trajectory.<sup>78</sup> Deprotonation of the ammonium is assisted by the side chain hydroxyl group of residue Thr353, located 3.6 Å away, top and back side of the imine carbon atom (Thr353 can be seen in the background of the active site of GABA AT in Figure 2.1). The threonine-assisted deprotonation and the nucleophilic attack imply that the ligand adopts the conformation shown in Scheme 3.40 with the torsion angle  $\tau_N = -60^\circ$ .



Scheme 3.40: Illustration of the dynamic binding process of (123) and (124). The conversion of (124) to the active conformation needs energy penalty as the C-F bond becomes *anti* to the C-N<sup>+</sup> bond. In (123), the C-F and the C-N<sup>+</sup> bonds remain *gauche*.<sup>77</sup>

This study suggests that GABA has a preferred binding conformation on GABA AT and that only the (3*R*)-F-GABA enantiomer can easily access this binding mode in solution.

The difference in activities observed between 3-F-GABA enantiomers on GABA AT validates for the first time the concept of using the C-F bond as a tool to influence the conformational mobility of biologically active amines. It also demonstrates that the C-F bond can be used as a conformational probe to reveal the binding conformation(s) of

GABA. Further conformational studies will now be conducted on other GABA recognition sites, such as GABA<sub>B</sub> receptors and GABA transporters.

### 3.6.3 Conclusions

(*R*)- and (*S*)- 3-Fluoro-GABA enantiomers have been found to possess similar activities on cloned GABA<sub>A</sub> receptors expressed in *Xenopus laevis* oocytes. They are respectively 14% and 10% as active as GABA. A clear difference in activity was observed *in vivo* on tadpoles. Interestingly, the (*S*)-enantiomer was found to be much more potent than the (*R*)-enantiomer. This difference could arise from GABA<sub>B</sub> selectivity but further experiments on cloned GABA<sub>B</sub> receptors are required. A marked difference was also noticed on GABA-AT, with the (*R*)-enantiomer being metabolised ten times quicker than the (*S*)-enantiomer. This study has shown that the stereoselective introduction of the C-F bond at the 3-position in 3-F-GABA influences the conformational mobility and the biological activity of the molecule.

Importantly, the concept of using the stereoelectronic influence of fluorine to limit the conformational mobility of bioactive molecules can potentially be applied to many other biological targets including amines and amides, in which the fluorine atom is known to exercise a strong conformational influence. This offers exciting prospects for future research.

## 3.7 Toward the synthesis of 3-fluoro-GABA analogues.

### 3.7.1 Synthesis of conformationally constrained GABA analogues

3-F-GABA, despite the conformational constraints introduced by the presence of the C-F bond, remains a flexible molecule. Its most stable conformations in solution do not inform for instance on the preferred orientation of the carbonyl group of GABA on GABA binding sites. An interesting example of a conformationally constrained GABA analogue is (1*S*,3*S*)-*trans*-3-aminocyclopentane carboxylic acid (**70**) (see Table 2.1) which exhibits high activity on GABA<sub>A</sub> receptors whereas its enantiomer is much less active.<sup>79</sup> The cyclopentane ring obviously induces conformational constraints but is still quite flexible.

Thus, compound (**70**) can access different conformations such as (**70a**) and (**70b**) as illustrated in Figure 3.19. In the scope of this work, it was thought that the introduction of a fluorine atom  $\beta$  to the amino group, at the 2-position (**206**) or at the 4-position (**207**) of the cyclopentane ring, could further constrain the conformational mobility of the cyclopentane ring. Indeed, conformations (**206b**) and (**207b**) are not expected to be significantly populated in solution due to the *anti* relationship between the C-F and the C-N<sup>+</sup> bonds.

Amino acids (1*R*,2*S*,3*S*)-3-amino-2-fluorocyclopentane carboxylic acid (**206**) and (1*R*,3*R*,4*R*)-3-amino-4-fluorocyclopentane carboxylic acid (**207**) are unknown and present challenging target molecules for synthesis. In particular, compound (**206**) and its (2*R*)-isomer can be regarded as conformationally restricted analogues of 3-F-GABA. For that reason, it was judged interesting to assess these analogues for testing on GABA<sub>A</sub> and GABA<sub>B</sub> receptors.



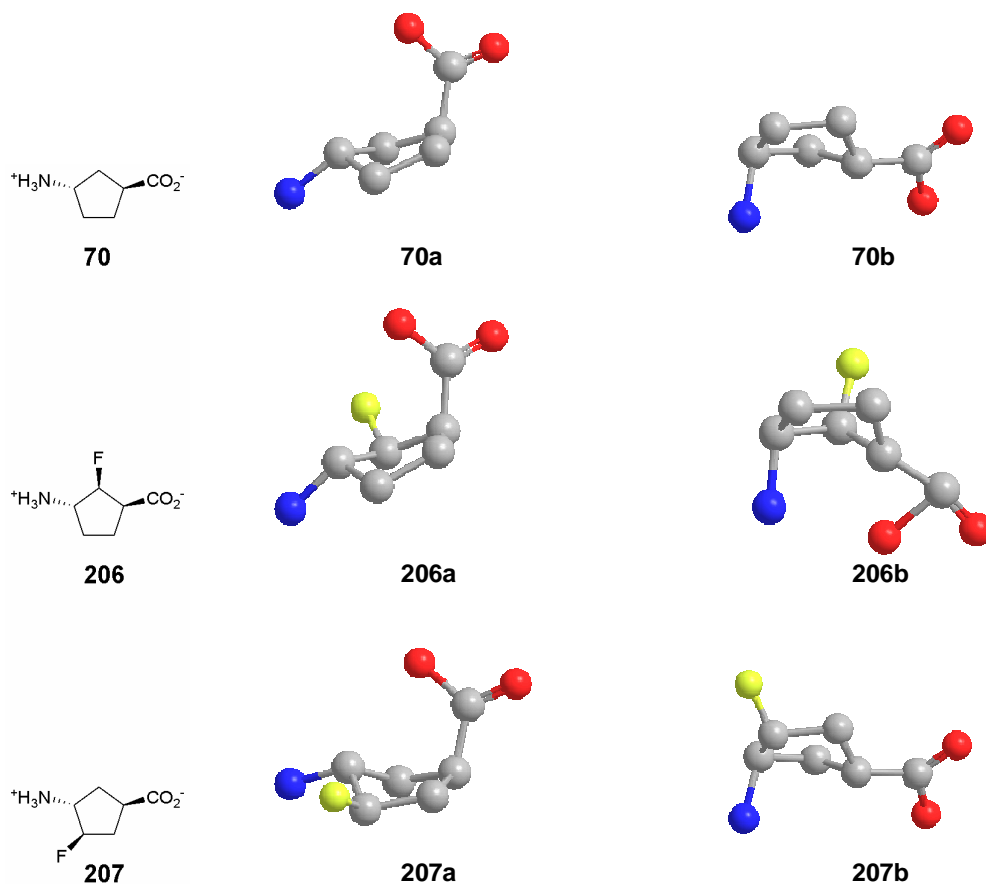
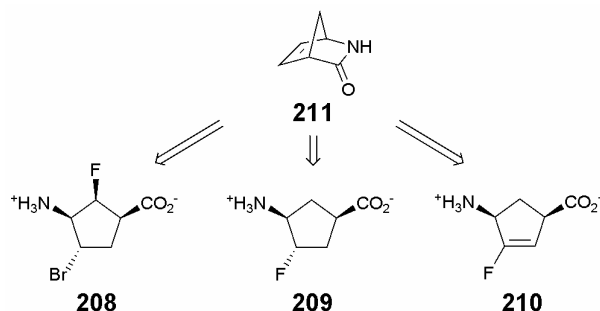


Figure 3.19: Illustration of the cyclopentane ring flexibility in (**70**) and the effect of the C-F bond on the conformational mobility of (**206**) and (**207**). Conformations (**206b**) and (**207b**) have the C-F and C-N<sup>+</sup> bonds in an *anti* relationship.

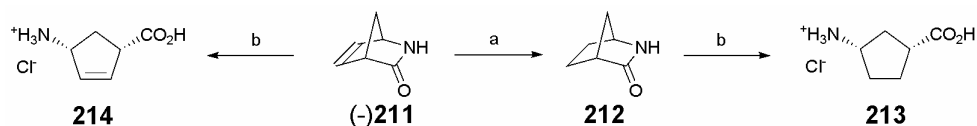
It should be noted that close analogues of (**206**) and (**207**) have already been prepared and tested as inhibitors of GABA-AT, but all of them (**208**), (**209**), (**210**) have the amino and the carboxylic acid groups in a *cis* relationship, which appears to be optimal for GABA AT inhibition. They were all synthesised from commercially available (-)-2-azabicyclo[2.2.1]hept-5-en-3-one (**211**) (Scheme 3.41).<sup>80, 81</sup>



Scheme 3.41: Preparation of halogenated 3-amino-cyclopentane carboxylic acid derivatives from (211).<sup>80, 81</sup>

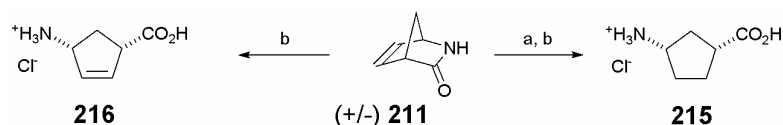
It is known that a *trans* relationship between the amino and carboxylic groups is preferable for GABA<sub>A</sub> binding activity.<sup>79</sup> *Trans* compounds such as (70) have been prepared by thermal isomerisation of *cis* compounds<sup>82</sup> or by re-crystallisations<sup>83</sup> of *cis/trans* mixtures, but no straightforward and appealing stereoselective synthesis of (70) has emerged. The synthesis of *cis*-3-aminocyclopentane carboxylic acids is however straightforward from (211). It was decided to prepare such compounds and then, to investigate the enantioselective synthesis of fluorinated and non-fluorinated analogues of (70) for biological evaluations.

Non-fluorinated *cis*-3-aminocyclopentane carboxylic acids were readily prepared following published procedures,<sup>84, 85</sup> starting from 2-azabicyclo[2.2.1]hept-5-en-3-one (211) which is commercially available in enantiomeric pure form and as a racemate. Accordingly, enantiopure amino acids (213) and (214) were synthesised from (-)-(211) by hydrogenation over Pd/C and/or acidic hydrolysis of the amine bond (Scheme 3.42).



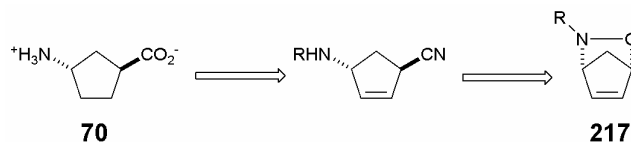
Scheme 3.42: Synthesis of enantiopure cyclopentane amino acids (213) and (214).<sup>84, 85</sup> Reagents and conditions: a) Pd/C, H<sub>2</sub>, EtOAc, 18 h, RT, 95%; b) HCl 4 N, AcOH, 5 h, 70 °C, 60-72%.

Similarly, racemic amino acids (**215**) and (**216**) were obtained from racemic ( $\pm$ )(**211**) (Scheme 3.43).

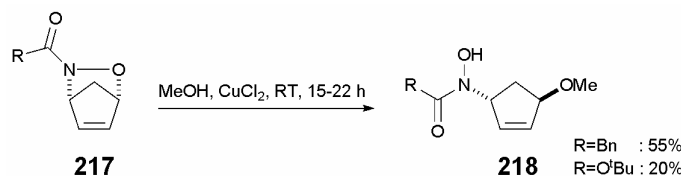


Scheme 3.43: Synthesis of racemic cyclopentane amino acids (**215**) and (**216**).<sup>84, 85</sup>  
Reagents and conditions: a) Pd/C, H<sub>2</sub>, EtOAc, 18 h, RT; b) HCl 4 N, AcOH, 5 h, 70 °C.

The synthesis of *trans*-3-aminocyclopentane carboxylic acid derivatives was then investigated. The proposed retrosynthetic analysis presented in Scheme 3.44 was motivated by the observation that oxazabicyclo[2.2.1]-hept-5-ene (**217**) reacts under specific conditions with alcohols or Grignard reagents to give *trans*-1,4-substituted cyclopentane derivatives as shown in Scheme 3.45.<sup>86-88</sup>



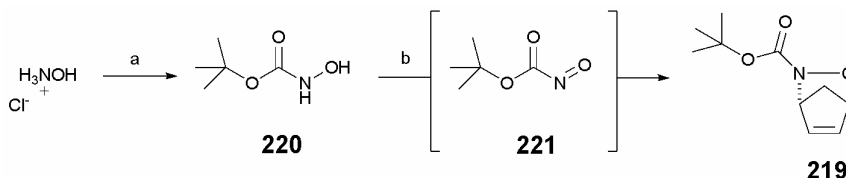
Scheme 3.44: Proposed retrosynthetic analysis of (**70**).



Scheme 3.45: Opening of (**217**) by methanol.<sup>87, 88</sup>

Accordingly, ( $\pm$ )-*N*-(carbo-*tert*-butoxy)-2,3-oxazabicyclo[2.2.1]hept-5-ene (**219**) was prepared using published procedures,<sup>89</sup> from cyclopentadiene and *t*-butyl-*N*-hydroxycarbamate (**220**). This compound was then oxidised with NaIO<sub>4</sub> to form the

dienophile nitroso species (**221**) which reacted *in situ* with cyclopentadiene in a hetero Diels-Alder reaction. The reaction proceeded cleanly and the product (**219**) was obtained as a brown solid in 72% yield (Scheme 3.46).



Scheme 3.46: Preparation of (**219**) by hetero Diels-Alder reaction.<sup>89</sup>  
 Reagents and conditions: a)  $\text{Boc}_2\text{O}$ ,  $\text{K}_2\text{CO}_3$ ,  $\text{Et}_2\text{O}$ ,  $0\text{ }^\circ\text{C}$ , 15 h, 89%;  
 b) Cyclopentadiene,  $\text{NaIO}_4$ ,  $\text{MeOH}$ ,  $0\text{ }^\circ\text{C}$ , 30 min, 72%.

The nucleophilic ring opening of (**219**) with cyanide was then attempted. Different sources of cyanide, such as potassium copper cyanide  $\text{K}_2\text{Cu}(\text{CN})_3$ , trimethylsilyl cyanide  $\text{Me}_3\text{SiCN}$  or potassium cyanide  $\text{KCN}$  were examined with different Lewis acids such as  $\text{CuSO}_4$  or  $\text{FeCl}_3$  under various conditions, but the target compound was never detected. Instead, when  $\text{Me}_3\text{SiCN}$  and  $\text{CuSO}_4$  were added to a solution of (**219**) in DMF and stirred at  $60\text{ }^\circ\text{C}$  for 20 h, an unexpected compound was obtained as a white solid in 57% yield. NMR and high resolution mass spectroscopy analyses allowed its structure to be solved. X-ray crystallography confirmed the structure to be oxazol-2-one (**222**) (Figure 3.20). A mechanism to account for its formation is suggested in Scheme 3.47.

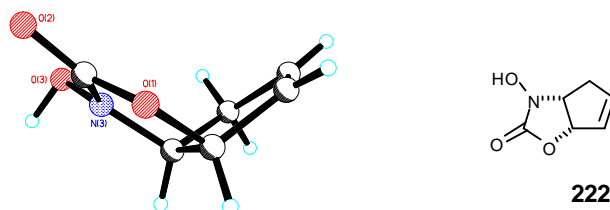
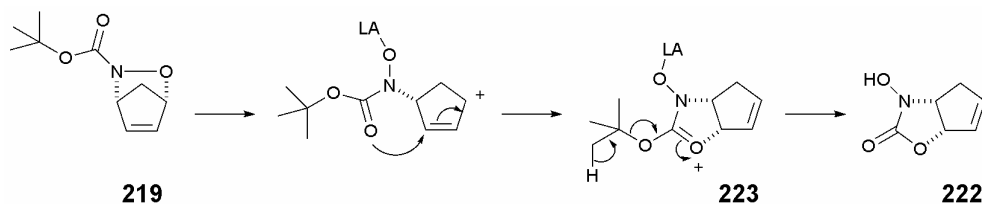
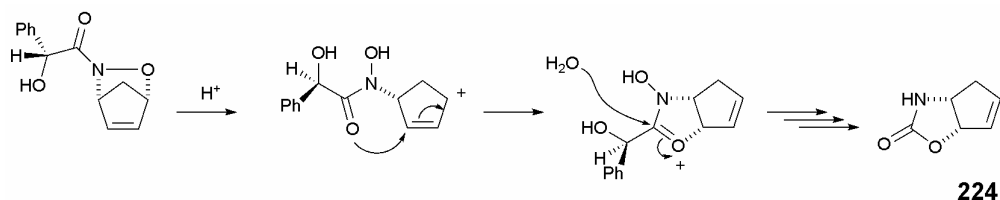


Figure 3.20: X-ray crystal structure of (**222**)

Scheme 3.47: Proposed mechanism for the formation of (**222**).

The Lewis acid  $\text{CuSO}_4$  promotes the opening of (**219**). The carbonyl of the carbamate then attacks the allyl cation to generate intermediate (**223**), which upon elimination of isobutene, generates the product (**222**). This mechanism is based on a reaction mechanism published by G. Procter for the formation of oxazolidinone (**224**) (Scheme 3.48).<sup>90, 91</sup>

Scheme 3.48: Formation of oxazolidinone (**224**).<sup>90, 91</sup>

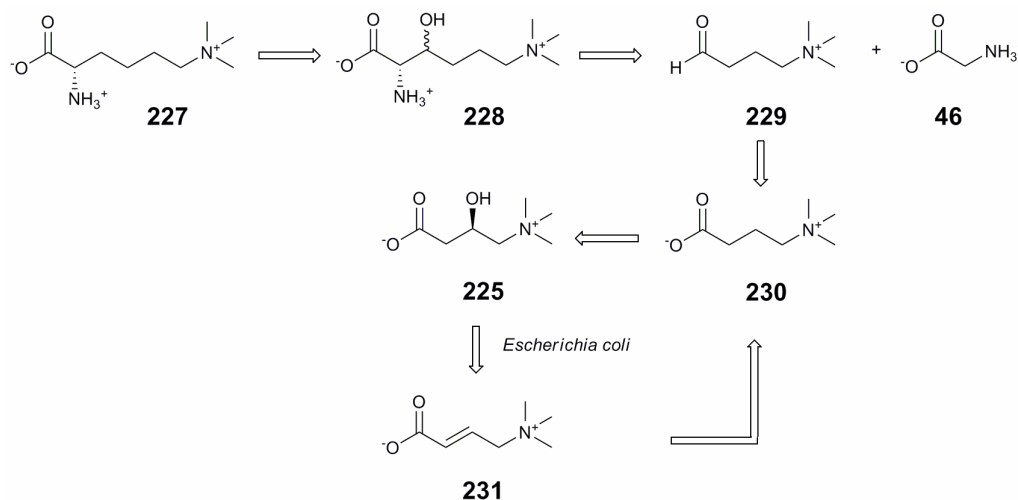
Presumably, the formation of compound (**222**) could be avoided by replacing the Boc protecting group by a benzyl group. However, this route was abandoned, mainly because the priorities of the project changed at this point, to address a synthesis of the enantiomers of 3-F-GABA. It may be worth in the future to re-investigate the synthesis of 3-F-GABA analogues (**206**) and (**207**).

### 3.7.2 Towards the synthesis of a fluorinated analogue of carnitine

(*R*)-Carnitine (**225**) is a close structural analogue of 3-hydroxy-GABA (**77**). It is ubiquitous in mammalian tissues and is essential for energy metabolism, transporting activated fatty acids to the mitochondria, where they are broken down *via*  $\beta$ -oxidation. Chemically, carnitine can be prepared from 3-hydroxy-GABA, and of relevance to this study, the 3-fluoro analogue of carnitine (**226**) is potentially accessible from 3-F-GABA.



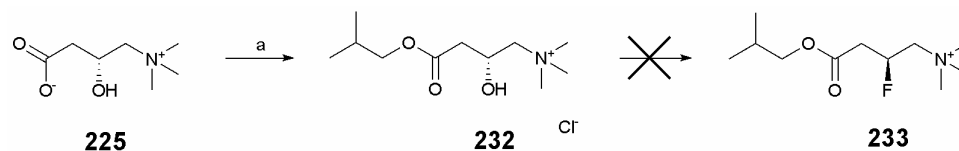
(*R*)-Carnitine biosynthesis (Scheme 3.49) starts from N<sup>6</sup>-trimethyl lysine (**227**) which is hydroxylated at the 3-position to give (**228**). Aldol cleavage of (**228**) then yields glycine (**46**) and 4-*N*-trimethylaminobutyraldehyde (**229**), the latter of which is oxidised to  $\gamma$ -butyrobetaine (**230**). In the last step,  $\gamma$ -butyrobetaine is hydroxylated at the 3-position by  $\gamma$ -butyrobetaine hydroxylase to yield (*R*)-carnitine (**225**).<sup>92, 93</sup> In *Escherichia coli*, carnitine is then metabolised by dehydration to  $\gamma$ -butyrobetaine *via* the formation of crotonobetaine (**231**).<sup>94</sup>



Scheme 3.49: Biosynthetic pathway and metabolism of (*R*)-carnitine.<sup>92, 93</sup>

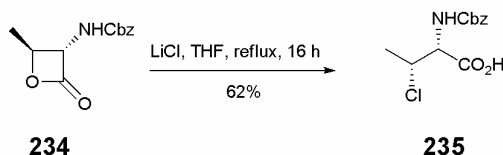
Fluorine, in addition to being a good hydrogen mimic can also mimic the hydroxyl group. Moreover, as for 3-F-GABA, the C-F and C-N<sup>+</sup> bonds are expected to orientate *gauche* to each other in (**226**), introducing conformational constraints in the molecule. 3-Fluoro-*N*-trimethylaminobutyric (**226**) could potentially be utilised for conformational binding studies or as a carnitine inhibitor of enzymes involved in carnitine biosynthesis or metabolism. As such, 3-fluoro-*N*-trimethylaminobutyric (**226**) emerged as an interesting carnitine analogue which could presumably be prepared by direct methylation of 3-F-GABA enantiomers. However, an alternative and perhaps more straightforward synthesis of (**226**) was sought.

Thus, carnitine isobutyl ester (**232**) was first prepared using a published procedure<sup>95</sup> and was then treated with Deoxofluor under various conditions. The best results were obtained when Deoxofluor (2 eq) was added at room temperature to a solution of (**232**) in DCM. Unfortunately, the desired product (**233**) was detected only by NMR analysis of the crude reaction mixture and in only 5-10% conversion and it could not be isolated. Addition of a larger excess of Deoxofluor may have resulted in a better yield but this was not attempted. Other deoxofluorination methods, such as the conversion of the hydroxyl group to a mesylate and fluorination with TBAF were explored, but again, these approaches led to a very poor conversion and/or elimination side products (Scheme 3.50). This study suggested that deoxofluorination of (**232**) was not a practical method for the synthesis of (**226**).



Scheme 3.50: Attempted synthesis of (**233**) by deoxofluorination from carnitine (**225**). Reagents and conditions: a) Isobutanol, HCl gas, reflux, 2 h, 92%.

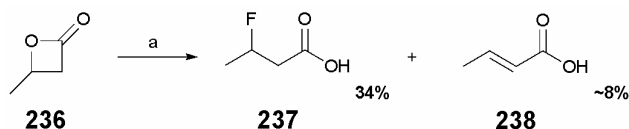
In 2006, J. Bonjoch *et al.*<sup>96</sup> demonstrated that the  $\beta$ -lactone (**234**) can be ring opened by chloride ion with full stereocontrol, to give the corresponding  $\beta$ -chloro- $\alpha$ -amino acid (**235**) (Scheme 3.51). Curiously, very few publications describe the ring opening of  $\beta$ -lactones by halogens<sup>96-100</sup> and there are none with fluorine. Therefore, it appeared worth exploring this reaction with fluoride.



Scheme 3.51: Opening of  $\beta$ -lactone (**234**) by chloride ion.<sup>96</sup>

Fluoride is a much poorer nucleophile than chloride but it was thought that triethylamine trihydrofluoride  $\text{Et}_3\text{N} \cdot 3\text{HF}$ , which is used to open epoxides, would be a suitable reagent for this kind of reaction. To test the feasibility of ring opening of  $\beta$ -lactones by fluoride, commercially available and inexpensive  $\beta$ -butyrolactone (**236**) was selected as a substrate.  $\text{Et}_3\text{N} \cdot 3\text{HF}$  (2 eq) was added to a solution of (**236**) in DCM and the mixture was heated under reflux for five days. After quenching and purification, the target product 3-fluorobutanoic acid (**237**) was isolated in 34% yield. The product of elimination, crotonic acid (**238**) was also formed and was difficult to separate from 3-fluorobutanoic acid. To ensure that crotonic acid was not an intermediate in the reaction and the substrate of an addition reaction with HF, crotonic acid was reacted with  $\text{Et}_3\text{N} \cdot 3\text{HF}$  in DCM and heated under reflux for ten days. No fluorinated product was detected in this case, suggesting that  $\beta$ -butyrolactone (**236**) is opened directly by nucleophilic attack of fluoride (Scheme 3.52).





Scheme **3.52**: Synthesis of 3-fluorobutanoic acid (**237**) by ring opening of β-butyrolactone (**236**).  
Reagents and conditions: a) Et<sub>3</sub>N·3HF, DCM, reflux, 5 days.

3-Fluorobutanoic acid was fully characterised by NMR analysis and although it is structurally a simple molecule, NMR simulation software DAISY proved useful to extract the coupling constants from the <sup>19</sup>F NMR spectrum. The fluorine signal is, as expected, a doublet of doublet of doublet of quadruplet (dddq). Coupling constants are 47.7 Hz (CHF), 28.8 Hz (CH<sub>2</sub>), 14.0 Hz (CH<sub>2</sub>) and 23.8 Hz (CH<sub>3</sub>).

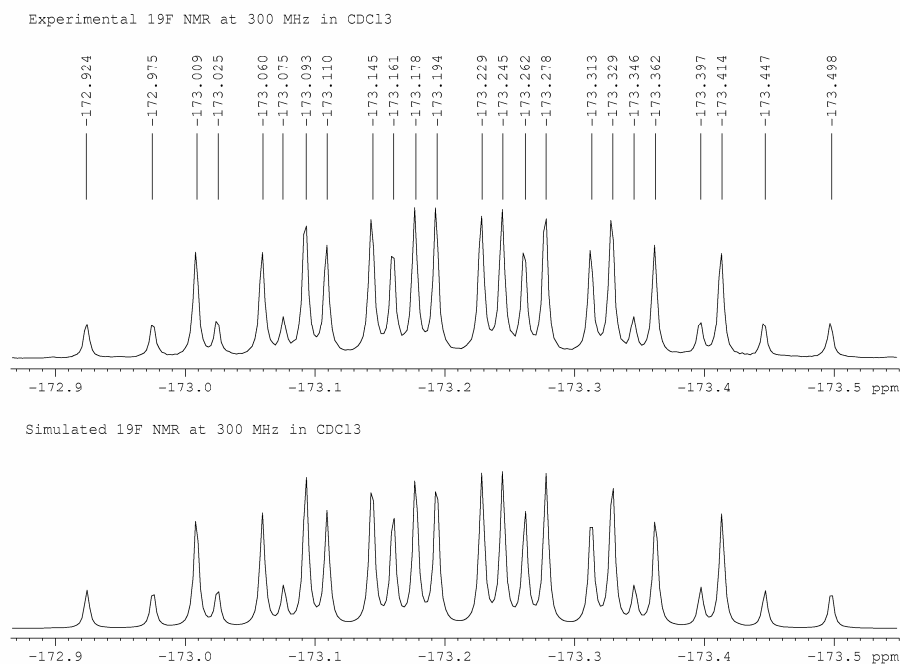
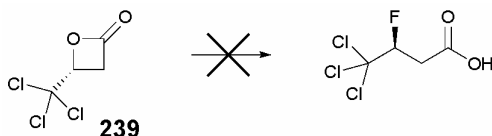


Figure **3.21**: Experimental (above) and simulated (below) <sup>19</sup>F NMR signal of (**237**).

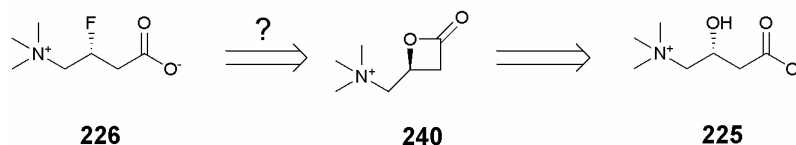
The synthesis of 3-fluorobutanoic acid from β-butyrolactone represents the first reported example of fluoride ion ring opening of a β-lactone. In order to evaluate the

enantioselectivity of this transformation, it was decided to test this reaction on enantiomerically pure (*R*)-4-(trichloromethyl)-2-oxetanone (**239**). Disappointingly, addition of Et<sub>3</sub>N·3HF to a solution of (**239**) in DCM and heating under reflux for ten days failed to produce any fluorinated product. This result indicated that the nucleophilic opening of β-lactone by fluoride is apparently deactivated by electron withdrawing substituents such as the trichloromethyl group (Scheme 3.53).



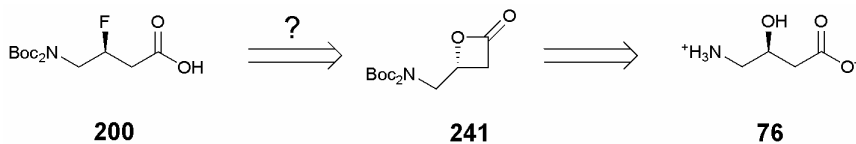
Scheme 3.53: (**239**) is inert to ring opening with Et<sub>3</sub>N·3HF.

In view of the inert nature of (**239**) to Et<sub>3</sub>N·3HF treatment, it seems unlikely that the opening of β-lactone by fluoride can be applied to the synthesis of 3-fluoro-*N*-trimethylaminobutyric acid (**226**) as drawn in Scheme 3.54 because of the electron withdrawing nature of the N<sup>+</sup>(CH<sub>3</sub>)<sub>3</sub> group. It has been reported however that intermediate (**240**) can be opened by sodium azide NaN<sub>3</sub>,<sup>95</sup> so perhaps conditions could be found to mediate a successful fluoride ion ring opening



Scheme 3.54: Improbable retrosynthesis of (**226**) from (*R*)-carnitine by fluorine ring opening of (**240**).

Assuming that the fluoride ring opening of β-lactone is enantioselective, which would of course have to be established, this methodology could potentially be applied in the future to an enantioselective synthesis of 3-F-GABA (Scheme 3.55).



The synthesis of 3-fluorobutanoic acid (**237**) from  $\beta$ -butyrolactone (**236**) has shown that ring opening of a  $\beta$ -lactone by fluoride is achievable and presents a novel approach towards the synthesis of  $\beta$ -fluorocarboxylic acids.

The enantioselective synthesis of 3-fluoro-GABA, which is both a  $\beta$ -fluorocarboxylic acid and a  $\beta$ -fluoroamine was presented in this chapter. The synthesis developed from L- and D- phenylalanine, has demonstrated that this  $\alpha$ -amino acid can be successfully converted to a  $\beta$ -fluoroamine in a stereoselective manner. The next chapter illustrates the feasibility and the practicality of this general transformation with another  $\alpha$ -amino acid.

### 3.8 References

- <sup>1</sup> J. Kollonitsch, S. Marburg, and L. M. Perkins, *J. Org. Chem.*, 1979, **44**, 771-777.
- <sup>2</sup> R. Gilmour, 'Novel approaches and a first synthesis of 4-amino-3-fluorobutyric acid', Senior Honours Project Report, St Andrews, 2002.
- <sup>3</sup> F. Chorki, 'Synthesis of 3-fluoro-GABA', Unpublished results, St Andrews, 2004.
- <sup>4</sup> J. Umezawa, O. Takahashi, K. Furuhashi, and H. Nohira, *Tetrahedron: Asymmetry*, 1993, **4**, 2053-2060.
- <sup>5</sup> E. J. Corey, W. L. Mock, and D. J. Pasto, *Tetrahedron Lett.*, 1961, 347-352.
- <sup>6</sup> I. Thomsen, B. V. Ernholz, and M. Bols, *Tetrahedron*, 1997, **53**, 9357-9364.
- <sup>7</sup> L. Somekh and A. Shanzer, *J. Am. Chem. Soc.*, 1982, **104**, 5836-5837.
- <sup>8</sup> D. F. Hook, F. Gessier, C. Noti, P. Kast, and D. Seebach, *ChemBioChem*, 2004, **5**, 691-706.
- <sup>9</sup> P. E. Floreancig, S. E. Swalley, J. W. Trauger, and P. B. Dervan, *J. Am. Chem. Soc.*, 2000, **122**, 6342-6350.
- <sup>10</sup> N. S. Chandrakumar, P. K. Yonan, A. Stapelfeld, M. Savage, E. Rorbacher, P. C. Contreras, and D. Hammond, *J. Med. Chem.*, 1992, **35**, 223-233.
- <sup>11</sup> D. Gani and D. W. Young, *J. Chem. Soc., Perkin Trans. 1*, 1985, 1355-1362.
- <sup>12</sup> F. Arndt and B. Eistert, *Ber. Deut. Chem. Ges.*, 1935, **68B**, 200-208.
- <sup>13</sup> J. Podlech and D. Seebach, *Angew. Chem., Int. Ed. Engl.*, 1995, **34**, 471-472.
- <sup>14</sup> G. M. Nicholas and T. F. Molinski, *J. Am. Chem. Soc.*, 2000, **122**, 4011-4019.
- <sup>15</sup> R. Ocampo, W. R. Dolbier, Jr., K. A. Abboud, and F. Zuluaga, *J. Org. Chem.*, 2002, **67**, 72-78.
- <sup>16</sup> A. Gaucher, L. Dutot, O. Barbeau, W. Hamchaoui, M. Wakselman, and J.-P. Mazaleyrat, *Tetrahedron: Asymmetry*, 2005, **16**, 857-864.
- <sup>17</sup> M. Hudlicky, *J. Org. Chem.*, 1980, **45**, 5377-5379.
- <sup>18</sup> A. G. Myers, J. K. Barbay, and B. Zhong, *J. Am. Chem. Soc.*, 2001, **123**, 7207-7219.
- <sup>19</sup> M. C. Pirrung, E. G. Rowley, and C. P. Holmes, *J. Org. Chem.*, 1993, **58**, 5683-5689.
- <sup>20</sup> V. Tolman and K. Veres, *Collect. Czech. Chem. Commun.*, 1964, **29**, 234-238.
- <sup>21</sup> L. Wolff, *Justus Liebigs Ann. Chem.*, 1912, **394**, 23-108.
- <sup>22</sup> W. Kirmse, *Eur. J. Org. Chem.*, 2002, 2193-2256.

- <sup>23</sup> P. G. Mahaffy, D. Visser, M. Torres, J. L. Bourdelande, and O. P. Strausz, *J. Org. Chem.*, 1987, **52**, 2680-2684.
- <sup>24</sup> J. D. Park, E. R. Larsen, H. V. Holler, and J. R. Lacher, *J. Org. Chem.*, 1958, **23**, 1166-1169.
- <sup>25</sup> P. Haiss and K.-P. Zeller, *Org. Biomol. Chem.*, 2003, **1**, 2556-2558.
- <sup>26</sup> F. Brown and W. K. R. Musgrave, *J. Chem. Soc.*, 1953, 2087-2089.
- <sup>27</sup> M. B. Giudicelli, D. Picq, and D. Anker, *Tetrahedron*, 1992, **48**, 6033-6042.
- <sup>28</sup> J.-W. Chern, J.-Y. Chang, C. O. Usifoh, and A. Gutsait, *Tetrahedron Lett.*, 1998, **39**, 8483-8486.
- <sup>29</sup> D. Gray, C. Concellon, and T. Gallagher, *J. Org. Chem.*, 2004, **69**, 4849-4851.
- <sup>30</sup> T. Markidis and G. Kokotos, *J. Org. Chem.*, 2001, **66**, 1919-1923.
- <sup>31</sup> N. Micale, R. Vairagoundar, A. G. Yakovlev, and A. P. Kozikowski, *J. Med. Chem.*, 2004, **47**, 6455-6458.
- <sup>32</sup> A. Tursun, B. Aboab, A.-S. Martin, M.-E. Sinibaldi, and I. Canet, *Synlett*, 2005, 2397-2399.
- <sup>33</sup> D. Coleman, *J. Chem. Soc.*, 1951, 2294-2295.
- <sup>34</sup> M. Rodriguez, M. Linares, S. Doulut, A. Heitz, and J. Martinez, *Tetrahedron Lett.*, 1991, **32**, 923-926.
- <sup>35</sup> J. S. Tou and B. D. Vineyard, *J. Org. Chem.*, 1985, **50**, 4982-4984.
- <sup>36</sup> U. Beifuss and M. Tietze, *Tetrahedron Lett.*, 2000, **41**, 9759-9763.
- <sup>37</sup> J. M. Andres, E. M. Munoz, R. Pedrosa, and A. Perez-Encabo, *Eur. J. Org. Chem.*, 2003, 3387-3397.
- <sup>38</sup> P. Gmeiner, *Arch. Pharm. (Weinheim, Ger.)*, 1991, **324**, 551-557.
- <sup>39</sup> S. Goldschmidt and G. Freyss, *Ber. Deut. Chem. Ges.*, 1933, **66B**, 784-785.
- <sup>40</sup> D. O'Hagan, H. S. Rzepa, M. Schuler, and A. M. Z. Slawin, *Beilstein J. Org. Chem.*, 2006, **2**, No pp given, doi:10.1186/1860-5397-2-19
- <sup>41</sup> M. Schueler, D. O'Hagan, and A. M. Z. Slawin, *Chem. Commun.*, 2005, 4324-4326.
- <sup>42</sup> D. O'Hagan, *J. Fluorine Chem.*, 1989, **43**, 371-377.
- <sup>43</sup> M. J. Sloan and K. L. Kirk, *Tetrahedron Lett.*, 1997, **38**, 1677-1680.
- <sup>44</sup> S. Arai, M. Oku, T. Ishida, and T. Shioiri, *Tetrahedron Lett.*, 1999, **40**, 6785-6789.
- <sup>45</sup> M. Kimura, T. Tominaga, and T. Kitazume, *J. Fluorine Chem.*, 2005, **126**, 135-139.
- <sup>46</sup> C. Audouard, I. Barsukov, J. Fawcett, G. A. Griffith, J. M. Percy, S. Pintat, and C. A. Smith, *Chem. Commun.*, 2004, 1526-1527.
- <sup>47</sup> M. T. Reetz, M. W. Drewes, and A. Schmitz, *Angew. Chem.*, 1987, **99**, 1186-1188.

- <sup>48</sup> P. O'Brien, H. R. Powell, P. R. Raithby, and S. Warren, *J. Chem. Soc., Perkin Trans. I*, 1997, 1031-1039.
- <sup>49</sup> J. Clayden, C. McCarthy, and J. G. Cumming, *Tetrahedron: Asymmetry*, 1998, **9**, 1427-1440.
- <sup>50</sup> R. P. Singh and J. n. M. Shreeve, *J. Fluorine Chem.*, 2002, **116**, 23-26.
- <sup>51</sup> C. Ye and J. n. M. Shreeve, *J. Fluorine Chem.*, 2004, **125**, 1869-1872.
- <sup>52</sup> J. A. Dale, D. L. Dull, and H. S. Mosher, *J. Org. Chem.*, 1969, **34**, 2543-2549.
- <sup>53</sup> M. Alcon, M. Poch, A. Moyano, M. A. Pericas, and A. Riera, *Tetrahedron: Asymmetry*, 1997, **8**, 2967-2974.
- <sup>54</sup> G. Veeresa and A. Datta, *Tetrahedron Lett.*, 1998, **39**, 3069-3070.
- <sup>55</sup> T. S. Cooper, P. Laurent, C. J. Moody, and A. K. Takle, *Org. Biomol. Chem.*, 2004, **2**, 265-276.
- <sup>56</sup> P. H. J. Carlsen, T. Katsuki, V. S. Martin, and K. B. Sharpless, *J. Org. Chem.*, 1981, **46**, 3936-3938.
- <sup>57</sup> S. Wolfe, S. K. Hasan, and J. R. Campbell, *J. Chem. Soc., Chem. Commun.*, 1970, 1420-1421.
- <sup>58</sup> M. T. Nunez and V. S. Martin, *J. Org. Chem.*, 1990, **55**, 1928-1932.
- <sup>59</sup> E. Kassab, J. Langlet, E. Evleth, and Y. Akacem, *THEOCHEM*, 2000, **531**, 267-282.
- <sup>60</sup> P. CarCabal, L. C. Snoek, and T. Van Mourik, *Mol. Phys.*, 2005, **103**, 1633-1639.
- <sup>61</sup> K. Odai, T. Sugimoto, M. Kubo, and E. Ito, *J. Biochem.*, 2003, **133**, 335-342.
- <sup>62</sup> M. Ramek and P. I. Nagy, *J. Phys. Chem. A*, 2000, **104**, 6844-6854.
- <sup>63</sup> M. L. Lorenzini, L. Bruno-Blanch, and G. L. Estiu, *THEOCHEM*, 1998, **454**, 1-16.
- <sup>64</sup> D. L. Crittenden, M. Chebib, and M. J. T. Jordan, *J. Phys. Chem. A*, 2005, **109**, 4195-4201.
- <sup>65</sup> D. L. Crittenden, M. Chebib, and M. J. T. Jordan, *J. Phys. Chem. A*, 2004, **108**, 203-211.
- <sup>66</sup> S. Miertus, E. Scrocco, and J. Tomasi, *Chem. Phys.*, 1981, **55**, 117-129.
- <sup>67</sup> A. D. Becke, *J. Chem. Phys.*, 1993, **98**, 5648-5652.
- <sup>68</sup> Y. Takahashi, C. Ueda, T. Tsuchiya, and Y. Kobayashi, *Carbohydr. Res.*, 1993, **249**, 57-76.
- <sup>69</sup> T. C. Rosen, S. Yoshida, R. Froehlich, K. L. Kirk, and G. Haufe, *J. Med. Chem.*, 2004, **47**, 5860-5871.
- <sup>70</sup> I. Brandariz, S. Fiol, R. Herrero, T. Vilarino, and M. Sastre de Vicente, *J. Chem. Eng. Data*, 1993, **38**, 531-533.

- <sup>71</sup> A. E. Martell and R. M. Smith, *Critical Stability Constants*, Vol. 1, Aminoacids, Plenum Press, 1982.
- <sup>72</sup> K. Sigfridsson, T. Andersson, L. Nilsson, V. Schoenbacher, and Y. Wang, *Eur. J. Pharm. Biopharm.*, 2007, **65**, 104-110.
- <sup>73</sup> A. Lehmann, A. Aurell Holmberg, U. Bhatt, M. Bremner-Danielsen, L. Braenden, S. Elg, T. Elebring, K. Fitzpatrick, W. B. Geiss, P. Guzzo, J. Jensen, G. Jerndal, J. P. Mattsson, K. Nilsson, and B.-M. Olsson, *Br. J. Pharmacol.*, 2005, **146**, 89-97.
- <sup>74</sup> K. Fitzpatrick, W. Geiss, A. Lehmann, G. Sunden, and S. Von Unge, ed. P. I. Appl., (Astrazeneca AB, Swed.), WO2002-SE1085, 2002.
- <sup>75</sup> J. Heygate, F. Chorki, D. O'Hagan, K. Sillar, and J. J. Lambert, 'Synthesis and biological evaluation of fluoro-gamma-amino-butyric acid (F-GABA)', Unpublished results, St Andrews University, St Andrews, 2003.
- <sup>76</sup> R. B. Silverman and M. A. Levy, *J. Biol. Chem.*, 1981, **256**, 11565-11568.
- <sup>77</sup> M. Clift, H. Ji, G. P. Deniau, D. O'Hagan, and R. B. Silverman, *Manuscript in preparation*, 2007.
- <sup>78</sup> H. B. Buergi, J. D. Dunitz, J. M. Lehn, and G. Wipff, *Tetrahedron*, 1974, **30**, 1563-1572.
- <sup>79</sup> R. D. Allan, H. W. Dickenson, and J. Fong, *Eur. J. Pharmacol.*, 1986, **122**, 339-348.
- <sup>80</sup> H. Lu and R. B. Silverman, *J. Med. Chem.*, 2006, **49**, 7404-7412.
- <sup>81</sup> J. Qiu and R. B. Silverman, *J. Med. Chem.*, 2000, **43**, 706-720.
- <sup>82</sup> R. D. Allan and J. Fong, *Aust. J. Chem.*, 1986, **39**, 855-864.
- <sup>83</sup> R. D. Allan, G. A. R. Johnston, and B. Twitchin, *Aust. J. Chem.*, 1979, **32**, 2517-2521.
- <sup>84</sup> C. Evans, R. McCague, S. M. Roberts, and A. G. Sutherland, *J. Chem. Soc., Perkin Trans. 1*, 1991, 656-657.
- <sup>85</sup> J. C. Jagt and A. M. Van Leusen, *J. Org. Chem.*, 1974, **39**, 564-566.
- <sup>86</sup> W. Lee, K.-H. Kim, M. D. Surman, and M. J. Miller, *J. Org. Chem.*, 2003, **68**, 139-149.
- <sup>87</sup> M. D. Surman, M. J. Mulvihill, and M. J. Miller, *J. Org. Chem.*, 2002, **67**, 4115-4121.
- <sup>88</sup> M. D. Surman and M. J. Miller, *J. Org. Chem.*, 2001, **66**, 2466-2469.
- <sup>89</sup> B. T. Shireman, M. J. Miller, M. Jonas, and O. Wiest, *J. Org. Chem.*, 2001, **66**, 6046-6056.
- <sup>90</sup> J. P. Muxworthy, J. A. Wilkinson, and G. Procter, *Tetrahedron Lett.*, 1995, **36**, 7539-7540.

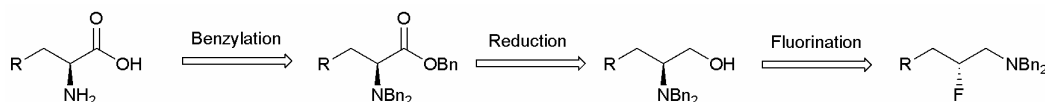
- <sup>91</sup> J. P. Muxworthy, J. A. Wilkinson, and G. Procter, *Tetrahedron Lett.*, 1995, **36**, 7535-7538.
- <sup>92</sup> W. A. Dunn, G. Rettura, E. Seifter, and S. England, *J. Biol. Chem.*, 1984, **259**, 10764-10770.
- <sup>93</sup> F. M. Vaz and R. J. A. Wanders, *Biochem. J.*, 2002, **361**, 417-429.
- <sup>94</sup> E. S. Rangarajan, Y. Li, P. Iannuzzi, M. Cygler, and A. Matte, *Biochemistry*, 2005, **44**, 5728-5738.
- <sup>95</sup> I. Bernabei, R. Castagnani, F. De Angelis, E. De Fusco, F. Giannessi, D. Misiti, S. Muck, N. Scafetta, and M. O. Tinti, *Chem.--Eur. J.*, 1996, **2**, 826-831.
- <sup>96</sup> N. Valls, M. Borregan, and J. Bonjoch, *Tetrahedron Lett.*, 2006, **47**, 3701-3705.
- <sup>97</sup> S. V. Pansare and J. C. Vederas, *J. Org. Chem.*, 1989, **54**, 2311-2316.
- <sup>98</sup> J. S. Bajwa and M. J. Miller, *J. Org. Chem.*, 1983, **48**, 1114-1116.
- <sup>99</sup> G. A. Olah, R. Karpeles, and S. C. Narang, *Synthesis*, 1982, 963-965.
- <sup>100</sup> T. Fujisawa, T. Sato, and M. Takeuchi, *Chem. Lett.*, 1982, 71-74.



## Chapter 4: Synthesis of 2-fluorohexane-1,6-diamine and 2-aminomethylpiperidine from L-lysine

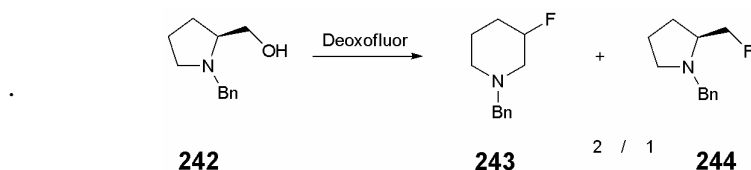
### 4.1 Introduction

The synthesis of the enantiomers of 3-F-GABA has proven that L- and D-phenylalanine can be converted in an enantioselective manner to a  $\beta$ -fluoroamine in three steps. Serine and aspartic acid emerged also as potential precursors of  $\beta$ -fluoroamines. In fact, all  $\alpha$ -amino acids can potentially be used as starting materials for the synthesis of  $\beta$ -fluoroamines as long as their side chain functional groups are compatible with the three chemical steps presented in Scheme 4.1. Despite the fact that this transformation is straightforward and that  $\beta$ -fluoroamines form an interesting class of compounds, this methodology has not been explored in much detail (Scheme 4.1).



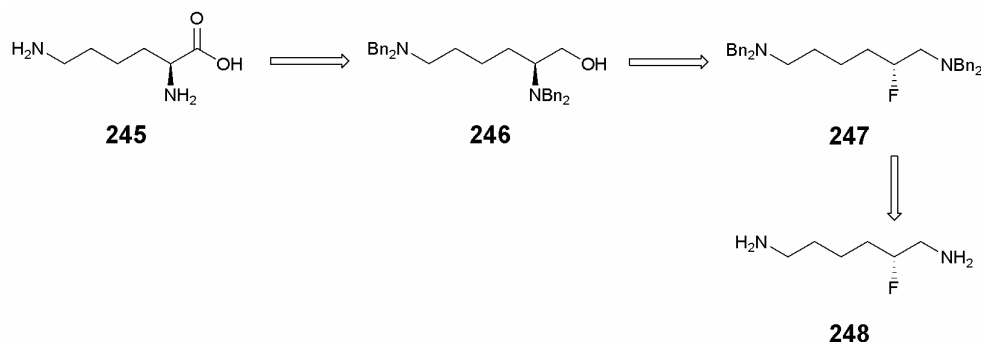
Scheme 4.1: Transformation of  $\alpha$ -amino acids into  $\beta$ -fluoroamines.

Interestingly, *N*-benzylprolinol (**242**) was reported by Shreeve *et al.*<sup>1</sup> to give 3-fluoropiperidine (**243**) *via* an aziridinium intermediate, and fluoromethylpyrrolidine (**244**) after reaction with Deoxofluor (Scheme 4.2). 3-Fluoropiperidine derivatives have interesting applications, not least because of the C-F...C-N<sup>+</sup> *gauche* relationships observed in these compounds. However, this method is not an efficient way to synthesise 3-fluoropiperidine (**243**) as it forms an inseparable mixture with (**244**).



Scheme 4.2: Preparation of *N*-benzyl-3-fluoropiperidine (**243**) from (**242**).<sup>1</sup>

From the list of the twenty proteinogenic  $\alpha$ -amino acids, L-lysine (**245**) emerged as an attractive starting material. Indeed, its transformation into the corresponding  $\beta$ -fluoroamine was anticipated to give (2*R*)-fluorohexane-1,6-diamine (**248**) (Scheme 4.3).



Scheme 4.3: Schematic synthesis of (2*R*)-fluorohexane-1,6-diamine (**248**) from L-lysine.

(2*R*)-Fluorohexane-1,6-diamine (**248**) is an analogue of 1,6-diaminohexane (**249**) which has found a wide range of applications, particularly in polymer chemistry, where it is used for example to produce nylon 6,6. In biology, 1,6-diaminohexane (**249**) can enter

the composition of polyamines which are known to bind to DNA molecules and induce bending of macroscopic DNA.<sup>2-4</sup> (2*R*)-Fluorohexane-1,6-diamine (**248**) can also be envisaged as a precursor for the synthesis of a 2-fluorinated analogue of hexamethonium (**250**) which is an important nicotinic acetylcholine receptor antagonist.<sup>5</sup> Although homology model crystal structures of nicotinic acetylcholine receptors have recently been published,<sup>6, 7</sup> little is known about the binding site of (**250**).<sup>8</sup>



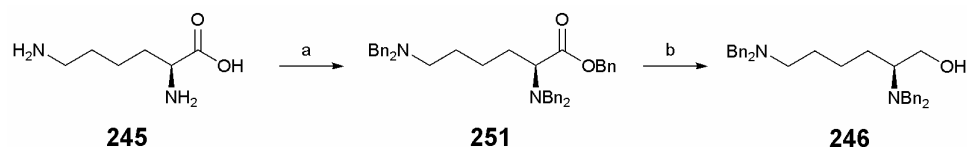
Compounds (**249**) and (**250**) highlight the interest in synthesising 2-fluorohexane-1,6-diamine (**248**) but obviously, the 1,6-diaminohexane moiety is part of many other important molecules, for which it might be interesting to explore a 2-fluoro analogue. At this position, the fluorine atom is likely to reduce the pK<sub>a</sub> value of the amine and the C-F bond is anticipated to align *gauche* to the C-N bond, particularly if the amine is protonated. The fact that 2-fluorohexane-1,6-diamine has not been reported yet, and the apparent simplicity of its preparation from L-lysine prompted us to investigate its synthesis.

## 4.2 Synthesis of (2*R*)-fluorohexane-1,6-diamine

### 4.2.1 The lysine approach

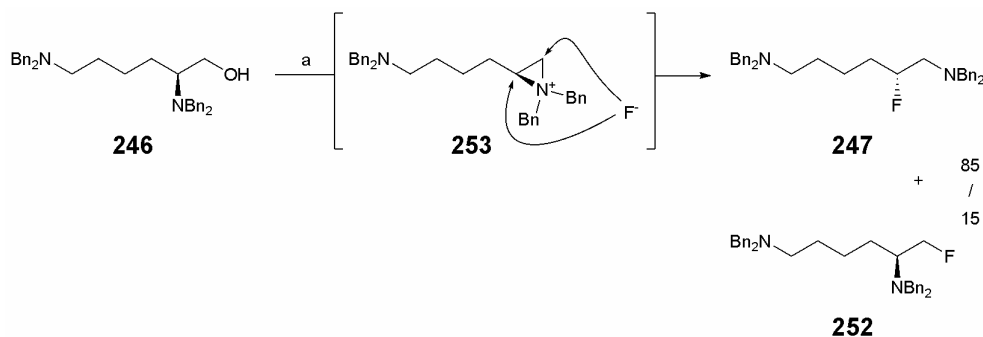
The methodology applied previously to the synthesis of 3-F-GABA was used in this study. Accordingly, L-lysine was perbenzylated by addition of benzyl bromide and K<sub>2</sub>CO<sub>3</sub> in DMF/water (10/1). The mixture was stirred at 60 °C for 3 days and the product was extracted into Et<sub>2</sub>O. The light yellow oil obtained was taken on directly for reduction,

but an analytical sample of perbenzylated lysine (**251**) was obtained after purification. The reduction was achieved with  $\text{LiAlH}_4$  and the resultant amino alcohol (**246**) was obtained after purification as a colourless oil in 62% yield over the two steps (Scheme 4.4).



Scheme 4.4: Preparation of dibenzyl- $\alpha$ -amino alcohol (**246**) from L-lysine. Reagents and conditions: a)  $\text{BnBr}$ ,  $\text{K}_2\text{CO}_3$ ,  $\text{DMF}/\text{H}_2\text{O}$ ,  $60\text{ }^\circ\text{C}$ , 3 days;  $\text{LiAlH}_4$ ,  $\text{THF}$ ,  $0\text{ }^\circ\text{C}$ , 2 h, 62%.

Fluorination of amino alcohol (**246**) was conducted with DAST (1.15 eq) in DCM at room temperature. The crude product was purified by chromatography and the early fractions contained a small amount of the desired fluorinated compound (**247**) and its isomer (**252**) in a 85/15 ratio (Scheme 4.5). This ratio was similar to that observed for the fluorination of *N,N*-dibenzylphenylalaninol (**178**) for which the ratio of rearranged/non-rearranged product isomers was 80/20. After two re-crystallisations from  $\text{Et}_2\text{O}$ /hexane, (**247**) was isolated as a colourless crystalline solid albeit in a low 11% yield.



Scheme 4.5: Preparation of (**247**) and (**252**). The conversion of (**246**) to fluorinated products (**247**) and (**252**) was low, yielding (**247**) in only 11% yield. Reagents and conditions: a) DAST, DCM, RT.

Tetrabenzyl-(2*R*)-fluorohexane-1,6-diamine (**247**) was fully characterised but its enantiopurity was not investigated. The crystals collected were amenable to X-ray structure analysis but were found to diffract very poorly. The structure was disordered about the C(3)/C(3A) bond, although a X-ray crystal structure of suitable quality for structure identification was obtained (Figure 4.1).

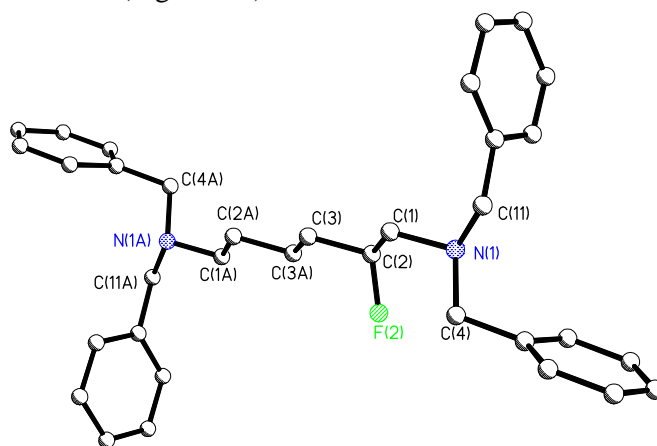
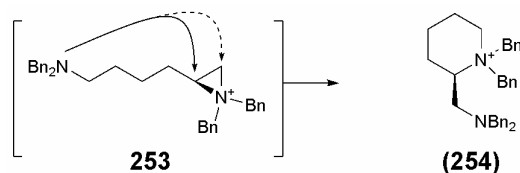


Figure 4.1: X-ray crystal structure of tetrabenzyl-(2*R*)-fluorohexane-1,6-diamine (**247**).

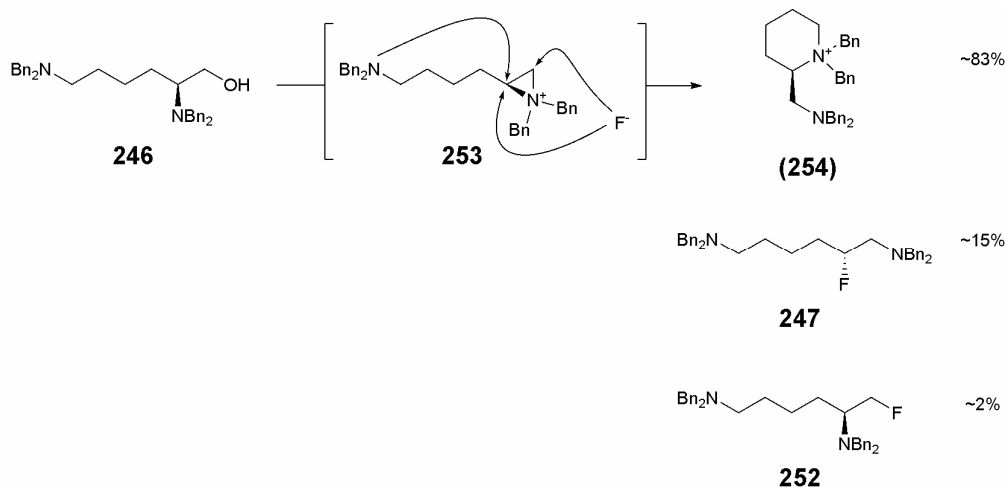
The very low conversion of amino alcohol (**246**) to  $\beta$ -fluoroamine (**247**) was disappointing and was most probably due to the formation of by-products occurring during the fluorination reaction. Although it was not possible to isolate any of these products, a very polar by-product was identified. High resolution mass spectroscopy analysis indicated that the compound had a mass of 475.3123, which matches the molecular formula  $(C_{34}H_{39}N_2)^+$  (-0.1 ppm). Presumably, this could correspond to the nucleophilic attack of  $N^6$ -nitrogen on aziridinium (**253**) (Scheme 4.6).



Scheme 4.6: Putative formation of polar by-product (**254**) occurring during fluorination of amino alcohol (**246**).

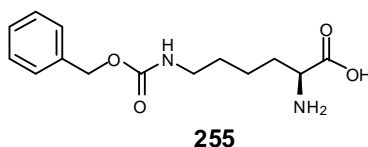
The structure (**254**) drawn in Scheme 4.6 is consistent with mass spectrometric analysis and is based on the hypothesis that aziridinium (**253**) is formed, and that nucleophilic attack on the aziridinium occurs preferentially at the most substituted carbon to form a six-membered ring (favoured six-exo-tet ring closure). An attack on the other carbon (dashed line in Scheme 4.6) would result in the less favourable formation of a seven-membered ring (unfavoured seven-endo-tet ring closure). At this stage however, the structure (**254**) could not be clearly established.

The formation of the putative cyclic by-product (**254**) is favoured over the formation of the fluorinated compound (**247**) which indicates that the dibenzyl-protected nitrogen is a better nucleophile than fluoride and consequently, that  $\beta$ -fluoroamine (**247**) will not be synthesised efficiently from 2,6-bis(dibenzylamino)hexan-1-ol (**246**). Nevertheless, the formation of (**247**), albeit in a low yield but in a good (**247**)/(**252**) ratio, suggests that if the nucleophilicity of the ( $\epsilon$ )-nitrogen could be suppressed, the desired fluorinated product (**247**) might be formed more efficiently.

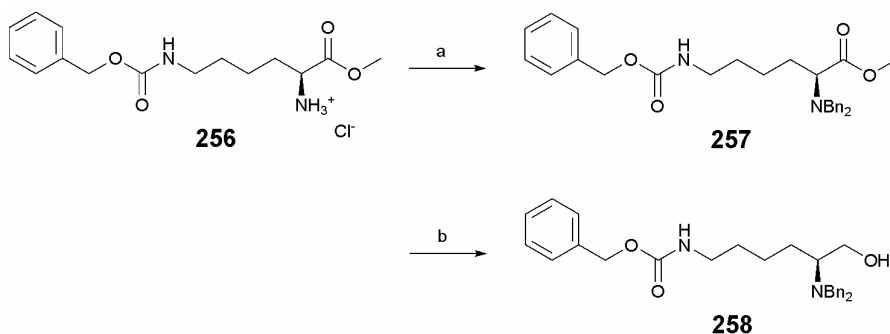


Scheme 4.7: The treatment of (**246**) with DAST in DCM at RT gives a complex mixture of at least three compounds, most probably (**254**), (**247**) and (**252**) in a 83/15/2 ratio of the crude reaction mixture.

### 4.2.2 The *N*( $\epsilon$ )-*Z*-L-lysine route



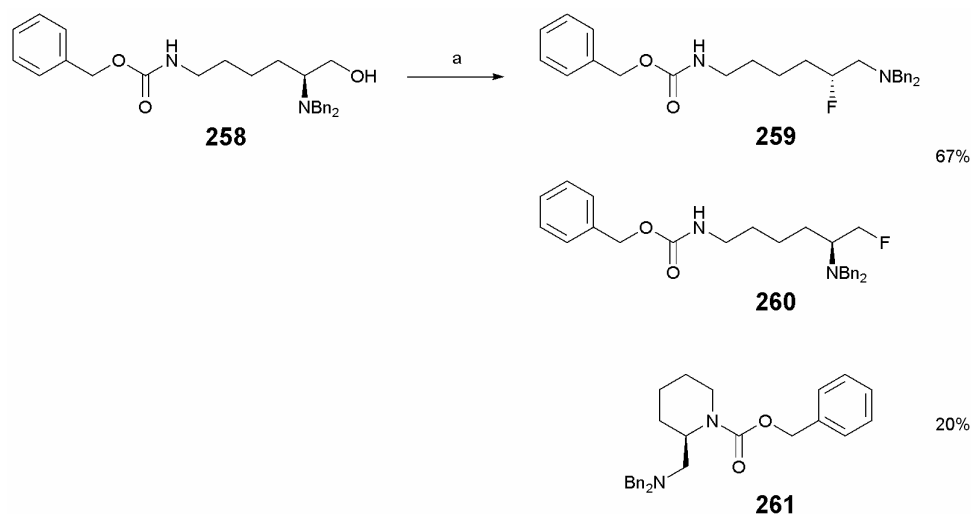
The chemistry of L-lysine, as one of the common amino acids, is well developed. Many derivatives of L-lysine, orthogonally protected or not, have been prepared and are now commercially available. For example, *N*( $\epsilon$ )-benzyloxycarbonyl-L-lysine (**255**) is available from Aldrich at £20.50 for 5 g. The benzyloxycarbonyl protecting group appears ideal at first sight, as it suppresses the nucleophilicity of the *N*( $\epsilon$ ) nitrogen and it can be cleaved by hydrogenolysis. Fortuitously, *N*( $\epsilon$ )-benzyloxycarbonyl-L-lysine methyl ester hydrochloride (**256**) was found in our laboratories and was used as starting material.



Scheme 4.8: Synthesis of dibenzyl- $\alpha$ -amino alcohol (**258**) from (**256**). Reagents and conditions: a) BnBr, K<sub>2</sub>CO<sub>3</sub>, MeCN, 80 °C, 20 h, 97%; b) LiAlH<sub>4</sub>, THF, -10 °C, 50 min, 94%.

Compound (**256**) was benzylated under standard conditions to give (**257**) in excellent yield (97%). (**256**) was then reduced with LiAlH<sub>4</sub> in THF at -10 °C to furnish dibenzyl- $\alpha$ -amino alcohol (**258**) after work-up and purification, in a very good yield. It is worth noting that the benzyloxycarbonyl group was stable under these conditions.

The fluorination of dibenzyl- $\alpha$ -amino alcohol (**258**) was carried out with Deoxofluor (1.2 eq) in DCM at  $-10^{\circ}\text{C}$ . The reaction mixture was allowed to warm to room temperature over six hours and was quenched by the addition of  $\text{K}_2\text{CO}_3$ .  $^{19}\text{F}$  NMR analysis of the crude reaction mixture revealed the presence of two fluorinated compounds in a 85/15 ratio, corresponding to the formation of (**259**) and (**260**). The ratio of rearranged (**259**) to non-rearranged (**260**) product was similar to that observed previously for (**247**) and (**252**).  $^1\text{H}$  NMR analysis of the crude product mixture was difficult to interpret but the existence of a non-fluorinated compound could also be detected in around 25% yield. This compound was less polar than the  $\beta$ -fluoroamines (**259**) and (**260**) and was isolated after purification by column chromatography, as a colourless oil and in a 20% yield. NMR and mass spectrometric analyses were consistent with structure (**261**) (Scheme 4.9). Compounds (**259**) and (**260**) which eluted after (**261**) were then collected as a 90/10 mixture and as a colourless oil in 67% yield.



Scheme 4.9: Formation of fluorinated compounds (**259**) and (**260**) along with cyclic (**261**) by treatment of (**258**) with Deoxofluor. Reagents and conditions: a) Deoxofluor,  $-10^{\circ}\text{C}$ , 6 h.



The formation of the fluorinated compounds (**259**) and (**260**) was anticipated and can be explained by nucleophilic attack (paths *a* and *b*) of fluoride on aziridinium (**262**) (Figure 4.2). The formation of the cyclic compound (**261**) was however more surprising but can be rationalised by nucleophilic addition of the benzyloxycarbonyl-protected nitrogen to the aziridinium (**262**) (path *c*). Under the conditions used, the N( $\epsilon$ )-nitrogen is apparently nucleophilic enough to attack (**262**), but cyclisation occurred with a much lower conversion than found with the dibenzyl-protected N<sup>6</sup>-nitrogen in compound (**246**).

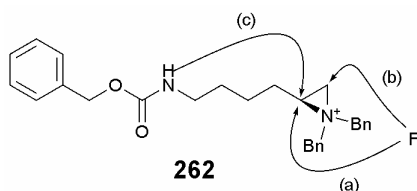


Figure 4.2: Reactivity of intermediate (**262**). The aziridinium ring can be opened in three different ways, producing compounds (**259**), (**260**) and (**261**). Attack at the most substituted carbon is favoured (paths *a* and *c*).

Compounds (**259**) and (**260**) could not be separated from each other by column chromatography and it was found more convenient to take the mixture directly through to the hydrogenolysis step. Nevertheless, an analytical sample of (**259**) was obtained as a colourless crystalline solid after re-crystallisation from Et<sub>2</sub>O/hexane. Crystals were amenable to X-ray structure analysis and a structure is shown in Figure 4.3.

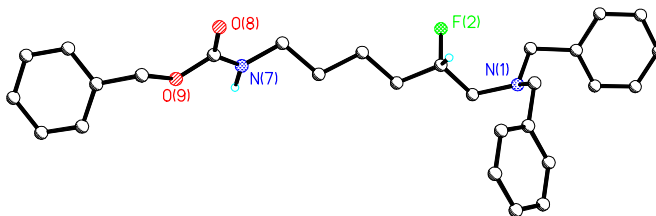
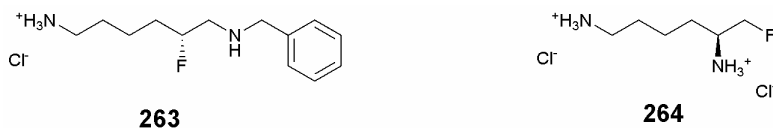
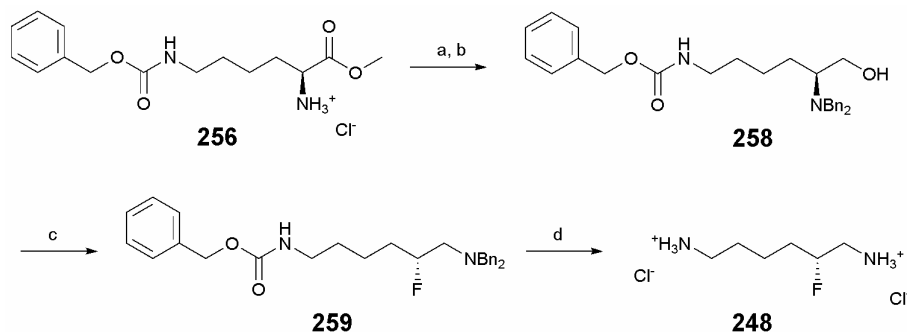


Figure 4.3: X-ray crystal structure of (**259**). Torsion angle N-C-C-F is 70.7 °.

Hydrogenolysis of (**259**) in MeOH was first conducted at atmospheric pressure with H<sub>2</sub> and a catalytic amount of Pd(OH)<sub>2</sub>/C. However, only partial debenzylation was observed under these conditions. Interestingly, compound (**263**) was isolated in a good yield and was identified by NMR analysis. However, it was re-subjected to hydrogenolysis to generate (**248**) and was not fully characterised.



Hydrogenolysis of (**259**) was then performed under a pressure of H<sub>2</sub> (20 bars) in an autoclave for two days. After filtration of the solids on Celite, 1 M HCl in Et<sub>2</sub>O was added and the mixture was re-crystallised from MeOH/EtOH/Et<sub>2</sub>O. Three successive re-crystallisations were required to purify dihydrochloride salt (**248**) from the by-product (**264**). In the end, (**248**) was obtained, as a colourless amorphous solid in 73% yield (Scheme 4.10).



Scheme 4.10: Synthesis of (2*R*)-fluorohexane-1,6-diamine dihydrochloride (**248**) from L-lysine derivative (**256**). Reagents and conditions: a) BnBr, K<sub>2</sub>CO<sub>3</sub>, MeCN, 80 °C, 20 h, 97%; b) LiAlH<sub>4</sub>, THF, -10 °C, 50 min, 94%; c) Deoxofluor, DCM, -10 °C, 67%; d) Pd(OH)<sub>2</sub>/C, MeOH, H<sub>2</sub> (20 bars), 48 h, 73%.

Standard re-crystallisations furnished (2*R*)-fluorohexane-1,6-diamine (**248**) as a white amorphous solid, presumably because of the long flexible alkane chain which is not

favourable for crystallisation. Nevertheless, very slow re-crystallisation by solvent diffusion at +4 °C yielded (**428**) as small white crystals which could be used for X-ray structure analysis (Figure 4.4).

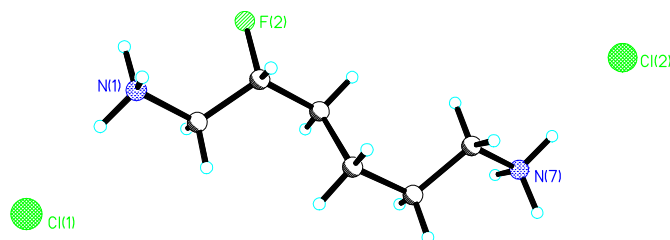


Figure 4.4: X-ray crystal structure of (2*R*)-fluorohexane-1,6-diamine dihydrochloride (**248**). Torsion angle F-C-C-N<sup>+</sup> is 62.7° and the absolute configuration, determined by X-ray is (*R*).

The absolute configuration of (**248**) was assessed by X-ray analysis to be (*R*), supporting the inversion of configuration *via* aziridinium intermediate (**262**). The enantiopurity of this compound was then investigated using (*S*)- and (*R*)- Mosher acids as derivatising reagents. In parallel procedures, (*S*)-(-)-Mosher acid and (*R*)-(+)-Mosher acid were added respectively to two mixtures containing 2-fluorohexane-1,6-diamine (**248**), Et<sub>3</sub>N and DMAP in DCM. The two reactions were stirred for twelve hours and after evaporation of the solvent, the residues were dissolved in CDCl<sub>3</sub> and analysed by <sup>19</sup>F NMR.

Compound (**265**) is the coupled product of (**248**) with two molecules of (*S*)-Mosher acid, and compound (**266**) comes from the coupling of (**248**) with two molecules of (*R*)-Mosher acids. The <sup>19</sup>F NMR signals for the fluorine at the stereogenic centres of respectively (**265**) and (**266**) are shown in Figure 4.5. Single peaks were found indicating that (**248**) was enantiopure. When compounds (**265**) and (**266**) were added in one tube, two distinct <sup>19</sup>F NMR signals were observed. This clearly demonstrates the enantiopurity of (2*R*)-fluorohexane-1,6-diamine (**248**) from the fluorination reaction with Deoxofluor.

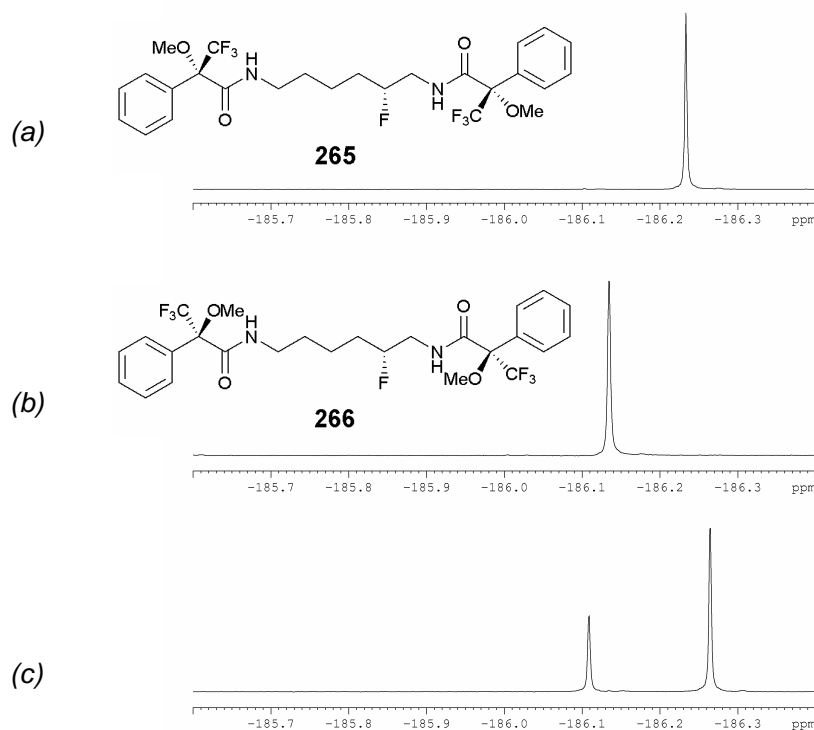


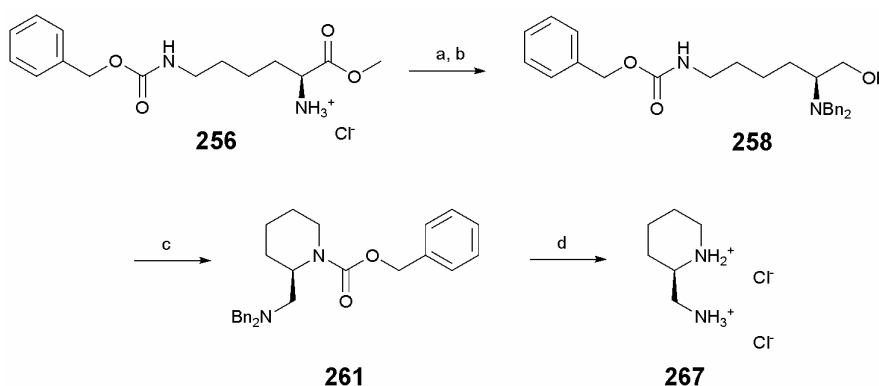
Figure 4.5:  $^{19}\text{F}$  NMR analysis (CDCl<sub>3</sub>, 375 MHz) of *(S)*-Mosher acid derivative (**265**) (a), *(R)*-Mosher acid derivative (**266**) (b) and the mixture of both (c) showing the high enantiopurity of (**248**).

The synthesis of (2*R*)-fluorohexane-1,6-diamine (**248**), developed from N( $\epsilon$ )-Z-L-lysine methyl ester (**256**) is another example that  $\alpha$ -amino acids can be converted to enantiopure  $\beta$ -fluoroamines. Around 500 mg of (**248**) was produced by this route, in a 45% overall yield from (**256**). This constitutes an efficient and robust synthesis of (**248**), using relatively cheap materials, with Deoxofluor being the most expensive. The main drawback of this route is probably the formation of the cyclic piperidine (**261**). It might be possible to avoid its formation with a more judicious choice of protecting group at the N<sup>6</sup>-nitrogen. A Boc protecting group for example, which could be installed prior to the fluorination step may give better results as it would reduce the nucleophilicity of the N<sup>6</sup>-nitrogen. However, it seems that the non-regioselective opening of the aziridinium intermediate (**262**) by fluoride, from which fluorinated compound (**260**) is formed as a by-product, is inherent to this kind of reaction and cannot be easily circumvented.

### 4.3 Synthesis of (2*R*)-aminomethylpiperidine

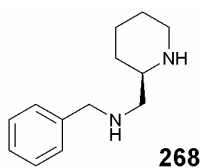
The formation of (2*R*)-((dibenzylamino)methyl)piperidine-1-benzoxycarbonate (**261**) as a minor product was judged to be worth investigation, because this compound could potentially be converted by hydrogenolysis to chiral diamine (2*R*)-aminomethylpiperidine (**261**) which has potential application in catalysis for example.

Hydrogenolysis of (**261**) with Pearlman's catalyst  $\text{Pd}(\text{OH})_2/\text{C}$  in MeOH under a pressure of  $\text{H}_2$  (20 bars) yielded, after addition of 1 M HCl and re-crystallisation from MeOH/Et<sub>2</sub>O, chiral diamine (**267**) as its dihydrochloride salt. The diamine (**267**) was obtained in 14% overall yield from (**256**) (Scheme 4.11).



Scheme 4.11: Synthesis of (2*R*)-aminomethylpiperidine dihydrochloride (**267**) from L-lysine derivative (**256**). Reagents and conditions: a) BnBr, K<sub>2</sub>CO<sub>3</sub>, MeCN, 80 °C, 20 h, 97%; b) LiAlH<sub>4</sub>, THF, -10 °C, 50 min, 94%; c) Deoxofluor, DCM, -10 °C, 20%; d)  $\text{Pd}(\text{OH})_2/\text{C}$ , MeOH,  $\text{H}_2$  (20 bars), 48 h, 75%.

Interestingly, benzylamine (**268**) was isolated in a good yield (79%) when hydrogenolysis was performed under an atmospheric pressure of  $\text{H}_2$ . Benzylamine (**268**) was characterised only by NMR and was then re-subjected to hydrogenolysis.



Re-crystallisation of the dihydrochloride salt of (**267**) yielded large, colourless crystals which were amenable to X-ray structure analysis. The absolute configuration was assigned unambiguously by X-ray to be (*R*), as shown in Figure 4.6.

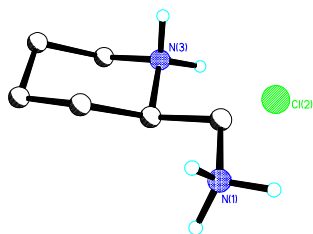
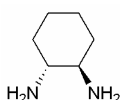
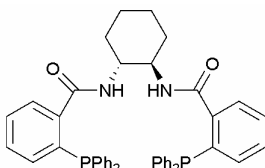


Figure 4.6: X-ray crystal structure of (2*R*)-aminomethyl-piperidine dihydrochloride (**261**).

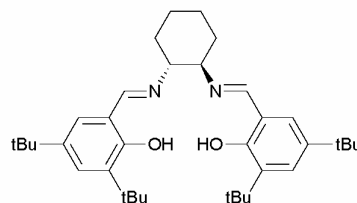
Chiral diamines form an important class of compounds which have found a wide range of applications in chemistry, particularly as bidentate ligands for the design of asymmetric catalysts. 1,2-Diaminocyclohexane (**269**) for example is used in Trost's catalyst (**270**) for asymmetric allylic alkylation reactions<sup>9, 10</sup> and also in salen-type ligands (Jacobsen's catalyst)<sup>11</sup> for enantioselective epoxidation (**271**).



**269**



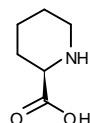
**270**



**271**

2-Aminomethylpiperidine however has not been widely used in the design of chiral ligands. A possible explanation for this could be its limited availability. Indeed, enantiopure 2-aminomethylpiperidine is not commercially available and although enantiomers can be prepared by the resolution of the racemate<sup>12</sup> or from pipercolic acid (**272**) by amidation and reduction,<sup>12-14</sup> this does not constitute a practical route to

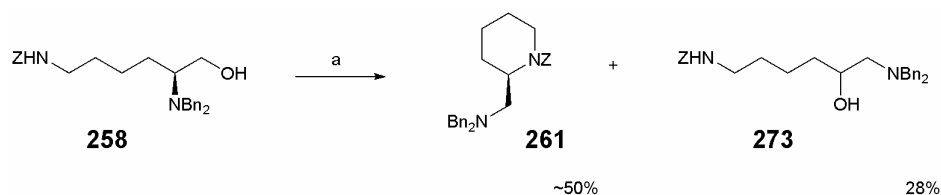
synthesise (**267**) in reasonable quantities. Pipecolic acid (**272**) is an expensive starting material, compared to L-lysine from which (2*R*)-aminomethylpiperidine (**267**) was prepared in this work. The synthesis from L-lysine constitutes a novel preparation of (**267**) and due to its high potential in asymmetric catalysis, it was decided to optimise the synthesis presented in Scheme 4.11.

**272**

The most vulnerable step in the synthesis of 2-aminomethylpiperidine (**267**) is clearly the low 20% yield obtained from the fluorination reaction. To improve this yield, the intramolecular nucleophilic attack of N<sup>6</sup>-nitrogen needs to be favoured over the intermolecular reaction with fluoride.

Taking advantage of the strength of the Si-F bond, silica (SiO<sub>2</sub>) was added to the reaction mixture of amino alcohol (**258**) in DCM. The idea was to trap fluoride anions with silica before they can react with the aziridinium intermediate (**262**). Empirically, it was chosen to add 200 mg of dry silica to a mixture of 200 mg of (**258**) in DCM at -78 °C. Deoxofluor (1.5 eq) was then added and the reaction was stirred at -78 °C for six hours. Pleasingly, only traces of fluorinated products (**259**) and (**260**) were detected by <sup>19</sup>F and <sup>1</sup>H NMR analysis of the crude reaction mixture. After purification, the piperidine (**261**) was isolated in ~50% yield, which represented a significant improvement on the 20% yield obtained from the reaction without silica at -10 °C.

Interestingly, another product was isolated in 28% yield from this reaction. Mass spectroscopy analysis revealed that this compound had the same mass as the starting material (**258**) but its NMR spectra were clearly different and suggested structure (**273**) (Scheme 4.12).



Scheme **4.12**: Fluorination of (**258**) with addition of silica. Reagents and conditions: a)  $\text{SiO}_2$ , Deoxofluor, DCM,  $-78\text{ }^\circ\text{C}$ , 6 h.

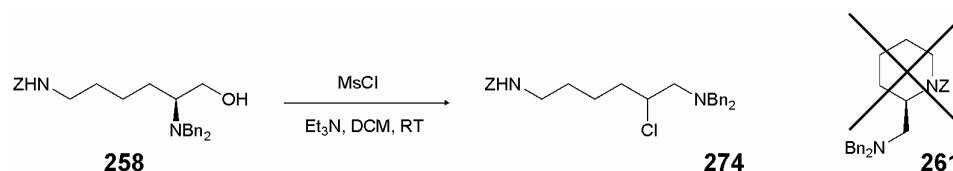
Compound (**273**) was not fully characterised and it is not clear how and when it is formed. Manifestly, it results from the opening of aziridinium (**262**) by a species containing a hydroxyl group.

The amount of silica added to this reaction was not optimised but this experiment proved that addition of silica is an efficient and effective method to suppress the nucleophilicity of fluoride anions in the reaction mixture.

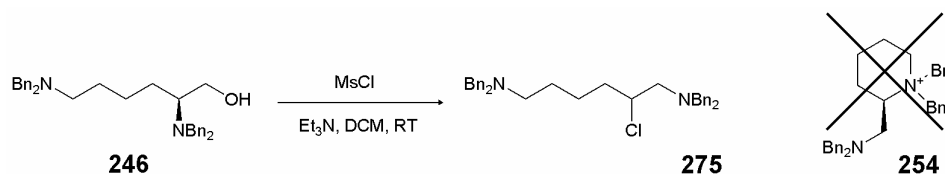
At this point, it seemed that the synthesis of 2-aminomethylpiperidine could be simplified and that Deoxofluor activation could be replaced by some alternative method. Mesylate activation was considered. This would, of course, suppress the problem encountered with side reactions involving fluoride anions because mesylate  $\text{MsO}^-$  is a relatively poor nucleophile which does not open the aziridinium ring. It is known that an aziridinium intermediate is formed by addition of  $\text{Ms}_2\text{O}$ ,  $\text{MsCl}$  or  $\text{Tf}_2\text{O}$  to solutions of *N,N*-dibenzyl- $\alpha$ -amino alcohols.<sup>15-19</sup>

Disappointingly, treatment of  $\text{Ms}_2\text{O}$  and  $\text{Et}_3\text{N}$  (1.5 eq) with amino alcohol (**258**) failed to produce the desired cyclic product (**261**). Addition of  $\text{MsCl}$  also failed and generated the chlorinated compound (**274**) instead, as evidenced by NMR and mass spectroscopy analyses (Scheme **4.13**). This type of reaction has already been reported and is not surprising given the higher nucleophilicity of chloride over the benzyloxycarbonyl-protected amine.<sup>19</sup>

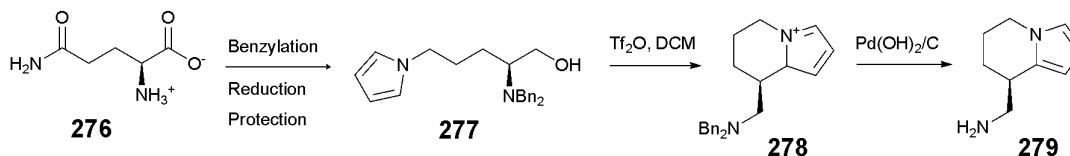


Scheme 4.13: Treatment of (**258**) with  $\text{MsCl}$  generates (**274**).

Similarly, treatment of (**246**) with  $\text{MsCl}$  also failed to form cyclic salt (**254**), which was formed initially in ~83% upon treatment with DAST. This time however, chlorinated compound (**272**) was detected by NMR and mass spectroscopy analyses (Scheme 4.14).

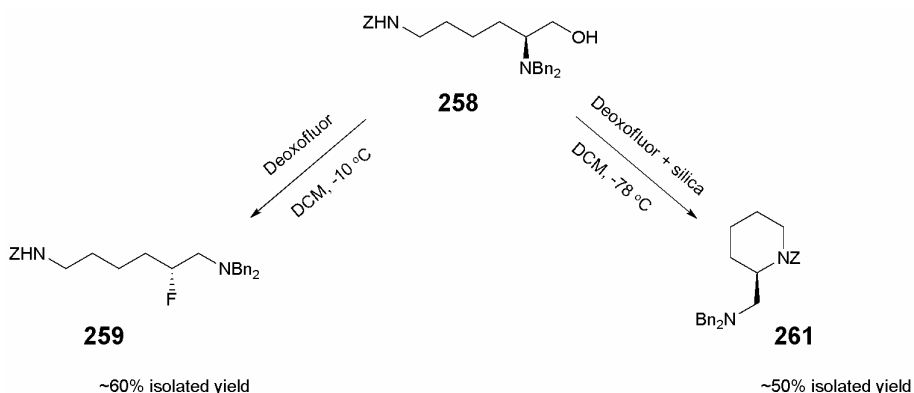
Scheme 4.14: Treatment of (**246**) with  $\text{MsCl}$  generates (**275**).

The intramolecular ring opening of *in situ*-generated aziridinium ring systems has been reported many times, but it is not clear why in our case it worked only with Deoxofluor. In a related reaction published by Gmeiner *et al.*, glutamine (**276**) was used to prepare dibenzyl- $\alpha$ -amino alcohol (**277**), which upon treatment with  $\text{Tf}_2\text{O}$ , underwent cyclisation *via* an aziridinium intermediate to give (**278**). After elimination and hydrogenolysis, the product (**279**) was obtained and was found to be enantiopure (Scheme 4.15).<sup>20</sup>

Scheme 4.15: Example of cyclisation from dibenzyl- $\alpha$ -amino alcohol (**277**) *via* an aziridinium intermediate.<sup>20</sup>

It is not clear why methanesulfonic anhydride did not promote the intramolecular reaction but the synthesis of (**261**) was not optimised any further. Nevertheless, (2*R*)-aminomethylpiperidine hydrochloride (**267**) could be prepared in 34% overall yield from commercially available N( $\epsilon$ )-Z-lysine methyl ester (**256**). The key step mediated by Deoxofluor, was significantly improved by the addition of silica gel to the reaction mixture.

It was shown in this study that dibenzyl- $\alpha$ -amino alcohol (**258**) can give mainly either the  $\beta$ -fluoroamine (**259**) or piperidine (**261**), depending on the conditions used (Scheme 4.16). The enantiopurity of (2*R*)-aminomethylpiperidine (**267**) has not been assessed in a definitive manner and the optical rotation found does not match satisfactorily that reported in the literature. Further work is required to optimise the synthesis of (**267**) and to assess its enantiopurity by the transformation shown in Scheme 4.16.



Scheme 4.16: Amino alcohol (**258**) as precursor of  $\beta$ -fluoroamine (**259**) and diamine (**261**).

## 4.4 References

- <sup>1</sup> C. Ye and J. M. Shreeve, *J. Fluorine Chem.*, 2004, **125**, 1869-1872.
- <sup>2</sup> D. Pastre, O. Pietrement, F. Landousy, L. Hamon, I. Sorel, M.-O. David, E. Delain, A. Zozime, and E. Le Cam, *Eur. Biophys. J.*, 2006, **35**, 214-223.
- <sup>3</sup> O. Phanstiel, H. L. Price, L. Wang, J. Juusola, M. Kline, and S. M. Shah, *J. Org. Chem.*, 2000, **65**, 5590-5599.
- <sup>4</sup> M. L. Edwards, R. D. Snyder, and D. M. Stemerick, *J. Med. Chem.*, 1991, **34**, 2414-2420.
- <sup>5</sup> B. Buisson and D. Bertrand, *Mol. Pharmacol.*, 1998, **53**, 555-563.
- <sup>6</sup> R. H. Henchman, H.-I. Wang, S. M. Sine, P. Taylor, and J. A. McCammon, *Biophys. J.*, 2003, **85**, 3007-3018.
- <sup>7</sup> T. K. Sixma and A. B. Smit, *Annu. Rev. Biophys. Biomol. Struct.*, 2003, **32**, 311-334.
- <sup>8</sup> F. Zheng, E. Bayram, S. P. Sumithran, J. T. Ayers, C.-G. Zhan, J. D. Schmitt, L. P. Dwoskin, and P. A. Crooks, *Bioorg. Med. Chem.*, 2006, **14**, 3017-3037.
- <sup>9</sup> B. M. Trost and X. Ariza, *Angew. Chem., Int. Ed.*, 1997, **36**, 2635-2637.
- <sup>10</sup> B. M. Trost, B. Breit, S. Peukert, J. Zambrano, and J. W. Ziller, *Angew. Chem., Int. Ed.*, 1995, **34**, 2386-2388.
- <sup>11</sup> E. N. Jacobsen, W. Zhang, A. R. Muci, J. R. Ecker, and L. Deng, *J. Am. Chem. Soc.*, 1991, **113**, 7063-7064.
- <sup>12</sup> G. Blaschke, U. Scheidemantel, and B. Walther, *Chem. Ber.*, 1985, **118**, 4616-4619.
- <sup>13</sup> V. Vecchietti, A. Giordani, G. Giardina, R. Colle, and G. D. Clarke, *J. Med. Chem.*, 1991, **34**, 397-403.
- <sup>14</sup> J. Perumattam, B. G. Shearer, W. L. Confer, and R. M. Mathew, *Tetrahedron Lett.*, 1991, **32**, 7183-7186.
- <sup>15</sup> S. E. de Sousa and P. O'Brien, *Tetrahedron Lett.*, 1997, **38**, 4885-4888.
- <sup>16</sup> P. Gmeiner, D. Junge, and A. Kaertner, *J. Org. Chem.*, 1994, **59**, 6766-6776.
- <sup>17</sup> P. O'Brien and T. D. Towers, *J. Org. Chem.*, 2002, **67**, 304-307.
- <sup>18</sup> C. McKay, R. J. Wilson, and C. M. Rayner, *Chem. Commun.*, 2004, 1080-1081.
- <sup>19</sup> K. Weber, S. Kuklinski, and P. Gmeiner, *Org. Lett.*, 2000, **2**, 647-649.
- <sup>20</sup> T. Lehmann and P. Gmeiner, *Heterocycles*, 2000, **53**, 1371-1378.

## Chapter 5: Experimental

### 5.1 General methods

#### 5.1.1 Reagents, solvents and reaction conditions

All reagents were of synthetic grade and were used without further purification unless otherwise stated. Dry diethyl ether and dry THF were distilled from sodium wire and benzophenone; dry methanol and dry DCM were distilled from calcium hydride. All moisture sensitive reactions were carried out under a positive pressure of nitrogen in oven-dried glassware (140 °C). Reaction temperatures of -78 °C to -40 °C were obtained using solid CO<sub>2</sub> in acetone or a bath cooling apparatus LP Technology RP-100-CD; reaction temperature of -10 °C was obtained using an ice/acetone bath. Organic extracts were dried over MgSO<sub>4</sub>.

#### 5.1.2 Chromatography and mass spectrometry

Thin layer chromatography (TLC) was performed using Macherey-Nagel Polygram Sil G/UV<sub>254</sub> plastic plates; visualisation was achieved by inspection under UV light (255 nm) or by the use of potassium permanganate stain, molybdenum-based stain, ferric chloride stain, bromocresol green stain or ninhydrin spray. Column chromatography was performed using silica gel 60 (40-63 micron) from Apollo Scientific Ltd. Ion-exchange chromatography was performed using Dowex® 50 W-X8100 resin with 50-100 mesh particules. GC-MS analyses were obtained using an Agilent 5890 gas chromatograph equipped with an Agilent 5973N mass-selective

detector. High-resolution mass spectrometry was performed by Mrs. C. Horsburgh on a Waters LCT or GCT time-of-flight mass spectrometer.

### 5.1.3 Nuclear magnetic resonance spectroscopy (NMR)

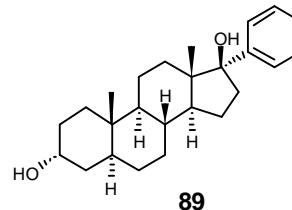
NMR spectra were recorded on either Bruker AV-300 ( $^1\text{H}$  at 300.06 MHz,  $^{13}\text{C}$  at 75.45 MHz,  $^{19}\text{F}$  at 282.34 MHz), or Bruker AV-300 ( $^1\text{H}$  at 300.13 MHz,  $^{13}\text{C}$  at 75.48 MHz), or Bruker AV-500 ( $^1\text{H}$  at 499.90 MHz,  $^{19}\text{F}$  at 470.33 MHz). Chemical shifts  $\delta$  are reported in parts per million (ppm) and quoted relative to internal standard  $\text{Me}_4\text{Si}$  for  $^1\text{H}$  and  $^{13}\text{C}$  and to external standard  $\text{CFCl}_3$  for  $^{19}\text{F}$ .  $^1\text{H}$ ,  $^{13}\text{C}$  and  $^{19}\text{F}$  spectroscopic data were assigned on a routine basis by a combination of one- and two- dimensional experiments (COSY, HSQC, HMBC, NOESY).

### 5.1.4 Other analysis

Melting points were measured using a Gallenkamp Griffin MPA350.BM2.5 melting point apparatus and are uncorrected. Optical rotations were determined using a A-1000 polarimeter (Optical Polarimeter Ltd) or a Perkin Elmer Model 341 polarimeter,  $[\alpha]_{\text{D}}$  values are measured at 589 nm and given in  $10^{-1}\text{deg.cm}^2.\text{g}^{-1}$ . Elemental analyses were carried out by Mrs. S. Williamson on a CE instrument EA 1110 CHNS analyser. IR spectra were recorded on a Perkin Elmer Spectrum GX FT-IR system as KBr disc or as thin film on NaCl plates. Single X-ray diffraction analyses were carried out by Prof. A.M.Z Slawin. pKa Determinations were conducted on a Fisherbrand Hydrus 300 pH meter equipped with a Hamilton biotrode pH electrode calibrated at pH 4 and pH 7 with standard buffer solutions.

## 5.2 Protocols

### 5.2.1 (3 $\alpha$ ,5 $\alpha$ ,17 $\beta$ )-17-Phenylandrosterane-3,17-diol (**89**)<sup>1</sup>

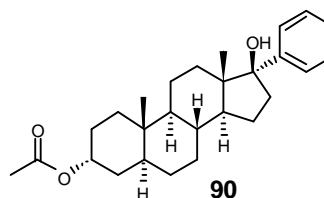


*n*-BuLi (3.2 cm<sup>3</sup>, 2.5 M in hexane, 8.0 mmol) was added at 0 °C under N<sub>2</sub> to a solution of bromobenzene (1.41 g, 9.0 mmol) in dry diethyl ether (6 cm<sup>3</sup>). The mixture was stirred for 30 min at 0 °C and 1 h at RT. The solution was then cooled to -10 °C and added dropwise *via* canula to a solution of androsterone (300 mg, 1.0 mmol) in dry THF (20 cm<sup>3</sup>). The reaction mixture was stirred 2 h at -10 °C and 16 h at RT. A saturated solution of NH<sub>4</sub>Cl (10 cm<sup>3</sup>) was added and the organic phase was extracted into EtOAc (3 × 50 cm<sup>3</sup>). The combined extracts were washed with brine and dried. After evaporation of the solvent under reduced pressure, the product was purified over silica gel (hexane/ EtOAc 6:1) to give (**89**) as a colourless solid (165 mg, 43%).

**Mp**: 190-192 °C (from hexane/EtOAc), lit<sup>1</sup> 193-196 °C (from hexanes/EtOAc);  **$\delta_{\text{H}}$**  (300 MHz, CDCl<sub>3</sub>) 7.19-7.27 (5 H, m, Ar-*H*), 3.89-3.93 (1 H, m, C<sup>3</sup>*H*), 2.30 (1 H, ddd, *J*=5.2 Hz, *J*=9.8 Hz, *J*=14.3 Hz, C<sup>16</sup>*H*<sub>A</sub>), 2.01 (1 H, ddd, *J*=4.6 Hz, *J*=12.5 Hz, *J*=14.3 Hz, C<sup>16</sup>*H*<sub>B</sub>), 0.73-1.78 (20 H, m), 0.97 (3 H, s, C<sup>18</sup>*H*<sub>3</sub>), 0.68 (3 H, s, C<sup>19</sup>*H*<sub>3</sub>), 0.23-0.40 (2 H, m);  **$\delta_{\text{C}}$**  (75 MHz, CDCl<sub>3</sub>) 146.5 (*Ar*), 127.7 (2 × C, *Ar*), 127.6 (2 × C, *Ar*), 127.1 (*Ar*), 86.4 (C<sup>17</sup>), 66.9 (C<sup>3</sup>), 54.1 (C<sup>9</sup>), 49.5 (C<sup>14</sup>), 47.1 (C<sup>13</sup>), 39.5 (C<sup>5</sup>), 39.0 (C<sup>16</sup>), 36.6 (C<sup>8</sup>), 36.5 (C<sup>10</sup>), 36.2 (C<sup>4</sup>), 34.0 (C<sup>12</sup>), 32.4 (C<sup>1</sup>), 32.1 (C<sup>7</sup>), 29.3 (C<sup>2</sup>), 28.8 (C<sup>6</sup>), 24.8 (C<sup>15</sup>), 20.7 (C<sup>11</sup>), 15.3 (C<sup>18</sup>), 11.6 (C<sup>19</sup>).

These data are in accordance with the literature.<sup>1</sup>

### 5.2.2 (3 $\alpha$ ,5 $\alpha$ ,17 $\beta$ )-17-Phenylandrostane-3,17-diol, 3-acetate (**90**)<sup>1</sup>

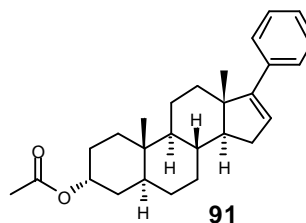


Ac<sub>2</sub>O (0.5 cm<sup>3</sup>) and 4-DMAP (24 mg) were added to a solution of (3 $\alpha$ ,5 $\alpha$ ,17 $\beta$ )-17-phenylandrostane-3,17-diol (**89**) (180 mg, 0.5 mmol) in pyridine (2.5 cm<sup>3</sup>). The mixture was stirred at RT for 15 min and poured into 10% NaHCO<sub>3</sub> (20 cm<sup>3</sup>). After the mixture was stirred for 10 min, the product was extracted into EtOAc (3  $\times$  40 cm<sup>3</sup>). The combined organic extracts were dried and evaporated under reduced pressure. The product was purified over silica gel (hexane/EtOAc 10:1) to give (**90**) as a colourless amorphous solid (180 mg, 90%).

**Mp**: 198-199 °C (from hexane/EtOAc), lit<sup>1</sup> 196-198 °C;  $\delta_{\text{H}}$  (300 MHz, CDCl<sub>3</sub>) 7.23-7.39 (5 H, m, Ar-*H*), 4.94-4.98 (1 H, m, C<sup>3</sup>*H*), 2.38 (1 H, ddd, *J*=4.8 Hz, *J*=9.7 Hz, *J*=14.3 Hz, C<sup>16</sup>*H*<sub>A</sub>), 2.04-2.15 (1 H, m, C<sup>16</sup>*H*<sub>B</sub>), 1.99 (3 H, s, CH<sub>3</sub>CO<sub>2</sub>), 0.79-1.88 (19 H, m), 1.05 (3 H, s, C<sup>18</sup>*H*<sub>3</sub>), 0.77 (3 H, s, C<sup>19</sup>*H*<sub>3</sub>), 0.32-0.49 (2 H, m);  $\delta_{\text{C}}$  (75 MHz, CDCl<sub>3</sub>) 171.1 (CO<sub>2</sub>), 146.7 (Ar), 127.8 (2  $\times$  C, Ar), 127.6 (2  $\times$  C, Ar), 127.1 (Ar), 86.3 (C<sup>17</sup>), 70.5 (CH), 54.0 (CH), 49.9 (CH<sub>2</sub>), 47.1 (C<sup>13</sup>), 40.3 (CH), 38.9 (CH<sub>2</sub>), 36.6 (CH), 36.2 (C<sup>10</sup>), 34.0 (CH<sub>2</sub>), 33.2 (CH<sub>2</sub>), 33.1 (CH<sub>2</sub>), 32.0 (CH<sub>2</sub>), 28.7 (CH<sub>2</sub>), 26.4 (CH<sub>2</sub>), 24.8 (CH<sub>2</sub>), 21.9 (CH<sub>2</sub>), 20.7 (CH<sub>3</sub>CO<sub>2</sub>), 15.3 (CH<sub>3</sub>), 11.8 (CH<sub>3</sub>).

These data are in accordance with the literature.<sup>1</sup>

### 5.2.3 (3 $\alpha$ ,5 $\alpha$ )-17-Phenylandrost-16-en-3-ol acetate (**91**)<sup>1</sup>

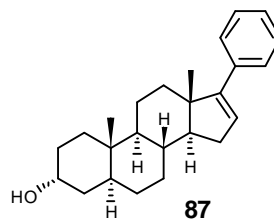


Et<sub>3</sub>N (0.6 cm<sup>3</sup>) and MsCl (0.18 cm<sup>3</sup>, 2.3 mmol) were added at 0 °C to a solution of (3 $\alpha$ ,5 $\alpha$ ,17 $\beta$ )-17-phenylandrostane-3,17-diol, 3-acetate (**90**) (170 mg, 0.4 mmol) in dry DCM (15 cm<sup>3</sup>). The solution was stirred for 1 h at 0 °C and DCM was removed under reduced pressure. The product was purified over silica gel (hexane/EtOAc 15:1) to give (**91**) as a colourless amorphous solid (140 mg, 86%).

**Mp**: 143-145 °C (from CHCl<sub>3</sub>), lit<sup>1</sup> 152-153 °C (from hexanes);  $\delta_{\text{H}}$  (300 MHz, CDCl<sub>3</sub>) 7.10-7.31 (5 H, m, Ar-*H*), 5.82 (1 H, dd,  $J=1.7$  Hz,  $J=3.2$  Hz, C<sup>16</sup>*H*), 4.92-4.96 (1 H, m, C<sup>3</sup>*H*), 2.12 (1 H, ddd,  $J=3.3$  Hz,  $J=6.3$  Hz,  $J=15.5$  Hz, C<sup>15</sup>*H*<sub>A</sub>), 1.86-2.01 (2 H, m), 1.97 (3 H, s, CH<sub>3</sub>CO<sub>2</sub>), 0.73-1.70 (17 H, m), 0.94 (3 H, s, C<sup>18</sup>*H*<sub>3</sub>), 0.77 (3 H, s, C<sup>19</sup>*H*<sub>3</sub>);  $\delta_{\text{C}}$  (75 MHz, CDCl<sub>3</sub>) 171.1 (CO<sub>2</sub>), 155.3 (C<sup>17</sup>), 137.8 (Ar), 128.5 (2  $\times$  C, Ar), 127.6 (C<sup>16</sup>), 127.1 (3  $\times$  C, Ar), 70.5 (CH), 58.1 (CH), 54.9 (CH), 47.8 (C<sup>13</sup>), 40.7 (CH), 36.4 (C<sup>10</sup>), 35.9 (CH<sub>2</sub>), 34.4 (CH), 33.3 (CH<sub>2</sub>), 33.2 (CH<sub>2</sub>), 32.2 (CH<sub>2</sub>), 31.9 (CH<sub>2</sub>), 28.8 (CH<sub>2</sub>), 26.5 (CH<sub>2</sub>), 22.0 (CH<sub>3</sub>CO<sub>2</sub>), 21.2 (CH<sub>2</sub>), 17.2 (CH<sub>3</sub>), 11.8 (CH<sub>3</sub>).

These data are in accordance with the literature.<sup>1</sup>

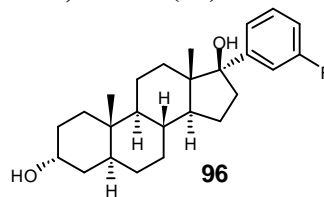


5.2.4 (3 $\alpha$ ,5 $\alpha$ )-17-Phenylandroster-16-en-3-ol (**87**)<sup>1</sup>

5 N NaOH (1 cm<sup>3</sup>) was added at RT to a solution of (3 $\alpha$ ,5 $\alpha$ )-17-phenylandroster-16-en-3-ol acetate (**91**) (130 mg, 0.33 mmol) in MeOH (15 cm<sup>3</sup>). The mixture was heated under reflux for 1 h and cooled to RT. Water (8 cm<sup>3</sup>) was added and the product was extracted into DCM (3  $\times$  40 cm<sup>3</sup>). The combined extracts were dried and the solvents removed under reduced pressure. The product was purified over silica gel (hexane/EtOAc 9:1) to give (3 $\alpha$ ,5 $\alpha$ )-17-phenylandroster-16-en-3-ol (**87**) as a colourless amorphous solid (104 mg, 89%).

**Mp**: 169-170 °C (from CHCl<sub>3</sub>), lit<sup>1</sup> 174.5-175.5 °C (from hexanes/EtOAc); **[ $\alpha$ ]<sub>D</sub><sup>20</sup>** +23.0 (c 1.5 CHCl<sub>3</sub>); (**Found**: C, 85.84; H, 10.21 %, C<sub>25</sub>H<sub>34</sub>O requires C, 85.66; H, 9.78 %);  **$\nu_{\max}$** (KBr plate)/cm<sup>-1</sup> 3361 (br), 2925, 2855, 1603, 1493, 1445, 1370, 1262, 1033, 753, 691;  **$\delta_{\text{H}}$**  (300 MHz, CDCl<sub>3</sub>) 7.18-7.38 (5 H, m, Ar-*H*), 5.88 (1 H, dd, *J*=1.7 Hz, *J*=3.1 Hz, C<sup>16</sup>*H*), 4.02-4.06 (1 H, m, C<sup>3</sup>*H*), 2.20 (1 H, ddd, *J*=3.3 Hz, *J*=6.2 Hz, *J*=15.4 Hz, C<sup>15</sup>*H*<sub>A</sub>), 1.93-2.07 (2 H, m), 0.81-1.78 (18 H, m), 1.02 (3 H, s, C<sup>18</sup>*H*<sub>3</sub>), 0.83 (3 H, s, C<sup>19</sup>*H*<sub>3</sub>);  **$\delta_{\text{C}}$**  (75 MHz, CDCl<sub>3</sub>) 155.3 (C<sup>17</sup>), 137.8 (*Ar*), 128.5 (2  $\times$  C, *Ar*), 127.6 (C<sup>16</sup>), 127.1 (2  $\times$  C, *Ar*), 127.0 (*Ar*), 67.0 (CH), 58.1 (CH), 55.1 (CH), 47.8 (C<sup>13</sup>), 39.8 (CH), 36.7 (C<sup>10</sup>), 36.3 (CH<sub>2</sub>), 35.9 (CH<sub>2</sub>), 34.5 (CH), 32.5 (CH<sub>2</sub>), 32.3 (CH<sub>2</sub>), 31.9 (CH<sub>2</sub>), 29.4 (CH<sub>2</sub>), 28.9 (CH<sub>2</sub>), 21.2 (CH<sub>2</sub>), 17.2 (CH<sub>3</sub>), 11.6 (CH<sub>3</sub>); ***m/z*** (+CI), found MH<sup>+</sup>: 351.2683, C<sub>25</sub>H<sub>35</sub>O requires 351.2688 (-1.5 ppm).

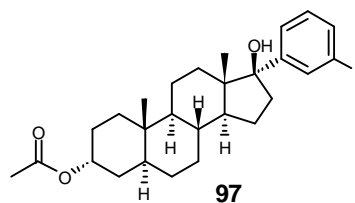
These data are in accordance with the literature.<sup>1</sup>

5.2.5 (3 $\alpha$ ,5 $\alpha$ ,17 $\beta$ )-17-(*m*-Fluorophenyl)androstane-3,17-diol (**96**)

*n*-BuLi (2.0 cm<sup>3</sup>, 2.5 M in hexane, 5.0 mmol) was added at -78 °C under N<sub>2</sub> to a solution of 3-fluoro-bromobenzene (0.55 cm<sup>3</sup>, 5.0 mmol) in dry diethyl ether (5 cm<sup>3</sup>). The mixture was stirred for 30 min at -78 °C and added dropwise *via* canula over 10 min to a solution of androsterone (300 mg, 1.0 mmol) in dry THF (20 cm<sup>3</sup>). The reaction mixture was stirred 3 h at -78 °C and the temperature was allowed to warm to RT over 15 h. A saturated solution of NH<sub>4</sub>Cl (10 cm<sup>3</sup>) was added and the organic phase was extracted into EtOAc (3 × 50 cm<sup>3</sup>). The combined organic extracts were washed with brine and dried. After evaporation of the solvent, the product was purified over silica gel (hexane/EtOAc 6:1) to give (**96**) as a colourless solid (125 mg, 31%).

**Mp**: 182-188 °C (from hexane/EtOAc); [ $\alpha$ ]<sub>D</sub><sup>20</sup> +25.3 (c 0.4, CHCl<sub>3</sub>);  $\nu_{\text{max}}$ (KBr plate)/cm<sup>-1</sup> 3422 (br), 2926, 2854, 1613, 1586, 1437, 1262, 1096, 1016, 804;  $\delta_{\text{H}}$  (300 MHz, CDCl<sub>3</sub>) 6.92-7.45 (4 H, m, Ar-*H*), 3.95-4.01 (1 H, m, C<sup>3</sup>*H*), 2.33 (1 H, ddd, *J*=5.3 Hz, *J*=9.7 Hz, *J*=14.4 Hz, C<sup>16</sup>*H*<sub>A</sub>), 2.08 (1 H, ddd, *J*=4.4 Hz, *J*=12.5 Hz, *J*=14.4 Hz, C<sup>16</sup>*H*<sub>B</sub>), 0.53-1.87 (20 H, m), 1.03 (3 H, s, C<sup>18</sup>*H*<sub>3</sub>), 0.76 (3 H, s, C<sup>19</sup>*H*<sub>3</sub>), 0.29-0.49 (2 H, m);  $\delta_{\text{C}}$  (75 MHz, CDCl<sub>3</sub>) 162.6 (d, *J*=244.2 Hz, Ar-F), 149.5 (d, *J*=6.4 Hz, Ar), 128.9 (d, *J*=8.1 Hz, Ar), 123.4 (d, *J*=2.4 Hz, Ar), 115.0 (d, *J*=22.1 Hz, Ar), 113.9 (d, *J*=21.1 Hz, Ar), 86.3 (C<sup>17</sup>), 66.8 (CH), 54.1 (CH), 49.5 (CH), 47.2 (C<sup>13</sup>), 39.4 (CH), 39.1 (CH<sub>2</sub>), 36.6 (CH), 36.4 (C<sup>10</sup>), 36.2 (CH<sub>2</sub>), 34.0 (CH<sub>2</sub>), 32.4 (CH<sub>2</sub>), 32.0 (CH<sub>2</sub>), 29.3 (CH<sub>2</sub>), 28.8 (CH<sub>2</sub>), 24.7 (CH<sub>2</sub>), 20.7 (CH<sub>2</sub>), 15.3 (CH<sub>3</sub>), 11.6 (CH<sub>3</sub>);  $\delta_{\text{F}}$  (282 MHz, CDCl<sub>3</sub>) -114.6 (1 F, ddd, *J*=6.1 Hz, *J*=8.4 Hz, *J*=11.0 Hz); *m/z* (+ES), found (M+Na<sup>+</sup>): 409.2512, C<sub>25</sub>H<sub>35</sub>O<sub>2</sub>NaF requires 409.2519 (-1.8 ppm).

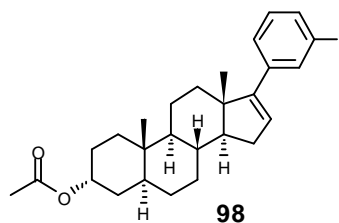
### 5.2.6 (3 $\alpha$ ,5 $\alpha$ ,17 $\beta$ )-17-(*m*-Fluorophenyl)androstane-3,17-diol, 3-acetate (**97**)



Ac<sub>2</sub>O (0.2 cm<sup>3</sup>) and 4-DMAP (8 mg) were added to a solution of (3 $\alpha$ ,5 $\alpha$ ,17 $\beta$ )-17-(*m*-fluorophenyl)androstane-3,17-diol (**96**) (62 mg, 0.16 mmol) in pyridine (0.5 cm<sup>3</sup>). The mixture was stirred at RT for 15 min and poured into 10% NaHCO<sub>3</sub> (8 cm<sup>3</sup>). After further stirring for 20 min, the product was extracted into EtOAc (3 × 20 cm<sup>3</sup>). The combined organic extracts were dried over MgSO<sub>4</sub> and evaporated under reduced pressure. The product was purified over silica gel (hexane/ EtOAc 10:1) to give (**97**) as a colourless solid (55 mg, 80%).

**Mp**: 195-197 °C (from CHCl<sub>3</sub>);  $\delta_{\text{H}}$  (300 MHz, CDCl<sub>3</sub>) 6.92-7.31 (4 H, Ar-*H*), 4.93-4.98 (1 H, m, C<sup>3</sup>*H*), 2.34 (1 H, ddd,  $J=5.3$  Hz,  $J=9.7$  Hz,  $J=14.5$  Hz, C<sup>16</sup>*H*<sub>A</sub>), 2.09 (1 H, ddd,  $J=4.2$  Hz,  $J=12.4$  Hz,  $J=14.4$  Hz, C<sup>16</sup>*H*<sub>B</sub>), 1.99 (3 H, s, CH<sub>3</sub>CO<sub>2</sub>), 0.57-1.94 (19 H, m), 1.04 (3 H, s, C<sup>18</sup>*H*<sub>3</sub>), 0.77 (3 H, s, C<sup>19</sup>*H*<sub>3</sub>), 0.31-0.51 (2 H, m);  $\delta_{\text{C}}$  (75 MHz, CDCl<sub>3</sub>) 171.1 (CO<sub>2</sub>), 162.6 (d,  $J=244.3$  Hz, Ar-F), 149.5 (d,  $J=6.3$  Hz, Ar), 128.9 (d,  $J=8.1$  Hz, Ar), 123.4 (d,  $J=2.4$  Hz, Ar), 115.0 (d,  $J=22.1$  Hz, Ar), 113.9 (d,  $J=21.0$  Hz, Ar), 86.3 (C<sup>17</sup>), 70.5 (CH), 54.0 (CH), 49.5 (CH<sub>2</sub>), 47.3 (C<sup>13</sup>), 40.3 (CH), 39.1 (CH<sub>2</sub>), 36.6 (CH), 36.2 (C<sup>10</sup>), 34.0 (CH<sub>2</sub>), 33.2 (CH<sub>2</sub>), 33.1 (CH<sub>2</sub>), 31.9 (CH<sub>2</sub>), 28.6 (CH<sub>2</sub>), 26.4 (CH<sub>2</sub>), 24.7 (CH<sub>2</sub>), 21.9 (CH<sub>3</sub>CO<sub>2</sub>), 20.7 (CH<sub>2</sub>), 15.3 (CH<sub>3</sub>), 11.7 (CH<sub>3</sub>);  $\delta_{\text{F}}$  (282 MHz, CDCl<sub>3</sub>) -114.6 (1 F, ddd,  $J=6.1$  Hz,  $J=8.4$  Hz,  $J=11.1$  Hz).

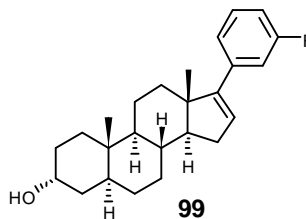
### 5.2.7 (3 $\alpha$ ,5 $\alpha$ )-17-(*m*-Fluorophenyl)androst-16-en-3-ol acetate (**98**)



Et<sub>3</sub>N (0.2 cm<sup>3</sup>) and MsCl (60  $\mu$ L, 0.77 mmol) were added at 0 °C to a solution of (3 $\alpha$ ,5 $\alpha$ ,17 $\beta$ )-17-(*m*-fluorophenyl)androstane-3,17-diol, 3-acetate (**97**) (50 mg, 0.12 mmol) in dry DCM (5 cm<sup>3</sup>). The solution was stirred for 45 min at 0 °C and DCM was removed under reduced pressure. The crude product was purified over silica gel (hexane/EtOAc 15:1) to give (**98**) as a colourless solid (32 mg, 67%).

**Mp**: 148-150 °C (from CHCl<sub>3</sub>);  $\delta_{\text{H}}$  (300 MHz, CDCl<sub>3</sub>) 7.20-7.28 (1 H, m, Ar-*H*), 7.12-7.16 (1 H, m, Ar-*H*), 7.03-7.09 (1 H, m, Ar-*H*), 6.87-6.94 (1 H, m, Ar-*H*), 5.94 (1 H, dd,  $J=1.8$  Hz,  $J=3.2$  Hz, C<sup>16</sup>*H*), 5.00-5.04 (1 H, m, C<sup>3</sup>*H*), 2.21 (1 H, ddd,  $J=3.3$  Hz,  $J=6.3$  Hz,  $J=15.7$  Hz, C<sup>15</sup>*H*<sub>A</sub>), 1.94-2.08 (2 H, m), 2.06 (3 H, s, CH<sub>3</sub>CO<sub>2</sub>), 0.78-1.78 (17 H, m), 1.01 (3 H, s, C<sup>18</sup>*H*<sub>3</sub>), 0.85 (3 H, s, C<sup>19</sup>*H*<sub>3</sub>);  $\delta_{\text{C}}$  (75 MHz, CDCl<sub>3</sub>) 171.2 (CH<sub>3</sub>CO<sub>2</sub>), 163.1 (d,  $J=244.4$  Hz, Ar-F), 154.2 (d,  $J=1.9$  Hz, C<sup>17</sup>), 140.0 (d,  $J=7.7$  Hz, Ar), 129.8 (d,  $J=8.4$  Hz, Ar), 128.9 (C<sup>16</sup>), 122.7 (d,  $J=2.6$  Hz, Ar), 113.8 (d,  $J=21.5$  Hz, Ar), 113.8 (d,  $J=21.1$  Hz, Ar), 70.5 (CH), 58.0 (CH), 54.9 (CH<sub>2</sub>), 47.8 (C<sup>13</sup>), 40.6 (CH), 36.4 (C<sup>10</sup>), 35.8 (CH<sub>2</sub>), 34.4 (CH), 33.3 (CH<sub>2</sub>), 33.1 (CH<sub>2</sub>), 32.2 (CH<sub>2</sub>), 31.9 (CH<sub>2</sub>), 28.7 (CH<sub>2</sub>), 26.5 (CH<sub>2</sub>), 22.0 (CH<sub>3</sub>CO<sub>2</sub>), 21.2 (CH<sub>2</sub>), 17.2 (CH<sub>3</sub>), 11.7 (CH<sub>3</sub>);  $\delta_{\text{F}}$  (282 MHz, CDCl<sub>3</sub>) -114.3 (1 F, ddd,  $J=6.1$  Hz,  $J=8.6$  Hz,  $J=10.6$  Hz); *m/z* (+ES), found (M+Na<sup>+</sup>): 433.2516, C<sub>27</sub>H<sub>35</sub>O<sub>2</sub>FNa requires 433.2519 (-0.7 ppm).

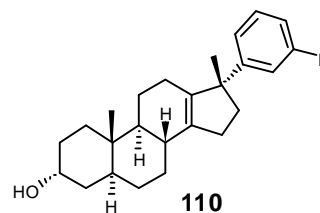
### 5.2.8 (3 $\alpha$ ,5 $\alpha$ )-17-(*m*-Fluorophenyl)androst-16-en-3-ol (**99**)



5 N NaOH (0.15 cm<sup>3</sup>) was added at RT to a solution of (3 $\alpha$ ,5 $\alpha$ )-17-(*m*-fluorophenyl)androst-16-en-3-ol acetate (**98**) (21 mg, 0.05 mmol) in MeOH (2.5 cm<sup>3</sup>). The mixture was heated under reflux for 1 h and cooled to RT. Water (2 cm<sup>3</sup>) was added and the product was extracted into DCM (3  $\times$  10 cm<sup>3</sup>). The combined organic extracts were dried and the solvent removed under reduced pressure. The product was purified over silica gel (hexane/EtOAc 9:1) to give (**99**) as a colourless solid (17 mg, 90%).

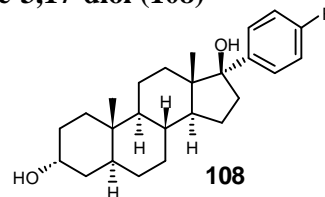
**Mp**: 179-184 °C (from CHCl<sub>3</sub>);  $\delta_{\text{H}}$  (300 MHz, CDCl<sub>3</sub>) 7.20-7.27 (1 H, m, Ar-*H*), 7.12-7.15 (1 H, m, Ar-*H*), 7.03-7.08 (1 H, m, Ar-*H*), 6.87-6.94 (1 H, m, Ar-*H*), 5.93 (1 H, *J*=1.8 Hz, *J*=3.1 Hz, C<sup>16</sup>*H*), 4.04-4.07 (1 H, m, C<sup>3</sup>*H*), 2.21 (1 H, ddd, *J*=3.3 Hz, *J*=6.2 Hz, *J*=15.6 Hz, C<sup>15</sup>*H*<sub>A</sub>), 1.94-2.01 (2 H, m), 0.75-1.78 (18 H, m), 1.01 (3 H, s, C<sup>18</sup>*H*<sub>3</sub>), 0.84 (3 H, s, C<sup>19</sup>*H*<sub>3</sub>);  $\delta_{\text{C}}$  (75 MHz, CDCl<sub>3</sub>) 163.1 (d, *J*=244.5 Hz, Ar-F), 154.3 (d, *J*=2.0 Hz, C<sup>17</sup>), 140.0 (d, *J*=7.8 Hz, Ar), 129.8 (d, *J*=8.5 Hz, Ar), 128.9 (C<sup>16</sup>), 122.7 (d, *J*=2.6 Hz, Ar), 113.8 (d, *J*=21.5 Hz, Ar), 113.7 (d, *J*=21.1 Hz, Ar), 67.0 (CH), 58.0 (CH), 55.0 (CH), 47.8 (C<sup>13</sup>), 39.7 (CH), 36.7 (C<sup>10</sup>), 36.3 (CH<sub>2</sub>), 35.8 (CH<sub>2</sub>), 34.4 (CH), 32.4 (CH<sub>2</sub>), 32.2 (CH<sub>2</sub>), 31.9 (CH<sub>2</sub>), 29.4 (CH<sub>2</sub>), 28.9 (CH<sub>2</sub>), 21.2 (CH<sub>2</sub>), 17.2 (CH<sub>3</sub>), 11.6 (CH<sub>3</sub>);  $\delta_{\text{F}}$  (282 MHz, CDCl<sub>3</sub>) -114.3 (1 F, ddd, *J*=6.2 Hz, *J*=8.7 Hz, *J*=10.7 Hz); *m/z* (+CI), found MH<sup>+</sup>: 369.2599, C<sub>25</sub>H<sub>34</sub>OF requires 369.2594 (+1.3 ppm).

### 5.2.9 17 $\alpha$ -(*m*-Fluorophenyl)-17 $\beta$ -methyl-5 $\alpha$ -androstene-13-3 $\alpha$ -ol (**110**)



*p*-Toluenesulfonic acid monohydrate (40 mg, 0.26 mmol) was added at RT to a solution of (3 $\alpha$ ,5 $\alpha$ ,17 $\beta$ )-17-(*m*-fluorophenyl)androstane-3,17-diol (**96**) (50 mg, 0.13 mmol) in dry DCM (10 cm<sup>3</sup>). The mixture was heated under reflux for 5 h, cooled down to RT, 1 M NaHCO<sub>3</sub> (5 cm<sup>3</sup>) was added and the solution was stirred for 15 min. The product was extracted into DCM (2  $\times$  20 cm<sup>3</sup>), the combined organic extracts were dried and the solvent was evaporated under reduced pressure. The product was purified over silica gel (hexane/EtOAc 10:1) to give (**110**) as a colourless oil (25 mg, 52%).

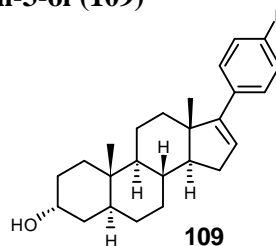
$\delta_{\text{H}}$  (500 MHz, CDCl<sub>3</sub>) 7.23 (1 H, ddd,  $J=6.4$  Hz,  $J=8.0$  Hz,  $J=8.0$  Hz, Ar-*H*), 7.03 (1 H, ddd,  $J=2.0$  Hz,  $J=2.0$  Hz,  $J=7.9$  Hz, Ar-*H*), 6.95 (1 H, ddd,  $J=2.0$  Hz,  $J=2.0$  Hz,  $J=11.1$  Hz, Ar-*H*), 6.84 (1 H, ddd,  $J=2.5$  Hz,  $J=8.3$  Hz,  $J=8.4$  Hz, Ar-*H*), 4.06-4.08 (1 H, m, C<sup>3</sup>*H*), 2.32-2.40 (1 H, m, C<sup>15</sup>*H*<sub>A</sub>), 2.12-2.21 (2 H, m, C<sup>15</sup>*H*<sub>B</sub> + C<sup>8</sup>*H*), 1.80-2.02 (5 H, m), 1.04-1.77 (14 H, m), 1.40 (3 H, C<sup>18</sup>*H*<sub>3</sub>), 0.78 (3 H, C<sup>19</sup>*H*<sub>3</sub>);  $\delta_{\text{C}}$  (75 MHz, CDCl<sub>3</sub>) 163.0 (d,  $J=244.2$  Hz, Ar), 152.0 (d,  $J=6.2$  Hz, Ar), 139.9 (C<sup>14</sup>), 139.6 (C<sup>13</sup>), 129.3 (d,  $J=8.2$  Hz, Ar), 121.6 (d,  $J=2.3$  Hz, Ar), 113.0 (d,  $J=21.4$  Hz, Ar), 112.1 (d,  $J=21.2$  Hz, Ar), 66.6 (C<sup>3</sup>), 53.1 (C<sup>17</sup>), 51.8 (C<sup>9</sup>), 42.2 (C<sup>16</sup>), 39.1 (C<sup>5</sup>), 36.9 (C<sup>8</sup>), 36.1 (C<sup>10</sup>), 35.7 (C<sup>4</sup>), 31.9 (C<sup>1</sup>), 31.5 (C<sup>7</sup>), 30.5 (C<sup>15</sup>), 29.0 (C<sup>6</sup>+C<sup>2</sup>), 24.2 (C<sup>18</sup>), 22.9 (C<sup>12</sup>), 22.2 (C<sup>11</sup>), 10.7 (C<sup>19</sup>);  $\delta_{\text{F}}$  (282 MHz, CDCl<sub>3</sub>) -114.3 (1 F, ddd,  $J=6.3$  Hz,  $J=8.5$  Hz,  $J=11.2$  Hz); *m/z* (+CI), found MH<sup>+</sup>: 369.2594, C<sub>25</sub>H<sub>34</sub>OF requires 369.2594 (+0.2 ppm).

5.2.10 (3 $\alpha$ ,5 $\alpha$ ,17 $\beta$ )-17-(*p*-Fluorophenyl)androsterane-3,17-diol (**108**)

*n*-BuLi (3.8 cm<sup>3</sup>, 2.5 M in hexane, 9.5 mmol) was added at -78 °C under N<sub>2</sub> to a solution of 4-fluoro-bromobenzene (1.1 cm<sup>3</sup>, 10.0 mmol) in dry diethyl ether (10 cm<sup>3</sup>). The mixture was stirred for 3 h at -78 °C and then 3 h at -40 °C. The solution was then added dropwise *via* canula at -40 °C to a solution of androsterone (300 mg, 1.0 mmol) in dry THF (15 cm<sup>3</sup>). The reaction mixture was stirred for 8 h at -40 °C and the temperature was allowed to warm to RT over 12 h. A saturated solution of NH<sub>4</sub>Cl (10 cm<sup>3</sup>) was added and the organic phase was extracted into EtOAc (3 × 50 cm<sup>3</sup>). The combined organic extracts were dried and evaporated and the product was purified over silica gel (hexane/EtOAc 6:1) to give (**108**) as a colourless solid (158 mg, 40%).

**Mp:** 173-176 °C (from CHCl<sub>3</sub>); [ $\alpha$ ]<sub>D</sub><sup>20</sup> +18.0 (c 1.5, CHCl<sub>3</sub>);  $\nu_{\text{max}}$ (KBr plate)/cm<sup>-1</sup> 3464 (br), 2932, 2855, 1603, 1508, 1226, 1162, 1075, 1016, 1005, 832;  $\delta_{\text{H}}$  (300 MHz, CDCl<sub>3</sub>) 7.23 (2 H, dd, *J*=5.6 Hz, *J*=8.8 Hz, Ar-*H*), 6.91 (2 H, dd, *J*=8.8 Hz, *J*=8.8 Hz, Ar-*H*), 3.94-3.99 (1 H, m, C<sup>3</sup>*H*), 2.24 (1 H, ddd, *J*=5.2 Hz, *J*=9.7 Hz, *J*=14.7 Hz, C<sup>16</sup>*H*<sub>A</sub>), 1.93-2.05 (1 H, m, C<sup>16</sup>*H*<sub>B</sub>), 0.72-1.77 (20 H, m), 0.95 (3 H, s, C<sup>18</sup>*H*<sub>3</sub>), 0.67 (3 H, s, C<sup>19</sup>*H*<sub>3</sub>); 0.20-0.39 (2 H, m);  $\delta_{\text{C}}$  (75 MHz, CDCl<sub>3</sub>) 162.1 (d, *J*=245.2 Hz, Ar-F), 142.1 (d, *J*=3.1 Hz, Ar), 129.3 (2 × C, d, *J*=7.8 Hz, Ar), 114.3 (2 × C, d, *J*=20.9 Hz, Ar), 86.1 (C<sup>17</sup>), 66.8 (CH), 54.1 (CH), 49.5 (CH), 47.0 (C<sup>13</sup>), 39.4 (CH), 39.1 (CH<sub>2</sub>), 36.6 (CH), 36.4 (C<sup>10</sup>), 36.1 (CH<sub>2</sub>), 33.9 (CH<sub>2</sub>), 32.4 (CH<sub>2</sub>), 32.0 (CH<sub>2</sub>), 29.3 (CH<sub>2</sub>), 28.8 (CH<sub>2</sub>), 24.6 (CH<sub>2</sub>), 20.7 (CH<sub>2</sub>), 15.2 (CH<sub>3</sub>), 11.5 (CH<sub>3</sub>);  $\delta_{\text{F}}$  (282 MHz, CDCl<sub>3</sub>) -117.0 (1 F, tt, *J*=5.4 Hz, *J*=8.6 Hz); *m/z* (+ES), found (M+Na<sup>+</sup>): 409.2517, C<sub>25</sub>H<sub>35</sub>O<sub>2</sub>NaF requires 409.2519 (-0.4 ppm).

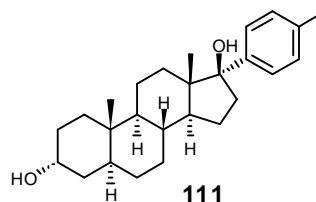
### 5.2.11 (3 $\alpha$ ,5 $\alpha$ )-17-(*p*-Fluorophenyl)androst-16-en-3-ol (**109**)



*p*-Toluenesulfonic acid monohydrate (10 mg, 0.05 mmol) was added at RT to a solution of (3 $\alpha$ ,5 $\alpha$ ,17 $\beta$ )-17-(*p*-fluorophenyl)androstane-3,17 $\beta$ -diol (**108**) (120 mg, 0.31 mmol) in dry DCM (20 cm<sup>3</sup>). The reaction solution was heated under reflux for 4 h and stirred at RT for 2 h. The reaction solution was washed with a 10% solution of NaHCO<sub>3</sub> (10 cm<sup>3</sup>) and the organic phase was extracted into diethyl ether (2  $\times$  40 cm<sup>3</sup>). The combined organic extracts were dried and the solvent was removed under reduced pressure. The residue was purified over silica gel (hexane/EtOAc 8:1) to give (**109**) as a colourless solid (65 mg, 57%).

**Mp**: 182-187 °C (from CHCl<sub>3</sub>); [ $\alpha$ ]<sub>D</sub><sup>18</sup> +25.6 (c 1.5, CHCl<sub>3</sub>);  $\nu_{\max}$ (KBr plate)/cm<sup>-1</sup> 3332 (br), 2929, 2858, 1601, 1505, 1442, 1230, 1218, 1034, 1005, 810;  $\delta_{\text{H}}$  (300 MHz, CDCl<sub>3</sub>) 7.28-7.33 (2 H, m, Ar-*H*), 6.94-7.00 (2 H, m, Ar-*H*), 5.83 (1 H, dd, *J*=1.8 Hz, *J*=3.2 Hz, C<sup>16</sup>*H*), 4.03-4.07 (1 H, m, C<sup>3</sup>*H*), 2.19 (1 H, ddd, *J*=3.3 Hz, *J*=6.2 Hz, *J*=15.4 Hz, C<sup>15</sup>*H*<sub>A</sub>), 1.92-2.04 (2 H, m), 0.73-1.77 (18 H, m), 0.99 (3 H, s, C<sup>18</sup>*H*<sub>3</sub>), 0.83 (3 H, s, C<sup>19</sup>*H*<sub>3</sub>);  $\delta_{\text{C}}$  (75 MHz, CDCl<sub>3</sub>) 162.3 (d, *J*=245.4 Hz, Ar), 154.3 (C<sup>17</sup>), 133.9 (d, *J*=3.2 Hz, Ar), 128.6 (2  $\times$  C, d, *J*=7.7 Hz, Ar), 127.5 (C<sup>16</sup>), 115.3 (2  $\times$  C, d, *J*=21.1 Hz, Ar), 67.0 (CH), 58.0 (CH), 55.0 (CH), 47.8 (C<sup>13</sup>), 39.7 (CH), 36.7 (C<sup>10</sup>), 36.3 (CH<sub>2</sub>), 35.9 (CH<sub>2</sub>), 34.5 (CH), 32.4 (CH<sub>2</sub>), 32.2 (CH<sub>2</sub>), 31.9 (CH<sub>2</sub>), 29.4 (CH<sub>2</sub>), 28.9 (CH<sub>2</sub>), 21.2 (CH<sub>2</sub>), 17.1 (CH<sub>3</sub>), 11.6 (CH<sub>3</sub>);  $\delta_{\text{F}}$  (282 MHz, CDCl<sub>3</sub>) -116.7 (1 F, tt, *J*=5.5 Hz, *J*=8.7 Hz); *m/z* (+CI), found MH<sup>+</sup>: 369.2585, C<sub>25</sub>H<sub>34</sub>OF requires 369.2594 (-2.3 ppm).

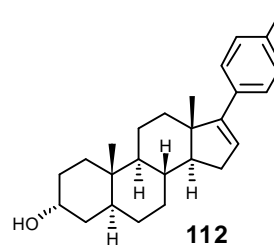


5.2.12 (3 $\alpha$ ,5 $\alpha$ ,17 $\beta$ )-(17-*p*-Toluene)androstane-3,17-diol (**111**)

*n*-BuLi (2 cm<sup>3</sup>, 2.5 M in hexane, 5.0 mmol) was added at RT under N<sub>2</sub> to a solution of *p*-bromotoluene (860 mg, 5.0 mmol) in dry diethyl ether (5 cm<sup>3</sup>). The mixture was stirred for 2 h at RT and added dropwise *via* canula to a solution of androsterone (262 mg, 0.9 mmol) in dry THF (10 cm<sup>3</sup>). The reaction mixture was stirred for 15 h at RT and then a 10% solution of NH<sub>4</sub>Cl (10 cm<sup>3</sup>) was added. The reaction mixture was extracted into EtOAc (3 × 40 cm<sup>3</sup>) and the combined extracts were washed with brine and dried. After evaporation of the solvent under reduced pressure, the product was purified over silica gel (hexane/EtOAc 7:1) to give (**111**) as a colourless solid (148 mg, 43%).

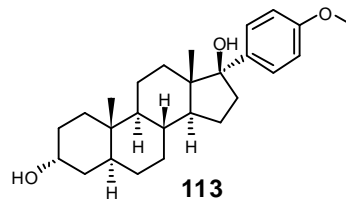
**Mp**: 173-174 °C (from CHCl<sub>3</sub>); **δ<sub>H</sub>** (500 MHz, CDCl<sub>3</sub>) 7.22 (2 H, d, *J*=8.0 Hz, Ar-*H*), 7.11 (2 H, d, *J*=8.0 Hz, Ar-*H*), 3.94-3.96 (1 H, m, C<sup>3</sup>*H*), 2.29-2.35 (1 H, ddd, *J*=5.2 Hz, *J*=9.8 Hz, *J*=14.4 Hz, C<sup>16</sup>*H<sub>A</sub>*), 2.33 (3 H, s, PhCH<sub>3</sub>), 2.03-2.09 (1 H, m, C<sup>16</sup>*H<sub>B</sub>*), 0.82-1.92 (20 H, m), 1.02 (3 H, s, C<sup>18</sup>*H<sub>3</sub>*), 0.74 (3 H, s, C<sup>19</sup>*H<sub>3</sub>*), 0.34-0.44 (2 H, m); **δ<sub>C</sub>** (75 MHz, CDCl<sub>3</sub>) 143.6 (*Ar*), 136.6 (*Ar*), 128.3 (2 × C, *Ar*), 127.6 (2 × C, *Ar*), 86.2 (C<sup>17</sup>), 66.8 (C<sup>3</sup>), 54.0 (C<sup>9</sup>), 49.5 (C<sup>14</sup>), 47.0 (C<sup>13</sup>), 39.4 (C<sup>5</sup>), 39.0 (C<sup>16</sup>), 36.6 (C<sup>8</sup>), 36.4 (C<sup>10</sup>), 36.2 (C<sup>4</sup>), 34.0 (C<sup>12</sup>), 32.4 (C<sup>1</sup>), 32.1 (C<sup>7</sup>), 29.3 (C<sup>2</sup>), 28.9 (C<sup>6</sup>), 24.8 (C<sup>15</sup>), 21.4 (C<sup>24</sup>), 20.7 (C<sup>11</sup>), 15.3 (C<sup>18</sup>), 11.6 (C<sup>19</sup>); ***m/z*** (+ES), found (M+Na<sup>+</sup>): 405.2766, C<sub>26</sub>H<sub>38</sub>O<sub>2</sub>Na requires 405.2770 (-0.8 ppm).

### 5.2.13 (3 $\alpha$ ,5 $\alpha$ )-(17-*p*-Toluene)androst-16-en-3-ol (**112**)



*p*-Toluenesulfonic acid monohydrate (10 mg, 0.05 mmol) was added at RT to a solution of (3 $\alpha$ ,5 $\alpha$ ,17 $\beta$ )-(17-*p*-toluene)androstane-3,17 $\beta$ -diol (**111**) (140 mg, 0.37 mmol) in dry DCM (20 cm<sup>3</sup>) and the reaction mixture was stirred at RT for 2 days. A 10% solution of NaHCO<sub>3</sub> (5 cm<sup>3</sup>) was then added, the organic phase was separated and the aqueous phase extracted into DCM (2  $\times$  20 cm<sup>3</sup>). The combined organic extracts were dried and the solvent was removed under reduced pressure. The residue was purified over silica gel (hexane/EtOAc 7:1) to give (**112**) as a colourless solid (95 mg, 71%).

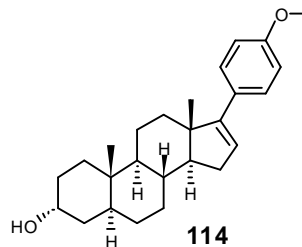
**Mp**: 182-185 °C (from CHCl<sub>3</sub>); [ $\alpha$ ]<sub>D</sub><sup>18</sup> +25.1 (c 1.5, CHCl<sub>3</sub>); (**Found**: C, 85.41; H, 10.38 %, C<sub>26</sub>H<sub>36</sub>O requires C, 85.66; H, 9.95 %);  $\nu_{\max}$  (KBr plate)/cm<sup>-1</sup> 3333 (br), 3048, 2924, 2846, 1508, 1443, 1368, 1357, 1001, 794;  $\delta_{\text{H}}$  (300 MHz, CDCl<sub>3</sub>) 7.26 (2 H, d,  $J$ =8.0 Hz), 7.10 (2 H, d,  $J$ =8.0 Hz), 5.84 (1 H, dd,  $J$ =1.8 Hz,  $J$ =3.2 Hz, C<sup>16</sup>H), 4.03-4.07 (1 H, m, C<sup>3</sup>H), 2.33 (3 H, s, PhCH<sub>3</sub>), 2.18 (1 H, ddd,  $J$ =3.3 Hz,  $J$ =6.3 Hz,  $J$ =15.4 Hz, C<sup>15</sup>H<sub>A</sub>), 1.92-2.07 (2 H, m), 0.77-1.77 (18 H, m), 1.00 (3 H, s, C<sup>18</sup>H<sub>3</sub>), 0.83 (3 H, s, C<sup>19</sup>H<sub>3</sub>);  $\delta_{\text{C}}$  (75 MHz, CDCl<sub>3</sub>) 154.7 (C<sup>17</sup>), 136.3 (Ar), 134.5 (Ar), 128.9 (2  $\times$  C, Ar), 126.6 (2  $\times$  C, Ar), 126.4 (C<sup>16</sup>), 66.6 (C<sup>3</sup>), 57.7 (C<sup>14</sup>), 54.7 (C<sup>9</sup>), 47.4 (C<sup>13</sup>), 39.4 (C<sup>5</sup>), 36.3 (C<sup>10</sup>), 35.9 (C<sup>4</sup>), 35.6 (C<sup>12</sup>), 34.1 (C<sup>8</sup>), 32.1 (C<sup>1</sup>), 31.9 (C<sup>7</sup>), 31.5 (C<sup>15</sup>), 29.1 (C<sup>2</sup>), 28.6 (C<sup>6</sup>), 21.1 (PhCH<sub>3</sub>), 20.8 (C<sup>11</sup>), 16.8 (C<sup>18</sup>), 11.2 (C<sup>19</sup>);  $m/z$  (+CI), found MH<sup>+</sup>: 365.2856, C<sub>26</sub>H<sub>37</sub>O requires 365.2844 (3.0 ppm).

**5.2.14 (3 $\alpha$ ,5 $\alpha$ ,17 $\beta$ )-17-(*p*-Methoxyphenyl)androsterane-3,17-diol (113)**


*n*-BuLi (2 cm<sup>3</sup>, 2.5 M in hexane, 5.0 mmol) was added at RT under N<sub>2</sub> to a solution of 4-bromoanisole (0.63 cm<sup>3</sup>, 5.0 mmol) in dry diethyl ether (5 cm<sup>3</sup>). The mixture was stirred for 2 h at RT and added dropwise *via* canula to a solution of androsterone (300 mg, 1.0 mmol) in dry THF (10 cm<sup>3</sup>). The reaction mixture was stirred at RT for 15 h. A 10% solution of NH<sub>4</sub>Cl (10 cm<sup>3</sup>) was added and the organic phase was extracted into Et<sub>2</sub>O (3 × 40 cm<sup>3</sup>). The combined organic extracts were dried and after evaporation of the solvent under reduced pressure, the product was purified over silica gel (hexane/EtOAc 5:1) to give (**113**) as a white foam (122 mg, 30%).

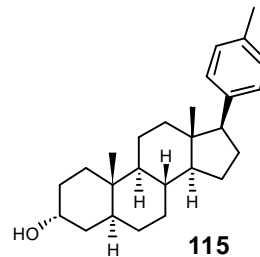
Note: (**113**) was not stable in solution and rapidly dehydrated to (**114**).

$\delta_{\text{H}}$  (300 MHz, CDCl<sub>3</sub>) 7.27 (2 H, *J*=9.0 Hz, Ar-*H*), 6.86 (2 H, d, *J*=9.0 Hz, Ar-*H*), 3.97-4.01 (1 H, m, C<sup>3</sup>*H*), 3.82 (3 H, s, OCH<sub>3</sub>), 2.33 (1 H, ddd, *J*=5.2 Hz, *J*=9.8 Hz, *J*=14.6 Hz, C<sup>16</sup>*H*<sub>A</sub>), 2.02-2.13 (1 H, m, C<sup>16</sup>*H*<sub>B</sub>), 0.81-1.83 (20 H, m), 1.03 (3 H, s, C<sup>18</sup>*H*<sub>3</sub>), 0.76 (3 H, s, C<sup>19</sup>*H*<sub>3</sub>); 0.34-0.52 (2 H, m);  $\delta_{\text{C}}$  (75 MHz, CDCl<sub>3</sub>) 158.7 (Ar), 138.5 (Ar), 128.8 (2 × C, Ar), 112.9 (2 × C, Ar), 86.1 (C<sup>17</sup>), 66.9 (CH), 55.6 (OCH<sub>3</sub>), 54.1 (CH), 49.5 (CH<sub>2</sub>), 47.1 (C<sup>13</sup>), 39.5 (CH), 39.1 (CH<sub>2</sub>), 36.6 (CH), 36.5 (C<sup>10</sup>), 36.2 (CH<sub>2</sub>), 34.0 (CH<sub>2</sub>), 32.4 (CH<sub>2</sub>), 32.1 (CH<sub>2</sub>), 29.4 (CH<sub>2</sub>), 28.9 (CH<sub>2</sub>), 24.7 (CH<sub>2</sub>), 20.7 (CH<sub>2</sub>), 15.3 (CH<sub>3</sub>), 11.6 (CH<sub>3</sub>); *m/z* (+ES), found (M+Na<sup>+</sup>): 421.2730, C<sub>26</sub>H<sub>38</sub>O<sub>3</sub>Na requires 421.2719 (+2.7 ppm).

5.2.15 (3 $\alpha$ ,5 $\alpha$ )-17-(*p*-Methoxyphenyl)androst-16-en-3-ol (**114**)

*p*-Toluenesulfonic acid monohydrate (2 mg) was added at RT to a solution of (3 $\alpha$ ,5 $\alpha$ ,17 $\beta$ )-17-(*p*-methoxyphenyl)androstane-3,17-diol (**113**) (55 mg, 0.14 mmol) in dry DCM (5 cm<sup>3</sup>). The reaction mixture turned pink very rapidly. After 8 h the colour had disappeared and DCM was removed under reduced pressure. The residue was purified over silica gel (petroleum ether/diethyl ether 3:1) to give (**114**) as a colourless solid (47 mg, 90%).

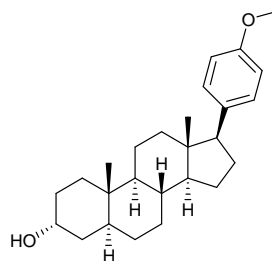
**Mp**: 171-176 °C (from CHCl<sub>3</sub>); [ $\alpha$ ]<sub>D</sub><sup>20</sup> +27.4 (c 1.5, CHCl<sub>3</sub>); (**Found**: C, 81.50; H, 9.85 %, C<sub>26</sub>H<sub>36</sub>O<sub>2</sub> requires C, 82.06; H, 9.53 %);  $\nu_{\max}$  (KBr plate)/cm<sup>-1</sup> 3322 (br), 2924, 2846, 1600, 1508, 1443, 1362, 1253, 1242, 1175, 1108, 1035;  $\delta_{\text{H}}$  (300 MHz, CDCl<sub>3</sub>) 7.30 (2 H, d, *J*=8.8 Hz, Ar-*H*), 6.83 (2 H, d, *J*=8.8 Hz, Ar-*H*), 5.79 (1 H, dd, *J*=1.7 Hz, *J*=3.1 Hz, C<sup>16</sup>*H*), 4.02-4.06 (1 H, m, C<sup>3</sup>*H*), 3.80 (3 H, s, OCH<sub>3</sub>), 2.18 (1 H, ddd, *J*=3.2 Hz, *J*=6.2 Hz, *J*=15.3 Hz, C<sup>15</sup>*H*<sub>A</sub>), 1.91-2.06 (2 H, m), 0.77-1.76 (18 H, m), 0.99 (3 H, s, C<sup>18</sup>*H*<sub>3</sub>), 0.83 (3 H, s, C<sup>19</sup>*H*<sub>3</sub>);  $\delta_{\text{C}}$  (75 MHz, CDCl<sub>3</sub>) 158.9 (*Ar*), 154.7 (C<sup>17</sup>), 130.5 (*Ar*), 128.2 (2  $\times$  C, *Ar*), 126.0 (C<sup>16</sup>), 113.9 (2  $\times$  C, *Ar*), 67.0 (CH), 58.0 (CH), 55.7 (OCH<sub>3</sub>), 55.1 (CH), 47.8 (C<sup>13</sup>), 39.8 (CH), 36.7 (C<sup>10</sup>), 36.3 (CH<sub>2</sub>), 36.0 (CH<sub>2</sub>), 34.5 (CH), 32.5 (CH<sub>2</sub>), 32.3 (CH<sub>2</sub>), 31.8 (CH<sub>2</sub>), 29.4 (CH<sub>2</sub>), 29.0 (CH<sub>2</sub>), 21.2 (CH<sub>2</sub>), 17.1 (CH<sub>3</sub>), 11.6 (CH<sub>3</sub>); *m/z* (+CI), found MH<sup>+</sup>: 381.2796, C<sub>26</sub>H<sub>37</sub>O<sub>2</sub> requires 381.2794 (+0.6 ppm).

5.2.16 (3 $\alpha$ ,5 $\alpha$ )-(17 $\beta$ -*p*-Toluene)androstan-3-ol (**115**)

Pd/C 5 % (5 mg) was added to a solution of (3 $\alpha$ ,5 $\alpha$ )-(17-*p*-toluene)androst-16-en-3-ol (**112**) (12 mg, 0.03 mmol) in EtOAc (5 cm<sup>3</sup>). The mixture was stirred at RT under a positive atmosphere of H<sub>2</sub>. After 12 h, the reaction mixture was filtered over Celite and the solvent was removed under reduced pressure. The product was purified over silica gel (hexane/EtOAc 6:1) to give (**115**) as a colourless solid (11 mg, 91 %).

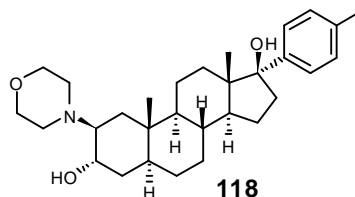
**Mp**: 230-234 °C (from hexane/EtOAc);  $[\alpha]_D^{20}$  +7.4 (c 0.65, CHCl<sub>3</sub>); (**Found**: C, 84.97; H, 10.82 %, C<sub>26</sub>H<sub>38</sub>O requires C, 85.19; H, 10.45 %);  $\nu_{\max}$  (KBr plate)/cm<sup>-1</sup> 3289 (br), 2931, 2869, 2842, 1514, 1446, 1262, 1098, 1035, 1002, 807;  $\delta_H$  (300 MHz, CDCl<sub>3</sub>) 7.00-7.05 (4 H, dd, Ar-*H*), 4.03-4.06 (1 H, m, C<sup>3</sup>*H*), 2.63 (1 H, t, *J*=9.9 Hz, C<sup>17</sup>*H*), 2.32 (3 H, s, PhCH<sub>3</sub>), 2.01-2.09 (1 H, m, C<sup>16</sup>*H*<sub>A</sub>), 1.88-1.96 (1 H, m, C<sup>16</sup>*H*<sub>B</sub>), 0.74-1.80 (21 H, m), 0.77 (3 H, s, C<sup>19</sup>*H*<sub>3</sub>), 0.45 (3 H, s, C<sup>18</sup>*H*<sub>3</sub>);  $\delta_C$  (75 MHz, CDCl<sub>3</sub>) 138.6 (*Ar*), 135.7 (*Ar*), 129.0 (2 × C, *Ar*), 128.8 (2 × C, *Ar*), 67.0 (CH), 57.1 (C<sup>17</sup>), 56.7 (CH), 55.0 (CH), 44.6 (C<sup>13</sup>), 39.7 (CH), 38.2 (CH<sub>2</sub>), 36.6 (C<sup>10</sup>), 36.4 (CH), 36.3 (CH<sub>2</sub>), 32.6 (CH<sub>2</sub>), 32.5 (CH<sub>2</sub>), 29.4 (CH<sub>2</sub>), 29.0 (CH<sub>2</sub>), 26.6 (CH<sub>2</sub>), 24.8 (CH<sub>2</sub>), 21.4 (PhCH<sub>3</sub>), 20.9 (CH<sub>2</sub>), 13.2 (CH<sub>3</sub>), 11.7 (CH<sub>3</sub>); *m/z* (+CI), found MH<sup>+</sup>: 367.2992, C<sub>26</sub>H<sub>39</sub>O requires 367.3001 (-2.4 ppm).

### 5.2.17 (3 $\alpha$ ,5 $\alpha$ )-(17 $\beta$ -*p*-Methoxyphenyl)androstan-3-ol (**116**)



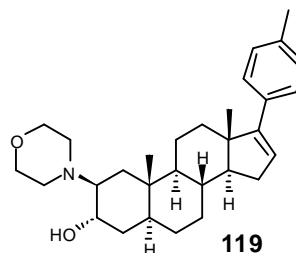
Pd/C 5 % (5 mg) was added to a solution of (3 $\alpha$ ,5 $\alpha$ )-(17-*p*-methoxyphenyl)androst-16-en-3-ol (**114**) (50 mg, 0.13 mmol) in EtOAc (10 cm<sup>3</sup>). The mixture was stirred at RT under a positive atmosphere of H<sub>2</sub>. After 12 h, the reaction mixture was filtered over Celite and the solvent was removed under reduced pressure. The product was purified over silica gel (petroleum ether/diethyl ether 2:1) to give (**116**) as a colourless solid (47 mg, 93 %).

**Mp:** 224-231 °C (from CHCl<sub>3</sub>); [ $\alpha$ ]<sub>D</sub><sup>20</sup> +8.0 (c 0.8, CHCl<sub>3</sub>); (**Found:** C, 81.76; H, 10.29 %, C<sub>26</sub>H<sub>38</sub>O<sub>2</sub> requires C, 81.63; H, 10.01 %);  $\nu_{\max}$  (KBr plate)/cm<sup>-1</sup> 3522 (br), 3457 (br), 2930, 2914, 1609, 1512, 1463, 1249, 1238, 1028;  $\delta_{\text{H}}$  (300 MHz, CDCl<sub>3</sub>) 7.12 (2 H, d,  $J$ =8.6 Hz, Ar-*H*), 6.82 (2 H, d,  $J$ =8.6 Hz, Ar-*H*), 4.02-4.06 (1 H, m, C<sup>3</sup>*H*), 3.79 (3 H, s, OCH<sub>3</sub>), 2.61 (1 H, t,  $J$ =9.8 Hz, C<sup>17</sup>*H*), 1.87-2.08 (2 H, m), 0.80-1.81 (21 H, m), 0.77 (3 H, s, C<sup>19</sup>*H*<sub>3</sub>), 0.44 (3 H, s, C<sup>18</sup>*H*<sub>3</sub>);  $\delta_{\text{C}}$  (75 MHz, CDCl<sub>3</sub>) 158.2 (*Ar*), 133.7 (*Ar*), 129.9 (2  $\times$  C, *Ar*), 113.4 (2  $\times$  C, *Ar*), 67.0 (C<sup>3</sup>), 56.6 (C<sup>14</sup>+C<sup>17</sup>), 55.6 (OCH<sub>3</sub>), 55.0 (C<sup>9</sup>), 44.5 (C<sup>13</sup>), 39.7 (C<sup>5</sup>), 38.2 (C<sup>12</sup>), 36.6 (C<sup>10</sup>), 36.4 (C<sup>8</sup>), 36.3 (C<sup>4</sup>), 32.6 (C<sup>1</sup>), 32.5 (C<sup>7</sup>), 29.4 (C<sup>2</sup>), 29.0 (C<sup>6</sup>), 26.8 (C<sup>16</sup>), 24.8 (C<sup>15</sup>), 20.9 (C<sup>11</sup>), 13.2 (C<sup>18</sup>), 11.7 (C<sup>19</sup>);  $m/z$  (+CI), found MH<sup>+</sup>: 383.2952, C<sub>26</sub>H<sub>39</sub>O<sub>2</sub> requires 383.2950 (+0.5 ppm).

5.2.18 2 $\beta$ -(4-Morpholinyl)-(3 $\alpha$ ,5 $\alpha$ ,17 $\beta$ )-(17-*p*-toluene)androstane-3,17-diol (**118**)

*p*-Bromotoluene (581 mg, 3.4 mmol) was added at RT under N<sub>2</sub> to a solution of *n*-BuLi (1.3 cm<sup>3</sup>, 2.5 M in hexane, 3.3 mmol) in dry diethyl ether (4 cm<sup>3</sup>). The mixture was stirred for 1.5 h at RT and was added dropwise *via* canula to a solution of 3 $\alpha$ -hydroxy-2 $\beta$ -(4-morpholinyl)-5 $\alpha$ -androstane-17-one (**117**) (257 mg, 0.7 mmol) in dry THF (15 cm<sup>3</sup>). The reaction mixture was stirred for 15 h at RT and then a 10% solution of NH<sub>4</sub>Cl (15 cm<sup>3</sup>) was added. The reaction mixture was extracted into EtOAc (3  $\times$  50 cm<sup>3</sup>) and the combined organic extracts were washed with brine and dried. After evaporation of the solvent under reduced pressure, the product was purified over silica gel (hexane/EtOAc 5:1) to give (**118**) as a colourless amorphous solid (160 mg, 50%).

**Mp**: 132-135 °C (from hexane/EtOAc); [ $\alpha$ ]<sub>D</sub><sup>16</sup> +46.2 (c 1.5, CHCl<sub>3</sub>); **v**<sub>max</sub> (KBr plate)/cm<sup>-1</sup> 3440 (br), 2924, 2852, 1511, 1449, 1382, 1292, 1262, 1116, 1069, 1015, 814;  $\delta$ <sub>H</sub> (300 MHz, CDCl<sub>3</sub>) 7.23 (2 H, d, *J*=8.1 Hz, Ar-*H*), 7.12 (2 H, d, *J*=8.1 Hz, Ar-*H*), 3.78 (1 H, ddd, *J*=5.5 Hz, *J*=8.1 Hz, *J*=9.9 Hz, C<sup>3</sup>*H*), 3.58-5.71 (4 H, m, 2  $\times$  CH<sub>2</sub>O), 2.43-2.57 (3 H, m), 2.28-2.38 (3 H, m), 2.34 (3 H, s, PhCH<sub>3</sub>), 2.02-2.13 (2 H, m), 1.65-1.83 (3 H, m), 0.73-1.56 (14 H, m), 1.03 (3 H, s, C<sup>18</sup>H<sub>3</sub>), 0.82 (3 H, s, C<sup>19</sup>H<sub>3</sub>), 0.35-0.45 (2 H, m);  $\delta$ <sub>C</sub> (75 MHz, CDCl<sub>3</sub>) 143.7 (Ar), 136.5 (Ar), 128.3 (2 $\times$ C, Ar), 127.7 (2 $\times$ C, Ar), 86.0 (C<sup>17</sup>), 67.8 (2 $\times$ CH<sub>2</sub>O), 65.3 (C<sup>2</sup>), 64.0 (C<sup>3</sup>), 55.7 (CH), 49.3 (CH), 49.2 (2 $\times$ CH<sub>2</sub>N), 47.1 (CH<sub>2</sub>), 38.9 (CH<sub>2</sub>), 38.8 (CH), 36.5 (CH), 36.1 (C<sup>10</sup>), 34.7 (CH<sub>2</sub>), 34.1 (CH<sub>2</sub>), 32.7 (CH<sub>2</sub>), 31.7 (CH<sub>2</sub>), 28.6 (CH<sub>2</sub>), 24.7 (CH<sub>2</sub>), 21.4 (PhCH<sub>3</sub>), 21.2 (CH<sub>2</sub>), 17.2 (C<sup>19</sup>), 15.4 (C<sup>18</sup>); **m/z** (+ES), found MH<sup>+</sup>: 468.3473, C<sub>30</sub>H<sub>46</sub>NO<sub>3</sub> requires 468.3478 (-1.0 ppm).

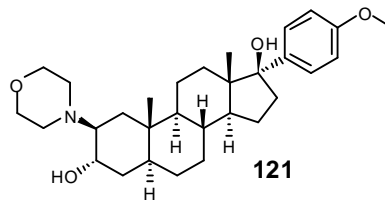
**5.2.19 2 $\beta$ -(4-Morpholinyl)-(3 $\alpha$ ,5 $\alpha$ )-(17-*p*-toluene)androst-16-en-3-ol (119)**

Chlorotrimethylsilane (0.10 cm<sup>3</sup>, 0.8 mmol, 5 eq) was added at RT to a solution of 2 $\beta$ -(4-morpholinyl)-(3 $\alpha$ ,5 $\alpha$ ,17 $\beta$ )-(17-*p*-toluene)androstane-3,17-diol (**118**) (78 mg, 0.16 mmol) in dry acetonitrile (15 cm<sup>3</sup>) and the mixture was stirred at 50 °C for 3 days. After cooling, a 10% solution of K<sub>2</sub>CO<sub>3</sub> (10 cm<sup>3</sup>) was added and the mixture was stirred for a further 5 h at RT. EtOAc (30 cm<sup>3</sup>) was added and the organic phase was separated. The aqueous phase was extracted into EtOAc (2  $\times$  30 cm<sup>3</sup>) and the combined organic extracts were washed with water and dried. After evaporation of the solvent under reduced pressure, the residue was purified over silica gel (hexane/EtOAc 6:1) to give (**119**) as a colourless amorphous solid (34 mg, 45%).

$\delta_{\text{H}}$  (300 MHz, CDCl<sub>3</sub>) 7.26 (2 H, d,  $J$ =8.1 Hz), 7.11 (2 H, d,  $J$ =7.9 Hz), 5.84 (1 H, dd,  $J$ =1.7 Hz,  $J$ =3.1 Hz, C<sup>16</sup>H), 3.89 (1 H, ddd,  $J$ =5.7 Hz,  $J$ =8.0 Hz,  $J$ =9.8 Hz, C<sup>3</sup>H), 3.65-3.78 (4 H, m, 2  $\times$  CH<sub>2</sub>O), 2.59-2.70 (3 H, m), 2.44-2.51 (2 H, m), 2.33 (3 H, s, PhCH<sub>3</sub>), 2.13-2.22 (1 H, m, C<sup>15</sup>H<sub>A</sub>), 0.81-2.07 (18 H, m), 1.00 (3 H, s, C<sup>18</sup>H<sub>3</sub>), 0.91 (3 H, s, C<sup>19</sup>H<sub>3</sub>);  $\delta_{\text{C}}$  (75 MHz, CDCl<sub>3</sub>) 155.0 (C<sup>17</sup>), 136.8 (Ar), 134.8 (Ar), 129.2 (2  $\times$  C, Ar), 127.0 (2  $\times$  C, Ar), 126.8 (C<sup>16</sup>), 67.8 (2  $\times$  CH<sub>2</sub>O), 65.5 (C<sup>2</sup>), 64.1 (C<sup>3</sup>), 57.8 (CH), 56.7 (CH), 49.3 (2  $\times$  CH<sub>2</sub>N), 47.8 (C<sup>13</sup>), 39.1 (CH), 36.4 (C<sup>10</sup>), 36.0 (CH<sub>2</sub>), 34.9 (CH<sub>2</sub>), 34.4 (CH), 32.9 (CH<sub>2</sub>), 31.9 (CH<sub>2</sub>), 31.8 (CH<sub>2</sub>), 28.7 (CH<sub>2</sub>), 21.6 (CH<sub>2</sub>), 21.5 (PhCH<sub>3</sub>), 17.3 (CH<sub>3</sub>), 17.2 (CH<sub>3</sub>);  $m/z$  (+CI), found MH<sup>+</sup>: 450.3387, C<sub>30</sub>H<sub>44</sub>NO<sub>2</sub> requires 450.3372 (+3.2 ppm).



**5.2.20 2 $\beta$ -(4-Morpholinyl)-(3 $\alpha$ ,5 $\alpha$ ,17 $\beta$ )-17-(*p*-methoxyphenyl)androstane-3,17-diol (**121**)**

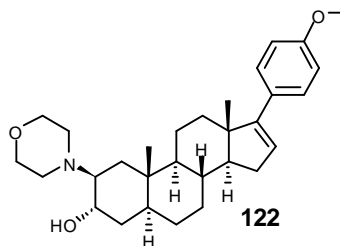


*p*-Bromoanisole (1.05 cm<sup>3</sup>, 8.4 mmol) was added at RT under N<sub>2</sub> to a solution of *n*-BuLi (3.2 cm<sup>3</sup>, 2.5 M in hexane, 8 mmol) in dry diethyl ether (5 cm<sup>3</sup>). The mixture was stirred for 2 h at RT and was then added dropwise *via* canula to a solution of 3 $\alpha$ -hydroxy-2 $\beta$ -(4-morpholinyl)-5 $\alpha$ -androstane-17-one (**117**) (380 mg, 1.0 mmol) in dry THF (40 cm<sup>3</sup>). The reaction mixture was stirred for 18 h at RT and then a 10% solution of NH<sub>4</sub>Cl (12 cm<sup>3</sup>) was added. The reaction mixture was extracted into EtOAc (3  $\times$  60 cm<sup>3</sup>) and the combined organic extracts were washed with brine and dried. After evaporation of the solvent under reduced pressure, the product was purified over silica gel (hexane/EtOAc 3:1) to give (**121**) as a colourless amorphous solid (180 mg, 37%).

**Mp:** 145-148 °C (from hexane/EtOAc); [ $\alpha$ ]<sub>D</sub><sup>16</sup> +38.2 (c 1.5, CHCl<sub>3</sub>); (**Found:** C, 74.39; H, 9.53; N, 2.89 %, C<sub>30</sub>H<sub>45</sub>NO<sub>4</sub> requires C, 74.50; H, 9.38; N, 2.90 %); **v**<sub>max</sub> (KBr plate)/cm<sup>-1</sup> 3434 (br), 2924, 2852, 1608, 1510, 1452, 1248, 1178, 1116, 1018, 825, 752;  **$\delta$ <sub>H</sub>** (300 MHz, CDCl<sub>3</sub>) 7.25 (2 H, d, *J*=8.7 Hz), 6.84 (2 H, d, *J*=8.9 Hz), 3.74-3.82 (1 H, m, C<sup>3</sup>H), 3.80 (3 H, s, OCH<sub>3</sub>), 3.55-3.71 (4 H, m, 2  $\times$  CH<sub>2</sub>O), 2.43-2.58 (3 H, m), 2.25-2.39 (3 H, m), 2.02-2.12 (2 H, m), 1.64-1.81 (3 H, m), 0.72-1.55 (14 H, m), 1.02 (3 H, s, C<sup>18</sup>H<sub>3</sub>), 0.82 (3 H, s, C<sup>19</sup>H<sub>3</sub>), 0.35-0.45 (2 H, m);  **$\delta$ <sub>C</sub>** (75 MHz, CDCl<sub>3</sub>) 158.3 (*Ar*), 138.3 (*Ar*), 128.5 (2  $\times$  C, *Ar*), 112.5 (2  $\times$  C, *Ar*), 85.5 (C<sup>17</sup>), 67.3 (2  $\times$  CH<sub>2</sub>O), 64.9 (C<sup>2</sup>), 63.7 (C<sup>3</sup>), 55.3 (CH), 55.2 (OCH<sub>3</sub>), 49.0 (CH), 48.8 (2  $\times$  CH<sub>2</sub>N), 46.7 (C<sup>13</sup>), 38.5 (CH<sub>2</sub>), 38.5 (CH), 36.1 (CH), 35.7 (C<sup>10</sup>), 34.3 (CH<sub>2</sub>), 33.6 (CH<sub>2</sub>), 32.4 (CH<sub>2</sub>), 31.3 (CH<sub>2</sub>), 28.2 (CH<sub>2</sub>), 24.3 (CH<sub>2</sub>), 20.9 (CH<sub>2</sub>), 16.9 (C<sup>19</sup>), 15.0 (C<sup>18</sup>); ***m/z*** (+CI), found MH<sup>+</sup>: 484.3445, C<sub>30</sub>H<sub>46</sub>NO<sub>4</sub> requires 484.3427 (+3.7 ppm).

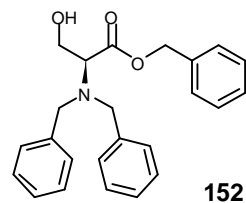
5.2.21 2 $\beta$ -(4-Morpholinyl)-(3 $\alpha$ ,5 $\alpha$ )-17-(*p*-methoxyphenyl)androst-16-en-3-ol

(122)



Chlorotrimethylsilane (64  $\mu$ L, 0.5 mmol, 5 eq) was added at RT to a solution of 2 $\beta$ -(4-morpholinyl)-(3 $\alpha$ ,5 $\alpha$ ,17 $\beta$ )-17-(*p*-methoxyphenyl)androstane-3,17-diol (121) (50 mg, 0.1 mmol) in dry DCM (15 cm<sup>3</sup>) and the mixture was stirred at RT for 24 h. A 10 % solution of K<sub>2</sub>CO<sub>3</sub> (10 cm<sup>3</sup>) was added and the mixture was stirred for 6 h at RT. The organic phase was separated and the aqueous phase was extracted into EtOAc (2  $\times$  30 cm<sup>3</sup>). The combined organic extracts were washed with water and dried. After evaporation of the solvent under reduced pressure, the residue was purified over silica gel (hexane/EtOAc 4:1) to give (122) as a colourless amorphous solid (30 mg, 62%).

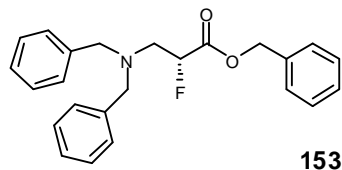
**Mp:** 193-196 °C (from DCM);  $[\alpha]_D^{17} +71.7$  (c 1.5, CHCl<sub>3</sub>);  $\nu_{\max}$  (KBr plate)/cm<sup>-1</sup> 3457 (br), 2920, 1608, 1597, 1507, 1445, 1303, 1256, 1240, 1116, 1033, 807;  $\delta_H$  (300 MHz, CDCl<sub>3</sub>) 7.30 (2 H, d,  $J=8.9$  Hz, Ar-*H*), 6.84 (2 H, d,  $J=8.9$  Hz, Ar-*H*), 5.79 (1 H, dd,  $J=1.7$  Hz,  $J=3.1$  Hz, C<sup>16</sup>*H*), 3.85-3.93 (1 H, m, C<sup>3</sup>*H*), 3.80 (3 H, s, OCH<sub>3</sub>), 3.65-3.79 (4 H, m, 2  $\times$  CH<sub>2</sub>O), 2.58-2.69 (3 H, m), 2.43-2.50 (2 H, m), 2.17 (1 H, ddd,  $J=3.3$  Hz,  $J=5.9$  Hz,  $J=15.4$  Hz, C<sup>15</sup>*H*<sub>A</sub>), 0.79-2.06 (18 H, m), 1.00 (3 H, s, C<sup>18</sup>*H*<sub>3</sub>), 0.91 (3 H, s, C<sup>19</sup>*H*<sub>3</sub>);  $\delta_C$  (75 MHz, CDCl<sub>3</sub>) 158.9 (*Ar*), 154.7 (C<sup>17</sup>), 130.3 (*Ar*), 128.2 (2  $\times$  C, *Ar*), 126.0 (C<sup>16</sup>), 113.9 (2  $\times$  C, *Ar*), 67.8 (2  $\times$  CH<sub>2</sub>O), 65.5 (C<sup>2</sup>), 64.1 (C<sup>3</sup>), 57.8 (CH), 56.7 (CH), 55.6 (OCH<sub>3</sub>), 49.3 (2  $\times$  CH<sub>2</sub>N), 47.8 (C<sup>13</sup>), 39.1 (CH), 36.4 (C<sup>10</sup>), 36.1 (CH<sub>2</sub>), 34.9 (CH<sub>2</sub>), 34.4 (CH), 32.9 (CH<sub>2</sub>), 31.9 (CH<sub>2</sub>), 31.8 (CH<sub>2</sub>), 28.7 (CH<sub>2</sub>), 21.7 (CH<sub>2</sub>), 17.3 (C<sup>19</sup>), 17.1 (C<sup>18</sup>); ***m/z*** (+ES), found MH<sup>+</sup>: 466.3313, C<sub>30</sub>H<sub>44</sub>NO<sub>3</sub> requires 466.3321 (-1.8 ppm).

5.2.22 (2*S*)-(Dibenzylamino)-3-hydroxypropionic acid benzyl ester (**152**)<sup>2,3</sup>

A solution of L-serine (10.5 g, 100 mmol), K<sub>2</sub>CO<sub>3</sub> (27.6 g, 200 mmol) and NaOH (8 g, 200 mmol) in H<sub>2</sub>O (200 cm<sup>3</sup>) was heated under reflux and then treated with BnBr (38 cm<sup>3</sup>, 320 mmol). After 1 h, the mixture was cooled to RT and extracted into Et<sub>2</sub>O (3 × 300 cm<sup>3</sup>). The combined organic extracts were dried and evaporated under reduced pressure. The product was purified over silica gel (hexane/EtOAc 6:1) to yield benzyl ester (**152**) as a colourless oil (19.3 g, 51%).

[ $\alpha$ ]<sub>D</sub><sup>20</sup> -125.1 (c 1.34 CHCl<sub>3</sub>), lit<sup>3</sup> [ $\alpha$ ]<sub>D</sub><sup>24</sup> -120.1 (c 1.34, CHCl<sub>3</sub>);  $\nu_{\max}(\text{film})/\text{cm}^{-1}$  3448 (br), 3063, 3030, 1730, 1602, 1495, 1455, 1174, 1028, 748, 698;  $\delta_{\text{H}}$  (300 MHz, CDCl<sub>3</sub>) 7.22-7.43 (15 H, m, Ar-*H*), 5.28 (1 H, d, *J*=12.2 Hz, PhCH<sub>A</sub>H<sub>B</sub>O), 5.20 (1 H, d, *J*=12.2 Hz, PhCH<sub>A</sub>H<sub>B</sub>O), 3.89 (2 H, d, *J*=13.4 Hz, 2 × PhCH<sub>A</sub>H<sub>B</sub>N), 3.77 (1 H, br d, *J*=7.9 Hz, CH<sub>2</sub>OH), 3.63 (2 H, d, *J*=13.4 Hz, 2 × PhCH<sub>A</sub>H<sub>B</sub>N), 3.59 (2 H, t, *J*=7.5 Hz, CHN), 2.50 (1 H, br s, OH);  $\delta_{\text{C}}$  (75 MHz, CDCl<sub>3</sub>) 171.6 (CO<sub>2</sub>), 139.0 (2 × C, *Ar*), 136.1 (*Ar*), 129.4 (4 × C, *Ar*), 129.1 (2 × C, *Ar*), 129.0 (5 × C, *Ar*), 128.9 (2 × C, *Ar*), 127.9 (2 × C, *Ar*), 66.9 (PhCH<sub>2</sub>O), 62.2 (CHN), 59.7 (CH<sub>2</sub>OH), 55.2 (2 × PhCH<sub>2</sub>N).

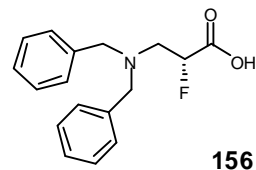
These data are in accordance with the literature.<sup>2,3</sup>

5.2.23 (2*R*)-3-(Dibenzylamino)-2-fluoropropanoic acid benzyl ester (**153**)<sup>2</sup>

DAST (2.36 cm<sup>3</sup>, 18 mmol) was added dropwise at 0 °C to a solution of (2*S*)-(dibenzylamino)-3-hydroxypropionic acid benzyl ester (**152**) (5.63 g, 15 mmol) in dry THF (30 cm<sup>3</sup>). The reaction mixture was stirred for 40 min, poured into cold water (30 cm<sup>3</sup>), neutralized by the addition of solid K<sub>2</sub>CO<sub>3</sub> and extracted into Et<sub>2</sub>O (2 × 50 cm<sup>3</sup>). The combined organic fractions were dried over MgSO<sub>4</sub> and evaporated under reduced pressure. The crude product was purified over silica gel (hexane/EtOAc 16:1) to yield (**153**) as a colourless oil (4.77 g, 85%).

[ $\alpha$ ]<sub>D</sub><sup>20</sup> +2.3 (c 1.0, CHCl<sub>3</sub>), lit<sup>2</sup> [ $\alpha$ ]<sub>D</sub><sup>RT</sup> +2.7 (c 1.0, CHCl<sub>3</sub>);  $\nu_{\max}$ (film)/cm<sup>-1</sup> 3063, 3030, 2807, 2385, 1763, 1495, 1455, 1276, 1197, 1067, 748, 698;  $\delta_{\text{H}}$  (300 MHz, CDCl<sub>3</sub>) 7.19-7.36 (15 H, m, Ar-*H*), 5.22 (1 H, d, *J*=12.2 Hz, PhCH<sub>A</sub>H<sub>B</sub>O), 5.09 (1 H, ddd, *J*=3.3 Hz, *J*=5.7 Hz, *J*=49.5 Hz, CHF), 5.05 (1 H, d, *J*=12.3 Hz, PhCH<sub>A</sub>H<sub>B</sub>O), 3.81 (2 H, d, *J*=13.7 Hz, 2 × PhCH<sub>A</sub>H<sub>B</sub>N), 3.54 (2 H, d, *J*=13.7 Hz, 2 × PhCH<sub>A</sub>H<sub>B</sub>N), 2.95-3.15 (2 H, m, CH<sub>2</sub>N);  $\delta_{\text{C}}$  (75 MHz, CDCl<sub>3</sub>) 169.1 (d, *J*=24.5 Hz, CO<sub>2</sub>), 139.1 (2 × C, Ar), 135.4 (Ar), 129.4 (4 × C, Ar), 129.0 (2 × C, Ar), 128.9 (Ar), 128.8 (2 × C, Ar), 128.7 (4 × C, Ar), 127.5 (2 × C, Ar), 89.6 (d, *J*=186.6 Hz, CHF), 67.4 (PhCH<sub>2</sub>O), 59.1 (2 × C, PhCH<sub>2</sub>N), 54.7 (d, *J*=20.1 Hz, CH<sub>2</sub>N);  $\delta_{\text{F}}$  (282 MHz, CDCl<sub>3</sub>) -190.6 (dt, *J*=25.8 Hz, *J*=50.6 Hz); *m/z* (+CI), found MH<sup>+</sup>: 378.1880, C<sub>24</sub>H<sub>25</sub>NO<sub>2</sub>F requires 378.1869 (+2.8 ppm).

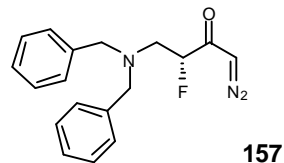
These data are in accordance with the literature.<sup>2</sup>

5.2.24 (2*R*)-3-(Dibenzylamino)-2-fluoropropanoic (156)<sup>4</sup>

0.5 N LiOH (12 cm<sup>3</sup>, 6 mmol) was added at 0 °C to a solution of (2*R*)-3-(dibenzylamino)-2-fluoropropanoic acid benzyl ester (**153**) (2.0 g, 5.3 mmol) in THF (30 cm<sup>3</sup>). The mixture was stirred at RT for 18 h and concentrated under reduced pressure to remove THF. The residue was acidified with acetic acid (10 cm<sup>3</sup>) and extracted into EtOAc (2 × 50 cm<sup>3</sup>). The combined organic extracts were washed with brine, dried and evaporated under reduced pressure. The product was purified over silica gel (hexane/EtOAc 1:1) to yield (**156**) as a viscous colourless oil (1.13 g, 74%).

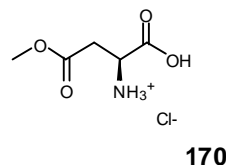
$[\alpha]_D^{20}$  -0.8 (c 2.43 CHCl<sub>3</sub>);  $\nu_{\max}(\text{film})/\text{cm}^{-1}$  3065, 2806, 2360, 2342, 1743 (br), 1618 (br), 1495, 1456, 1270, 1090, 738, 700;  $\delta_{\text{H}}$  (300 MHz, CDCl<sub>3</sub>) 9.49 (1 H, br s, CO<sub>2</sub>H), 7.28-7.40 (10 H, m, Ar-H), 4.98 (1 H, dt,  $J=5.6$  Hz,  $J=48.8$  Hz, CHF), 4.00 (2 H, d,  $J=13.5$  Hz, 2 × PhCH<sub>A</sub>H<sub>B</sub>N), 3.90 (2 H, d,  $J=13.5$  Hz, 2 × PhCH<sub>A</sub>H<sub>B</sub>N), 3.16-3.26 (2 H, m, CH<sub>2</sub>N);  $\delta_{\text{C}}$  (75 MHz, CDCl<sub>3</sub>) 171.4 (d,  $J=21.7$  Hz, CO<sub>2</sub>), 134.2 (2 × C, Ar), 130.4 (4 × C, Ar), 129.3 (4 × C, Ar), 129.0 (2 × C, Ar), 86.5 (d,  $J=186.0$  Hz, CHF), 58.6 (2 × C, PhCH<sub>2</sub>N), 53.7 (d,  $J=23.1$  Hz, CH<sub>2</sub>N);  $\delta_{\text{F}}$  (282 MHz, CDCl<sub>3</sub>) -188.5 (dt,  $J=20.3$  Hz,  $J=48.7$  Hz);  $m/z$  (+EI), found MH<sup>+</sup>: 288.1399, C<sub>17</sub>H<sub>19</sub>NO<sub>2</sub>F requires 288.1400 (-0.3 ppm).

These data are in accordance with the literature.<sup>4</sup>

5.2.25 (3*R*)-1-Diazo-4-(dibenzylamino)-3-fluorobutan-2-one (**157**)

Freshly distilled  $\text{SOCl}_2$  ( $0.29 \text{ cm}^3$ , 3.6 mmol, 6 eq) was added at RT to a solution of (2*R*)-3-(dibenzylamino)-2-fluoropropanoic (**156**) (189 mg, 0.6 mmol) in dry DCM ( $6 \text{ cm}^3$ ). The solution was heated under reflux for 2 h and the solvent was evaporated under reduced pressure. The residue was dissolved in dry THF and evaporated again under reduced pressure to remove excess of  $\text{SOCl}_2$ . The resultant white foam was dissolved in dry THF ( $5 \text{ cm}^3$ ) and added dropwise at  $0^\circ\text{C}$  under  $\text{N}_2$  to a stirred solution of diazomethane, prepared from Diazald® (11 mmol).<sup>5, 6</sup> The yellow reaction mixture was stirred for 14 h at RT under  $\text{N}_2$ . Evaporation of the solvent under reduced pressure gave a yellow paste which contained the diazo-ketone (**157**) and the methyl ester (**161**) in a 70/30 % mixture as determined by NMR analysis.

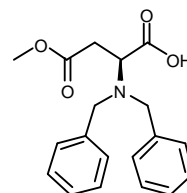
$\nu_{\text{max}}(\text{KBr plate})/\text{cm}^{-1}$  2112 (N=N), 1641 (C=O);  $\delta_{\text{H}}$  (300 MHz,  $\text{CDCl}_3$ ) 7.13-7.30 (10 H, m, Ar-*H*), 5.55 (1 H, d,  $J=3.0 \text{ Hz}$ ,  $\text{CHN}_2$ ), 4.81-5.05 (1 H, dm,  $J=50.1 \text{ Hz}$ ,  $\text{CHF}$ ), 3.69 (2 H, d,  $J=13.9 \text{ Hz}$ ,  $2 \times \text{PhCH}_A\text{H}_B\text{N}$ ), 3.56 (2 H, d,  $J=13.9 \text{ Hz}$ ,  $2 \times \text{PhCH}_A\text{H}_B\text{N}$ ), 2.92-3.05 (2 H, m,  $\text{CH}_2\text{N}$ );  $\delta_{\text{C}}$  (75 MHz,  $\text{CDCl}_3$ ) 192.4 (d,  $J=24.2 \text{ Hz}$ , CO), 139.2 ( $2 \times \text{C}$ , Ar), 129.3 ( $4 \times \text{C}$ , Ar), 128.7 ( $4 \times \text{C}$ , Ar), 127.6 ( $2 \times \text{C}$ , Ar), 94.7 (d,  $J=189.5 \text{ Hz}$ ,  $\text{CHF}$ ), 58.9 ( $2 \times \text{C}$ ,  $\text{PhCH}_2\text{N}$ ), 55.4 (d,  $J=19.3 \text{ Hz}$ ,  $\text{CH}_2\text{N}$ ), 54.2 (d,  $J=9.5 \text{ Hz}$ ,  $\text{CHN}_2$ );  $\delta_{\text{F}}$  (282 MHz,  $\text{CDCl}_3$ ) -191.9 (1 F, m,  $\text{CHF}$ ).

5.2.26  $\beta$ -Methyl-(*S*)-aspartate hydrochloride (**170**)<sup>7,8</sup>

$\text{SOCl}_2$  (1.55 cm<sup>3</sup>, 21.2 mmol, 1.4 eq) was added dropwise at 0 °C to a solution of L-aspartic acid (2 g, 15 mmol) in dry methanol (10 cm<sup>3</sup>). The reaction mixture was stirred for 30 min while slowly warming up to room temperature. Diethyl ether (50 cm<sup>3</sup>) was then added and the mixture was cooled to -10 °C. The resultant white precipitate was filtered, washed with ice cold diethyl ether and dried under vacuum. The solid was re-crystallised from methanol/diethyl ether (1:5) to yield  $\beta$ -methyl-(*S*)-aspartate hydrochloride (**170**) as a colourless amorphous solid (1.7 g, 62%).

**Mp:** 190-192 °C (from MeOH/Et<sub>2</sub>O), lit<sup>9</sup> 184-186 °C (from MeOH/Et<sub>2</sub>O);  $[\alpha]_{\text{D}}^{20} + 9.8$  (c 0.6, H<sub>2</sub>O), lit<sup>9</sup>  $[\alpha]_{\text{D}}^{25} + 9.7$  (c 0.6, H<sub>2</sub>O);  $\delta_{\text{H}}$  (300 MHz, D<sub>2</sub>O) 4.23 (1 H, t,  $J=5.5$  Hz, CHN), 4.60 (3 H, s, OCH<sub>3</sub>), 2.97-3.00 (CH<sub>2</sub>);  $\delta_{\text{C}}$  (75 MHz, D<sub>2</sub>O) 172.2 (CO<sub>2</sub>Me), 171.2 (CO<sub>2</sub>H), 53.2 (OCH<sub>3</sub>), 49.6 (CHN), 34.1 (CH<sub>2</sub>).

These data are in accordance with the literature.<sup>7,8</sup>

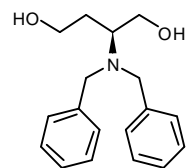
5.2.27 (*S*)-*N,N*-Dibenzylaspartic acid  $\beta$ -methyl ester (**172**)<sup>10</sup>**172**

A solution of  $\beta$ -methyl-(*S*)-aspartate hydrochloride (**170**) (500 mg, 2.7 mmol) in dry methanol (25 cm<sup>3</sup>) was treated with Et<sub>3</sub>N (~0.27 cm<sup>3</sup>, 2 mmol) to neutralise pH to ~7. Benzaldehyde (1.66 cm<sup>3</sup>, 16.3 mmol, 6 eq) was added and the mixture was stirred at RT for 2 h. NaCNBH<sub>3</sub> (679 mg, 10.8 mmol, 4 eq) was then added portion wise and the reaction mixture was stirred for 16 h at RT. The reaction was quenched by the addition of acetic acid (25 cm<sup>3</sup>) and the mixture was concentrated under reduced pressure. Water (15 cm<sup>3</sup>) was added and the aqueous phase was extracted into DCM (2  $\times$  50 cm<sup>3</sup>). After evaporation of the solvent, the resultant oil was purified over silica gel (hexane/EtOAc 4:1) to give (*S*)-*N,N*-dibenzylaspartic acid  $\beta$ -methyl ester (**172**) as a viscous colourless oil (570 mg, 64%).

$[\alpha]_D^{20}$  -33.6 (c 0.5, CHCl<sub>3</sub>), lit<sup>11</sup>  $[\alpha]_D^{23}$  -55 (c 0.5, CHCl<sub>3</sub>);  $\nu_{\max}(\text{film})/\text{cm}^{-1}$  3029, 2952, 2850, 1735, 1624, 1495, 1455, 1437, 1174, 700;  $\delta_{\text{H}}$  (300 MHz, CDCl<sub>3</sub>) 10.53 (1 H, br s, CO<sub>2</sub>H), 7.20-7.49 (10 H, m, Ar-*H*), 3.98 (1 H, t, *J*=7.4 Hz, CHN), 3.83 (2 H, AB d, *J*=13.5 Hz, 2  $\times$  PhCH<sub>A</sub>H<sub>B</sub>), 3.76 (2 H, AB d, *J*=13.5 Hz, 2  $\times$  PhCH<sub>A</sub>H<sub>B</sub>), 3.59 (3 H, s, OCH<sub>3</sub>), 2.94 (1 H, dd, *J*=7.1 Hz, *J*=15.8 Hz, CH<sub>A</sub>H<sub>B</sub>), 2.73 (1 H, dd, *J*=7.7 Hz, *J*=15.8 Hz, CH<sub>A</sub>H<sub>B</sub>);  $\delta_{\text{C}}$  (75 MHz, CDCl<sub>3</sub>) 175.7 (CO<sub>2</sub>H), 172.2 (CO<sub>2</sub>Me), 138.3 (2  $\times$  C, Ar), 129.6 (4  $\times$  C, Ar), 128.9 (4  $\times$  C, Ar), 128.0 (2  $\times$  C, Ar), 58.9 (CHN), 55.2 (2  $\times$  PhCH<sub>2</sub>), 52.4 (OCH<sub>3</sub>), 34.5 (CH<sub>2</sub>).

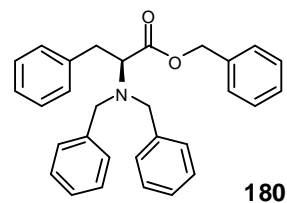
These data are in accordance with the literature.<sup>10, 11</sup>



5.2.28 (2*S*)-(Dibenzylamino)butane-1,4-diol (**173**)**173**

$\text{BH}_3$  (1 M solution in THF) ( $1.6 \text{ cm}^3$ , 1.6 mmol, 4 eq) was added at RT under  $\text{N}_2$  to a solution of (*S*)-*N,N*-dibenzylaspartic acid  $\beta$ -methyl ester (**172**) (130 mg, 0.4 mmol) in dry THF ( $8 \text{ cm}^3$ ). The mixture was heated under reflux for 8 h till TLC analysis showed completion of the reaction. After cooling down to RT, the reaction was quenched by the addition of water ( $5 \text{ cm}^3$ ) and acetic acid ( $5 \text{ cm}^3$ ). The aqueous phase was extracted into EtOAc ( $3 \times 20 \text{ cm}^3$ ) and the product was purified over silica gel (hexane/EtOAc 2:1) to give (2*S*)-(dibenzylamino)butane-1,4-diol (**173**) as a colourless oil (86 mg, 75%).

$[\alpha]_{\text{D}}^{20} +16.5$  (c 1,  $\text{CHCl}_3$ ), lit<sup>12</sup>  $[\alpha]_{\text{D}}^{23} +17$  (c 1,  $\text{CHCl}_3$ );  $\nu_{\text{max}}(\text{film})/\text{cm}^{-1}$  3358 (br), 3028, 2932, 1602, 1495, 1453, 1130, 1028, 749, 699;  $\delta_{\text{H}}$  (300 MHz,  $\text{CDCl}_3$ ) 7.20-7.33 (10 H, m, Ar-*H*), 3.71 (2 H, d,  $J=13.3 \text{ Hz}$ ,  $2 \times \text{PhCH}_A\text{H}_B$ ), 3.58 (2 H, d,  $J=13.3 \text{ Hz}$ ,  $2 \times \text{PhCH}_A\text{H}_B$ ), 3.49-3.67 (4 H, m,  $2 \times \text{CH}_2\text{OH}$ ), 2.93 (1 H, tt,  $J=5.9 \text{ Hz}$ ,  $J=7.8 \text{ Hz}$ , CHN), 2.70 (2 H, br s,  $2 \times \text{CH}_2\text{OH}$ ), 1.92-2.02 (1 H, m,  $\text{CH}_A\text{H}_B$ ), 1.46 (1 H, ddt,  $J=5.7 \text{ Hz}$ ,  $J=7.3 \text{ Hz}$ ,  $J=11.3 \text{ Hz}$ ,  $\text{CH}_A\text{H}_B$ );  $\delta_{\text{C}}$  (75 MHz,  $\text{CDCl}_3$ ) 139.5 ( $2 \times \text{C}$ , Ar), 129.5 ( $4 \times \text{C}$ , Ar), 128.9 ( $4 \times \text{C}$ , Ar), 127.7 ( $2 \times \text{C}$ , Ar), 61.8 ( $\text{CH}_2\text{OH}$ ), 61.6 ( $\text{CH}_2\text{OH}$ ), 57.3 (CHN), 54.0 ( $2 \times \text{PhCH}_2$ ), 29.3 ( $\text{CH}_2$ ).

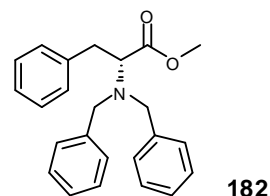
5.2.29 (2*S*)-(Dibenzylamino)-3-phenylpropanoic acid benzyl ester (**180**)

Anhydrous potassium carbonate (13.8 g, 99.9 mmol, 3.3 eq) and benzyl bromide (15.8 g, 92.3 mmol, 3.05 eq) were added to a solution of L-phenylalanine (5 g, 30.26 mmol) in ethanol (100 cm<sup>3</sup>). The mixture was then stirred at 70 °C for 3 days. After cooling, the solids were filtered and washed with EtOAc. The filtrate was concentrated under reduced pressure to give (**180**) as a light yellow oil in nearly quantitative yield.

An analytical sample was obtained after chromatography over silica gel (hexane/EtOAc 12:1) to give (**180**) as a colourless oil.

$[\alpha]_{\text{D}}^{18}$  -83.3 (c 1.8 CHCl<sub>3</sub>), lit<sup>13</sup>  $[\alpha]_{\text{D}}^{20}$  -72.9 (c 1.8, CHCl<sub>3</sub>);  $\nu_{\text{max}}(\text{film})/\text{cm}^{-1}$  3062, 3028, 2935, 2844, 2360, 2341, 1730, 1602, 1585, 1495, 1454, 1212, 1160;  $\delta_{\text{H}}$  (300 MHz, CDCl<sub>3</sub>) 6.07-7.39 (20 H, m, Ar-*H*), 5.22 (1 H, d,  $J=12.2$  Hz, PhCH<sub>A</sub>H<sub>B</sub>O), 5.11 (1 H, d,  $J=12.2$  Hz, PhCH<sub>A</sub>H<sub>B</sub>O), 3.92 (2 H, d,  $J=14.0$  Hz, 2 × PhCH<sub>A</sub>H<sub>B</sub>N), 3.71 (1 H, t,  $J=7.7$  Hz, CHN), 3.53 (2 H, d,  $J=14.0$  Hz, 2 × PhCH<sub>A</sub>H<sub>B</sub>N), 3.13 (1 H, dd,  $J=7.3$  Hz,  $J=13.9$  Hz, PhCH<sub>A</sub>H<sub>B</sub>), 2.99 (1 H, dd,  $J=8.2$  Hz,  $J=13.9$  Hz, PhCH<sub>A</sub>H<sub>B</sub>);  $\delta_{\text{C}}$  (75 MHz, CDCl<sub>3</sub>) 172.6 (CO<sub>2</sub>), 139.7 (2 × C, Ar), 138.5 (Ar), 136.4, (Ar), 129.9 (2 × C, Ar), 129.1 (4 × C, Ar), 129.0 (2 × C, Ar), 128.9 (2 × C, Ar), 128.7 (Ar), 128.6 (6 × C, Ar), 127.4 (2 × C, Ar), 126.7 (Ar), 66.5 (PhCH<sub>2</sub>O), 62.8 (CHN), 54.8 (2 × PhCH<sub>2</sub>N), 36.1 (PhCH<sub>2</sub>).

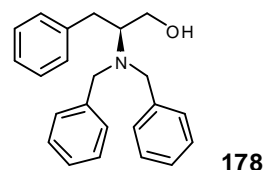
These data are in accordance with the literature.<sup>13</sup>

**5.2.30 (2*R*)-(Dibenzylamino)-3-phenylpropanoic acid methyl ester (182)**

Anhydrous potassium carbonate (8.0 g, 57.5 mmol, 3.1 eq) and benzyl bromide (7.0 g, 40.8 mmol, 2.2 eq) were added to a solution of D-phenylalanine methyl ester hydrochloride (**181**) (4.0 g, 18.5 mmol) in acetonitrile (100 cm<sup>3</sup>). The mixture was then heated under reflux for 16 h. After cooling, the solids were filtered and washed with EtOAc. The filtrate was concentrated under reduced pressure and the product was purified over silica gel (hexane/EtOAc 12:1) to give (**182**) as a colourless oil (5.25 g, 79%).

$[\alpha]_{\text{D}}^{16} +74.5$  (c 1.8, CHCl<sub>3</sub>), lit<sup>14</sup>  $[\alpha]_{\text{D}}^{20} -77.8$  (c 2.2, CHCl<sub>3</sub>, (*S*)-enantiomer);  $\delta_{\text{H}}$  (300 MHz, CDCl<sub>3</sub>) 6.98-7.26 (15 H, m, Ar-*H*), 3.95 (2 H, d,  $J=14.0$  Hz, 2 × PhCH<sub>A</sub>H<sub>B</sub>N), 3.72 (3 H, s, OCH<sub>3</sub>), 3.67 (1 H, dd,  $J=7.2$  Hz,  $J=8.2$  Hz, CHN), 3.54 (2 H, d,  $J=14.0$  Hz, 2 × PhCH<sub>A</sub>H<sub>B</sub>N), 3.12 (1 H, dd,  $J=7.2$  Hz,  $J=14.0$  Hz, PhCH<sub>A</sub>H<sub>B</sub>), 2.98 (1 H, dd,  $J=8.2$  Hz,  $J=14.0$  Hz, PhCH<sub>A</sub>H<sub>B</sub>);  $\delta_{\text{C}}$  (75 MHz, CDCl<sub>3</sub>) 173.2 (CO<sub>2</sub>), 139.7 (2 × C, *Ar*), 138.6 (*Ar*), 129.9 (2 × C, *Ar*), 129.2 (4 × C, *Ar*), 128.6 (6 × C, *Ar*), 127.4 (2 × C, *Ar*), 126.7 (*Ar*), 62.8 (CHN), 54.9 (2 × PhCH<sub>2</sub>N), 51.6 (OCH<sub>3</sub>), 36.2 (PhCH<sub>2</sub>).

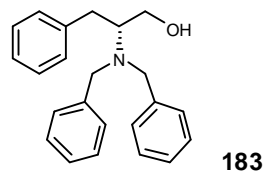
These data are in accordance with the literature.<sup>14</sup>

5.2.31 (2*S*)-(Dibenzylamino)-3-phenylpropan-1-ol (**178**)<sup>13</sup>

A solution of ester (**180**) (9 g, 20.7 mmol) in dry THF (50 cm<sup>3</sup>) was added dropwise at 0 °C to a suspension of LiAlH<sub>4</sub> (1.96 g, 51.6 mmol, 2.5 eq) in dry THF (150 cm<sup>3</sup>). The reaction mixture was stirred for 2 h at 0 °C and the excess of hydride was quenched by the addition of EtOAc and water. Et<sub>2</sub>O was added and the mixture was filtered over Celite. Filtrates were concentrated under reduced pressure and the residue was purified over silica gel (hexane/EtOAc 7:1) to give (**178**) as a colourless solid (5.84 g, 85%).

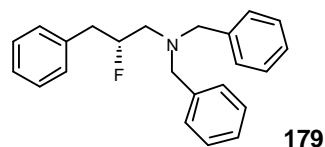
**Mp** 73-74 °C (from DCM), lit<sup>13</sup> 69-71 °C from Et<sub>2</sub>O/hexane;  $[\alpha]_{\text{D}}^{20} +43.0$  (c 1.5, CHCl<sub>3</sub>), lit<sup>13</sup>  $[\alpha]_{\text{D}}^{20} +38.4$  (c 1.5, CHCl<sub>3</sub>), lit<sup>15</sup>  $[\alpha]_{\text{D}}^{20} +42.5$  (c 1, CHCl<sub>3</sub>);  $\nu_{\text{max}}$ (KBr plate)/cm<sup>-1</sup> 3393 (br), 3063, 3026, 2924, 1601, 1583, 1494, 1454, 1412, 1259, 1103, 1042;  $\delta_{\text{H}}$  (300 MHz, CDCl<sub>3</sub>) 7.09-7.36 (15 H, m, Ar-*H*), 3.93 (2 H, d, *J*=13.3 Hz, 2 × PhCH<sub>A</sub>H<sub>B</sub>N), 3.48-3.55 (1 H, m, CH<sub>A</sub>H<sub>B</sub>OH), 3.49 (2 H, d, *J*=13.3 Hz, 2 × PhCH<sub>A</sub>H<sub>B</sub>N), 3.33 (1 H, dd, *J*=4.4 Hz, *J*=10.6 Hz, CH<sub>A</sub>H<sub>B</sub>OH), 3.04-3.15 (2 H, m, CHN and PhCH<sub>A</sub>H<sub>B</sub>), 3.02 (1 H, br s, OH), 2.43 (1 H, dd, *J*=9.4 Hz, *J*=12.9 Hz, PhCH<sub>A</sub>H<sub>B</sub>);  $\delta_{\text{C}}$  (75 MHz, CDCl<sub>3</sub>) 139.6 (*Ar*), 139.5 (2 × C, *Ar*), 129.5 (6 × C, *Ar*), 129.0 (6 × C, *Ar*), 127.8 (2 × C, *Ar*), 126.7 (*Ar*), 61.3 (CHN), 60.8 (CH<sub>2</sub>OH), 53.7 (2 × PhCH<sub>2</sub>N), 32.1 (PhCH<sub>2</sub>).

These data are in accordance with the literature.<sup>13</sup>

**5.2.32 (2*R*)-(Dibenzylamino)-3-phenylpropan-1-ol (183)** <sup>13</sup>

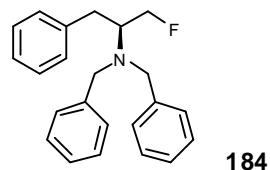
This product was prepared following the procedure for the (*S*)-enantiomer (**178**) (see **5.2.31**), starting with (*2R*)-(dibenzylamino)-3-phenylpropanoic acid methyl ester (**182**). The product was obtained as a colourless amorphous solid (93%).

Spectroscopic data were identical to the (*S*)-enantiomer (**178**); **mp** 70-72 °C (from hexane/EtOAc),  $[\alpha]_D^{20}$  -43.6 (c 1.5 CHCl<sub>3</sub>).

5.2.33 (2*R*)-*N,N*-Dibenzyl-2-fluoro-3-phenylpropan-1-amine (**179**)<sup>16</sup>

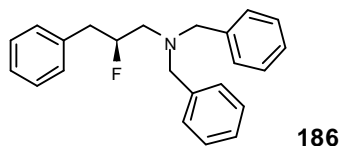
A solution of Deoxofluor<sup>TM</sup> (2.67 g, 12.1 mmol, 1 eq) in dry DCM (20 cm<sup>3</sup>) was added dropwise over 15 min at -10 °C to a stirred solution of amino alcohol (**178**) (4.0 g, 12.1 mmol) in dry DCM (100 cm<sup>3</sup>). The reaction was allowed to warm to RT, stirred for 15 h and was then quenched by the addition of a 10% solution of K<sub>2</sub>CO<sub>3</sub> (10 cm<sup>3</sup>). The organic phase was separated and the aqueous phase washed with DCM. The combined organic extracts were concentrated under reduced pressure and the residue was purified over silica gel (hexane/DCM 5:1). Side product (**184**) eluted first and was obtained as a colourless oil (0.350 g, 9%). The desired and major product (**179**) was then collected as a colourless oil (3.03 g, 75%).

**R<sub>f</sub>**: 0.25 (hexane/DCM 2:1); [ $\alpha$ ]<sub>D</sub><sup>20</sup> + 1.1 (c 6, CHCl<sub>3</sub>); **v**<sub>max</sub>(film)/cm<sup>-1</sup> 3062, 3028, 2929, 2802, 2360, 1602, 1495, 1455, 1369, 1028, 745, 699; **δ**<sub>H</sub> (300 MHz, CDCl<sub>3</sub>) 7.07-7.35 (15 H, m, Ar-*H*), 4.81 (1 H, d m, *J*=49.3 Hz, *CHF*), 3.65 (4 H, s, 2 × PhCH<sub>2</sub>N), 2.75-2.87 (2 H, m, PhCH<sub>2</sub>CF), 2.65-2.78 (2 H, m, CFCH<sub>2</sub>N); **δ**<sub>C</sub> (75 MHz, CDCl<sub>3</sub>) 139.8 (2 × C, *Ar*), 137.8 (d, *J*=3.9 Hz, *Ar*), 129.7 (2 × C, *Ar*), 129.4 (4 × C, *Ar*), 128.9 (2 × C, *Ar*), 128.7 (4 × C, *Ar*), 127.5 (2 × C, *Ar*), 126.9 (*Ar*), 94.0 (d, *J*=172.7 Hz), 59.6 (2 × C), 57.1 (d, *J*=22.0 Hz), 40.2 (d, *J*=21.1 Hz); **δ**<sub>F</sub> (280 MHz, CDCl<sub>3</sub>) -180.4 (m, 1 F); **m/z** (+EI), found MH<sup>+</sup>: 334.1972, C<sub>23</sub>H<sub>25</sub>NF requires 334.1971 (+0.1 ppm).

5.2.34 (2*S*)-*N,N*-Dibenzyl-1-fluoro-3-phenylpropan-2-amine (**184**)<sup>16</sup>

Compound (**184**) was obtained as a side product (9%) from the synthesis of (**179**) (see 5.2.33).

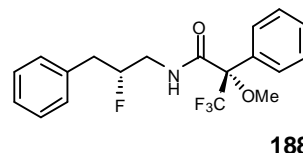
**R<sub>f</sub>**: 0.42 Hexane/DCM (2:1); [ $\alpha$ ]<sub>D</sub><sup>20</sup> -19.2 (c 1, CHCl<sub>3</sub>), lit<sup>17</sup> [ $\alpha$ ]Hg<sub>23</sub><sup>546</sup> -45 (c 1, CH<sub>2</sub>Cl<sub>2</sub>);  $\nu_{\text{max}}$ (film)/cm<sup>-1</sup> 3062, 3027, 2953, 2803, 1602, 1495, 1454, 1365, 1143, 1029, 743, 698;  $\delta_{\text{H}}$  (300 MHz, CDCl<sub>3</sub>) 7.05-7.29 (15 H, m, Ar-*H*), 4.57 (1 H, ddd, *J*=3.2 Hz, *J*=9.8 Hz, *J*=47.8 Hz, CH<sub>A</sub>H<sub>B</sub>F), 4.46 (1 H, ddd, *J*=5.3 Hz, *J*=9.8 Hz, *J*=47.9 Hz, CH<sub>A</sub>H<sub>B</sub>F), 3.72-3.82 (4 H, dd, 2 × PhCH<sub>2</sub>N), 3.02-3.19 (1 H, m, CHN), 2.97 (1 H, ddd, *J*=1.6 Hz, *J*=6.4 Hz, *J*=13.4 Hz, PhCH<sub>A</sub>H<sub>B</sub>), 2.80 (1 H, dd, *J*=8.5 Hz, *J*=13.4 Hz, PhCH<sub>A</sub>H<sub>B</sub>);  $\delta_{\text{C}}$  (75 MHz, CDCl<sub>3</sub>) 140.0 (2 × C, *Ar*), 139.7 (*Ar*), 129.4 (2 × C, *Ar*), 128.6 (4 × C, *Ar*), 128.4 (2 × C, *Ar*), 128.3 (4 × C, *Ar*), 126.9 (2 × C, *Ar*), 126.2 (*Ar*), 83.6 (d, *J*=172.4 Hz, CH<sub>2</sub>F), 59.3 (d, *J*=17.4 Hz, CHN), 54.5 (d, *J*=1.5 Hz, 2 × PhCH<sub>2</sub>N), 33.1 (d, *J*=6.0 Hz, PhCH<sub>2</sub>);  $\delta_{\text{F}}$  (280 MHz, CDCl<sub>3</sub>) -226.7 (1 F, dt, *J*=26.1 Hz, *J*=47.8 Hz); *m/z* (+EI), found MH<sup>+</sup>: 334.1969, C<sub>23</sub>H<sub>25</sub>NF requires 334.1971 (-0.5 ppm).

**5.2.35 (2S)-N,N-Dibenzyl-2-fluoro-3-phenylpropan-1-amine (186)**

This product was prepared following the procedure for the (*R*)-enantiomer (**179**) (see **5.2.33**), starting with (*2R*)-(dibenzylamino)-3-phenylpropan-1-ol (**183**). The product (**186**) was obtained as a colourless oil (76%).

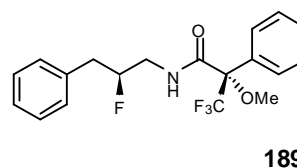
Spectroscopic data were identical to the (*R*)-enantiomer (**179**);  $[\alpha]_D^{20}$  -1.0 (c 6, CHCl<sub>3</sub>); *m/z* (+EI), found MH<sup>+</sup>: 334.1971, C<sub>23</sub>H<sub>25</sub>NF requires 334.1971 (+0.1 ppm)



**5.2.36 *N*-((2*R*)-Fluoro-3-phenylpropyl)-(S)-MTPA amide (188)**

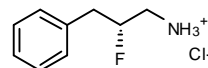
Et<sub>3</sub>N (18 μL, 2.5 eq), 4-DMAP (3 mg) and (*R*)-(-)-α-methoxy-α-(trifluoromethyl)phenylacetyl chloride (**187**) (20 mg, 1.5 eq) were added at RT to a suspension of (2*R*)-fluoro-3-phenylpropan-1-amine (**190**) (10 mg, 5.3 × 10<sup>-2</sup> mmol) in DCM (2 cm<sup>3</sup>). The reaction mixture was stirred for 4 h and was quenched by the addition of water. Solvents were removed under reduced pressure and the residue was dissolved in CDCl<sub>3</sub> and filtered through a glass cotton plug directly into a NMR tub.

$\delta_F \{^1H\}$  (470 MHz, CDCl<sub>3</sub>) -68.8 (3 F, s, CF<sub>3</sub> Mosher amide), -70.7 (s, CF<sub>3</sub> Mosher acid in excess), -184.9 (1 F, s, CHF); *m/z* (+EI), found (M+Na<sup>+</sup>): 392.1247, C<sub>19</sub>H<sub>19</sub>NO<sub>2</sub>F<sub>4</sub>Na requires 392.1250 (-0.6 ppm).

**5.2.37 *N*-((2*S*)-Fluoro-3-phenylpropyl)-(S)-MTPA amide 189**

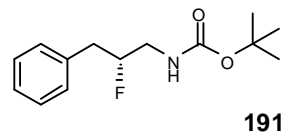
(**189**) was prepared in an identical manner to that described above (5.2.36), starting with (2*S*)-fluoro-3-phenylpropan-1-amine hydrochloride.

$\delta_F \{^1H\}$  (470 MHz, CDCl<sub>3</sub>) -68.8 (3 F, s, CF<sub>3</sub> Mosher amide), -70.7 (s, CF<sub>3</sub> Mosher acid in excess), -184.7 (1 F, s, CHF).

**5.2.38 (2R)-Fluoro-3-phenylpropan-1-amine hydrochloride (190)****190**

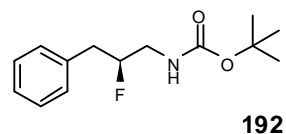
20% Pd(OH)<sub>2</sub>/C (40 mg) was added to a solution of (2*R*)-*N,N*-dibenzyl-2-fluoro-3-phenylpropan-1-amine (**179**) (0.125 g, 0.37 mmol) in methanol (10 cm<sup>3</sup>). The mixture was stirred at RT under a positive pressure of H<sub>2</sub> for 2 h. The palladium catalyst was removed by filtration over Celite and 1 M HCl in diethyl ether (2 cm<sup>3</sup>) was added to the filtrate. The solution was concentrated under reduced pressure and the product was re-crystallised from EtOH/Et<sub>2</sub>O. (2*R*)-Fluoro-3-phenylpropan-1-amine hydrochloride (**190**) was obtained as a colourless crystalline solid (0.053 g, 76%).

**Mp** 129-132 °C (from EtOH/Et<sub>2</sub>O), [ $\alpha$ ]<sub>D</sub><sup>20</sup> +9.81 (c 3.18, MeOH); (**Found**: C, 56.86; H, 6.95; N, 7.25 %, C<sub>9</sub>H<sub>13</sub>NFCl requires C, 57.00; H, 6.91; N, 7.39 %);  $\nu_{\text{max}}$ (KBr plate)/cm<sup>-1</sup> 2993 (br), 1588, 1486, 1457, 1375, 1148, 1037, 993, 958, 753, 745, 697;  $\delta_{\text{H}}$  (300 MHz, D<sub>2</sub>O) 7.19-7.32 (5 H, m, Ar-*H*), 4.82-5.07 (1 H, m, CHF), 3.07-3.28 (2 H, m, CH<sub>2</sub>N), 2.88-2.99 (2 H, m, PhCH<sub>2</sub>);  $\delta_{\text{C}}$  (75 MHz, D<sub>2</sub>O) 135.9 (d, *J*=4.0 Hz, Ar), 129.8 (2 × C, Ar), 129.2 (2 × C, Ar), 127.6 (Ar), 91.4 (d, *J*=171.3 Hz, CHF), 42.9 (d, *J*=20.4 Hz, CH<sub>2</sub>N), 38.2 (d, *J*=19.9 Hz, PhCH<sub>2</sub>);  $\delta_{\text{F}}$  (280 MHz, CDCl<sub>3</sub>) -188.4 (m, 1 F); *m/z* (+EI), found (M-Cl<sup>-</sup>):154.1033, C<sub>9</sub>H<sub>13</sub>NF requires 154.1032 (+0.9 ppm).

5.2.39 *tert*-Butyl-(2*R*)-fluoro-3-phenylpropylcarbamate (**191**)

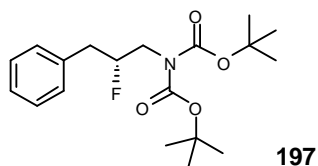
20% Pd(OH)<sub>2</sub>/C (200 mg) was added to a solution of (2*R*)-*N,N*-dibenzyl-2-fluoro-3-phenylpropan-1-amine (**179**) (0.675 g, 2.0 mmol) in methanol (30 cm<sup>3</sup>). The mixture was stirred for 3 h at RT under a positive atmosphere of H<sub>2</sub> and then di-*tert*-butyl dicarbonate (0.664 g, 3.04 mmol, 1.5 eq) was added. The reaction was then stirred for 14 h at RT. The palladium catalyst was removed by filtration over Celite, the filtrate was concentrated to dryness and the crude residue was purified over silica gel (hexane/DCM 10:1). The product (**191**) was obtained after re-crystallisation from hexane/DCM as a colourless crystalline solid (0.462 g, 90%).

**Mp** 66-76 °C (from hexane/DCM),  $[\alpha]_D^{20}$  -11.2 (c 1, CHCl<sub>3</sub>);  $\nu_{\max}$ (KBr plate)/cm<sup>-1</sup> 3374, 2991, 2970, 1696, 1525, 1248, 1165, 1076, 990, 896, 754, 703; (**Found**: C, 66.59; H, 7.61; N, 5.39 %, C<sub>14</sub>H<sub>20</sub>NO<sub>2</sub>F requires C, 66.38; H, 7.96; N, 5.53 %);  $\delta_H$  (300 MHz, CDCl<sub>3</sub>) 7.15-7.32 (5 H, m, Ar-*H*), 4.96 (1 H, br s, N-*H*), 4.61-4.86 (1 H, m, CHF), 3.40-3.57 (1 H, m, CH<sub>A</sub>H<sub>B</sub>N), 3.11-3.27 (1 H, m, CH<sub>A</sub>H<sub>B</sub>N), 2.79-3.01 (2 H, m, PhCH<sub>2</sub>), 1.44 (9 H, s, C(CH<sub>3</sub>)<sub>3</sub>);  $\delta_C$  (75 MHz, CDCl<sub>3</sub>) 156.3 (NCO), 136.7 (d, *J*=4.3 Hz, Ar), 129.8 (2 × C, *Ar*), 129.0 (2 × C, *Ar*), 127.2 (*Ar*), 93.8 (d, *J*=172.4 Hz, CHF), 80.0 (C(CH<sub>3</sub>)<sub>3</sub>), 44.6 (d, *J*=20.7 Hz, CH<sub>2</sub>N), 39.3 (d, *J*=20.8 Hz, PhCH<sub>2</sub>), 28.8 (C(CH<sub>3</sub>)<sub>3</sub>);  $\delta_F$  (280 MHz, CDCl<sub>3</sub>) -185.4 (1 F, m); *m/z* (+EI), found (M+Na<sup>+</sup>): 276.1378, C<sub>14</sub>H<sub>20</sub>NO<sub>2</sub>FNa requires 276.1376 (+1.0 ppm).

**5.2.40 *tert*-Butyl-(2*S*)-fluoro-3-phenylpropylcarbamate (192)**

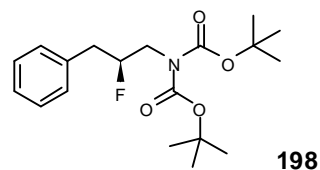
This product was prepared following the procedure for the (*R*)-enantiomer (**191**) (see **5.2.39**), starting with (*2S*)-*N,N*-dibenzyl-2-fluoro-3-phenylpropan-1-amine (**186**). The product was obtained as a colourless crystalline solid (85%).

Spectroscopic data were identical to the (*R*)-enantiomer (**191**); **mp** 68-76 °C (from hexane/DCM);  $[\alpha]_{\text{D}}^{20} +10.6$  (c 1, CHCl<sub>3</sub>); *m/z* (+ES), found (M+Na<sup>+</sup>): 276.1369, C<sub>14</sub>H<sub>20</sub>NO<sub>2</sub>FNa requires 276.1376 (-2.6 ppm).

5.2.41 Di(*tert*-butyl)-(2*R*)-fluoro-3-phenylpropyldicarbamate (**197**)

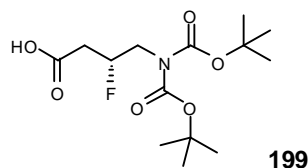
20% Pd(OH)<sub>2</sub>/C (300 mg) was added to a solution of (**179**) (1.45 g, 4.3 mmol) in methanol (50 cm<sup>3</sup>). The mixture was stirred for 3 h at RT under a positive atmosphere of H<sub>2</sub> and then di-*tert*-butyl dicarbonate (1.90 g, 8.7 mmol, 2 eq) was added. The reaction was then stirred for 14 h at RT. The palladium catalyst was removed by filtration over Celite and the solution was concentrated to dryness. The residue was dissolved in MeCN (50 cm<sup>3</sup>), then di-*tert*-butyl dicarbonate (1.90 g, 8.7 mmol, 2 eq) and 4-DMAP (80 g, 0.65 mmol, 15% mol) were added and the solution was heated under reflux for 14 h. After cooling, the solvent was evaporated under reduced pressure, the residue dissolved in Et<sub>2</sub>O and the organic phase washed with water. After evaporation of the organic phase under reduced pressure, the product was purified over silica gel (hexane/EtOAc 18:1) to give (**197**) as a colourless oil (1.23 g, 80%).

$[\alpha]_D^{20}$  -16.4 (c 2, CHCl<sub>3</sub>),  $\nu_{\max}(\text{film})/\text{cm}^{-1}$  2980, 2935, 1792, 1749, 1699, 1429, 1368, 1234, 1146, 1122, 856, 752, 700;  $\delta_{\text{H}}$  (300 MHz, CDCl<sub>3</sub>) 7.20-7.33 (5 H, m, Ar-*H*), 4.76-5.01 (1 H, m, CHF), 3.59-4.06 (2 H, m, CFCH<sub>2</sub>N), 2.81-3.03 (2 H, m, PhCH<sub>2</sub>CF), 1.47 (18 H, s, 6 × CH<sub>3</sub>);  $\delta_{\text{C}}$  (75 MHz, CDCl<sub>3</sub>) 152.9 (2 × NCO<sub>2</sub>), 136.8 (d, *J*=3.9 Hz, Ar), 129.7 (2 × C, Ar), 128.9 (2 × C, Ar), 127.15 (Ar), 92.9 (d, *J*=175.0 Hz, CHF), 83.0 (2 × C(CH<sub>3</sub>)), 49.9 (d, *J*=22.3 Hz, CH<sub>2</sub>N), 39.7 (d, *J*=20.6 Hz, PhCH<sub>2</sub>), 29.37 (6 × CH<sub>3</sub>);  $\delta_{\text{F}}$  (280 MHz, CDCl<sub>3</sub>) -186.8 (1 F, m); *m/z* (+EI), found (M+Na<sup>+</sup>): 376.1905, C<sub>19</sub>H<sub>28</sub>NO<sub>4</sub>FNa requires 376.1900 (+1.4 ppm).

**5.2.42 Di(*tert*-butyl)-(2*S*)-fluoro-3-phenylpropyldicarbamate (198)**

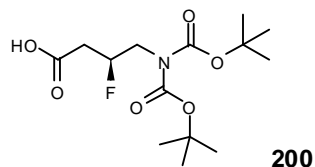
This product was prepared following the procedure for the (*R*)-enantiomer (**197**) (see **5.2.41**), starting with (*2S*)-*N,N*-dibenzyl-2-fluoro-3-phenylpropan-1-amine (**186**). The product was obtained as a colourless oil (78%).

Spectroscopic data were identical to the (*R*)-enantiomer (**197**);  $[\alpha]^{20}_{\text{D}} +16.2$  (c 2,  $\text{CHCl}_3$ );  $m/z$  (+EI), found ( $\text{M}+\text{Na}^+$ ): 376.1906,  $\text{C}_{19}\text{H}_{28}\text{NO}_4\text{FNa}$  requires 376.1900 (+1.5 ppm).

5.2.43 4-(Bis(*tert*-butoxycarbonyl)amino)-(3*R*)-fluorobutanoic acid (**199**)**199**

NaIO<sub>4</sub> (5.584 g, 26 mmol, 18 eq) was added to a stirred solution of (**197**) (512 mg, 1.45 mmol) in the biphasic solvent system CCl<sub>4</sub>/MeCN/H<sub>2</sub>O (12 /12 /15 cm<sup>3</sup>). The mixture was treated with RuCl<sub>3</sub> · xH<sub>2</sub>O (23 mg, 0.09 mmol, 6% mol) and the reaction was stirred vigorously at 25 °C for 3 days. The mixture was then filtered through a large Celite pad and the solids were washed with EtOAc. The filtrate was concentrated to dryness and the product was purified over silica gel (hexane/EtOAc 2.5:1). Carboxylic acid (**199**) was obtained as a colourless oil (356 mg, 76%).

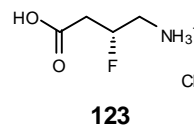
[ $\alpha$ ]<sub>D</sub><sup>20</sup> -19.1 (c 2, CHCl<sub>3</sub>),  $\nu_{\text{max}}$ (film)/cm<sup>-1</sup> 2982, 2936, 1785, 1720, 1429, 1370, 1125, 1043, 854, 736,  $\delta_{\text{H}}$  (300 MHz, CDCl<sub>3</sub>) 9.51 (1 H, br s, CO<sub>2</sub>H), 4.99-5.23 (1 H, m, CHF), 3.72-4.09 (2 H, m, CFCH<sub>2</sub>N), 2.60-2.82 (2 H, m, CH<sub>2</sub>CO<sub>2</sub>), 1.51 (18 H, s, 6 × CH<sub>3</sub>);  $\delta_{\text{C}}$  (75 MHz, CDCl<sub>3</sub>) 175.4 (d, *J*=5.0 Hz, CO<sub>2</sub>H), 152.8 (2 × NCO<sub>2</sub>), 88.6 (d, *J*=173.9 Hz, CHF), 83.5 (2 × C(CH<sub>3</sub>)<sub>3</sub>), 49.1 (d, *J*=23.5 Hz, CH<sub>2</sub>N), 38.2 (d, *J*=23.8 Hz, CH<sub>2</sub>CO<sub>2</sub>), 28.31 (6 × CH<sub>3</sub>);  $\delta_{\text{F}}$  (280 MHz, CDCl<sub>3</sub>) -186.9 (1 F, m); *m/z* (-EI), found (M-H<sup>+</sup>): 320.1504, C<sub>14</sub>H<sub>23</sub>NO<sub>6</sub>F requires 320.1509 (-1.6 ppm).

**5.2.44 4-(Bis(*tert*-butoxycarbonyl)amino)-(3*S*)-fluorobutanoic acid (200)**

This product was prepared following the procedure for the (*R*)-enantiomer (**199**) (see **5.2.43**), starting with di(*tert*-butyl)-(2*S*)-fluoro-3-phenylpropyl-dicarbamate (**198**). The product was obtained as a colourless oil (75%).

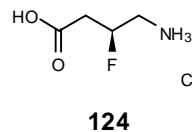
Spectroscopic data were identical to the (*R*)-enantiomer XX;  $[\alpha]_D^{20} +18.9$  (c 2, CHCl<sub>3</sub>); *m/z* (-EI), found (M-H<sup>+</sup>): 320.1512, C<sub>14</sub>H<sub>23</sub>NO<sub>6</sub>F requires 320.1509 (+0.6 ppm).



**5.2.45 (3R)-Fluoro-4-aminobutyric acid hydrochloride (123)**

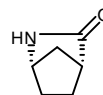
HCl gas was bubbled for 20 min into an ice-cooled solution of (**199**) (350 mg, 1.1 mmol) in dry DCM (40 cm<sup>3</sup>). After the formation of a white precipitate, nitrogen gas was bubbled through the reaction mixture at RT until evaporation of the solvent was complete. The off-white solid was dissolved in ethanol and re-crystallised twice from diethyl ether to yield (3*R*)-fluoro-4-aminobutyric acid hydrochloride (**123**) as a colourless crystalline solid (137 mg, 80%).

**Mp** 116-118 °C (from EtOH/Et<sub>2</sub>O);  $[\alpha]_D^{20}$  -15.5 (c 2.21, MeOH); (**Found**: C, 30.28; H, 5.51; N, 8.68 %, C<sub>4</sub>H<sub>9</sub>NO<sub>2</sub>FCl requires C, 30.49; H, 5.76; N, 8.89 %);  $\nu_{\max}(\text{KBr plate})/\text{cm}^{-1}$  3027 (br), 1701, 1610, 1572, 1506, 1448, 1394, 1306, 1255, 1222, 1036, 1005;  $\delta_{\text{H}}$  (300 MHz, CD<sub>3</sub>OD) 5.05-5.31 (1 H, d m,  $J=49.2$  Hz, CHF), 2.24-3.41 (2 H, m, CH<sub>2</sub>N), 2.75-2.86 (2 H, m, CH<sub>2</sub>CO<sub>2</sub>H);  $\delta_{\text{C}}$  (75 MHz, CD<sub>3</sub>OD) 172.7 (d,  $J=6.0$  Hz, CO<sub>2</sub>), 88.9 (d,  $J=171.5$  Hz, CHF), 44.2 (d,  $J=20.6$  Hz, CH<sub>2</sub>N), 38.4 (d,  $J=22.4$  Hz, CH<sub>2</sub>CO<sub>2</sub>);  $\delta_{\text{F}}$  (280 MHz, CD<sub>3</sub>OD) -190.0 (1 F, m);  $m/z$  (+EI) found (M-Cl<sup>-</sup>): 122.0615, C<sub>4</sub>H<sub>9</sub>NO<sub>2</sub>F requires 122.0617 (-2.3 ppm).

**5.2.46 (3S)-Fluoro-4-aminobutyric acid hydrochloride (124)**

This product was prepared following the procedure for the (*R*)-enantiomer (**123**) (see **5.2.45**), starting with 4-(bis(*tert*-butoxycarbonyl)amino)-(*3S*)-fluorobutanoic acid (**200**). The product was obtained as a colourless crystalline solid (84%).

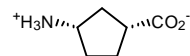
Spectroscopic data were identical to (*R*)-enantiomer; **mp** 116-117 °C (from EtOH/Et<sub>2</sub>O);  $[\alpha]_D^{20}$  +15.6 (c 2.22, MeOH); (**Found**: C, 30.63; H, 5.70; N, 8.71 %, C<sub>4</sub>H<sub>9</sub>NO<sub>2</sub>FCl requires C, 30.49; H, 5.76; N, 8.89 %); *m/z* (+EI) found (M-Cl<sup>+</sup>): 122.0614, C<sub>4</sub>H<sub>9</sub>NO<sub>2</sub>F requires 122.0617 (-2.6 ppm).

**5.2.47 (1*S*, 4*R*)-2-Azabicyclo[2.2.1]heptan-3-one (212)**<sup>18, 19</sup>**212**

10% Pd/C (8 mg) was added to a solution of (1*S*, 4*R*)-2-azabicyclo[2.2.1]hept-5-en-3-one (150 mg, 1.4 mmol) in EtOAc (15 cm<sup>3</sup>). The suspension was stirred at room temperature for 18 h under a positive pressure of H<sub>2</sub>. The reaction solution was then filtered through Celite and the stationary phase washed with EtOAc. Evaporation of the combined organic phases gave (**212**) as a colourless hygroscopic solid (145 mg, 95%), which liquefied rapidly when exposed to air.

$[\alpha]_{\text{D}}^{20}$  -552 (c 1, CHCl<sub>3</sub>), lit<sup>20</sup>  $[\alpha]_{\text{D}}$  -560 (c 1.1 CHCl<sub>3</sub>);  $\delta_{\text{H}}$  (300 MHz, CDCl<sub>3</sub>) 6.36 (1 H, br s, NH), 3.83 (1 H, m, CHN), 2.62 (1 H, m, CHCO), 1.30-1.80 (6 H, m, 3 × CH<sub>2</sub>);  $m/z$  (+EI): 111 (M, 100%), 96 (10), 83 (96), 67 (83), 55 (73).

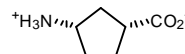
These data are in accordance with the literature.<sup>18, 19</sup>

**5.2.48 (1*R*, 3*S*)-3-Aminocyclopentane carboxylic acid (213)**<sup>21, 22</sup>**213**

4 N HCl (8 cm<sup>3</sup>) was added to a solution of (1*S*, 4*R*)-2-azabicyclo[2.2.1]heptan-3-one (**212**) (120 mg, 1.1 mmol) in acetic acid (8 cm<sup>3</sup>). The mixture was stirred for 5 h at 70 °C and after evaporation of the solvents under reduced pressure, the residue was dissolved in water (2 cm<sup>3</sup>). The solution was passed down an ion-exchange column (Dowex AG 50W-X8100), eluting with 2 N NH<sub>3</sub>. After evaporation of the solvent, the resultant solid was re-crystallised from methanol/EtOAc to give (1*R*, 3*S*)-3-aminocyclopentane carboxylic acid (**213**) as a colourless amorphous solid (128 mg, 72%).

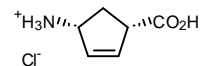
**Mp:** 253-255 °C (from MeOH/EtOAc), lit<sup>21</sup> 250-255 °C, [ $\alpha$ ]<sub>D</sub><sup>20</sup> -7.5 (c 1, H<sub>2</sub>O), lit<sup>21</sup> -7 (c 1, H<sub>2</sub>O); (**Found** C, 55.69; H, 8.55; N, 10.79 %, C<sub>6</sub>H<sub>11</sub>NO<sub>2</sub> requires C, 55.78; H, 8.60; N, 10.85 %);  $\delta_{\text{H}}$  (300 MHz, D<sub>2</sub>O) 3.56-3.64 (1 H, m, CHN), 2.62-2.70 (1 H, m, CHCO<sub>2</sub>), 1.64-2.14 (6 H, m, 3  $\times$  CH<sub>2</sub>);  $\delta_{\text{C}}$  (75 MHz, D<sub>2</sub>O) 180.3 (CO<sub>2</sub>), 51.8 (CHN), 42.8 (CHCO<sub>2</sub>), 34.0 (CH<sub>2</sub>), 30.1 (CH<sub>2</sub>), 28.0 (CH<sub>2</sub>).

These data are in accordance with the literature.<sup>21, 22</sup>

**5.2.49 (±)-Cis-3-aminocyclopentane carboxylic acid (215)****215**

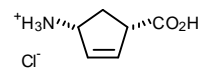
Racemic (±)-*cis*-3-aminocyclopentane carboxylic acid was obtained following the procedure for (1*R*, 3*S*)-3-aminocyclopentane carboxylic acid (**213**), starting with (±)-2-aza-bicyclo-[2.2.1]hept-5-en-3-one (see **5.2.47**). The product (**215**) was isolated as a colourless amorphous solid (85% over 2 steps).

Spectroscopic data were identical to (1*R*, 3*S*) enantiomer (**213**); **mp.** 243-246 °C (from H<sub>2</sub>O/EtOH/Et<sub>2</sub>O), lit<sup>23</sup>: 242-244 °C (from H<sub>2</sub>O/EtOH/Et<sub>2</sub>O).

**5.2.50 (1*S*, 4*R*)-4-Aminocyclopent-2-ene carboxylic acid hydrochloride (214)****214**

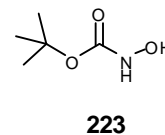
4 N HCl (8 cm<sup>3</sup>) was added to a solution of (1*S*, 4*R*)-2-azabicyclo[2.2.1]hepten-3-one (150 mg, 1.38 mmol) in acetic acid (8 cm<sup>3</sup>). The mixture was stirred for 5 h at 70 °C. After evaporation of the solvents under reduced pressure, the residue was dissolved in water (2 cm<sup>3</sup>) and was passed down an ion-exchange column (Dowex AG 50W-X8100), eluting with 2 N NH<sub>3</sub>. After evaporation of the solvent, the off-white solid was dissolved in 0.1 N HCl (1.4 cm<sup>3</sup>, 1 eq) and freeze-dried. The amino acid hydrochloride was then re-crystallised from acetic acid to give (1*S*, 4*R*)-4-aminocyclopent-2-ene carboxylic acid hydrochloride (**214**) as a colourless amorphous solid (135 mg, 60%).

**Mp:** 178-180 °C (from AcOH),  $[\alpha]_D^{20}$  -96.6 (c 1, H<sub>2</sub>O); (**Found** C, 44.20; H, 6.75; N, 8.58 %, C<sub>6</sub>H<sub>10</sub>NO<sub>2</sub>Cl requires C, 44.05; H, 6.16; N, 8.56 %);  $\delta_H$  (300 MHz, D<sub>2</sub>O) 6.11 (1 H, ddd,  $J=1.6$  Hz,  $J=2.4$  Hz,  $J=5.7$  Hz, CH=C), 5.85 (1 H, dt,  $J=2.3$  Hz,  $J=5.6$  Hz, CH=C), 4.25-4.30 (1 H, m, CHN), 3.59-3.66 (1 H, m, CHCO<sub>2</sub>), 2.56 (1 H, dt,  $J=8.6$  Hz,  $J=14.5$  Hz, CH<sub>A</sub>H<sub>B</sub>), 1.96 (1 H, dt,  $J=4.9$  Hz,  $J=14.4$  Hz, CH<sub>A</sub>H<sub>B</sub>);  $\delta_C$  (75 MHz, D<sub>2</sub>O) 177.9 (CO<sub>2</sub>), 136.6 (CH=C), 129.9 (CH=C), 56.5 (CHN), 50.0 (CHCO<sub>2</sub>), 31.6 (CH<sub>2</sub>).

**5.2.51 (±)-Cis-4-Aminocyclopent-2-ene carboxylic acid hydrochloride (216)<sup>24</sup>****216**

Racemic (±)-*cis*-4-aminocyclopent-2-ene carboxylic acid hydrochloride was obtained following the procedure for the (1*S*, 4*R*) enantiomer (**214**), starting with (±)-2-aza-bicyclo-[2.2.1]hept-5-en-3-one (see **5.2.50**). The product (**216**) was obtained as a colourless amorphous solid (55%).

Spectroscopic data were identical to (1*S*, 4*R*) enantiomer (**214**), **mp**: 168-172 °C (from AcOH), lit<sup>24</sup>: 167-170 °C (from AcOH).

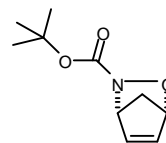
**5.2.52 *tert*-Butyl-*N*-hydroxycarbamate (220)<sup>25, 26</sup>**

A suspension of hydroxylamine hydrochloride (3.2 g, 45 mmol, 1.5 eq) and  $\text{K}_2\text{CO}_3 \cdot 3/2\text{H}_2\text{O}$  (3.8 g, 23 mmol) in diethyl ether (20 cm<sup>3</sup>) and water (0.35 cm<sup>3</sup>) was stirred for 1 h at RT with evolution of CO<sub>2</sub>. A solution of *t*-butyl dicarbonate (6.33 g, 29 mmol) in diethyl ether (12 cm<sup>3</sup>) was then added dropwise at 0 °C and the suspension was stirred at RT for 15 h. The organic phase was decanted, the solids washed with diethyl ether and the organic fractions evaporated to dryness. *tert*-Butyl-*N*-hydroxycarbamate (**220**) was obtained as a colourless solid (3.42 g, 89%) which could be used directly without further purification.

**Mp:** 59-61 °C (from Et<sub>2</sub>O), lit<sup>26</sup>: 58-59 °C; **δ<sub>H</sub>** (300 MHz, CDCl<sub>3</sub>) 7.15-7.40 (1 H, br s, NH), 1.47 (9 H, s, 3 × CH<sub>3</sub>).

These data are in accordance with the literature.<sup>26</sup>

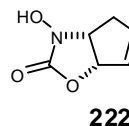


5.2.53 (±)-*N*-(Carbo-*tert*-butoxy)-2,3-oxazabicyclo[2.2.1]hept-5-ene (**219**)<sup>27</sup>**219**

Freshly generated cyclopentadiene (7.2 g, 110 mmol) was added at 0 °C to a stirred solution of *t*-butyl-*N*-hydroxycarbamate (**220**) (3.25 g, 24.4 mmol) in MeOH (240 cm<sup>3</sup>). A solution of NaIO<sub>4</sub> (5.77 g, 27 mmol) in H<sub>2</sub>O (65 cm<sup>3</sup>) was then added dropwise over 20 min. After stirring at 0 °C for 30 min, the reaction mixture was partitioned between brine (325 cm<sup>3</sup>) and EtOAc (325 cm<sup>3</sup>). The layers were separated, the aqueous layer was saturated with NaCl and extracted into EtOAc (3 × 80 cm<sup>3</sup>). The combined organic layers were washed with saturated NaHCO<sub>3</sub>, dried and concentrated under reduced pressure to give a brown oil which was purified over silica gel (hexane/EtOAc 2:1) to give (**219**) as a brown solid (3.44 g, 72%).

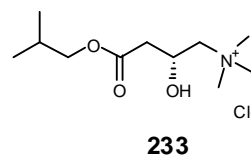
**Mp**: 41-43 °C (from hexane/EtOAc), lit<sup>27</sup> 43-45 °C; **δ<sub>H</sub>** (300 MHz, CDCl<sub>3</sub>) 5.38-5.44 (2 H, m, CH=CH), 5.20-5.22 (1 H, m, CHN), 4.97-4.99 (1 H, m, CHO), 1.99 (1 H, ddd, *J*=1.8 Hz, *J*=1.8 Hz, *J*=8.6 Hz, CH<sub>A</sub>H<sub>B</sub>), 1.71-1.75 (1 H, m, CH<sub>A</sub>H<sub>B</sub>), 1.47 (9 H, s, 3 × CH<sub>3</sub>); **δ<sub>C</sub>** (75 MHz, CDCl<sub>3</sub>) 158.8 (NCO<sub>2</sub>), 134.5 (CH=C), 133.3 (CH=C), 83.9 (CHO), 82.5 (C(CH<sub>3</sub>)<sub>3</sub>), 65.4 (CHN), 48.5 (CH<sub>2</sub>), 28.5 (3 × CH<sub>3</sub>).

These data are in accordance with the literature.<sup>27</sup>

5.2.54 ( $\pm$ )-3-Hydroxy-3,3a,4,6a-tetrahydro-2H-cyclopentaoxazol-2-one (**222**)

A solution of trimethylsilane cyanide (200 mg, 2 mmol) in DMF (6 cm<sup>3</sup>) was added dropwise over 10 min to a solution of ( $\pm$ )-*N*-(carbo-*tert*-butoxy)-2,3-oxazabicyclo[2.2.1]hept-5-ene (**219**) (200 mg, 1 mmol) and CuSO<sub>4</sub> (360 mg, 1.5 mmol) in DMF (10 cm<sup>3</sup>) stirred at 0 °C under N<sub>2</sub>. The reaction mixture was then stirred at 60 °C for 20 h and the reaction was quenched with a 10% solution of EDTA (35 cm<sup>3</sup>). The mixture was extracted into EtOAc (3 × 60 cm<sup>3</sup>) and the combined organic phases were evaporated under reduced pressure. The residue was purified over silica gel (hexane/ EtOAc 1:2) to give the title product (**222**) as a colourless crystalline solid (80 mg, 57%), which was re-crystallised from DCM/hexane.

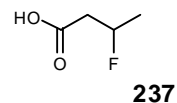
**Mp**: 134-138 °C (from DCM/hexane);  $\nu_{\max}$ (KBr plate)/cm<sup>-1</sup> 3115 (br), 2954 (br), 1748 (br), 1490, 1365, 1283, 1231, 1161, 1110, 992, 884;  $\delta_{\text{H}}$  (300 MHz, CDCl<sub>3</sub>) 9.17 (1 H, br s, OH), 6.11-6.14 (1 H, m, CH=C), 5.82 (1 H, ddd, *J*=2.1 Hz, *J*=4.2 Hz, *J*=6.0 Hz, CH=C), 5.43-5.46 (1 H, m, CHO), 4.47-4.51 (1 H, m, CHN), 2.82-2.88 (1 H, m, CH<sub>A</sub>H<sub>B</sub>), 2.53-2.61 (1 H, m, CH<sub>A</sub>H<sub>B</sub>);  $\delta_{\text{C}}$  (75 MHz, CDCl<sub>3</sub>) 158.8 (NCO<sub>2</sub>), 137.5 (CH=C), 127.7 (CH=C), 83.6 (CHO), 59.9 (CHN), 36.9 (CH<sub>2</sub>); *m/z* (+ES), found (M+Na<sup>+</sup>): 164.0319, C<sub>6</sub>H<sub>7</sub>NO<sub>3</sub>Na requires 164.0324 (-3.0 ppm).

**5.2.55 (S)-Carnitine isobutyl ester (233)<sup>28, 29</sup>**

A suspension of (S)-carnitine hydrochloride (1.15 g, 5.8 mmol) in isobutyl alcohol (8 cm<sup>3</sup>) was saturated with HCl gas and the resultant solution was heated under reflux for 3 h. The solution was then concentrated under reduced pressure and the residue was taken up twice into isobutyl alcohol (2 × 8 cm<sup>3</sup>) and concentrated to dryness. The residue was triturated with acetone to give after filtration (**233**) as a colourless solid (1.38 g, 93%).

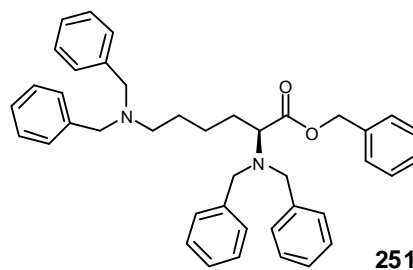
**Mp:** 140-142 °C (from isobutyl alcohol), lit<sup>29</sup> 150 °C (decomp.); [ $\alpha$ ]<sub>D</sub><sup>20</sup> +14.2 (c 1, H<sub>2</sub>O), lit<sup>29</sup> [ $\alpha$ ]<sub>D</sub><sup>25</sup> +15.0 (c 1, H<sub>2</sub>O);  $\delta_{\text{H}}$  (300 MHz, D<sub>2</sub>O); 4.55-4.65 (1 H, m, *CHOH*), 3.82-3.93 (2 H, m, *OCH*<sub>2</sub>), 3.49-3.42 (2 H, m, *CH*<sub>2</sub>N<sup>+</sup>), 3.15 (9 H, 3 × *CH*<sub>3</sub>), 2.53-2.68 (2 H, m, *CH*<sub>2</sub>CO<sub>2</sub>), 1.78-1.96 (1 H, m, *CH*(CH<sub>3</sub>)<sub>2</sub>), 0.83 (6 H, d, *J*=6.8 Hz, 2 × *CH*<sub>3</sub>);  $\delta_{\text{C}}$  (75 MHz, D<sub>2</sub>O); 172.8 (CO<sub>2</sub>), 72.2 (*OCH*<sub>2</sub>), 70.0 (*CH*<sub>2</sub>N<sup>+</sup>), 63.3 (*CHOH*), 54.5 (3 × *CH*<sub>3</sub>), 40.6 (*CH*<sub>2</sub>CO<sub>2</sub>), 27.5 (*CH*(CH<sub>3</sub>)<sub>2</sub>), 18.6 (2 × *CH*<sub>3</sub>).

These data are in accordance with the literature.<sup>28</sup>

5.2.56 3-Fluorobutanoic acid (**237**)

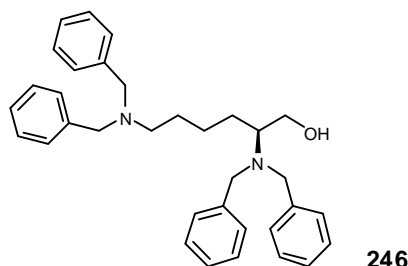
Triethylamine trihydrofluoride (3.8 cm<sup>3</sup>, 23.3 mmol, 2 eq) was added at RT to a solution of  $\beta$ -butyrolactone (1 g, 11.6 mmol) in dry DCM (10 cm<sup>3</sup>). The mixture was then heated under reflux for 5 days. After cooling, the reaction was quenched by the addition of a saturated solution of K<sub>2</sub>CO<sub>3</sub> (10 cm<sup>3</sup>), stirred for 2 h and acidified with HCl 1 N till pH 2. EtOAc (40 cm<sup>3</sup>) was added and the organic phase was separated. The aqueous phase was extracted further with EtOAc (3  $\times$  40 cm<sup>3</sup>) and the combined organic extracts were evaporated under reduced pressure. The residue was purified over silica gel (hexane/EtOAc 5/1) to give (**237**) as a colorless oil (370 mg, 30%).

$\nu_{\text{max}}(\text{film})/\text{cm}^{-1}$  2989, 2942, 2680, 1718, 1433, 1389, 1311, 1214, 1137, 1065, 940, 842;  $\delta_{\text{H}}$  (300 MHz, CDCl<sub>3</sub>) 11.51 (1 H, br s, CO<sub>2</sub>H), 5.10 (1 H, dddq,  $J=47.6$  Hz,  $J=4.6$  Hz,  $J=8.0$  Hz,  $J=6.2$  Hz, CHF), 2.77 (1 H, ddd,  $J=8.0$  Hz,  $J=14.0$  Hz,  $J=16.2$  Hz, CH<sub>A</sub>H<sub>B</sub>CO<sub>2</sub>H), 2.61 (1 H, ddd,  $J=4.6$  Hz,  $J=16.2$  Hz,  $J=28.8$  Hz, CH<sub>A</sub>H<sub>B</sub>CO<sub>2</sub>H), 1.43 (3 H, dd,  $J=6.2$  Hz,  $J=23.8$  Hz, CH<sub>3</sub>);  $\delta_{\text{C}}$  (75 MHz, CDCl<sub>3</sub>); 177.1 (d,  $J=6.4$  Hz, CO<sub>2</sub>), 87.1 (d,  $J=167.3$  Hz, CHF), 42.1 (d,  $J=24.1$  Hz, CH<sub>2</sub>CO<sub>2</sub>), 21.1 (d,  $J=22.3$  Hz, CH<sub>3</sub>);  $\delta_{\text{F}}$  (282 MHz, CDCl<sub>3</sub>) -173.2 (1 F, dddq,  $J=47.8$  Hz,  $J=29.5$  Hz,  $J=23.6$  Hz,  $J=13.6$  Hz);  $m/z$  (+ES), found (M+Na<sup>+</sup>): 129.0322, C<sub>4</sub>H<sub>7</sub>FO<sub>2</sub>Na requires 129.0328 (-4.6 ppm).

5.2.57 Benzyl (S)-2,6-bis(dibenzylamino)hexanoate (**251**)<sup>30</sup>

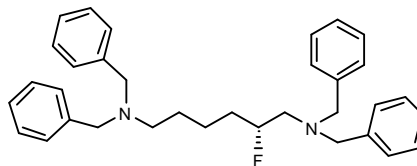
Anhydrous  $\text{K}_2\text{CO}_3$  (30.25 g, 220 mmol, 8 eq) and benzyl bromide (18 cm<sup>3</sup>, 150 mmol, 5.5 eq) were added to a solution of *L*-lysine (4.0 g, 27.4 mmol) in DMF/water (10:1 v/v mixture, 60 cm<sup>3</sup>). After stirring at 60 °C for 3 days, the resulting white slurry was diluted with water (150 cm<sup>3</sup>) and extracted into diethyl ether. The combined organic extracts were washed with 10% NaCl solution and the solvent was removed under reduced pressure to give a light yellow oil (16 g) which could be used for the next step. An analytical sample was obtained after chromatography over silica gel (hexane/EtOAc 10:1) to give the perbenzylated lysine (**251**) as a colourless oil.

$[\alpha]_D^{20}$  -53.2 (c 2.8,  $\text{CHCl}_3$ ), lit<sup>30</sup> -52.5 (c 2.8,  $\text{CHCl}_3$ );  $\nu_{\text{max}}(\text{film})/\text{cm}^{-1}$  3029, 2942, 2798, 1731, 1494, 1454, 1365, 1138, 1028, 969, 745, 698;  $\delta_{\text{H}}$  (300 MHz,  $\text{CDCl}_3$ ) 7.17-7.40 (25 H, m, Ar-*H*), 5.23 (1 H, d,  $J=12.3$  Hz,  $\text{PhCH}_A\text{H}_B\text{O}$ ), 5.11 (1 H, d,  $J=12.3$  Hz,  $\text{PhCH}_A\text{H}_B\text{O}$ ), 3.89 (2 H, d,  $J=13.9$  Hz,  $2 \times \text{PhCH}_A\text{H}_B\text{N}$ ), 3.49 (2 H, d,  $J=13.9$  Hz,  $2 \times \text{PhCH}_A\text{H}_B\text{N}$ ), 3.42-3.52 (4 H, dd,  $\text{PhCH}_2\text{N}'$ ), 3.32 (1 H, dd,  $J=6.2$  Hz,  $J=8.7$  Hz, *CHN*), 2.33 (2 H, t,  $J=6.8$  Hz,  $\text{CH}_2\text{N}'$ ), 1.14-1.76 (6 H, m,  $\text{CH}_2$ );  $\delta_{\text{C}}$  (75 MHz,  $\text{CDCl}_3$ ) 173.0 ( $\text{CO}_2$ ), 140.1 ( $2 \times \text{C}$ , Ar), 139.7 ( $2 \times \text{C}$ , Ar), 136.2 (Ar), 128.9 ( $4 \times \text{C}$ , Ar), 128.8 ( $4 \times \text{C}$ , Ar), 128.6 ( $2 \times \text{C}$ , Ar), 128.5 ( $2 \times \text{C}$ , Ar), 128.4 (Ar), 128.3 ( $4 \times \text{C}$ , Ar), 128.2 ( $4 \times \text{C}$ , Ar), 127.0 ( $2 \times \text{C}$ , Ar), 126.8 ( $2 \times \text{C}$ , Ar), 65.9 ( $\text{PhCH}_2\text{O}$ ), 60.7 (*CHN*), 58.3 ( $2 \times \text{PhCH}_2\text{N}'$ ), 54.5 ( $2 \times \text{PhCH}_2\text{N}$ ), 53.2 ( $\text{CH}_2\text{N}'$ ), 29.3 ( $\text{CH}_2$ ), 26.7 ( $\text{CH}_2$ ), 23.8 ( $\text{CH}_2$ );  $m/z$  (+EI), found  $\text{MH}^+$ : 597.3477,  $\text{C}_{41}\text{H}_{45}\text{N}_2\text{O}_2$  requires 597.3481 (-0.6 ppm).

**5.2.58 (S)-2,6-bis(dibenzylamino)hexan-1-ol (246)**

A solution of the crude benzyl ester (**251**) (14 g, 23.4 mmol) in dry THF (50 cm<sup>3</sup>) was added dropwise over 15 min at 0 °C to a suspension of LiAlH<sub>4</sub> (1.78 g, 46.9 mmol, 2 eq) in dry THF (150 cm<sup>3</sup>). The mixture was stirred for 2 h at 0 °C and the excess of hydride was quenched by successive addition of isopropanol (20 cm<sup>3</sup>) and water (300 cm<sup>3</sup>). The mixture was extracted into diethyl ether (2 × 500 cm<sup>3</sup>), the organic extracts were combined and the solvent removed under reduced pressure. The product was purified over silica gel (hexane/EtOAc 3:1) to yield the amino alcohol (**246**) as a viscous colourless oil (7.2 g, 62% yield over 2 steps).

$[\alpha]_D^{20}$  +56.7 (c 2.8, CHCl<sub>3</sub>),  $\nu_{\max}(\text{film})/\text{cm}^{-1}$  3443, 3027, 2935, 2799, 2360, 1602, 1494, 1453, 1365, 1129, 1028, 747, 698;  $\delta_{\text{H}}$  (300 MHz, CDCl<sub>3</sub>) 7.19-7.38 (20 H, m, Ar-H), 3.75 (2 H, d,  $J=13.3$  Hz, PhCH<sub>A</sub>H<sub>B</sub>N), 3.57 (2 H, d,  $J=13.6$  Hz, PhCH<sub>A</sub>H<sub>B</sub>N'), 3.48 (2 H, d,  $J=13.6$  Hz, PhCH<sub>A</sub>H<sub>B</sub>N'), 3.31-3.45 (2 H, m, CH<sub>2</sub>OH), 3.32 (2 H, d,  $J=13.3$  Hz, PhCH<sub>A</sub>H<sub>B</sub>N), 3.14 (1 H, br s, OH), 2.67-2.77 (1 H, m, CHN), 2.34-2.47 (2 H, m, CH<sub>2</sub>N'), 1.40-1.63 (3 H, m), 1.00-1.37 (3 H, m);  $\delta_{\text{C}}$  (75 MHz, CDCl<sub>3</sub>) 139.9 (2 × C, Ar), 139.3 (2 × C, Ar), 129.0 (4 × C, Ar), 128.7 (4 × C, Ar), 128.4 (4 × C, Ar), 128.1 (4 × C, Ar), 127.1 (2 × C, Ar), 126.7 (2 × C, Ar), 60.8 (CH<sub>2</sub>OH), 58.9 (CHN), 58.4 (2 × PhCH<sub>2</sub>N'), 53.1 (2 × PhCH<sub>2</sub>N), 52.8 (CH<sub>2</sub>N'), 27.3 (CH<sub>2</sub>), 24.7 (CH<sub>2</sub>), 24.5 (CH<sub>2</sub>);  $m/z$  (+EI), found MH<sup>+</sup>: 493.3236, C<sub>34</sub>H<sub>41</sub>N<sub>2</sub>O requires 493.3219 (+3.4 ppm).

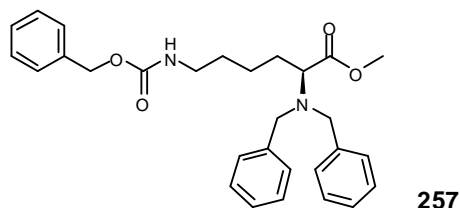
5.2.59  $N^1, N^1, N^6, N^6$ -Tetrabenzyl-(2*R*)-fluorohexane-1,6-diamine (**247**)**247**

DAST (0.4 cm<sup>3</sup>, 3.3 mmol, 1.15 eq) was added dropwise at 0 °C to a solution of (**246**) (1.4 g, 2.8 mmol) in dry DCM (40 cm<sup>3</sup>). The reaction mixture was stirred at RT for 8 h and the reaction was quenched by the addition of 10% K<sub>2</sub>CO<sub>3</sub> (5 cm<sup>3</sup>). Solvents were evaporated to dryness under reduced pressure and the residue was purified over silica gel (hexane/EtOAc 1/1). The early fractions were collected and evaporated to give an off-white solid (280 mg) containing the title compound (**247**) and (*S*)- $N^1, N^1, N^5, N^5$ -tetrabenzyl-6-fluorohexane-1,5-diamine (**252**) as a 85/15 mixture. Re-crystallisation from Et<sub>2</sub>O/hexane gave (**247**) as a colourless crystalline solid (160 mg, 11%).

**Mp**: 93-94 °C (from Et<sub>2</sub>O/hexane); [ $\alpha$ ]<sub>D</sub><sup>20</sup> 0.0 (c 1.1, CHCl<sub>3</sub>); (**Found**: C, 82.15; H, 8.17; N, 5.69 %, C<sub>34</sub>H<sub>39</sub>N<sub>2</sub>F requires C, 82.55; H, 7.95; N, 5.66 %);  $\nu_{\max}$ (KBr plate)/cm<sup>-1</sup> 3027, 2920, 2796, 1948, 1494, 1454, 1117, 1029, 972, 746, 668;  $\delta_H$  (300 MHz, CDCl<sub>3</sub>) 7.17-7.36 (20 H, m, Ar-*H*), 4.57 (1 H, d m, *J*=49.6 Hz, CHF), 3.63 (4 H, s, 2 × PhCH<sub>2</sub>N<sup>1</sup>), 3.51 (4 H, s, 2 × PhCH<sub>2</sub>N<sup>6</sup>), 2.45-2.76 (2 H, m, CHFCH<sub>2</sub>N<sup>1</sup>), 2.34 (2 H, t, *J*=7.1 Hz, CH<sub>2</sub>N<sup>6</sup>), 1.10-1.54 (6 H, m, 3 × CH<sub>2</sub>);  $\delta_C$  (75 MHz, CDCl<sub>3</sub>) 140.0 (2 × C, Ar), 139.5 (2 × C, Ar), 128.9 (4 × C, Ar), 128.8 (4 × C, Ar), 128.3 (4 × C, Ar), 128.2 (4 × C, Ar), 127.0 (2 × C, Ar), 126.8 (2 × C, Ar), 93.4 (d, *J*=169.2 Hz, CHF), 59.1 (2 × PhCH<sub>2</sub>N<sup>1</sup>), 58.4 (2 × PhCH<sub>2</sub>N<sup>6</sup>), 57.0 (d, *J*=21.6 Hz, CH<sub>2</sub>N<sup>1</sup>), 53.1 (CH<sub>2</sub>N<sup>6</sup>), 33.0 (d, *J*=20.6 Hz, CHFCH<sub>2</sub>), 26.9 (CH<sub>2</sub>), 22.5 (d, *J*=4.6 Hz, CH<sub>2</sub>);  $\delta_F$  (376 MHz, CDCl<sub>3</sub>) -181.2 (1 F, dddd, *J*=49.6 Hz, *J*=28.9 Hz, *J*=17.4 Hz, *J*=19.3 Hz, *J*=26.7 Hz); *m/z* (+Cl), found MH<sup>+</sup>: 495.3172 C<sub>34</sub>H<sub>40</sub>N<sub>2</sub>F requires 495.3176. (-0.7 ppm).

5.2.60 Methyl 6-(benzyloxycarbonylamino)-(2*S*)-(dibenzylamino)hexanoate

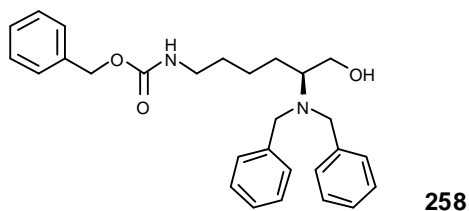
(257)



Anhydrous potassium carbonate (6.265 g, 45.3 mmol, 3 eq) and benzyl bromide (4.31 cm<sup>3</sup>, 36.2 mmol, 2.4 eq) were added to a solution of *N*(ε)-benzyloxycarbonyl-*L*-lysine methyl ester hydrochloride (5 g, 15.1 mmol) in acetonitrile (40 cm<sup>3</sup>). The mixture was heated under reflux for 20 h and after cooling, the solids were filtered and washed with EtOAc. Solvents were removed under reduced pressure and the product was purified over silica gel (hexane/EtOAc 4:1) to yield compound (**257**) as a colourless oil (6.96 g, 97%).

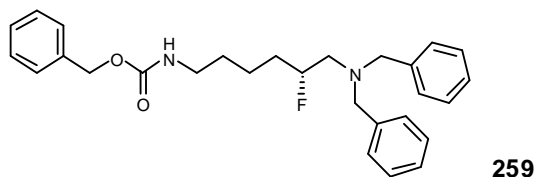
$[\alpha]_D^{20}$  -63.6 (c 2.8 CHCl<sub>3</sub>);  $\nu_{\max}(\text{film})/\text{cm}^{-1}$  3350, 3030, 2948, 1728, 1524, 1455, 1246, 1140, 1028, 748, 699;  $\delta_{\text{H}}$  (300 MHz, CDCl<sub>3</sub>) 7.19-7.36 (15 H, m, Ar-*H*), 5.08 (2 H, s, PhCH<sub>2</sub>O), 4.65 (1 H, br s, NH), 3.90 (2 H, d,  $J=13.8$  Hz, PhCH<sub>A</sub>H<sub>B</sub>N), 3.75 (3 H, s, OCH<sub>3</sub>), 3.50 (2 H, d,  $J=13.8$  Hz, PhCH<sub>A</sub>H<sub>B</sub>N), 3.29 (1 H, dd,  $J=6.5$  Hz,  $J=8.4$  Hz, CHN), 3.10 (2 H, dd,  $J=6.5$  Hz,  $J=12.7$  Hz, CH<sub>2</sub>N'), 1.64-1.78 (2 H, m, CH<sub>2</sub>), 1.37-1.46 (1 H, m, CH<sub>A</sub>H<sub>B</sub>), 1.19-1.32 (3 H, m, CH<sub>2</sub> + CH<sub>A</sub>H<sub>B</sub>);  $\delta_{\text{C}}$  (75 MHz, CDCl<sub>3</sub>) 173.8 (CO<sub>2</sub>), 156.7 (CON), 140.0 (2 × C, Ar), 137.1 (Ar), 129.3 (4 × C, Ar), 128.9 (2 × C, Ar), 128.7 (4 × C, v), 128.5 (3 × C, Ar), 127.4 (2 × C, Ar), 67.0 (PhCH<sub>2</sub>O), 60.7 (CHN), 54.9 (2 × PhCH<sub>2</sub>N), 51.5 (OCH<sub>3</sub>), 41.2 (CH<sub>2</sub>N'), 29.7 (CH<sub>2</sub>), 29.5 (CH<sub>2</sub>), 23.5 (CH<sub>2</sub>);  $m/z$  (+Cl), found MH<sup>+</sup>: 475.2585, C<sub>29</sub>H<sub>35</sub>N<sub>2</sub>O<sub>4</sub> requires 475.2597 (-2.5 ppm).



5.2.61 6-(Benzyloxycarbonylamino)-(2*S*)-(dibenzylamino)hexan-1-ol (**258**)

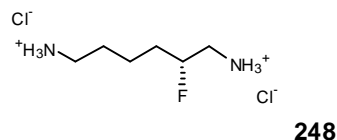
A solution of (**257**) (2.15 g, 4.5 mmol) in dry THF (10 cm<sup>3</sup>) was added dropwise at -10 °C to a suspension of LiAlH<sub>4</sub> (0.344 g, 9.1 mmol, 2 eq) in dry THF (30 cm<sup>3</sup>). The reaction mixture was stirred for 50 min at -10 °C until TLC analysis indicated completion. The reaction was then quenched by careful addition of water and stirred for 1 h. The mixture was acidified with 1 N HCl till pH 7 and extracted into EtOAc. The combined organic extracts were dried and the solvents were evaporated under reduced pressure. The resultant oil was purified over silica gel (hexane/EtOAc 2:1) to yield the amino alcohol (**258**) as a viscous colourless oil (1.90 g, 94%).

$[\alpha]_D^{20} +62.2$  (c 3, CHCl<sub>3</sub>);  $\nu_{\max}(\text{film})/\text{cm}^{-1}$  3421, 3335, 3029, 2860, 1702, 1534, 1455, 1252, 1132, 1028, 749, 699;  $\delta_{\text{H}}$  (300 MHz, CDCl<sub>3</sub>) 7.19-7.36 (15 H, m, Ar-*H*), 5.10 (2 H, s, PhCH<sub>2</sub>O), 4.84 (1 H, br s, NH), 3.79 (2 H, d, *J*=13.3 Hz, 2 × PhCH<sub>A</sub>H<sub>B</sub>N), 3.38-3.50 (2 H, m, CH<sub>2</sub>OH), 3.40 (2 H, d, *J*=13.3 Hz, 2 × PhCH<sub>A</sub>H<sub>B</sub>N), 3.15-3.21 (3 H, m, CH<sub>2</sub>N' and OH), 2.71-2.79 (1 H, m, CHN), 1.66-1.77 (1 H, m, CH<sub>A</sub>H<sub>B</sub>), 1.40-1.54 (2 H, m, CH<sub>2</sub>), 1.14-1.34 (3 H, m, CH<sub>2</sub> and C'H<sub>A</sub>H<sub>B</sub>);  $\delta_{\text{C}}$  (75 MHz, CDCl<sub>3</sub>) 156.5 (CO<sub>2</sub>N), 139.3 (2 × C, Ar), 136.6 (Ar), 129.0 (4 × C, Ar), 128.6 (2 × C, Ar), 128.5 (4 × C, Ar), 128.2 (3 × C, Ar), 127.3 (2 × C, Ar), 66.7 (PhCH<sub>2</sub>O), 60.9 (CH<sub>2</sub>OH), 58.9 (CHN), 53.2 (2 × PhCH<sub>2</sub>N), 40.8 (CH<sub>2</sub>N'), 30.3 (CH<sub>2</sub>), 24.8 (CH<sub>2</sub>), 24.2 (CH<sub>2</sub>); *m/z* (+CI), found MH<sup>+</sup>: 447.2652, C<sub>28</sub>H<sub>35</sub>N<sub>2</sub>O<sub>3</sub> requires 447.2648 (+1.0 ppm).

5.2.62 Benzyl 6-(dibenzylamino)-(5*R*)-fluorohexylcarbamate (**259**)**259**

Deoxofluor 50% in THF (3.02 g, 6.8 mmol, 1.2 eq) was added dropwise at -10 °C to a solution of (**258**) (2.54 g, 5.7 mmol) in dry DCM (40 cm<sup>3</sup>). The mixture was stirred for 6 h, slowly warming from -10 °C to 0 °C and the reaction was quenched by addition of 10% K<sub>2</sub>CO<sub>3</sub> (10 cm<sup>3</sup>). The product was extracted into EtOAc and the combined organic extracts were evaporated under reduced pressure. The residue was purified over silica gel (hexane/EtOAc 5:1) to yield (**259**) and (**260**) as a 90/10 mixture (1.7 g, 67%) as a colourless oil. Re-crystallisation from Et<sub>2</sub>O/hexane gave an analytical sample of (**259**) as a colourless crystalline solid.

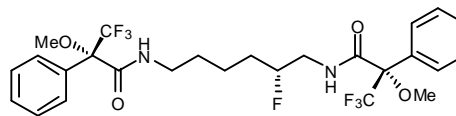
**R<sub>f</sub>**: 0.20 Hexane/EtOAc (5:1); **mp**: 60-62 °C (from Et<sub>2</sub>O/hexane); **[α]<sup>20</sup><sub>D</sub>** +3.2 (c 3.5, CHCl<sub>3</sub>); (**Found**: C, 74.75; H, 7.42; N, 6.43 %, C<sub>28</sub>H<sub>33</sub>N<sub>2</sub>O<sub>2</sub>F requires C, 74.97; H, 7.42; N, 6.25 %); **ν<sub>max</sub>**(KBr plate)/cm<sup>-1</sup> 3361, 2933, 1685, 1539, 1453, 1370, 1266, 1144, 1022, 748, 701; **δ<sub>H</sub>** (300 MHz, CDCl<sub>3</sub>) 7.19-7.37 (15 H, m, Ar-*H*), 5.08 (2 H, s, PhCH<sub>2</sub>O), 4.72 (1 H, br s, NH), 4.59 (1 H, d m, *J*=49.6 Hz, CHF), 3.63 (4 H, s, 2 × PhCH<sub>2</sub>N) 3.12 (2 H, dd, *J*=6.7 Hz, *J*=13.1 Hz, CH<sub>2</sub>N'), 2.50-2.73 (2 H, m, CHFCH<sub>2</sub>N), 1.13-1.60 (6 H, m, 3 × CH<sub>2</sub>); **δ<sub>C</sub>** (75 MHz, CDCl<sub>3</sub>) 156.8 (CO<sub>2</sub>N), 139.8 (2 × C, Ar), 137.0 (Ar), 129.3 (4 × C, Ar), 129.0 (2 × C, Ar), 128.7 (4 × C, Ar), 128.5 (3 × C, Ar), 127.4 (2 × C, Ar), 93.6 (d, *J*=169.3 Hz, CHF), 67.0 (PhCH<sub>2</sub>O), 59.6 (2 × PhCH<sub>2</sub>N), 57.2 (d, *J*=21.9 Hz, CHFCH<sub>2</sub>N), 41.3 (CH<sub>2</sub>N'), 33.1 (d, *J*=20.7 Hz, CH<sub>2</sub>CF), 30.1 (CH<sub>2</sub>), 22.5 (d, *J*=4.3 Hz, CH<sub>2</sub>); **δ<sub>F</sub>** (282 MHz, CDCl<sub>3</sub>) -182.1 (1 F, m); **m/z** (+CI), found MH<sup>+</sup>: 449.2621, C<sub>28</sub>H<sub>34</sub>N<sub>2</sub>O<sub>2</sub>F requires 449.2604 (+3.6 ppm).

**5.2.63 (2R)-Fluorohexane-1,6-diamine dihydrochloride (248)**

$\text{Pd}(\text{OH})_2/\text{C}$  (20% dry weight) (350 mg) was added to a solution of the 90/10 mixture of (**259**) and (**260**) (1.45 g, 3.2 mmol) in methanol (60 cm<sup>3</sup>) (see **5.2.62**). The mixture was stirred in an autoclave at RT for 2 days under a pressure of H<sub>2</sub> (20 bars). The reaction mixture was then filtered over Celite, 1 M HCl in diethyl ether (8 cm<sup>3</sup>) was added and the product was re-crystallised 3 times from methanol/ethanol/diethyl ether till <sup>19</sup>F-NMR spectroscopy indicated only one peak. (2*R*)-Fluorohexane-1,6-diamine dihydrochloride (**248**) was obtained as a colourless amorphous solid (490 mg, 73%).

**Mp:** 235-237 °C (from MeOH/Et<sub>2</sub>O);  $[\alpha]_D^{16}$  0.0 (c 4, MeOH);  $\nu_{\text{max}}$ (KBr plate)/cm<sup>-1</sup> 2996 (br), 2058, 1603, 1485, 1474, 1230, 1152, 1108, 1040, 970, 931, 782;  $\delta_{\text{H}}$  (300 MHz, CD<sub>3</sub>OD) 4.89 (6 H, s, 6 × NH), 4.71-4.96 (1 H, m, CHF), 3.13-3.34 (2 H, m, CHFCH<sub>2</sub>N), 2.95-3.00 (2 H, m, CH<sub>2</sub>N'), 1.67-1.85 (4 H, m, 2 × CH<sub>2</sub>), 1.50-1.70 (2 H, m, CH<sub>2</sub>);  $\delta_{\text{C}}$  (75 MHz, CD<sub>3</sub>OD) 91.7 (d, *J*=170.6 Hz, CHF), 44.3 (d, *J*=20.9 Hz, CHFCH<sub>2</sub>N), 40.5 (CH<sub>2</sub>N'), 32.8 (d, *J*=19.9 Hz, CH<sub>2</sub>), 28.2 (CH<sub>2</sub>), 22.84 (d, *J*=4.1 Hz, CH<sub>2</sub>);  $\delta_{\text{F}}$  (282 MHz, CD<sub>3</sub>OD) -190.9 (1 F, m); *m/z* (+CI), found (M-HCl<sub>2</sub><sup>-</sup>): 135.1298, C<sub>6</sub>H<sub>16</sub>N<sub>2</sub>F requires 135.1298 (+0.4 ppm).

**5.2.64** *N,N*-((2*R*)-Fluorohexane-1,6-diyl)bis((2*S*)-methoxy-2-trifluoromethyl-phenylacetamide) (**265**)

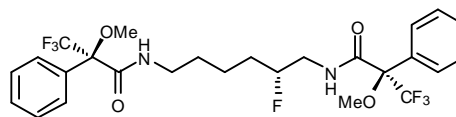


**265**

Et<sub>3</sub>N (27  $\mu$ L, 4 eq), 4-DMAP (5 mg), DCC (40 mg, 4 eq) and (*S*)-(-)- $\alpha$ -methoxy- $\alpha$ -(trifluoromethyl)-phenylacetic acid (37 mg, 3 eq) were added at RT to a suspension of (2*R*)-fluorohexane-1,6-diamine dihydrochloride (**248**) (10 mg, 4.8  $10^{-2}$  mmol) in DCM (1 cm<sup>3</sup>). The reaction mixture was stirred for 12 h and the solvent was removed under reduced pressure. The residue was dissolved in CDCl<sub>3</sub> and filtered through a glass cotton plug directly into a NMR tub.

$\delta_F \{^1H\}$  (375 MHz, CDCl<sub>3</sub>) -68.8 (3 F, s, CF<sub>3</sub> Mosher amide), -68.9 (3 F, s, CF<sub>3</sub> Mosher amide), -70.5 (s, CF<sub>3</sub> Mosher acid in excess), -186.2 (1 F, s, CHF); *m/z* (+CI), found (MH<sup>+</sup>): 567.2093, C<sub>26</sub>H<sub>30</sub>F<sub>7</sub>N<sub>2</sub>O<sub>4</sub> requires 567.2094 (-0.1 ppm).

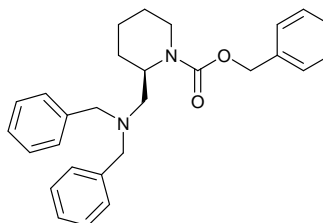
**5.2.65** *N,N*-((2*R*)-Fluorohexane-1,6-diyl)bis((2*R*)-methoxy-2-trifluoromethyl-phenylacetamide) (**266**)



**266**

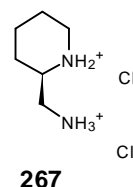
(**266**) was prepared in an identical manner to that described above (**5.2.64**) using (*R*)-(+)- $\alpha$ -methoxy- $\alpha$ -(trifluoromethyl) phenylacetic acid.

$\delta_F \{^1H\}$  (375 MHz, CDCl<sub>3</sub>) -68.9 (6 F, s, 2  $\times$  CF<sub>3</sub> Mosher amide), -70.5 (s, CF<sub>3</sub> Mosher acid in excess), -186.1 (1 F, s, CHF).

**5.2.66 (2R)-((dibenzylamino)methyl)piperidine-1-benzoxycarbonate (261)**

Silica gel (40-63 micron) was added to a solution of **(258)** (200 mg, 0.45 mmol) in dry DCM (10 cm<sup>3</sup>). The mixture was then cooled to -78 °C and Deoxofluor 50% in THF (0.25 cm<sup>3</sup>, 0.7 mmol, 1.5 eq) was added. The mixture was stirred for 6 h at -78 °C and allowed to warm to 0 °C. The reaction was then quenched by the addition of 10% K<sub>2</sub>CO<sub>3</sub> (2 cm<sup>3</sup>). The product was extracted into DCM and the combined organic extracts were evaporated under reduced pressure. The residue was purified over silica gel (hexane/EtOAc 5:1) to yield **(261)** as a colourless oil (96 mg, 50%).

**R<sub>f</sub>**: 0.40 Hexane/EtOAc (5:1); [ $\alpha$ ]<sub>D</sub><sup>20</sup> +93.9 (c 3, CHCl<sub>3</sub>); **v**<sub>max</sub>(film)/cm<sup>-1</sup> 3029, 2936, 2797, 1696, 1495, 1425, 1354, 1256, 1150, 1069, 748, 699; **δ**<sub>H</sub> (300 MHz, CDCl<sub>3</sub>) 7.20-7.33 (15 H, m, Ar-H), 4.99-5.21 (2 H, m, PhCH<sub>2</sub>O), 4.48 (1 H, br d, *J*=42.7 Hz, CHN'), 3.89 (1 H, br s, CH<sub>A</sub>H<sub>B</sub>N'), 3.54 (4 H, br s, 2 × PhCH<sub>2</sub>N), 2.44-2.56 (2 H, m, CH<sub>2</sub>N), 2.35 (1 H, dt, *J*=3.0 Hz, *J*=13.1 Hz, CH<sub>A</sub>H<sub>B</sub>N'), 1.77 (1 H, d, *J*=11.1 Hz, CH<sub>A</sub>H<sub>B</sub>), 1.24-1.53 (4 H, m, 2 × CH<sub>2</sub>), 0.85-0.99 (1 H, m, C'H<sub>A</sub>H<sub>B</sub>); **δ**<sub>C</sub> (75 MHz, CDCl<sub>3</sub>) 155.6 (CO<sub>2</sub>N), 139.6 (2 × C, Ar), 137.0 (Ar), 129.0 (4 × C, Ar), 128.5 (2 × C, Ar), 128.2 (6 × C, Ar), 127.9 (Ar), 126.9 (2 × C, Ar), 67.0 (PhCH<sub>2</sub>O), 58.7 (2 × PhCH<sub>2</sub>N), 52.2 (CH<sub>2</sub>N), 48.2 (CHN'), 39.6 (CH<sub>2</sub>N'), 26.0 (CH<sub>2</sub>), 25.3 (CH<sub>2</sub>), 18.7 (CH<sub>2</sub>); **m/z** (+EI), found MH<sup>+</sup>: 429.2534, C<sub>28</sub>H<sub>33</sub>N<sub>2</sub>O<sub>2</sub> requires 429.2542 (-1.8 ppm).

5.2.67 Piperidine-(2*R*)-methylamine dihydrochloride (**267**)

Pd(OH)<sub>2</sub>/C (20% dry weight) (150 mg) was added to a solution of benzyl-(2*R*)-((dibenzylamino)methyl)piperidine-1-carboxylate (**261**) (500 mg, 1.2 mmol) in methanol (30 cm<sup>3</sup>). The mixture was stirred for 2 days in an autoclave at room temperature under H<sub>2</sub> (20 bars). The black suspension was then filtered over Celite and 1 M HCl in Et<sub>2</sub>O (4 cm<sup>3</sup>) was added to the filtrate. Solvents were removed under reduced pressure and the crude product was re-crystallised from methanol/diethyl ether to yield piperidine-(2*R*)-methylamine dihydrochloride (**267**) (164 mg, 75%) as a colourless crystalline solid.

**Mp**: 213-215 °C (from MeOH/Et<sub>2</sub>O), lit<sup>31</sup> 240-242 °C (from MeOH/Et<sub>2</sub>O, (*S*)-enantiomer); [ $\alpha$ ]<sub>D</sub><sup>20</sup> +2.3 (c 1.4, MeOH), lit<sup>31</sup> [ $\alpha$ ]<sub>D</sub><sup>20</sup> -5.7 (c 0.42, MeOH, (*S*)-enantiomer); (**Found**: C, 38.86; H, 8.31; N, 14.66 %, C<sub>6</sub>H<sub>16</sub>N<sub>2</sub>Cl<sub>2</sub> requires C, 38.51; H, 8.62; N, 14.97 %);  $\nu_{\text{max}}$ (KBr plate)/cm<sup>-1</sup> 3416, 2955 (br), 2842 (br), 1584, 1514, 1484, 1476, 1440, 1407, 1133, 1022, 1008;  $\delta_{\text{H}}$  (300 MHz, CD<sub>3</sub>OD) 4.77 (5 H, s, 5 × NH), 3.38-3.48 (1 H, m, CHN), 3.34-3.42 (1 H, m, CH<sub>A</sub>H<sub>B</sub>N), 3.28 (1 H, dd, *J*=5.8 Hz, *J*=13.6 Hz, CH<sub>A</sub>H<sub>B</sub>N'), 3.14 (1 H, dd, *J*=6.5 Hz, *J*=13.6 Hz, CH<sub>A</sub>H<sub>B</sub>N'), 3.00 (1 H, dt, *J*=3.3 Hz, *J*=12.5 Hz, CH<sub>A</sub>H<sub>B</sub>N), 1.46-2.04 (6 H, m, 3 × CH<sub>2</sub>);  $\delta_{\text{C}}$  (75 MHz, CD<sub>3</sub>OD); 55.8 (CHN), 46.5 (CH<sub>2</sub>N), 42.9 (CH<sub>2</sub>N'), 27.8 (CH<sub>2</sub>), 23.3 (CH<sub>2</sub>), 23.0 (CH<sub>2</sub>); *m/z* (+Cl), found (M-HCl<sub>2</sub><sup>-</sup>): 115.1236, C<sub>6</sub>H<sub>15</sub>N<sub>2</sub> requires 115.1235 (+0.4 ppm).

## 5.3 References

- <sup>1</sup> S. Mennerick, Y. He, X. Jiang, B. D. Manion, M. Wang, A. Shute, A. Benz, A. S. Evers, D. F. Covey, and C. F. Zorumski, *Mol. Pharmacol.*, 2004, **65**, 1191-1197.
- <sup>2</sup> D. F. Hook, F. Gessier, C. Noti, P. Kast, and D. Seebach, *ChemBioChem*, 2004, **5**, 691-706.
- <sup>3</sup> G. M. Nicholas and T. F. Molinski, *J. Am. Chem. Soc.*, 2000, **122**, 4011-4019.
- <sup>4</sup> N. S. Chandrakumar, P. K. Yonan, A. Stapelfeld, M. Savage, E. Rorbacher, P. C. Contreras, and D. Hammond, *J. Med. Chem.*, 1992, **35**, 223-233.
- <sup>5</sup> M. Hudlicky, *J. Org. Chem.*, 1980, **45**, 5377-5379.
- <sup>6</sup> A. Gaucher, L. Dutot, O. Barbeau, W. Hamchaoui, M. Wakselman, and J.-P. Mazaleyrat, *Tetrahedron: Asymmetry*, 2005, **16**, 857-864.
- <sup>7</sup> R. J. Cox and P. S. H. Wang, *J. Chem. Soc., Perkin Trans. 1*, 2001, 2022-2034.
- <sup>8</sup> D. Coleman, *J. Chem. Soc.*, 1951, 2294-2295.
- <sup>9</sup> D. Gani, D. W. Young, D. M. Carr, J. P. Poyser, and I. H. Sadler, *J. Chem. Soc., Perkin Trans. 1*, 1983, 2811-2814.
- <sup>10</sup> M. Marastoni, M. Bazzaro, F. Bortolotti, and R. Tomatis, *Bioorg. Med. Chem.*, 2003, **11**, 2477-2483.
- <sup>11</sup> P. Gmeiner, *Arch. Pharm. (Weinheim, Ger.)*, 1991, **324**, 551-557.
- <sup>12</sup> P. Gmeiner, D. Junge, and A. Kaertner, *J. Org. Chem.*, 1994, **59**, 6766-6776.
- <sup>13</sup> P. O'Brien, H. R. Powell, P. R. Raithby, and S. Warren, *J. Chem. Soc., Perkin Trans. 1*, 1997, 1031-1039.
- <sup>14</sup> R. V. Hoffman and J. Tao, *J. Org. Chem.*, 1997, **62**, 2292-2297.
- <sup>15</sup> J. Schwerdtfeger, S. Kolczewski, B. Weber, R. Frohlich, and D. Hoppe, *Synthesis*, 1999, 1573-1592.
- <sup>16</sup> C. Ye and J. n. M. Shreeve, *J. Fluorine Chem.*, 2004, **125**, 1869-1872.
- <sup>17</sup> R. P. Singh and J. n. M. Shreeve, *J. Fluorine Chem.*, 2002, **116**, 23-26.
- <sup>18</sup> C. Evans, R. McCague, S. M. Roberts, and A. G. Sutherland, *J. Chem. Soc., Perkin Trans. 1*, 1991, 656-657.
- <sup>19</sup> J. C. Jagt and A. M. Van Leusen, *J. Org. Chem.*, 1974, **39**, 564-566.

- <sup>20</sup> H. Nakano, K. Iwasa, Y. Okuyama, and H. Hongo, *Tetrahedron: Asymmetry*, 1996, **7**, 2381-2386.
- <sup>21</sup> R. D. Allan, G. A. R. Johnston, and B. Twitchin, *Aust. J. Chem.*, 1979, **32**, 2517-2521.
- <sup>22</sup> R. Chenevert and R. Martin, *Tetrahedron: Asymmetry*, 1992, **3**, 199-200.
- <sup>23</sup> H. Berger, H. Paul, and G. Hilgetag, *Chem. Ber.*, 1968, **101**, 1525-1531.
- <sup>24</sup> R. D. Allan and B. Twitchin, *Aust. J. Chem.*, 1980, **33**, 599-604.
- <sup>25</sup> J.-B. Behr, C. Chevrier, A. Defoin, C. Tarnus, and J. Streith, *Tetrahedron*, 2003, **59**, 543-553.
- <sup>26</sup> A. Defoin, J. Pires, and J. Streith, *Helv. Chim. Acta*, 1991, **74**, 1653-1670.
- <sup>27</sup> B. T. Shireman, M. J. Miller, M. Jonas, and O. Wiest, *J. Org. Chem.*, 2001, **66**, 6046-6056.
- <sup>28</sup> R. Castagnani, F. De Angelis, E. De Fusco, F. Giannessi, D. Misiti, D. Meloni, and M. O. Tinti, *J. Org. Chem.*, 1995, **60**, 8318-8319.
- <sup>29</sup> I. Bernabei, R. Castagnani, F. De Angelis, P. De Witt Scalfaro, F. Giannessi, D. Misiti, S. Muck, N. Scafetta, and M. O. Tinti, *Angew. Chem., Int. Ed. Engl.*, 1994, **33**, 2076-2078.
- <sup>30</sup> M. G. Banwell, M. J. Coster, M. J. Harvey, and J. Moraes, *J. Org. Chem.*, 2003, **68**, 613-616.
- <sup>31</sup> O. Froelich, P. Desos, M. Bonin, J.-C. Quirion, H.-P. Husson, and J. Zhu, *J. Org. Chem.*, 1996, **61**, 6700-6705.



## 5.4 Crystallographic data

### 5.4.1 (3 $\alpha$ ,5 $\alpha$ )-17-Phenylandrost-16-en-3-ol (87)

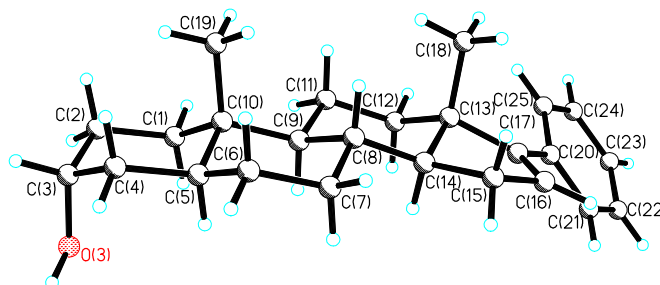


Table 1. Crystal data and structure refinement for gddh2.

Identification code	gddh2	
Empirical formula	C <sub>25</sub> H <sub>34</sub> O	
Formula weight	350.52	
Temperature	93(2) K	
Wavelength	0.71073 Å	
Crystal system	Monoclinic	
Space group	P2(1)	
Unit cell dimensions	a = 14.011(3) Å	$\alpha = 90^\circ$ .
	b = 6.6880(9) Å	$\beta = 97.499(5)^\circ$ .
	c = 21.436(4) Å	$\gamma = 90^\circ$ .
Volume	1991.5(6) Å <sup>3</sup>	
Z	4	
Density (calculated)	1.169 Mg/m <sup>3</sup>	
Absorption coefficient	0.069 mm <sup>-1</sup>	
F(000)	768	
Crystal size	0.2000 x 0.1000 x 0.0200 mm <sup>3</sup>	
Theta range for data collection	1.85 to 25.34°.	
Index ranges	-16 ≤ h ≤ 15, -6 ≤ k ≤ 7, -25 ≤ l ≤ 19	
Reflections collected	12835	
Independent reflections	6604 [R(int) = 0.0512]	
Completeness to theta = 25.34°	98.7 %	
Absorption correction	Multiscan	
Max. and min. transmission	1.0000 and 0.2034	
Refinement method	Full-matrix least-squares on F <sup>2</sup>	
Data / restraints / parameters	6604 / 3 / 479	
Goodness-of-fit on F <sup>2</sup>	0.966	
Final R indices [I > 2sigma(I)]	R1 = 0.0645, wR2 = 0.1495	
R indices (all data)	R1 = 0.0921, wR2 = 0.1694	
Absolute structure parameter	1(2)	
Extinction coefficient	0.012(2)	
Largest diff. peak and hole	0.280 and -0.267 e.Å <sup>-3</sup>	

### 5.4.2 2 $\beta$ -(4-Morpholinyl)-(3 $\alpha$ ,5 $\alpha$ ,17 $\beta$ )-17-(*p*-methoxyphenyl)androstane-3,17-diol (121)

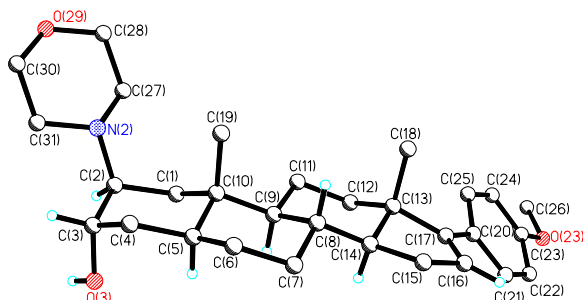


Table 1. Crystal data and structure refinement for gddh3.

Identification code	gddh3	
Empirical formula	C <sub>30</sub> H <sub>43</sub> N O <sub>3</sub>	
Formula weight	465.65	
Temperature	93(2) K	
Wavelength	0.71073 Å	
Crystal system	Orthorhombic	
Space group	P2(1)2(1)2(1)	
Unit cell dimensions	a = 6.2862(5) Å	α = 90°.
	b = 12.3500(9) Å	β = 90°.
	c = 32.739(2) Å	γ = 90°.
Volume	2541.7(3) Å <sup>3</sup>	
Z	4	
Density (calculated)	1.217 Mg/m <sup>3</sup>	
Absorption coefficient	0.077 mm <sup>-1</sup>	
F(000)	1016	
Crystal size	0.150 x 0.030 x 0.010 mm <sup>3</sup>	
Theta range for data collection	2.07 to 25.34°.	
Index ranges	-7 ≤ h ≤ 6, -14 ≤ k ≤ 8, -39 ≤ l ≤ 39	
Reflections collected	18475	
Independent reflections	4392 [R(int) = 0.0281]	
Completeness to theta = 25.34°	95.5 %	
Absorption correction	Multiscan	
Max. and min. transmission	1.0000 and 0.9310	
Refinement method	Full-matrix least-squares on F <sup>2</sup>	
Data / restraints / parameters	4392 / 1 / 314	
Goodness-of-fit on F <sup>2</sup>	1.112	
Final R indices [I > 2σ(I)]	R1 = 0.0356, wR2 = 0.0773	
R indices (all data)	R1 = 0.0396, wR2 = 0.0794	
Absolute structure parameter	0.8(11)	
Extinction coefficient	0.0022(13)	
Largest diff. peak and hole	0.173 and -0.155 e.Å <sup>-3</sup>	

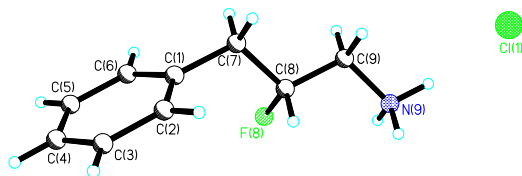
5.4.3 (2*R*)-Fluoro-3-phenylpropan-1-amine hydrochloride (190)

Table 1. Crystal data and structure refinement for gddh6.

Identification code	gddh6	
Empirical formula	C <sub>9</sub> H <sub>13</sub> Cl F N	
Formula weight	189.65	
Temperature	173(2) K	
Wavelength	1.54178 Å	
Crystal system	Orthorhombic	
Space group	P2(1)2(1)2(1)	
Unit cell dimensions	a = 4.522(6) Å	α = 90°.
	b = 5.804(6) Å	β = 90°.
	c = 37.62(2) Å	γ = 90°.
Volume	987.3(18) Å <sup>3</sup>	
Z	4	
Density (calculated)	1.276 Mg/m <sup>3</sup>	
Absorption coefficient	3.131 mm <sup>-1</sup>	
F(000)	400	
Crystal size	0.1500 x 0.1000 x 0.0300 mm <sup>3</sup>	
Theta range for data collection	4.70 to 68.08°.	
Index ranges	-5 ≤ h ≤ 5, -6 ≤ k ≤ 6, -44 ≤ l ≤ 45	
Reflections collected	10441	
Independent reflections	1699 [R(int) = 0.0525]	
Completeness to theta = 68.08°	96.2 %	
Absorption correction	Multiscan	
Max. and min. transmission	1.0000 and 0.5730	
Refinement method	Full-matrix least-squares on F <sup>2</sup>	
Data / restraints / parameters	1699 / 3 / 122	
Goodness-of-fit on F <sup>2</sup>	1.097	
Final R indices [I > 2σ(I)]	R1 = 0.0333, wR2 = 0.0917	
R indices (all data)	R1 = 0.0401, wR2 = 0.1098	
Absolute structure parameter	0.04(2)	
Largest diff. peak and hole	0.255 and -0.409 e.Å <sup>-3</sup>	

Table 2. Torsion angles [°] for gddh6.

C(6)-C(1)-C(2)-C(3)	0.6(4)	C(2)-C(1)-C(7)-C(8)	76.2(3)
C(7)-C(1)-C(2)-C(3)	-178.1(3)	C(6)-C(1)-C(7)-C(8)	-102.4(3)
C(1)-C(2)-C(3)-C(4)	-0.3(4)	C(1)-C(7)-C(8)-F(8)	62.0(3)
C(2)-C(3)-C(4)-C(5)	-0.1(4)	C(1)-C(7)-C(8)-C(9)	-178.3(2)
C(3)-C(4)-C(5)-C(6)	0.2(4)	F(8)-C(8)-C(9)-N(9)	-62.9(2)
C(4)-C(5)-C(6)-C(1)	0.1(4)	C(7)-C(8)-C(9)-N(9)	176.4(2)
C(2)-C(1)-C(6)-C(5)	-0.5(4)		
C(7)-C(1)-C(6)-C(5)	178.2(2)		

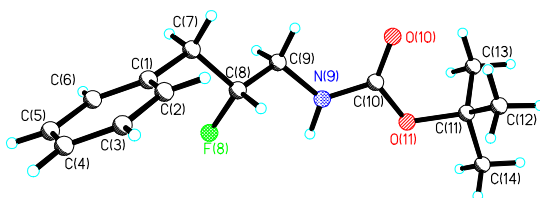
5.4.4 *tert*-Butyl-(2*R*)-fluoro-3-phenylpropylcarbamate (191)

Table 1. Crystal data and structure refinement for gddh5.

Identification code	gddh5	
Empirical formula	C <sub>14</sub> H <sub>20</sub> F N O <sub>2</sub>	
Formula weight	253.31	
Temperature	173(2) K	
Wavelength	1.54178 Å	
Crystal system	Monoclinic	
Space group	P2(1)	
Unit cell dimensions	a = 5.2329(8) Å	α = 90°.
	b = 8.9769(14) Å	β = 90.272(4)°.
	c = 14.679(2) Å	γ = 90°.
Volume	689.53(18) Å <sup>3</sup>	
Z	2	
Density (calculated)	1.220 Mg/m <sup>3</sup>	
Absorption coefficient	0.740 mm <sup>-1</sup>	
F(000)	272	
Crystal size	0.200 x 0.200 x 0.200 mm <sup>3</sup>	
Theta range for data collection	3.01 to 44.82°.	
Index ranges	-4 ≤ h ≤ 4, -8 ≤ k ≤ 8, -13 ≤ l ≤ 13	
Reflections collected	3099	
Independent reflections	1010 [R(int) = 0.0318]	
Completeness to theta = 25.00°	66.2 %	
Absorption correction	Multiscan	
Max. and min. transmission	1.0000 and 0.4133	
Refinement method	Full-matrix least-squares on F <sup>2</sup>	
Data / restraints / parameters	1010 / 2 / 169	
Goodness-of-fit on F <sup>2</sup>	1.091	
Final R indices [I > 2σ(I)]	R1 = 0.0262, wR2 = 0.0651	
R indices (all data)	R1 = 0.0262, wR2 = 0.0651	
Absolute structure parameter	-0.03(17)	
Extinction coefficient	0.053(9)	
Largest diff. peak and hole	0.080 and -0.078 e.Å <sup>-3</sup>	

Table 2. Torsion angles [°] for gddh5.

C(6)-C(1)-C(2)-C(3)	0.6(4)	F(8)-C(8)-C(9)-N(9)	-66.8(2)
C(7)-C(1)-C(2)-C(3)	-177.35(19)	C(7)-C(8)-C(9)-N(9)	173.53(18)
C(1)-C(2)-C(3)-C(4)	0.0(4)	C(8)-C(9)-N(9)-C(10)	-130.9(2)
C(2)-C(3)-C(4)-C(5)	-1.2(4)	C(9)-N(9)-C(10)-O(10)	1.0(3)
C(3)-C(4)-C(5)-C(6)	1.8(4)	C(9)-N(9)-C(10)-O(11)	179.92(17)
C(2)-C(1)-C(6)-C(5)	0.1(3)	O(10)-C(10)-O(11)-C(11)	-1.9(3)
C(7)-C(1)-C(6)-C(5)	177.9(2)	N(9)-C(10)-O(11)-C(11)	179.20(16)
C(4)-C(5)-C(6)-C(1)	-1.3(4)	C(10)-O(11)-C(11)-C(14)	-177.97(16)
C(6)-C(1)-C(7)-C(8)	-99.4(2)	C(10)-O(11)-C(11)-C(12)	64.8(2)
C(2)-C(1)-C(7)-C(8)	78.4(3)	C(10)-O(11)-C(11)-C(13)	-60.0(2)
C(1)-C(7)-C(8)-F(8)	61.2(2)		
C(1)-C(7)-C(8)-C(9)	-178.92(17)		

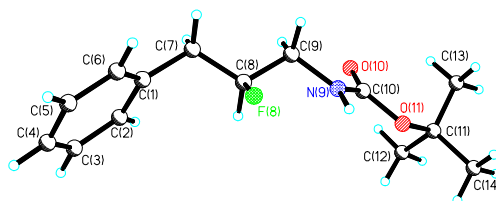
5.4.5 *tert*-Butyl-(2*S*)-fluoro-3-phenylpropylcarbamate (192)

Table 1. Crystal data and structure refinement for gddh4.

Identification code	gddh4	
Empirical formula	C <sub>14</sub> H <sub>20</sub> F N O <sub>2</sub>	
Formula weight	253.31	
Temperature	173(2) K	
Wavelength	1.54178 Å	
Crystal system	Monoclinic	
Space group	P2(1)	
Unit cell dimensions	a = 5.2346(9) Å	α = 90°.
	b = 8.9661(15) Å	β = 90.445(5)°.
	c = 14.681(3) Å	γ = 90°.
Volume	689.0(2) Å <sup>3</sup>	
Z	2	
Density (calculated)	1.221 Mg/m <sup>3</sup>	
Absorption coefficient	0.740 mm <sup>-1</sup>	
F(000)	272	
Crystal size	0.300 x 0.300 x 0.030 mm <sup>3</sup>	
Theta range for data collection	8.47 to 44.70°.	
Index ranges	-4 ≤ h ≤ 4, -8 ≤ k ≤ 8, -13 ≤ l ≤ 13	
Reflections collected	3190	
Independent reflections	1041 [R(int) = 0.0464]	
Completeness to theta = 25.00°	84.8 %	
Absorption correction	Multiscan	
Max. and min. transmission	1.0000 and 0.2371	
Refinement method	Full-matrix least-squares on F <sup>2</sup>	
Data / restraints / parameters	1041 / 2 / 169	
Goodness-of-fit on F <sup>2</sup>	1.058	
Final R indices [I > 2σ(I)]	R1 = 0.0337, wR2 = 0.0821	
R indices (all data)	R1 = 0.0338, wR2 = 0.0822	
Absolute structure parameter	0.0(2)	
Extinction coefficient	0.029(5)	
Largest diff. peak and hole	0.108 and -0.121 e.Å <sup>-3</sup>	

Table 2. Torsion angles [°] for gddh4.

C(6)-C(1)-C(2)-C(3)	-0.7(4)	C(1)-C(7)-C(8)-C(9)	178.9(2)
C(7)-C(1)-C(2)-C(3)	177.5(2)	F(8)-C(8)-C(9)-N(9)	66.4(3)
C(1)-C(2)-C(3)-C(4)	0.3(5)	C(7)-C(8)-C(9)-N(9)	-173.9(2)
C(2)-C(3)-C(4)-C(5)	0.7(5)	C(8)-C(9)-N(9)-C(10)	131.4(3)
C(3)-C(4)-C(5)-C(6)	-1.1(5)	C(9)-N(9)-C(10)-O(10)	-1.5(4)
C(4)-C(5)-C(6)-C(1)	0.7(5)	C(9)-N(9)-C(10)-O(11)	-179.8(2)
C(2)-C(1)-C(6)-C(5)	0.3(4)	O(10)-C(10)-O(11)-C(11)	2.2(4)
C(7)-C(1)-C(6)-C(5)	-178.0(2)	N(9)-C(10)-O(11)-C(11)	-179.5(2)
C(6)-C(1)-C(7)-C(8)	99.8(3)	C(10)-O(11)-C(11)-C(12)	-65.0(3)
C(2)-C(1)-C(7)-C(8)	-78.4(3)	C(10)-O(11)-C(11)-C(13)	60.0(3)
C(1)-C(7)-C(8)-F(8)	-61.0(3)	C(10)-O(11)-C(11)-C(14)	177.8(2)

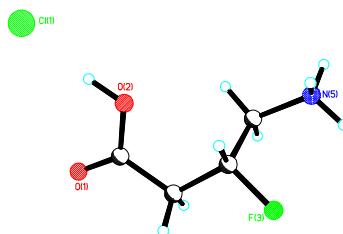
5.4.6 (3*R*)-Fluoro-4-aminobutyric acid hydrochloride (123)

Table 1. Crystal data and structure refinement for gddh8.

Identification code	gddh8	
Empirical formula	C4 H9 Cl F N O2	
Formula weight	157.57	
Temperature	173(2) K	
Wavelength	1.54178 Å	
Crystal system	Orthorhombic	
Space group	P2(1)2(1)2(1)	
Unit cell dimensions	a = 5.3327(5) Å	$\alpha = 90^\circ$ .
	b = 10.1855(10) Å	$\beta = 90^\circ$ .
	c = 13.0250(13) Å	$\gamma = 90^\circ$ .
Volume	707.47(12) Å <sup>3</sup>	
Z	4	
Density (calculated)	1.479 Mg/m <sup>3</sup>	
Absorption coefficient	4.458 mm <sup>-1</sup>	
F(000)	328	
Crystal size	0.100 x 0.100 x 0.020 mm <sup>3</sup>	
Theta range for data collection	6.80 to 44.70°.	
Index ranges	-4 ≤ h ≤ 4, -9 ≤ k ≤ 9, -11 ≤ l ≤ 11	
Reflections collected	3269	
Independent reflections	533 [R(int) = 0.0369]	
Completeness to theta = 25.00°	82.8 %	
Absorption correction	Multiscan	
Max. and min. transmission	1.0000 and 0.1973	
Refinement method	Full-matrix least-squares on F <sup>2</sup>	
Data / restraints / parameters	533 / 4 / 100	
Goodness-of-fit on F <sup>2</sup>	1.072	
Final R indices [I > 2σ(I)]	R1 = 0.0189, wR2 = 0.0480	
R indices (all data)	R1 = 0.0189, wR2 = 0.0480	
Absolute structure parameter	0.009(17)	
Extinction coefficient	0.0121(16)	
Largest diff. peak and hole	0.085 and -0.091 e.Å <sup>-3</sup>	

Table 2. Torsion angles [°] for gddh8.

O(1)-C(1)-C(2)-C(3)	174.3(2)
O(2)-C(1)-C(2)-C(3)	-5.7(3)
C(1)-C(2)-C(3)-F(3)	172.4(2)
C(1)-C(2)-C(3)-C(4)	-70.3(3)
F(3)-C(3)-C(4)-N(5)	-56.0(3)
C(2)-C(3)-C(4)-N(5)	-173.8(2)

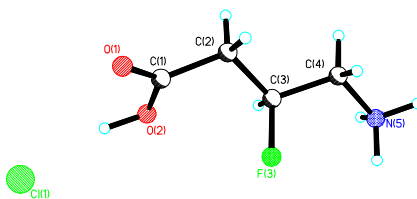
5.4.7 (3*S*)-Fluoro-4-aminobutyric acid hydrochloride (124)

Table 1. Crystal data and structure refinement for gddh15.

Identification code	gddh15	
Empirical formula	C <sub>4</sub> H <sub>9</sub> Cl F N O <sub>2</sub>	
Formula weight	157.57	
Temperature	93(2) K	
Wavelength	0.71073 Å	
Crystal system	Orthorhombic	
Space group	P2(1)2(1)2(1)	
Unit cell dimensions	a = 5.4219(6) Å	α = 90°.
	b = 8.5384(10) Å	β = 90°.
	c = 15.4796(19) Å	γ = 90°.
Volume	716.62(15) Å <sup>3</sup>	
Z	4	
Density (calculated)	1.460 Mg/m <sup>3</sup>	
Absorption coefficient	0.483 mm <sup>-1</sup>	
F(000)	328	
Crystal size	0.200 x 0.030 x 0.030 mm <sup>3</sup>	
Theta range for data collection	3.98 to 25.35°.	
Index ranges	-6 ≤ h ≤ 6, -10 ≤ k ≤ 10, -18 ≤ l ≤ 18	
Reflections collected	6233	
Independent reflections	1252 [R(int) = 0.0395]	
Completeness to theta = 25.00°	95.7 %	
Absorption correction	Multiscan	
Max. and min. transmission	1.0000 and 0.5768	
Refinement method	Full-matrix least-squares on F <sup>2</sup>	
Data / restraints / parameters	1252 / 4 / 99	
Goodness-of-fit on F <sup>2</sup>	1.048	
Final R indices [I > 2σ(I)]	R1 = 0.0198, wR2 = 0.0469	
R indices (all data)	R1 = 0.0206, wR2 = 0.0473	
Absolute structure parameter	0.07(6)	
Largest diff. peak and hole	0.157 and -0.157 e.Å <sup>-3</sup>	

Table 2. Torsion angles [°] for gddh15.

O(1)-C(1)-C(2)-C(3)	142.93(14)
O(2)-C(1)-C(2)-C(3)	-37.65(18)
C(1)-C(2)-C(3)-F(3)	-52.84(16)
C(1)-C(2)-C(3)-C(4)	-170.51(13)
F(3)-C(3)-C(4)-N(5)	64.81(14)
C(2)-C(3)-C(4)-N(5)	-176.80(12)

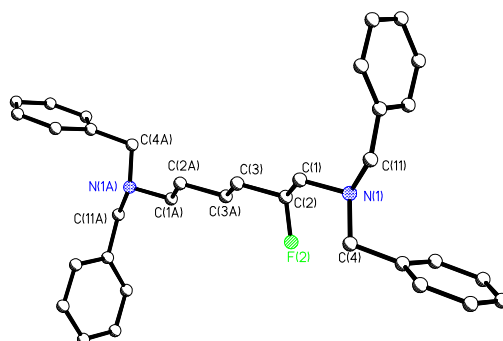
5.4.8  $N^1, N^1, N^6, N^6$ -Tetrabenzyl-(2*R*)-fluorohexane-1,6-diamine (247)

Table 1. Crystal data and structure refinement for GDDH12.

Identification code	gddh12	
Empirical formula	C <sub>34</sub> H <sub>39</sub> F N <sub>2</sub>	
Formula weight	494.67	
Temperature	93(2) K	
Wavelength	0.71073 Å	
Crystal system	Triclinic	
Space group	P-1	
Unit cell dimensions	a = 5.6765(11) Å	$\alpha = 104.607(11)^\circ$
	b = 9.5940(18) Å	$\beta = 90.735(12)^\circ$
	c = 13.544(2) Å	$\gamma = 90.574(13)^\circ$
Volume	713.6(2) Å <sup>3</sup>	
Z	1	
Density (calculated)	1.151 Mg/m <sup>3</sup>	
Absorption coefficient	0.071 mm <sup>-1</sup>	
F(000)	266	
Crystal size	0.200 x 0.050 x 0.020 mm <sup>3</sup>	
Theta range for data collection	2.99 to 25.34°	
Index ranges	-6 ≤ h ≤ 6, -11 ≤ k ≤ 11, -16 ≤ l ≤ 13	
Reflections collected	6233	
Independent reflections	2446 [R(int) = 0.0704]	
Completeness to theta = 25.00°	94.8 %	
Absorption correction	Multiscan	
Max. and min. transmission	1.0000 and 0.1867	
Refinement method	Full-matrix least-squares on F <sup>2</sup>	
Data / restraints / parameters	2446 / 0 / 174	
Goodness-of-fit on F <sup>2</sup>	2.060	
Final R indices [I > 2sigma(I)]	R1 = 0.1580, wR2 = 0.4444	
R indices (all data)	R1 = 0.1674, wR2 = 0.4495	
Extinction coefficient	0.8(2)	
Largest diff. peak and hole	1.450 and -0.473 e.Å <sup>-3</sup>	



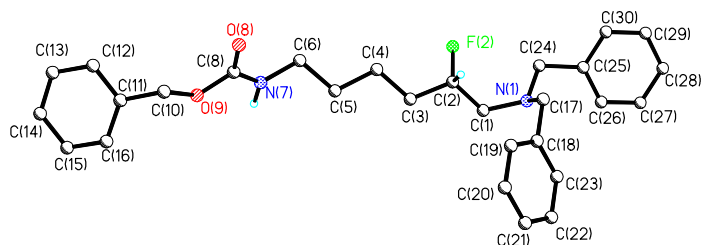
5.4.9 Benzyl 6-(dibenzylamino)-(5*R*)-fluorohexylcarbamate (259)

Table 1. Crystal data and structure refinement for gddh13.

Identification code	gddh13	
Empirical formula	C <sub>28</sub> H <sub>33</sub> F N <sub>2</sub> O <sub>2</sub>	
Formula weight	448.56	
Temperature	93(2) K	
Wavelength	0.71073 Å	
Crystal system	Monoclinic	
Space group	P2(1)	
Unit cell dimensions	a = 12.536(4) Å	α = 90°.
	b = 5.0626(13) Å	β = 101.254(17)°.
	c = 19.426(6) Å	γ = 90°.
Volume	1209.2(6) Å <sup>3</sup>	
Z	2	
Density (calculated)	1.232 Mg/m <sup>3</sup>	
Absorption coefficient	0.082 mm <sup>-1</sup>	
F(000)	480	
Crystal size	0.1000 x 0.0300 x 0.0300 mm <sup>3</sup>	
Theta range for data collection	1.07 to 25.36°.	
Index ranges	-15 ≤ h ≤ 12, -6 ≤ k ≤ 5, -21 ≤ l ≤ 23	
Reflections collected	6860	
Independent reflections	3755 [R(int) = 0.0465]	
Completeness to theta = 25.00°	97.1 %	
Absorption correction	Multiscan	
Max. and min. transmission	1.0000 and 0.5079	
Refinement method	Full-matrix least-squares on F <sup>2</sup>	
Data / restraints / parameters	3755 / 2 / 304	
Goodness-of-fit on F <sup>2</sup>	1.048	
Final R indices [I > 2σ(I)]	R1 = 0.0661, wR2 = 0.1319	
R indices (all data)	R1 = 0.1147, wR2 = 0.1626	
Absolute structure parameter	1.3(19)	
Extinction coefficient	0.018(3)	
Largest diff. peak and hole	0.244 and -0.262 e.Å <sup>-3</sup>	

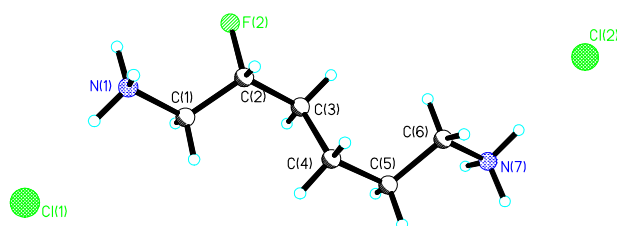
5.4.10 (2*R*)-Fluorohexane-1,6-diamine dihydrochloride (248)

Table 1. Crystal data and structure refinement for GDDH14.

Identification code	gddh14	
Empirical formula	C <sub>6</sub> H <sub>17</sub> Cl <sub>2</sub> F N <sub>2</sub>	
Formula weight	207.12	
Temperature	93(2) K	
Wavelength	0.71073 Å	
Crystal system	Monoclinic	
Space group	P2(1)	
Unit cell dimensions	a = 9.0111(12) Å b = 5.7519(7) Å c = 10.1529(13) Å	α = 90°. β = 108.070(6)°. γ = 90°.
Volume	500.28(11) Å <sup>3</sup>	
Z	2	
Density (calculated)	1.375 Mg/m <sup>3</sup>	
Absorption coefficient	0.610 mm <sup>-1</sup>	
F(000)	220	
Crystal size	0.100 x 0.100 x 0.030 mm <sup>3</sup>	
Theta range for data collection	2.64 to 25.34°.	
Index ranges	-10 ≤ h ≤ 10, -6 ≤ k ≤ 5, -12 ≤ l ≤ 12	
Reflections collected	4502	
Independent reflections	1487 [R(int) = 0.0503]	
Completeness to theta = 25.00°	96.1 %	
Absorption correction	Multiscan	
Max. and min. transmission	1.0000 and 0.3506	
Refinement method	Full-matrix least-squares on F <sup>2</sup>	
Data / restraints / parameters	1487 / 7 / 119	
Goodness-of-fit on F <sup>2</sup>	1.062	
Final R indices [I > 2σ(I)]	R1 = 0.0472, wR2 = 0.1288	
R indices (all data)	R1 = 0.0475, wR2 = 0.1293	
Absolute structure parameter	0.01(14)	
Largest diff. peak and hole	0.805 and -0.439 e.Å <sup>-3</sup>	

Table 2. Torsion angles [°] for GDDH14.

N(1)-C(1)-C(2)-F(2)	-62.7(4)
N(1)-C(1)-C(2)-C(3)	176.0(3)
F(2)-C(2)-C(3)-C(4)	165.0(2)
C(1)-C(2)-C(3)-C(4)	-75.0(4)
C(2)-C(3)-C(4)-C(5)	-177.1(3)
C(3)-C(4)-C(5)-C(6)	70.5(5)
C(4)-C(5)-C(6)-N(7)	-169.9(4)

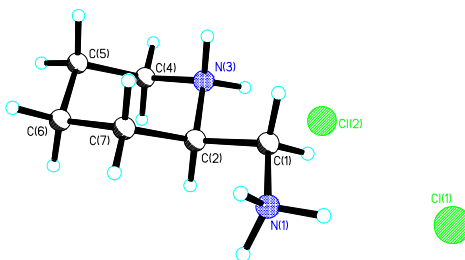
5.4.11 Piperidine-(2*R*)-methylamine dihydrochloride (267)

Table 1. Crystal data and structure refinement for gddh11.

Identification code	gddh11	
Empirical formula	C <sub>6</sub> H <sub>16</sub> Cl <sub>2</sub> N <sub>2</sub>	
Formula weight	187.11	
Temperature	93(2) K	
Wavelength	0.71073 Å	
Crystal system	Monoclinic	
Space group	P2(1)	
Unit cell dimensions	a = 7.036(2) Å	α = 90°.
	b = 9.112(2) Å	β = 106.010(7)°.
	c = 7.702(2) Å	γ = 90°.
Volume	474.6(2) Å <sup>3</sup>	
Z	2	
Density (calculated)	1.309 Mg/m <sup>3</sup>	
Absorption coefficient	0.621 mm <sup>-1</sup>	
F(000)	200	
Crystal size	0.1000 x 0.1000 x 0.0200 mm <sup>3</sup>	
Theta range for data collection	2.75 to 25.35°.	
Index ranges	-8 ≤ h ≤ 8, -10 ≤ k ≤ 10, -9 ≤ l ≤ 6	
Reflections collected	3060	
Independent reflections	1638 [R(int) = 0.0170]	
Completeness to theta = 25.00°	98.4 %	
Absorption correction	Multiscan	
Max. and min. transmission	1.0000 and 0.8985	
Refinement method	Full-matrix least-squares on F <sup>2</sup>	
Data / restraints / parameters	1638 / 6 / 112	
Goodness-of-fit on F <sup>2</sup>	1.053	
Final R indices [I > 2σ(I)]	R1 = 0.0194, wR2 = 0.0415	
R indices (all data)	R1 = 0.0202, wR2 = 0.0418	
Absolute structure parameter	0.00(5)	
Largest diff. peak and hole	0.156 and -0.137 e.Å <sup>-3</sup>	

Table 2. Torsion angles [°] for gddh11.

N(1)-C(1)-C(2)-N(3)	177.21(12)
N(1)-C(1)-C(2)-C(7)	56.30(19)
C(7)-C(2)-N(3)-C(4)	-59.60(17)
C(1)-C(2)-N(3)-C(4)	176.26(13)
C(2)-N(3)-C(4)-C(5)	59.86(16)
N(3)-C(4)-C(5)-C(6)	-56.94(17)
C(4)-C(5)-C(6)-C(7)	54.74(18)
N(3)-C(2)-C(7)-C(6)	56.29(19)
C(1)-C(2)-C(7)-C(6)	175.37(12)
C(5)-C(6)-C(7)-C(2)	-54.60(1)

